

**CIVIL ENGINEERING STUDY 76-1
STRUCTURAL SERIES**

**DYNAMIC INSTABILITY
AND ULTIMATE CAPACITY
OF INELASTIC SYSTEMS
PARAMETRICALLY EXCITED
BY EARTHQUAKES-- PART II**

by

**Franklin Y. Cheng
Professor**

**Kenneth B. Oster
Graduate Assistant**

**Department of Civil Engineering
University of Missouri - Rolla
Rolla, Missouri
August, 1976**



BIBLIOGRAPHIC DATA SHEET	1. Report No. Civil Eng. Study 76-1	2.	3. Recipient's Accession No.
	4. Title and Subtitle Dynamic Instability and Ultimate Capacity of Inelastic Systems Parametrically Excited by Earthquakes--Part II		5. Report Date August, 1976
7. Author(s) Franklin Y. Cheng and Kenneth B. Oster		8. Performing Organization Rept. No. Civil Eng. Study 76-1	
9. Performing Organization Name and Address Civil Engineering Department University of Missouri-Rolla Rolla, Missouri 65401		10. Project/Task/Work Unit No.	
		11. Contract/Grant No. NSF-GI-34966	
12. Sponsoring Organization Name and Address Division of Advanced Environmental Research and Technology National Science Foundation Washington, D.C. 20550		13. Type of Report & Period Covered Technical Report	
		14.	
15. Supplementary Notes			
16. Abstracts An analytical study is presented for the behavior of multi-story framed structures subjected to the interaction of horizontal and vertical components of an earthquake. Frameworks having three to ten stories and one to three bays are studied on the basis of two lumped mass models with elastic, elasto-plastic and bilinear material behavior. The studies include the characteristics of input energy, kinetic energy, elastic strain energy, dissipated strain, and damping energy; the reduction of plastic moment capacity of columns; ductility and excursion rations; and the P-Δ effect. Numerical results show that the inclusion of the vertical ground motion can significantly influence the response parameters of lateral displacements and ductility requirements and consequently causes structural collapse.			
17. Key Words and Document Analysis. 17a. Descriptors Earthquake Engineering Inelastic Behavior Dynamic Instability Structural Dynamics Matrix Method			
17b. Identifiers/Open-Ended Terms			
17c. COSATI Field/Group			
18. Availability Statement		19. Security Class (This Report) UNCLASSIFIED	21. No. of Pages 339
		20. Security Class (This Page) UNCLASSIFIED	22. Price \$10.00-3.00

DYNAMIC INSTABILITY AND ULTIMATE CAPACITY
OF INELASTIC SYSTEMS PARAMETRICALLY
EXCITED BY EARTHQUAKES--PART II

by

Franklin Y. Cheng

Professor

Kenneth B. Oster

Graduate Assistant

Department of Civil Engineering
University of Missouri-Rolla
Rolla, Missouri

August, 1976

Prepared for the National Science Foundation Under Grant No. NSF-GI-34966

ia

ABSTRACT

An analytical study is presented for the behavior of multi-story framed structures subjected to the interaction of horizontal and vertical components of an earthquake.

Typical structures having three to ten stories and one to three bays are studied on the basis of a lumped mass model with elastic, elasto-plastic and bilinear material behavior. The studies include the characteristics of energy absorption in the form of input energy, kinetic energy, elastic strain energy, and dissipated strain and damping energy; the reduction of plastic moment capacity of columns; ductility and excursion ratios; and the P-delta effect as well as the effect of two different lumped mass models on the response parameters.

The response parameters selected to describe the investigative results are: maximum horizontal floor displacements, maximum relative floor displacements, maximum vertical displacements and accelerations at the centers of girders, ductility and excursion ratios of girders and columns, and the variation of input, stored and dissipated energy. The energy evaluation is not only used to indicate the response behavior of various structural systems but also to check the accuracy of step-by-step numerical solutions by determining the maximum percent error at every time increment.

Numerical results show that the inclusion of the vertical ground motion can significantly influence the response parameters. For example, the ductility requirements of girders are remarkably increased. A new concept of ductility ratio based on energy is proposed in this

work and has been compared with other ductility concepts of symmetric bending and curvature. The proposed ductility evaluation has been proved to be advantageous over the other two in both qualitative and quantitative measurements.

Other results may be simply summarized as: Structures having a certain range of natural frequencies are sensitive to vertical earthquake motions. The reduction in plastic moment capacity of columns can increase the influence of vertical earthquake motion on weak column-strong girder systems. Although the consideration of damping in an elastic or inelastic analysis results in a reduction in response as expected, the general behavior of the significant influence of vertical earthquake component on response parameters remains the same as that of undamped systems.

The computer program has been comprehensively developed and can be conveniently used by research workers and practitioners for seismic analysis of large structures.

ACKNOWLEDGEMENTS

This report forms the last phase of the investigation, "Dynamic Instability and Ultimate Capacity of Inelastic Systems Parametrically Excited by Earthquakes," carried out at the University of Missouri-Rolla under the direction of Dr. Franklin Y. Cheng. Part of the work described in this report was presented by the junior author to the faculty of the graduate committee of the University of Missouri-Rolla for partial fulfillment of the requirements for doctor of philosophy in Civil Engineering, summer, 1976.

TABLE OF CONTENTS

	Page
ABSTRACT.....	ii
ACKNOWLEDGEMENTS.....	iv
LIST OF FIGURES.....	ix
LIST OF TABLES.....	xvii
LIST OF SYMBOLS.....	xviii
I. INTRODUCTION.....	1
A. SCOPE OF INVESTIGATION.....	1
B. REVIEW OF LITERATURE.....	4
II. SEISMIC LOADING.....	6
A. EARTHQUAKE RECORDS.....	6
B. GROUND VELOCITY AND DISPLACEMENT.....	6
C. FREQUENCY SPECTRUM.....	15
D. ORIGINAL RECORD BY FOURIER SUMMATION.....	20
III. DYNAMIC ANALYSIS OF A SINGLE-DEGREE-OF-FREEDOM SYSTEM.....	25
A. MOTION EQUATION.....	25
B. COMPARISON OF P-DELTA EFFECT WITH KNOWN SOLUTION.....	29
C. COMPARISON OF RESPONSES WITH PREVIOUS RESULTS BASED ON MATERIAL BEHAVIOR.....	35
D. EFFECT OF VERTICAL FORCES ON TOTAL RESPONSE OF SINGLE-DEGREE-OF-FREEDOM SYSTEM.....	37
IV. MATHEMATICAL FORMULATION OF A MULTI-DEGREE-OF-FREEDOM SYSTEM.....	52
A. MOTION EQUATION.....	52
1. Incremental Form of Motion Equation.....	54
2. Mass Matrix.....	55

Table of Contents (continued)	Page
3. Damping Coefficient Matrix.....	56
4. Geometric Stiffness Matrix.....	57
B. NONLINEAR RESPONSE.....	58
1. Mechanical Equivalent.....	60
2. Moment-Rotation Equations.....	62
3. Stiffness of a Member.....	67
4. Total Stiffness of a Structure.....	74
C. REDUCTION OF ALLOWABLE MOMENT IN COLUMNS.....	74
D. ENERGY.....	76
1. Input Energy.....	77
2. Stored Energy Due to Elastic Strain.....	78
3. Kinetic Energy.....	83
4. Dissipated Energy Due to Damping.....	84
5. Dissipated Energy Due to Plastic Rotation.....	85
6. Elastic Strain Energy For Bilinear Response.....	87
E. DUCTILITY AND EXCURSION RATIOS.....	88
1. Ductility Ratio Based on Symmetrical Bending.....	88
2. Ductility Ratio Based on Curvature.....	92
3. Consideration of Stress Reversal.....	94
4. Ductility Ratio Based on Energy.....	97
V. NUMERICAL METHODS OF INTEGRATION OF INCREMENTAL MOTION EQUATIONS.....	106
A. NEWMARK BETA METHOD.....	106
B. FOURTH ORDER RUNGE-KUTTA.....	109
C. WILSON'S θ -METHOD.....	112

Table of Contents (continued)	Page
VI. ELASTIC RESPONSE OF MULTI-STORY STRUCTURES TO VARIABLE LOADS.....	119
A. COMPARISON OF STEP-BY-STEP INTEGRATION TECHNIQUES WITH THEORETICAL RESULTS OF A TWO-DEGREE-OF-FREEDOM SYSTEM.....	119
B. P-DELTA EFFECT ON DYNAMIC RESPONSE OF A LINEAR SYSTEM DUE TO AN EARTHQUAKE.....	123
C. EFFECT OF VERTICAL EARTHQUAKE MOTION ON DYNAMIC RESPONSE.....	129
D. SENSITIVE STRUCTURES TO VERTICAL EARTHQUAKE EXCITATIONS.....	138
E. FREQUENCIES OF THE VERTICAL FREQUENCY SPECTRUM CONTROLLING THE HORIZONTAL RESPONSE.....	140
VII. INELASTIC RESPONSE OF MULTI-STORY STRUCTURES TO HORIZONTAL AND VERTICAL EARTHQUAKE LOADS.....	142
A. FUNDAMENTAL FREQUENCY IN DAMPING FORMULATION OF INELASTIC STRUCTURES.....	144
1. Effect of Misestimating Fundamental Frequency.....	144
2. Effect of Change in Fundamental Frequency Due to Plastic Deformations.....	151
B. BEHAVIOR COMPARISONS BASED ON STRUCTURAL MODEL.....	154
1. 4-Story, 3-Bay Frame (Frame B).....	155
2. 10-Story, 1-Bay Frame (Frame C).....	159
3. Conclusions of Model Study.....	168
C. COMPARISON OF DUCTILITY AND EXCURSION RATIOS BASED ON DEFINITION.....	168
1. 3-Story, 1-Bay Frame (Frame A).....	170
2. 4-Story, 3-Bay Frame (Frame B).....	175
3. 10-Story, 1-Bay Frame (Frame C).....	175
4. Observations Based on Ductility Studies.....	175

Table of Contents (continued)	Page
D. EFFECT OF INELASTIC ACTION ON RESPONSE PARAMETERS.....	181
1. 3-Story, 1-Bay Frame (Frame A).....	183
2. 4-Story, 3-Bay Frame (Frame B).....	189
3. 10-Story, 1-Bay Frame (Frame C).....	200
4. Observations Based on Response Parameter Studies....	213
E. EFFECT OF M_p REDUCTION ON RESPONSE PARAMETERS.....	214
1. 3-Story, 1-Bay Frame (Frame A).....	214
2. 4-Story, 3-Bay Frame (Frame B).....	216
3. Conclusions on the Effect of M_p Reduction.....	222
F. EFFECT OF VISCOUS DAMPING ON RESPONSE PARAMETERS.....	226
1. 4-Story, 3-Bay Frame (Frame B).....	226
2. 10-Story, 1-Bay Frame (Frame C).....	226
3. Conclusions on the Effect of Damping.....	232
VIII. REVIEW AND CONCLUSIONS.....	238
BIBLIOGRAPHY.....	242
APPENDIX--DESCRIPTION OF INPUT DATA, FORTRAN IV LISTING OF PROGRAM, AND EXAMPLE INPUT AND OUTPUT.....	246

LIST OF FIGURES

Figure	Page
2.1 1940 El Centro Earthquake, N-S Component.....	7
2.2 1940 El Centro Earthquake, Vertical Component.....	7
2.3 1952 Taft Earthquake, N69°W Component.....	8
2.4 1952 Taft Earthquake, Vertical Component.....	8
2.5 Ground Velocity, 1940 El Centro, N-S Component.....	10
2.6 Ground Displacement, 1940 El Centro, N-S Component.....	10
2.7 Ground Velocity, 1940 El Centro, Vertical Component.....	11
2.8 Ground Displacement, 1940 El Centro, Vertical Component.....	11
2.9 Ground Velocity, 1952 Taft, N69°W Component.....	12
2.10 Ground Displacement, 1952 Taft, N69°W Component.....	12
2.11 Ground Velocity, 1952 Taft, Vertical Component.....	13
2.12 Ground Displacement, 1952 Taft, Vertical Component.....	13
2.13 Frequency Spectrum, 1940 El Centro, N-S Component.....	18
2.14 Frequency Spectrum, 1940 El Centro, Vertical Component.....	19
2.15 Fourier Summation, Impulse Load, 206 Frequencies (0-5Hz)....	22
2.16 Frequency Spectrum of Impulse Load.....	22
2.17 Fourier Summation, 1940 El Centro Earthquake (N-S).....	23
3.1 Horizontal Ground Motion Acting on a Single-Degree- of-Freedom System.....	26
3.2 Horizontal Plus Vertical Ground Motion Acting on a Single-Degree-of-Freedom System.....	28
3.3 Horizontal Forcing Function Acting on a Single-Degree- of-Freedom System.....	31
3.4 Simple Bent with Variable Horizontal Load and Constant Vertical Load.....	33

Figure	Page
3.5 Comparison of Methods of Analysis When Considering P-delta Effect on Single-Degree-of-Freedom System.....	34
3.6 Shear Structure for Comparison, $T_n = 1.20$ sec.....	36
3.7 Bilinear Response Based on $2M_p$ Stress Range.....	38
3.8 Elastic Response of Fig. 3.6, $T_n = 1.20$ sec.....	39
3.9 Bilinear Response of Fig. 3.6, $T_n = 1.20$ sec.....	39
3.10 Elasto-Plastic Response of Fig. 3.6, $T_n = 1.20$ sec.....	39
3.11 Horizontal Displacement of Single-Degree-of-Freedom System, $T_n = 2.0$ sec., 1940 El Centro (N-S).....	41
3.12 Frequency Spectrum (0.25-0.67 Hz), 1940 El Centro Earthquake (N-S).....	42
3.13 Horizontal Displacement of Single-Degree-of-Freedom System, $T_n = 3.0$ sec., 1940 El Centro (N-S).....	44
3.14 Response of Single Mass Subjected to Sinusoidal Loads in the Horizontal and Vertical Directions.....	45
3.15 Response of Single Mass Subjected to Sinusoidal Loads in the Horizontal and Vertical Directions ($\alpha_v \neq 0$).....	47
3.16 Response of Single Mass Subjected to Sinusoidal Loads in the Horizontal and Vertical Directions ($\omega_v = 2p_n$).....	48
3.17 Response of a Single Mass Subjected to an Impulse F_s and $F_v = A_v \sin(\omega_v t)$	50
3.18 Response of a Single Mass Subjected to an Impulse F_s and $F_v = A_v \sin(\omega_v t + \alpha_v)$	51
4.1 Idealized Moment-Rotation Relationship.....	59
4.2 Equivalent Mechanical System for Bilinear System.....	61
4.3 M- θ Relationship for Model Components.....	61
4.4 Two Component Model of Inelastic Member.....	63
4.5 Forces and Deformations of a Typical Member.....	68
4.6 Member Moment Diagram.....	79
4.7 Elastic Moment-Rotation Relationship.....	82

Figure	Page
4.8 Inelastic Moment-Rotation Relationship.....	86
4.9 Moment-Rotation, Ductility Based on Symmetrical Bending.....	89
4.10 Moment-Rotation, Ductility Based on Curvature.....	93
4.11 Effect of $2M_p$ Stress Range on Ductility.....	96
4.12 Moment-Rotation, Ductility Based on Energy.....	98
4.13 M- θ Curve of Node 3 for Horizontal and Vertical Ground Motions of 1940 El Centro.....	100
4.14 Moment-Rotation Boundary for One End of a Member.....	101
4.15 Elastic Strain Energy of a Member Based on M- θ Relationship.....	103
5.1 Period Elongation and Amplitude Decay of Single Mass Using Wilson's θ -Method.....	117
6.1 Two-Degree System.....	120
6.2 Spring-Mass Model for Two-Degree System.....	120
6.3 Response of Two-Degree System Based on Initial Conditions...	122
6.4 Three-Story Frame.....	124
6.5 Top Floor Response of 3-Story Bldg, 1940 El Centro.....	124
6.6 Comparison of Maximum Response with Frequency Spectrum of Earthquake (N-S, 1940 El Centro).....	126
6.7 Response of 3-Story Bldg, Equal Response Frequencies, 1940 El Centro.....	128
6.8 Response of 3-Story Bldg, 1940 El Centro.....	130
6.9 Loads on Multi-Story Structure to Study Effect of Vertical Ground Motion.....	131
6.10 Top Floor Displacement, Impulse Only ($p_n = 3.0$ Hz).....	131
6.11 Top Floor Displacement, Impulse Plus Vertical Up Positive ($p_n = 3.0$ Hz).....	133
6.12 Top Floor Displacement, Impulse Plus Vertical Down Positive ($p_n = 3.0$ Hz).....	133

Figure	Page
6.13 Top Floor Displacement, Impulse Only ($p_n = 4.37$ Hz).....	134
6.14 Top Floor Displacement, Impulse Plus Vertical Up Positive ($p_n = 4.37$ Hz).....	134
6.15 Top Floor Displacement, Impulse Plus Vertical Down Positive ($p_n = 4.37$ Hz).....	135
6.16 Top Floor Displacement ($p_n = 1.22$ Hz).....	136
6.17 Top Floor Displacement, Impulse Plus Vertical Up Positive ($p_n = 1.22$ Hz).....	137
6.18 Top Floor Displacement, Impulse Plus Vertical Down Positive ($p_n = 1.22$ Hz).....	137
7.1 3-Story, 1-Bay Frame (Frame A).....	147
7.2 Linear Combination of Mass and Stiffness Damping, Top Floor Displacement, Frame A ($p_n = 0.833$ Hz).....	149
7.3 Mass and Stiffness Proportional Damping, Top Floor Displacement, Frame A ($p_n = 0.833$ Hz).....	150
7.4 Comparison of Elasto-Plastic Responses, Frame A, ($p_n = 0.833$ Hz).....	153
7.5 4-Story, 3-Bay Frame (Frame B).....	156
7.6 Models 1 and 2, Top Floor Displacement of Frame B, Elasto-Plastic System, 3% Damping, 1940 El Centro.....	156
7.7 Models 1 and 2, Energy Plot of Frame B, Elastic System, 3% Damping, 1940 El Centro, N-S Component Only.....	157
7.8 Models 1 and 2, Energy Plot of Frame B, Elastic System, 3% Damping, 1940 El Centro, N-S Plus Vertical.....	158
7.9 Models 1 and 2, Energy Plot of Frame B, Elasto-Plastic System, 3% Damping, 1940 El Centro, N-S Component Only.....	160
7.10 Models 1 and 2, Energy Plot of Frame B, Elasto-Plastic System, 3% Damping, 1940 El Centro, N-S Plus Vertical.....	161
7.11 Models 1 and 2, Ductility Requirement of Frame B, Elasto-Plastic System, 1940 El Centro.....	162
7.12 Maximum Vertical Displacement at Center of Girders, Model 2 of Frame B, 1940 El Centro, N-S Plus Vertical.....	162

Figure	Page
7.13 10-Story, 1-Bay Frame (Frame C).....	163
7.14 Maximum Vertical Displacement at Center of Girders, Model 2 of Frame C, 1940 El Centro, N-S Plus Vertical.....	165
7.15 Models 1 and 2, Maximum Relative Floor Displacement of Frame C, 1940 El Centro.....	166
7.16 Models 1 and 2 Ductility Requirement of Frame C, 1940 El Centro.....	167
7.17 Elasto-Plastic Ductility Ratios for Girders of Frame A, 1952 Taft.....	171
7.18 Elasto-Plastic Excursion Ratios for Girders of Frame A, 1952 Taft.....	172
7.19 Bilinear Ductility Ratios for Girders of Frame A, 1952 Taft.....	173
7.20 Bilinear Excursion Ratios for Girders of Frame A, 1952 Taft.....	174
7.21 Elasto-Plastic Girder Ductility and Excursion Ratios of Frame B, 1940 El Centro.....	176
7.22 Elasto-Plastic Column Ductility and Excursion Ratios of Frame B, 1940 El Centro.....	177
7.23 Elasto-Plastic Girder Ductility Ratios of Frame C, 1940 El Centro.....	178
7.24 Elasto-Plastic Girder Excursion Ratios of Frame C, 1940 El Centro.....	179
7.25 Maximum Floor Displacement, Frame A, Elastic and Elasto-Plastic Systems, 1940 El Centro.....	184
7.26 Maximum Floor Displacement, Frame A, Elasto-Plastic and Bilinear ($p = 0.05$) Systems, 1940 El Centro.....	185
7.27 Top Floor Displacement of Frame A, Elastic and Elasto-Plastic Systems, 1940 El Centro.....	186
7.28 Top Floor Displacement of Frame A With and Without Static Loads, Elasto-Plastic System, 1940 El Centro.....	186
7.29 Maximum Relative Floor Displacements, Frame A, Elastic and Elasto-Plastic Systems, 1940 El Centro.....	187

Figure	Page
7.30 Maximum Relative Floor Displacement, Frame A, Elasto-Plastic and Bilinear ($p = 0.05$) Systems, 1940 El Centro.....	188
7.31 Maximum Vertical Displacement at Center of Girder, Frame A, 1940 El Centro, N-S Plus Vertical.....	190
7.32 Maximum Vertical Acceleration at Center of Girder, Frame A, 1940 El Centro, N-S Plus Vertical.....	191
7.33 Maximum Ductility Ratios, Frame A, 1940 El Centro.....	192
7.34 Maximum Girder Ductility Ratios at Face of Column, Frame A, 1940 El Centro.....	193
7.35 Maximum Girder Ductility Ratios at Center of Span, Frame A, 1940 El Centro.....	193
7.36 Top Floor Displacement of Frame B, 1940 El Centro, N-S Plus Vertical.....	194
7.37 Maximum Floor Displacements, Frame B, 1940 El Centro.....	196
7.38 Maximum Relative Floor Displacements, Frame B, 1940 El Centro.....	196
7.39 Maximum Vertical Displacement at Center of Girders, Frame B, 1940 El Centro.....	197
7.40 Maximum Vertical Acceleration at Center of Girders, Frame B, 1940 El Centro.....	197
7.41 Maximum Girder Ductility and Excursion Ratios, Frame B, 1940 El Centro.....	198
7.42 Maximum Column Ductility and Excursion Ratios, Frame B, 1940 El Centro.....	199
7.43 Effect of P-delta on Energy, Frame B, Elasto-Plastic System, 1940 El Centro, N-S Only.....	201
7.44 Effect of Response Condition on Energy, Frame B, N-S Only...	202
7.45 Effect of the Vertical Ground Motion on Energy, Frame B, 3% Damping, Elastic System, 1940 El Centro.....	203
7.46 Elastic and Elasto-Plastic Energy, Frame B, 3% Damping, 1940 El Centro, N-S Plus Vertical.....	204
7.47 Effect of the Vertical Ground Motion on Energy, Frame B, 3% Damping, Elasto-Plastic System, 1940 El Centro.....	205

Figure	Page
7.48 Maximum Floor Displacement, Frame C, 1940 El Centro.....	207
7.49 Top Floor Displacement, Frame C, 1940 El Centro, N-S Plus Vertical.....	208
7.50 Maximum Relative Floor Displacements, Frame C, 1940 El Centro.....	209
7.51 Maximum Vertical Displacement, Frame C, 1940 El Centro.....	210
7.52 Maximum Vertical Acceleration, Frame C, 1940 El Centro.....	210
7.53 Girder Ductility Ratios, Frame C, 1940 El Centro.....	211
7.54 Girder Excursion Ratios, Frame C, 1940 El Centro.....	211
7.55 Effect of Response Condition on Energy, Frame C, 1940 El Centro, N-S Plus Vertical.....	212
7.56 Effect of M_p Reduction on Horizontal Response, Frame A, 1940 El Centro.....	215
7.57 Maximum and Minimum Floor Displacements, Frame A, Elasto- Plastic and Bilinear ($p = 0.05$) Systems, 1940 El Centro.....	217
7.58 Effect of M_p Reduction on Vertical Response, Frame A, 1940 El Centro.....	218
7.59 Effect of M_p Reduction on Ductility, Frame A, 1940 El Centro.....	219
7.60 Effect of M_p Reduction on Horizontal Response, Frame B, 3% Damping, Elasto-Plastic System, 1940 El Centro, N-S Plus Vertical.....	220
7.61 Effect of M_p Reduction on Top Floor Displacement, Frame B, 3% Damping, Elasto-Plastic System, 1940 El Centro, N-S Plus Vertical.....	221
7.62 Effect of M_p Reduction on Vertical Response, Frame B, 3% Damping, Elasto-Plastic System, 1940 El Centro, N-S Plus Vertical.....	223
7.63 Effect of M_p Reduction on Ductility Requirement, Frame B, 3% Damping, Elasto-Plastic System, 1940 El Centro, N-S Plus Vertical.....	224
7.64 Effect of M_p Reduction on Energy, Frame B, 3% Damping, Elasto-Plastic System, 1940 El Centro, N-S Plus Vertical....	225

Figure	Page
7.65 Effect of Damping on Horizontal Response, Frame B, 1940 El Centro, N-S Plus Vertical.....	227
7.66 Effect of Damping on Displacement of Top Floor, Frame B, Elasto-Plastic System, 1940 El Centro, N-S Plus Vertical....	228
7.67 Effect of Damping on Vertical Response, Frame B, 1940 El Centro, N-S Plus Vertical.....	229
7.68 Effect of Damping on Ductility Requirements, Frame B, Elasto-Plastic System, 1940 El Centro, N-S Plus Vertical....	230
7.69 Effect of Damping on Energy, Frame B, Elasto-Plastic System, 1940 El Centro, N-S Plus Vertical.....	231
7.70 Effect of Damping on Maximum Horizontal Response, Frame C, Elasto-Plastic System, 1940 El Centro, N-S Plus Vertical.....	233
7.71 Effect of Damping on Displacement of Top Floor, Frame C, Elasto-Plastic System, 1940 El Centro, N-S Plus Vertical....	234
7.72 Effect of Damping on Vertical Response, Frame C, Elasto-Plastic System, 1940 El Centro, N-S Plus Vertical....	235
7.73 Effect of Damping on Girder Ductility Requirements, Frame C, Elasto-Plastic System, 1940 El Centro, N-S Plus Vertical.....	236
7.74 Effect of Damping on Energy, Frame C, Elasto-Plastic System, 1940 El Centro, N-S Plus Vertical.....	237

LIST OF TABLES

Table	Page
4.1 Value of C in $\theta_y = CM_{pL}/EI$ Based on Different Conditions at Opposite End of a Member.....	91
7.1 Linear Response of Frame A Using Different Damping Formulation and Estimated Fundamental Frequency (1940 El Centro, P-delta Included, 5% Damping).....	148
7.2 Elasto-Plastic Response of Frame A Using Different Damping Formulation (1940 El Centro, P-delta Included, 5% Damping).....	152

LIST OF SYMBOLS

a	= member end (2i-1); moment-deformation relationship term = $4EI/L$
a_r	= real part of A_r
A	= cross-sectional area; constant
A_r	= rth coefficient of the discrete Fourier transform
$\{A\}$	= intermediate matrix in Newmark and Runge-Kutta integration techniques
$[A]$	= static equilibrium matrix
b	= member end (2i); moment-deformation relationship term = $2EI/L$
b_r	= imaginary part of A_r
B	= constant
$\{B\}$	= intermediate matrix in Newmark and Runge-Kutta integration techniques
c	= moment-deformation relationship term = $6EI/L^2$
c_0, c_1, c_2	= constraints in equation for base line of an accelerogram
c_m	= coefficient for calculating M_p reduction based on bracing and loading of a member
C	= coefficient of $\theta_y = CM_p L/EI$ based on the moment condition at opposite end of the member
$[C]$	= damping coefficient matrix
d	= moment-deformation relationship term = $12EI/L^3$
DFT	= discrete Fourier transform
$\{D\}$	= intermediate matrix in Runge-Kutta integration technique
e	= moment-deformation relationship term = $3EI/L$
E	= modulus of elasticity
E_{bx}	= bilinear strain energy

E_d	= dissipated energy
E_{dd}	= dissipated energy due to damping
E_{ds}	= dissipated strain energy
E_{es}	= elastic strain energy
E_i	= input energy
E_k	= kinetic energy
E_s	= stored energy
$\{E\}$	= intermediate matrix in Runge-Kutta integration technique
f	= moment-deformation relationship term = $3EI/L^2$
F	= force
F_a	= allowable working stress by elastic design rules, ksi
F_p	= horizontal force due to P-delta effect
F_y	= yield stress of material in tension
F'_e	= allowable Euler stress = $\pi^2 EK_1 / 1.92 (K\ell_b / r_b)^2$
FFT	= fast Fourier transform
$\{F\}$	= multiple forcing function
g	= moment-deformation relationship term = $3EI/L^3$; acceleration of gravity = 32.2 fps^2 (9.81 m/sec^2)
H	= floor height relative to floor below
i	= beam member no.; counter; $\sqrt{-1}$
I	= moment of inertia of cross-sectional area
IDFT	= inverse of discrete Fourier transform
j	= floor number; counter
k	= node stiffness; counter
k_1	= elastic component of node stiffness
k_2	= elasto-plastic component of node stiffness

K	= column stiffness; effective length factor in the plane of bending
$K_s, [K_s]$	= geometric stiffness
K_1	= earthquake and wind factor per AISC = 1.3
$[K]$	= stiffness matrix of structural system
$[K_{11}], [K_{12}],$ $[K_{22}]$	= submatrices of $[K]$
$[K'']$	= condensed stiffness matrix of structural system
ℓ_b	= actual unbraced length in the plane of bending
L	= length of a structural member
m	= mass of a single-degree-of-freedom system
M	= moment at one end of a member
M_m	= maximum moment a member can resist without an axial load
M_p	= plastic moment
M_{pc}	= permissible load based on axial plus bending loads
M_y	= yield moment
$\{M\}$	= member end-moments
$[M]$	= mass matrix
n	= some positive number, number of floor levels
N	= number of Nyquist data points
N_f	= number of floor levels; $N/2$
N_μ	= total number of times the node of a member is plastic during loading
NPH	= number of degrees of freedom in horizontal direction
NPR	= number of degrees of freedom in rotation
NPS	= number of degrees of freedom in translation
NPV	= number of degrees of freedom in vertical direction

p	= strain hardening ratio = k_2/k ; mode frequency
p_n	= natural frequency without vertical load
p_s	= natural frequency when including vertical load
P	= axial load in column
P_{cr}	= $1.7AF_a$, kips (1 kip = 4448 Newton)
P_e	= $1.92AF_e$, kips (1 kip = 4448 Newton)
P_y	= allowable axial load
q	= ratio of elastic component to total elastic stiffness = k_1/k
q_y	= yield strength restoring force per unit mass
Q_y	= yield strength restoring force
r_b	= radius of gyration in plane of bending
R_y	= vertical column reactions
S	= member section modulus
$[S]$	= member stiffness matrix
t	= time
T_n	= fundamental period
T_s	= fundamental period when including vertical loads
u	= end displacement of a beam
u_s	= absolute nodal displacement in horizontal direction
$\{u_s\}$	= absolute nodal displacement vector in horizontal direction
v_s	= absolute nodal displacement in vertical direction
V	= member end shears
$\{v_s\}$	= absolute nodal displacement vector in vertical direction
W	= total weight of structure; work
W_j	= weight of floor j

x	= displacement
x_g	= horizontal movement of ground
x_s	= horizontal displacement relative to ground
x_v	= vertical displacement relative to ground
x_k	= kth sample of a time series; displacement amplitude
$\{x\}$	= deformation vector
$\{\ddot{x}_g\}$	= ground acceleration vector
$\{x_s\}$	= horizontal displacement vector
$\{x_v\}$	= vertical displacement vector
$\{x_\theta\}$	= rotation vector
y_g	= vertical movement of ground
Z	= plastic modulus
α	= plastic rotation; damping coefficient parameter; phase angle
β	= damping coefficient parameter; coefficient used in Newmark's integration technique
Δ	= horizontal displacement of a floor relative to the one below it; increment
Δt	= time increment
ϵ	= excursion ratio
θ	= end-rotation of a member; factor used in Wilson's θ -Method
λ	= damping ratio
μ	= ductility ratio
τ	= projected time increment used in Wilson's θ -Method
ω	= end rotation of central beam of the elasto-plastic component of a member; forcing frequency

Subscripts

a	= end (2i-1) of member i
ab	= absolute value
act	= actual
ave	= average
b	= end 2i of member i
c	= column
cr	= critical
est	= estimated
eq	= equivalent
f	= floor
g	= ground; girder
max	= maximum
min	= minimum
n	= natural
s	= horizontal
t	= total; at time t
t+ Δt	= at time t + Δt
v	= vertical
y	= yield

Superscripts

.	= 1st derivative, velocity
''	= 2nd derivative, acceleration
T	= transpose of matrix
-1	= inverse of matrix

I. INTRODUCTION

The increasing population density in regions of the world having high seismicity has resulted in an increasing potential for catastrophic structural damage due to earthquakes. The use of multi-story structures as required to meet the needs for more space in high density areas can be one of the major potential dangers.

The capacity of a multi-story structure to absorb energy released by earthquakes of significant magnitude will depend mainly on the structure's ability to respond in a nonlinear manner without extreme structural damage resulting in possible loss of lives. Large quantities of energy will be required to be dissipated by plastic deformations. It is apparent that a comparison of the response behavior of structural systems is essential for a satisfactory design of multi-story seismic structures. To be able to determine this behavior by structural analysis, it is necessary to have an adequate mathematical model as well as adequate response parameters to describe the behavior sufficiently.

A. SCOPE OF INVESTIGATION

In the analysis of multi-story frame structures subjected to seismic loading it has been common practice to disregard the vertical component of the ground motion. Cheng and Tseng have recently studied the dynamic instability and response of structural systems subject to pulsating axial loads, time dependent lateral forces, or foundation movements.²² They have reported the significant effect of time-dependent longitudinal excitations on the lateral displacements of various elastic and inelastic structures. However, the effect of interaction

between horizontal and vertical earthquake components on a structural response is yet to be explored. The purpose of this study is to determine the behavior of various structural models subjected to a combined loading of the horizontal and vertical earthquake components.

Besides considering the two components of an earthquake, the following additional considerations are made to further exemplify the actual structural conditions. Inelastic material behavior due to bending is considered by employing a bilinear or elasto-plastic model. The P-delta effect is included for the overturning effect produced by the vertical loads. The AISC specifications are used for the reduction in the plastic moment M_p due to axial loads in column members. Also included is viscous damping to account for the friction between structural surfaces and other parts of the structure during motion.

The response parameters employed in this study are:

- (1) maximum horizontal floor displacements,
- (2) maximum relative floor displacements,
- (3) maximum vertical displacement and acceleration at the center of girder members,
- (4) ductility requirements of all members as determined by the ductility and excursion ratios, and
- (5) quantity of energy input, stored and dissipated by the frame during the seismic loading.

The above response parameters were determined for the different loading and material conditions where comparisons are warranted.

A computer program has been developed for this research and the results presented herein are obtained by using the IBM 370/168 Computer through the Computer Network of the University of Missouri. Different

from the previous study of consistant mass formulation,^{22,23} this work considers a step-by-step analysis of a lumped mass system. The acceleration, velocity and displacement at the beginning of a time increment are used to obtain the corresponding results at the end of the time increment. Continuation of this process over the total earthquake record results in a complete response history of the structure.

A brief discussion as to contents of each chapter of this report is given as follows. Each chapter provides theoretical studies and numerical results to fulfill the purpose of this study.

Chapter II describes the seismic load and the associated velocities and displacements. A spectrum analysis of the earthquake records is included.

The fundamental behavior of a single-degree-of-freedom system is given in Chapter III to establish basic concepts and to verify the validity of the computer program based on different loading and response conditions. The effect of vertical forces are included for the single-degree-of-freedom system.

Complete formulation of a multi-degree system is derived in Chapter IV. The general motion equation is formulated for a nonlinear response for which the interaction between moment and axial load is considered for reducing the plastic moment of columns. The energy absorption and the ductility requirements are also included in this chapter.

Chapter V presents the methods of numerical integration of incremental motion equations.

Results of the elastic analysis of multi-story structures are given in Chapter VI. The elastic response of a 3-story frame is shown for revealing the effect of P-delta along with vertical earthquake component. Structures sensitive to vertical excitations and the possible vertical frequencies controlling horizontal responses are also discussed.

Chapter VII reports the response results of inelastic multi-story structures. The effects of the inelastic action, structural models, the M_p reduction and damping on the response parameters of individual systems are studied.

Chapter VII reviews the work done and lists the conclusions based on the results obtained in this work.

B. REVIEW OF LITERATURE

Efforts in the dynamic analysis of inelastic framed structures due to seismic loading have increased since the advent of the high speed digital computer. Berg,⁸ Saul,³⁹ Thomaides,⁴¹ Clough, Bensuka and Wilson,²⁴ Saul, Fleming and Lee,³⁸ Giberson,²⁹ Goel,³⁰ Guru and Heidebrecht³¹ and Walpole and Shepherd⁴⁵ are among early research workers who have made contributions in the analysis of inelastic structural systems. Later Anderson and Bertero,^{2,3} Anderson and Gupta,⁴ Cheng and Tseng²² and Cheng and Oster²¹ are among those providing refined efforts in the analysis of inelastic structures.

The inclusion of the P-delta effect in the dynamic structural analysis has been considered by Anderson and Bertero³ and others. Sun, Berg and Hanson⁴⁰ studied the effect of gravity loads on an inelastic system consisting of a single story braced frame with

hinged joints. Cheng and Botkin^{15,16} investigated the P-delta effect on the response behavior of tall buildings.

Inclusion of vertical loads on the girder nodes of multi-story frames was early studied by Guru and Heidebrecht³¹ for determining the influence of live load on the structural response. Similarly, Anderson and Bertero² included both the gravity loads and the ground motion in their investigation. Cheng and Oster further reported on the structural response due to vertical earthquake motions acting on the masses lumped at the centers of the constituent girders.¹⁷ The parametric instability of structural systems subject to axial concentrated uniform dynamic loads or time dependent vertical ground motions was investigated by Cheng and others.^{14,5,12} The effect of parametric earthquake motions on the ultimate capacity of framed structures was also studied by Cheng and Oster.^{19,20}

In the analysis of inelastic structures the ductility ratio has been usually obtained by employing the total plastic joint rotation divided by the yielding rotation. Clough, Bensuka and Wilson,²⁴ Giberson,^{28,29} Goel,³⁰ Walpole and Shepherd⁴⁵ and Guru and Heidebrecht³¹ used this definition in their analyses. Anderson and Bertero^{2,3} proposed to determine the ductility requirement of a structure based on curvature instead of end rotation. Cheng and Oster²¹ proposed a new definition for the ductility ratio and the results are compared with those obtained by using the previous definitions.

II. SEISMIC LOADING

The type of earthquake loading used to actuate a multi-story structure as analyzed in this study consists of the dynamic type of ground motions. Though other types of ground motion may occur during an earthquake such as a ground settlement, fault displacements in the vicinity of the structure and landslides, the inertia forces produced as a result of ground accelerations are of concern here.

A. EARTHQUAKE RECORDS

One of the horizontal components and the vertical component for two earthquakes are considered in this study. They are:

1. 1940 El Centro, California (May 18) North-South and Vertical components; and
2. 1952 Taft, California (July 21) N 69°W and Vertical components.

Figures 2.1 through 2.4 show the variation in the ground acceleration of each of the above components of earthquake records. These variations were obtained by plotting the digitized earthquake data with $\Delta t = 0.01$ sec. for each earthquake record as obtained from its accelerogram. The accuracy of the response behavior of a mathematical structural model when using this type of data will be mainly based on the accuracy of the accelerometer used to obtain the data and that of the digitized data in representing an accelerogram.

B. GROUND VELOCITY AND DISPLACEMENT

The ground velocities and displacements associated with the above ground accelerations are obtained by the integration of the ground acceleration with the initial ground velocity and displacement set to zero. The linear acceleration method is used here as formulated in

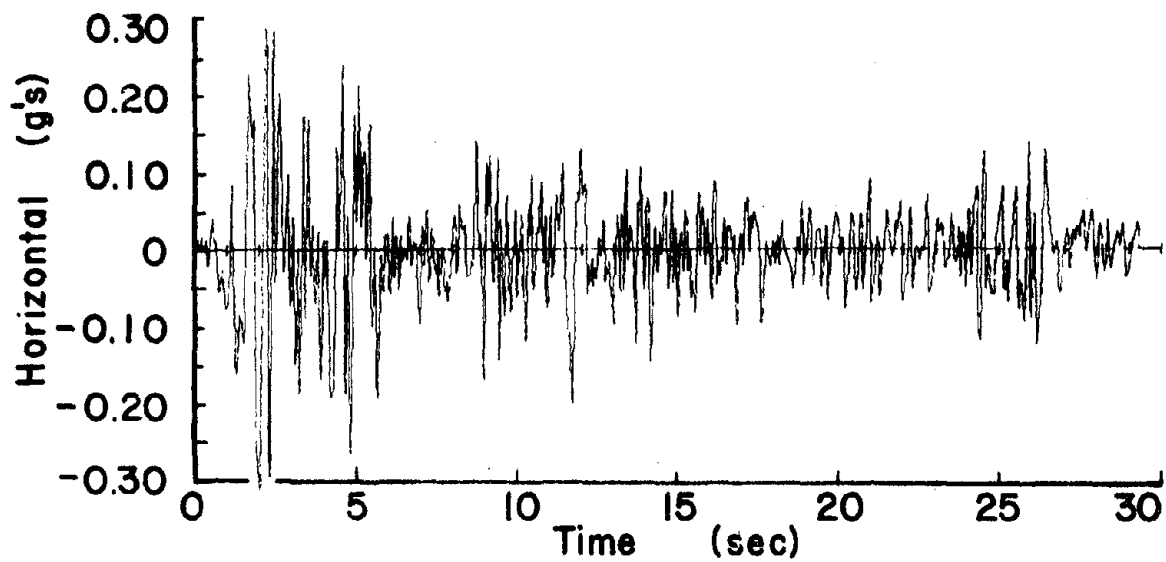


Figure 2.1. 1940 El Centro Earthquake, N-S Component

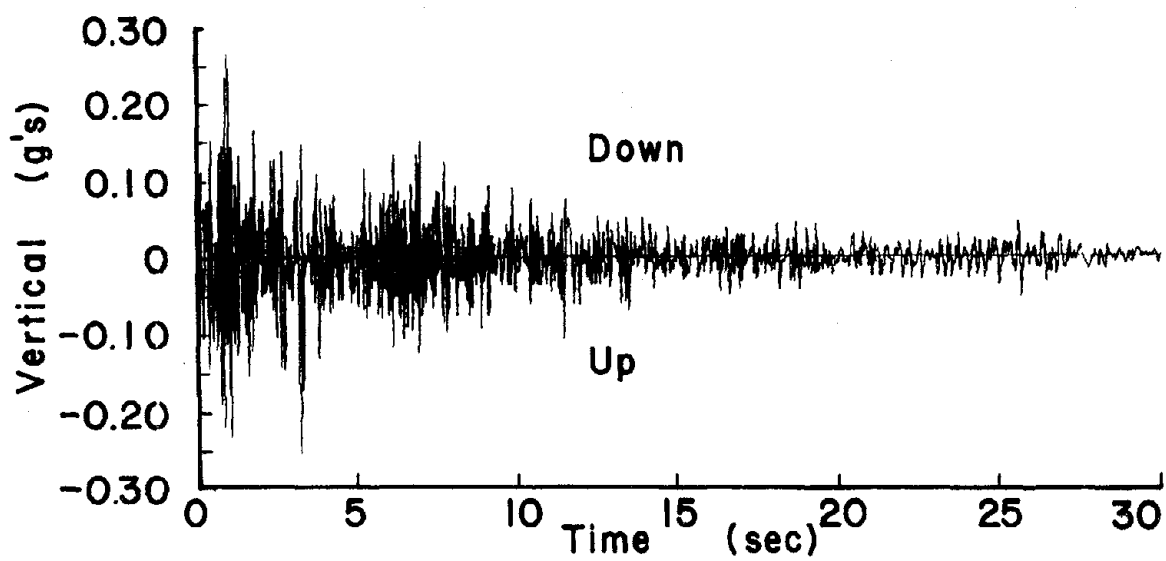


Figure 2.2. 1940 El Centro Earthquake, Vertical Component

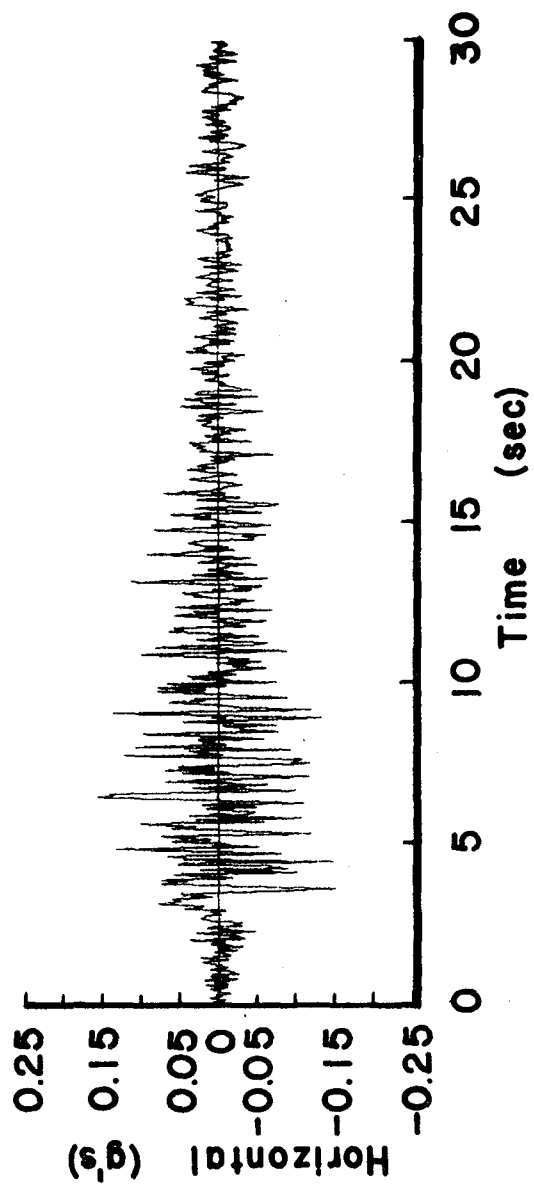


Figure 2.3. 1952 Taft Earthquake, N69°W Component

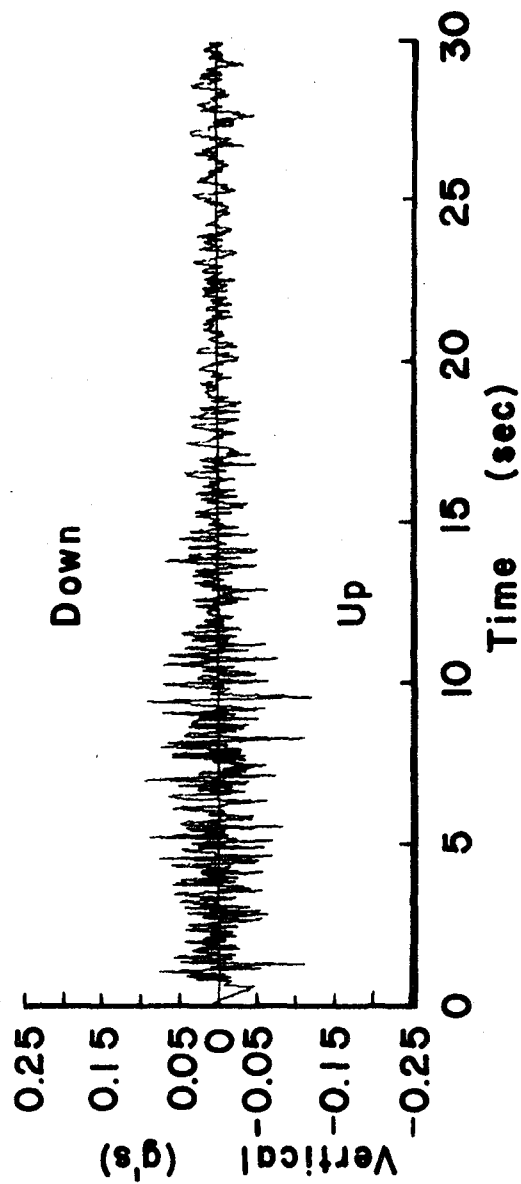


Figure 2.4. 1952 Taft Earthquake, Vertical Component

Section V-A for $\beta = 1/6$ in Newmark's method of integration. The following equations for the velocity and displacement of the ground in the horizontal direction are obtained from this method. Similar relationships can be written for the vertical ground motion.

$$\dot{x}_g(t+\Delta t) = \dot{x}_g(t) + \frac{(\Delta t)}{2} [\ddot{x}_g(t) + \ddot{x}_g(t+\Delta t)] \quad (2.1)$$

$$x_g(t+\Delta t) = x_g(t) + (\Delta t)\dot{x}_g(t) + \frac{(\Delta t)^2}{6} [2\ddot{x}_g(t) + \ddot{x}_g(t+\Delta t)] \quad (2.2)$$

where $\ddot{x}_g(t+\Delta t)$, $\dot{x}_g(t+\Delta t)$, $x_g(t+\Delta t)$ = acceleration, velocity and displacement of ground at time $t + \Delta t$,

$\ddot{x}_g(t)$, $\dot{x}_g(t)$, $x_g(t)$ = acceleration, velocity and displacement of ground at time t , and

Δt = time increment.

Figures 2.5 through 2.8 show the variation in ground velocity and displacement based on Eqs. 2.1 and 2.2 for the N-S and vertical components of the 1940 El Centro earthquake. Similarly, Figs. 2.9 and 2.10 show the variation in ground velocity and displacement for the N 69°W component of the 1952 Taft earthquake. The ground velocity in the vertical direction for the same earthquake is shown in Fig. 2.11. An overall shift in the base line is shown by the approximate improved base line as indicated. The vertical ground displacements corresponding to these velocities substantiate this shift by the corrections shown in Fig. 2.12.

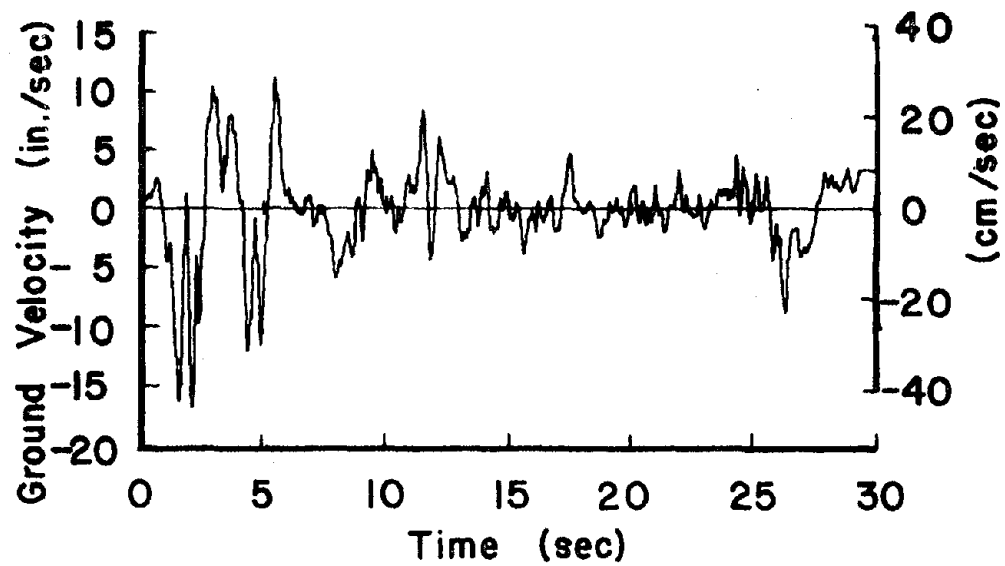


Figure 2.5. Ground Velocity, 1940 El Centro, N-S Component

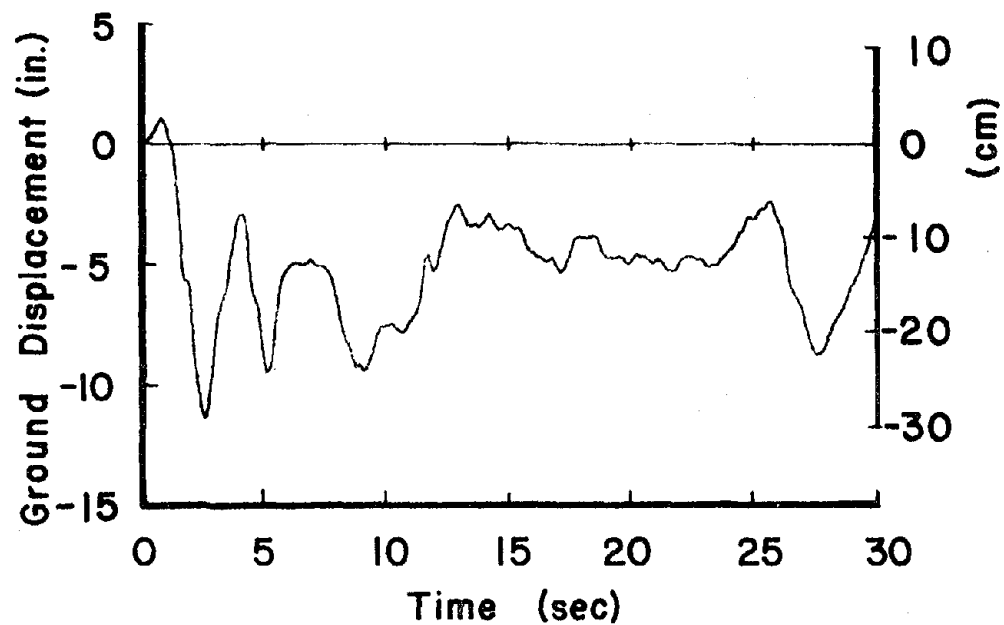


Figure 2.6. Ground Displacement, 1940 El Centro, N-S Component

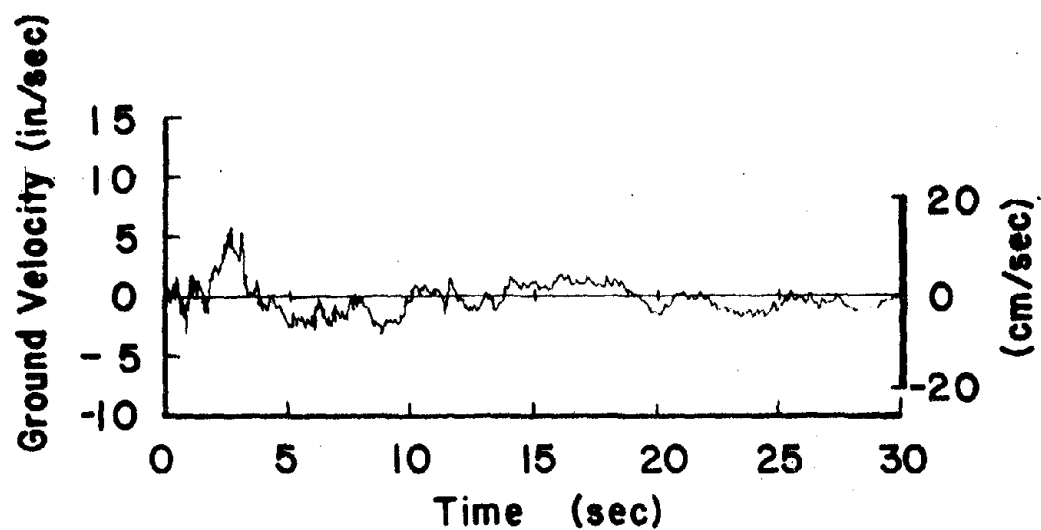


Figure 2.7. Ground Velocity, 1940 El Centro, Vertical Component

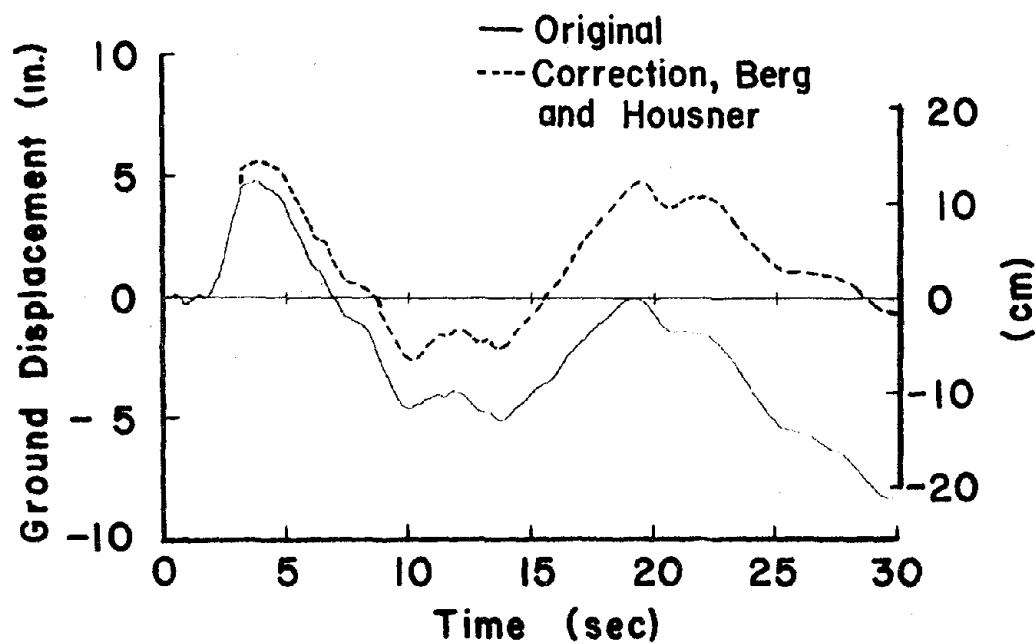


Figure 2.8. Ground Displacement, 1940 El Centro, Vertical Component

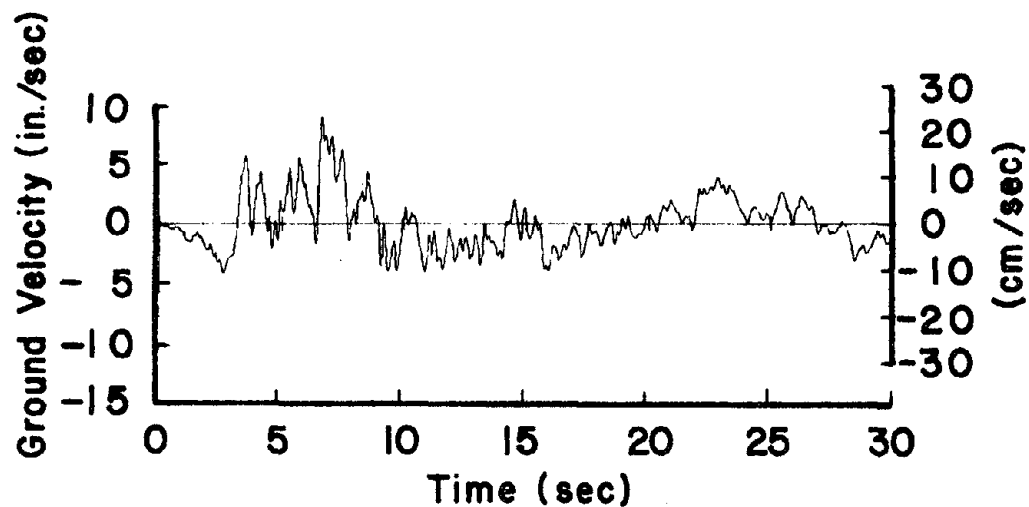


Figure 2.9. Ground Velocity, 1952 Taft, N69°W Component

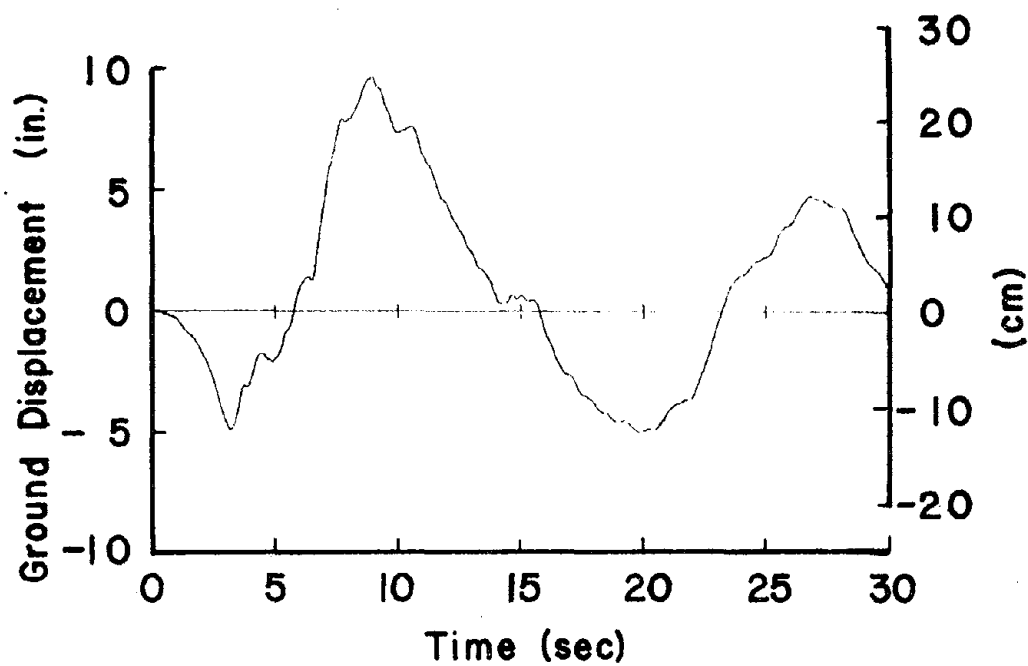


Figure 2.10. Ground Displacement, 1952 Taft, N69°W Component

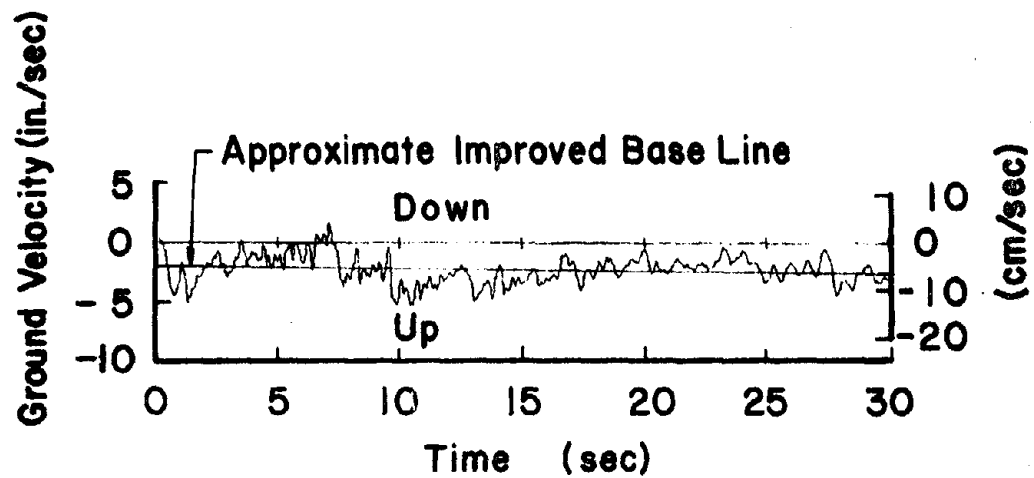


Figure 2.11. Ground Velocity, 1952 Taft, Vertical Component

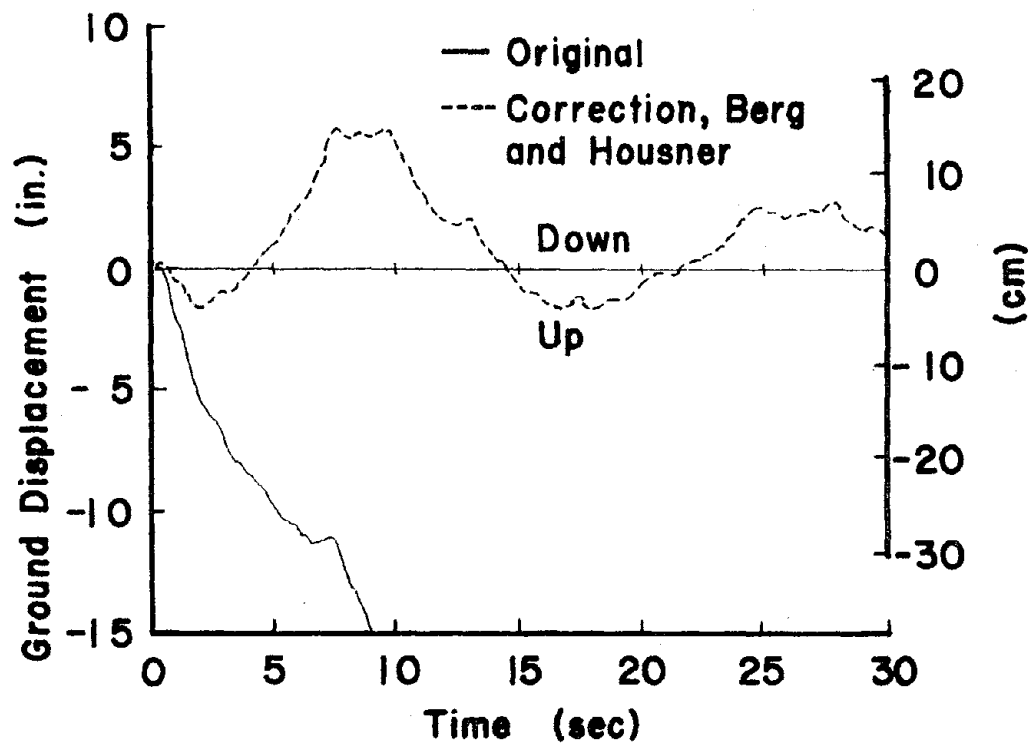


Figure 2.12. Ground Displacement, 1952 Taft, Vertical Component

Berg and Housner⁹ made a correction to the shift of the base line by adjusting the acceleration readings to meet certain restrictions. They assumed that in the true time acceleration coordinates, the equation of the temporary base line would take the form $c_0 + c_1 t + c_2 t^2$. The constraints c_0 , c_1 and c_2 would have the values that would make the mean square computed ground velocity a minimum. The results of the corrected velocity by Berg and Housner are indicated by dotted lines in each of the ground displacement curves for the two earthquakes. Dotted lines are not shown where there is an insignificant amount of difference in ground displacement, as for the N-S component of the 1940 El Centro earthquake. Correction was found less necessary for the El Centro earthquake.

Other methods have been used to correct the baseline shift of an accelerogram. In an earlier study Berg⁸ selected the improved axis of the accelerogram to be parallel to the horizontal base line appearing on the record and then located the position such that if a zero initial velocity were assumed, the computed velocity at the end of the punched card accelerogram would also be zero. Berg and Thomaides¹⁰ further learned to minimize the mean square displacement to justify the initial ground velocity, initial ground displacement and the adjusted location of the zero axis of the accelerogram.

Based on the greater similarities in the response patterns for the 1940 El Centro earthquake record as shown in Figs. 2.5-2.12, the original earthquake components for the El Centro earthquake were used in this study more extensively. The same horizontal displacement curve is realized for both the original and corrected data for the N-S component as shown in Fig. 2.6. Also, the zero velocity in the

vertical direction at the end of the original earthquake record as shown in Fig. 2.7 satisfies the end condition of zero velocity for this component. Berg⁸ found that while slight differences in ground accelerations resulted in a substantial difference in computed ground motion, their effect on structural response was negligible.

The velocities and displacements of the ground as determined from Eqs. 2.1 and 2.2 are used in calculating the quantities of energy. Energy in the form of input, stored and dissipated is absorbed during the earthquake excitation by the lumped mass system. Horizontal and vertical ground displacements are used to calculate the input energy produced by the horizontal and vertical reactions at the supports. Stored energy in the form of kinetic energy and dissipated energy due to damping are each a function of the absolute velocity of the lumped mass system.

C. FREQUENCY SPECTRUM

To describe further the seismic loading, an amplitude frequency spectrum of an earthquake record can be obtained by a Fourier transform. A correlation of these frequencies, making up the earthquake loading that have the larger amplitudes, can be made with the natural frequencies of a structural system.

The earthquake records used in this study are classified as digitized nonperiodic signals since they consist of a sequence of numbers in a random order of magnitude. A frequency analysis of this signal consists of breaking up the signal into a set of sinusoids such that, when these sinusoids are added, the original signal results. To accomplish this signal breakdown for the earthquake records for this study, the fast Fourier transform (FFT) is used.^{25,27,43}

The FFT is an iterative method which efficiently computes the discrete Fourier transform (DFT) of an earthquake record or any time series of data samples. The time series provided by these equally spaced data points (Nyquist samples) completely represent the continuous waveform (earthquake accelerations) as long as this waveform is frequency band-limited and the samples are taken at a rate that is at least twice the highest frequency present in the waveform.

The DFT is defined here in complex form as:

$$A_r = \sum_{k=0}^{N-1} \frac{X_k}{N} \exp(-2\pi i r k / N), \quad r = 0, \dots, N-1 \quad (2.3)$$

where A_r = rth coefficient of the DFT,

X_k = kth sample of the time series,

N = number of samples in time series, and

$i = \sqrt{-1}$.

The FFT sequentially combines progressively larger weighted sums of data so as to produce the DFT coefficients, A_r , as defined in Eq. 2.3. In other words the FFT combines the DFT of the individual data samples such that the occurrence times of these samples are taken into account sequentially and applied to the DFT's of the progressively larger mutually exclusive subgroups of data samples, which are combined to ultimately produce the DFT of the complete series of data samples. The inverse of the discrete Fourier transform (IDFT) is

$$x_k = \sum_{r=0}^{N-1} A_r \exp(2\pi i r k / N), \quad k = 0, \dots, N-1 \quad (2.4)$$

The amplitude frequency spectrums for the 1940 El Centro earthquake components are determined using the above procedure as programmed in Subroutine NLOGN by Robinson³⁷. Figures 2.13 and 2.14 show the resulting frequency spectrums for the N-S and vertical earthquake components, respectively, for frequencies having the larger amplitudes ranging from 0-17 Hz. The total frequency spectrum ranges from 0-50 Hz with a fundamental frequency of $2.44(10)^{-2}$ Hz. The highest frequency of 50 Hz is the folding frequency based on the Δt ($\Delta t = 0.01$ sec.). The folding frequency and fundamental frequency are obtained from the following equations:

$$\text{Folding frequency} = \frac{1}{2(\Delta t)} = \frac{1}{0.02} = 50 \text{ Hz}$$

$$\text{Fundamental frequency} = \frac{1}{N(\Delta t)} = \frac{1}{40.96} = 2.44(10)^{-2} \text{ Hz}$$

where $\Delta t = 0.01$ sec = time increment of the digitized data,

$N = 2^n = 2^{12} = 4096$ = number of data points, and

n = some positive number.

The minimum number for n is 12 based on the 30 seconds of earthquake with $\Delta t = 0.01$ sec. (3000 data points). Zeros are added to the 3000 data points to obtain the 4096 data points required for $n = 12$. Frequencies between 17 and 50 Hz are not included in Figs. 2.13 and 2.14 due to their insignificant magnitude.

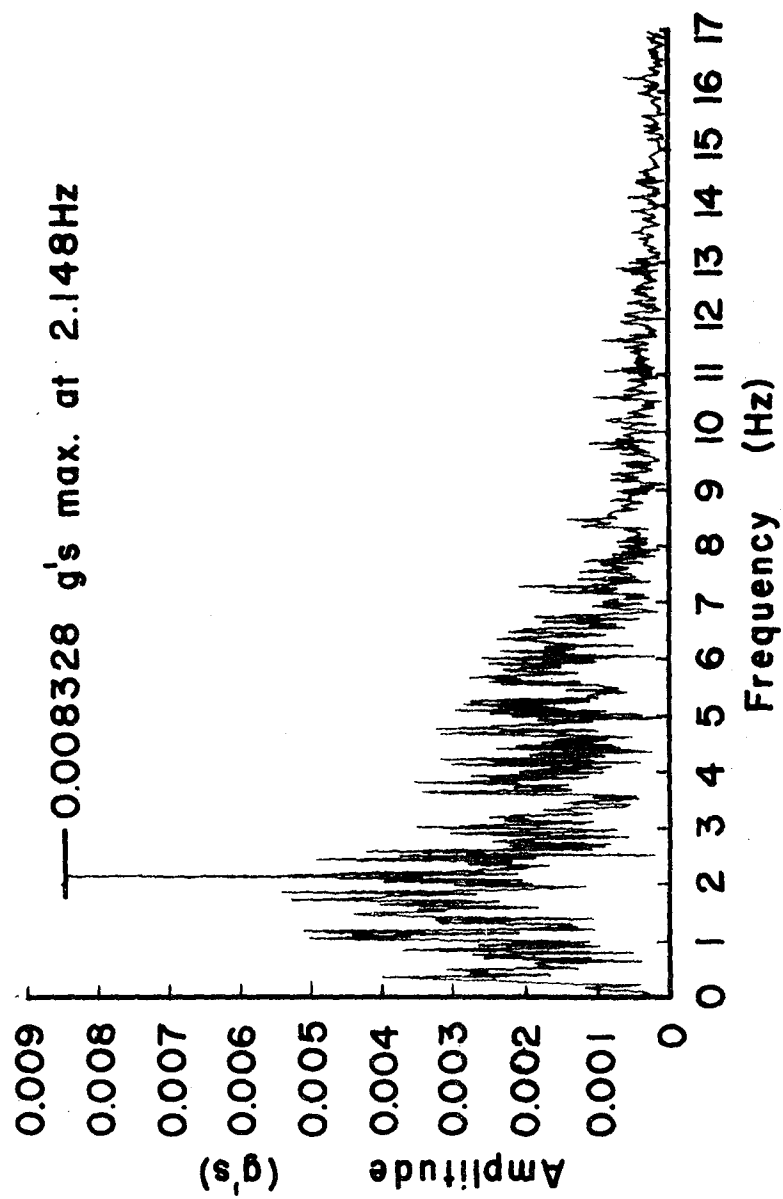


Figure 2.13. Frequency Spectrum, 1940 E1 Centro, N-S Component

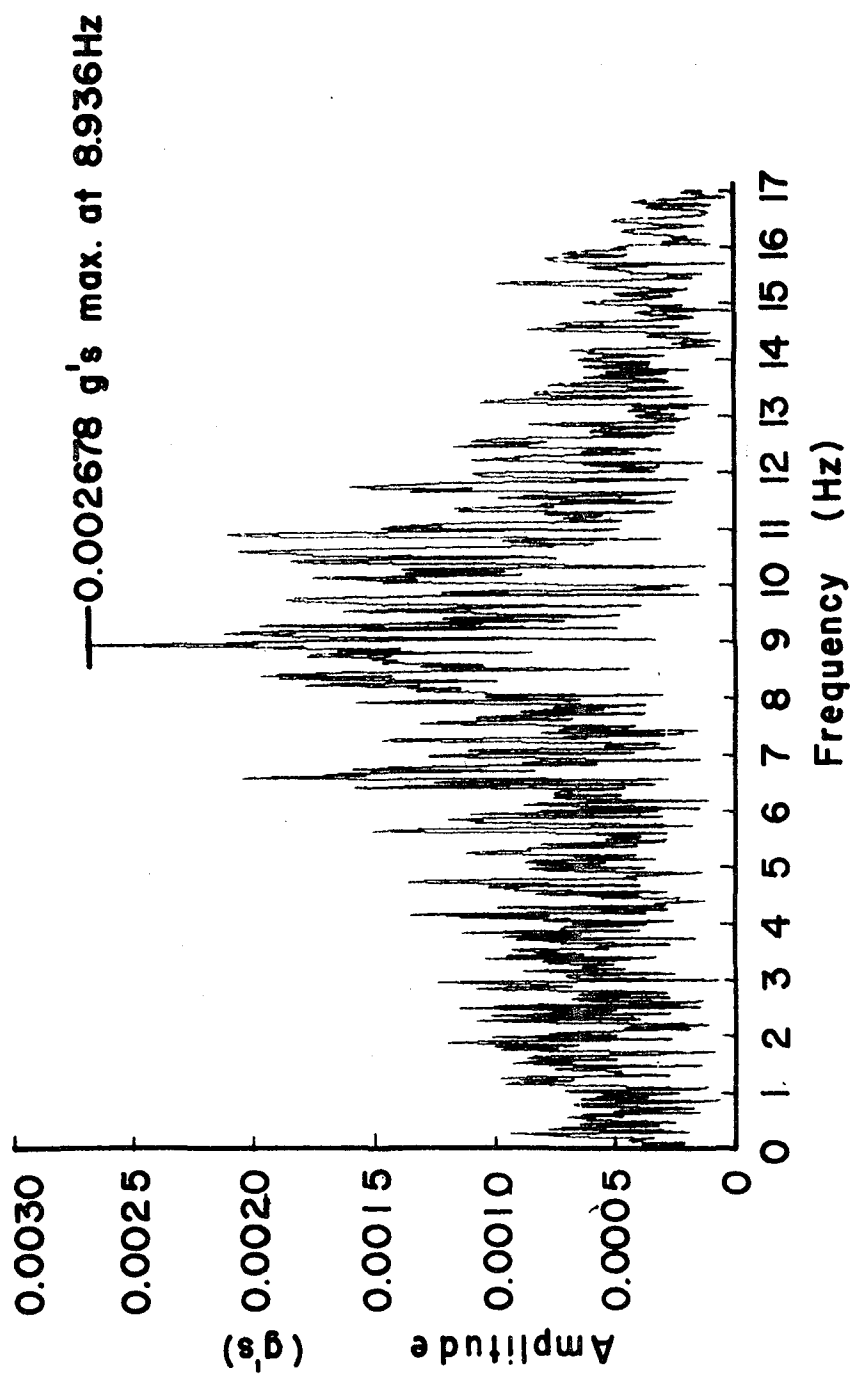


Figure 2.14. Frequency Spectrum, 1940 El Centro, Vertical Component

D. ORIGINAL RECORD BY FOURIER SUMMATION

The continuous form of the original earthquake record can be obtained from the DFT as determined from Eq. 2.3. The expansion of the DFT into a Fourier series provides a way of utilizing all or portions of the frequency spectrum. To obtain the total original record in a continuous form the Fourier series will be as follows.

$$\ddot{x}(t) = 2 \sum_{r=0}^{N_f-1} \{a_r \cos(r\omega_f t) + b_r \sin(r\omega_f t)\} \quad (2.5)$$

where $N_f = N/2$ = number of data points divided by 2,

a_r = real part of A_r ,

b_r = imaginary part of A_r ,

ω_f = fundamental frequency of data,

t = time at which function is evaluated, and

r = DFT coefficient subscript.

The factor 2 is used in conjunction with the N_f since the DFT values represent the folding values of the DFT. Another form of Eq. 2.5 is more adaptable to a digital computer by containing only one trigonometric function. This can be used to sum just portions of the DFT.

$$\ddot{x}(t) = 2 \sum_{i=0}^{N_t} |A_i| \cos(\omega_i t + \alpha_i) \quad (2.6)$$

where N_t = number of DFT values to be added,

$$|A_i| = (a_r^2 + b_r^2)^{1/2} = \text{absolute value of } i\text{th coefficient of DFT,}$$

$$\omega_i = r\omega_f = \text{frequency of } i\text{th coefficient of DFT, and}$$

$$\alpha_i = \arctan(b_r/a_r) = \text{phase angle.}$$

An example in the use of Eq. 2.6 is illustrated with the use of a triangular impulse load shown in Fig. 2.15. This load decreases from 1000 units linearly to zero in 10 units of time (sec). The frequency spectrum for this impulse was obtained based on 4096 data points at 0.01 sec time increment corresponding to the number of data points and Δt used for the 30 second earthquake data frequency spectrum. The resulting frequency spectrum is shown in Fig. 2.16 with frequencies greater than 6 Hz having insignificant amplitudes.

A reproduction of the original impulse load is obtained by using the inverse feature of subroutine NLOGN as given by Eq. 2.4. The resulting inverse is shown in Fig. 2.15, the identical impulse load. Also shown is the results of the Fourier series summation based on Eq. 2.6 and using the first 206 frequencies (0-5 Hz) from the frequency spectrum out of the total of 2048 frequencies.

While Fig. 2.16 illustrates the use of the Fourier summation of Eq. 2.6 for a given triangular impulse load, a similar approach can be used on a random loading such as an earthquake record. A Fourier summation of the frequencies for the N-S component of the 1940 El Centro earthquake as shown in Fig. 2.13 results in the record shown in Fig. 2.17. The solid line is based on the 364 frequencies from the frequency spectrum having amplitudes greater than 0.0005g. The small circles shown are corresponding to the maximum g's obtained from the

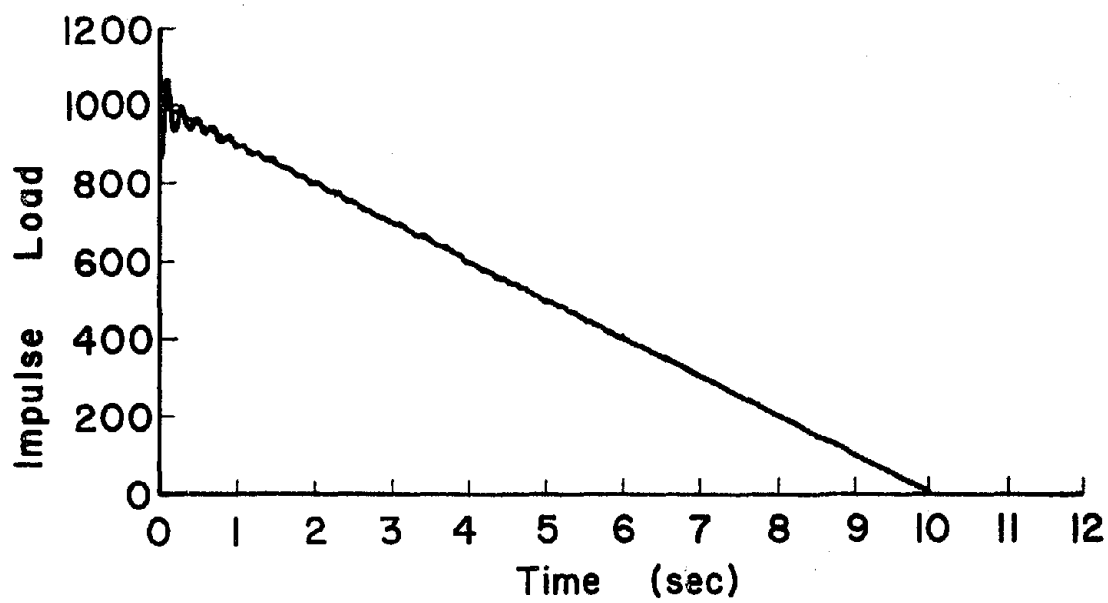


Figure 2.15. Fourier Summation, Impulse Load, 206 Frequencies (0-5Hz)

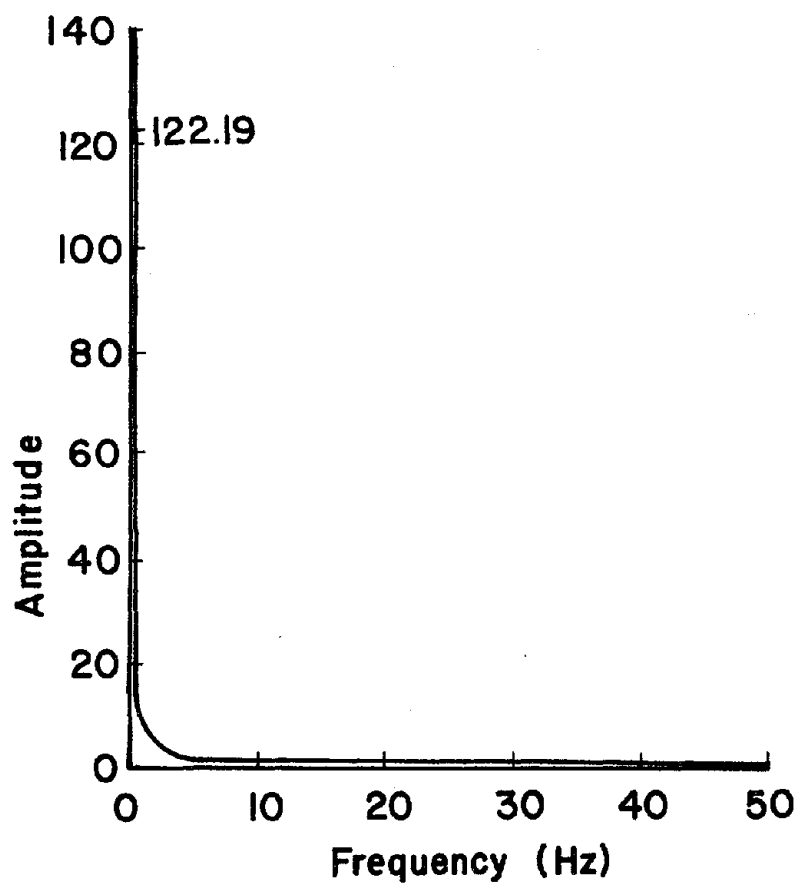


Figure 2.16. Frequency Spectrum of Impulse Load

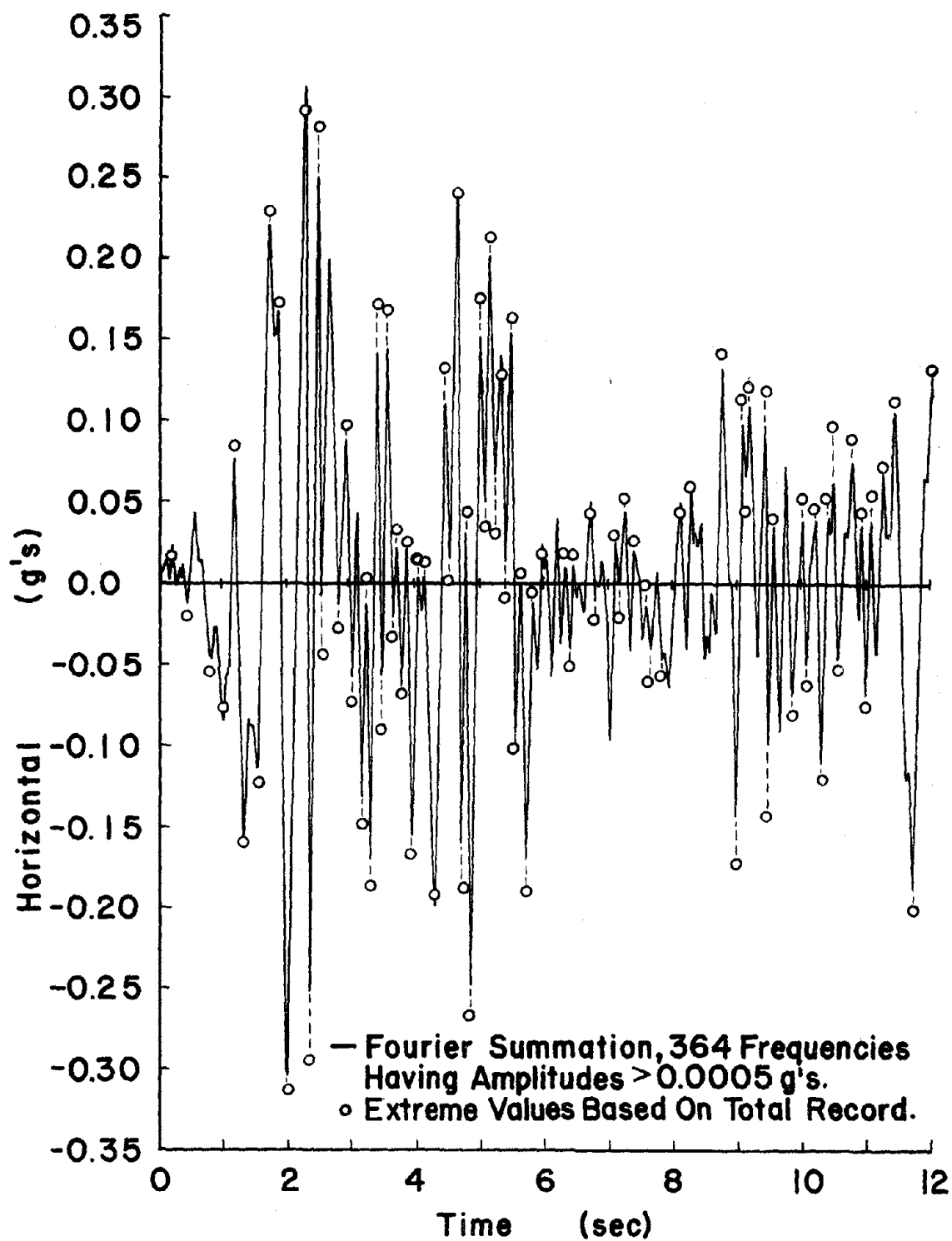


Figure 2.17. Fourier Summation, 1940 El Centro Earthquake (N-S)

total record. Except for a few of these points, most of the maximum g-load values based on the total record are greater than the corresponding maximum values based on the 364 frequencies having the largest amplitudes.

III. DYNAMIC ANALYSIS OF A SINGLE-DEGREE-OF-FREEDOM SYSTEM

A. MOTION EQUATION

The motion equation for a single-degree-of-freedom system, later to be generalized for multiple-degree-of-freedom systems using matrix methods (Chapter IV), can best be realized from a free body diagram (f.b.d.) shown in Fig. 3.1. Figure 3.1b shows the f.b.d. for a single degree system (horizontal) that is being actuated by the horizontal motion of the ground as shown in Fig. 3.1a. Due to the movement of the ground an inertia force equal to the product of the mass m and the absolute acceleration of the mass, \ddot{u}_s , will act in the opposite direction of motion. Also, a spring force will be equal to the product of the column stiffness K and the relative displacement x_s of the mass to the ground. Positive direction of acceleration, velocity and displacement is taken to the right. Using D'Alembert's principle, the motion equation for the above single-degree-of-freedom system without damping is

$$m\ddot{u}_s + Kx_s = 0 \quad (3.1)$$

where $\ddot{u}_s = \ddot{x}_g + \ddot{x}_s$,

\ddot{x}_g = acceleration of ground, and

\ddot{x}_s = acceleration of mass relative to ground.

Equation 3.1 can then be written

$$m\ddot{x}_s + Kx_s = -m\ddot{x}_g \quad (3.2)$$

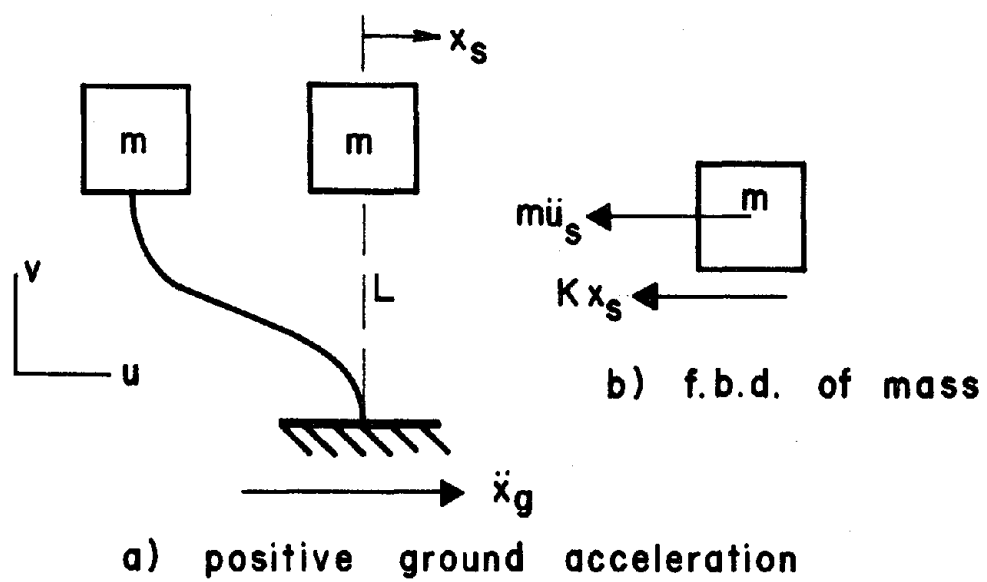


Figure 3.1. Horizontal Ground Motion Acting on a Single-Degree-of-Freedom System

The term to the right of the equal sign represents the forcing function acting on the system.

In addition to the horizontal motion of the ground, this study considers a secondary effect due to the weight of the mass plus the vertical motion of the ground during an earthquake. This secondary effect is known as the P-delta effect. Assuming down as the positive vertical direction as shown in Fig. 3.2a, the f.b.d. of a single mass system can be illustrated by Fig. 3.2b where $K_s = (W - m\ddot{y}_g)/L$, defined as the geometric stiffness determined from the f.b.d. of the supporting column (Fig. 3.2c). The couple produced by vertical forces are in equilibrium with the horizontal shears causing an additional force on the mass in the horizontal direction. The vertical acceleration \ddot{y}_s of the mass m is equal to the vertical ground acceleration \ddot{y}_g since axial deformations are not considered in the column members. Based on the f.b.d. of Fig. 3.2b including the P-delta effect, the motion equation of Eq. 3.2 for time t is written as follows.

$$m\ddot{x}_s + (K - K_s)x_s = -m\ddot{x}_g \quad (3.3)$$

where $K_s = (W - m\ddot{y}_g)/L$ = geometric stiffness,

L = column length,

\ddot{y}_g = vertical ground acceleration,

$W = mg$, and

g = acceleration of gravity.

The incremental form of Eq. 3.3 is obtained by subtracting the motion equation for time t from the motion equation for time $t + \Delta t$

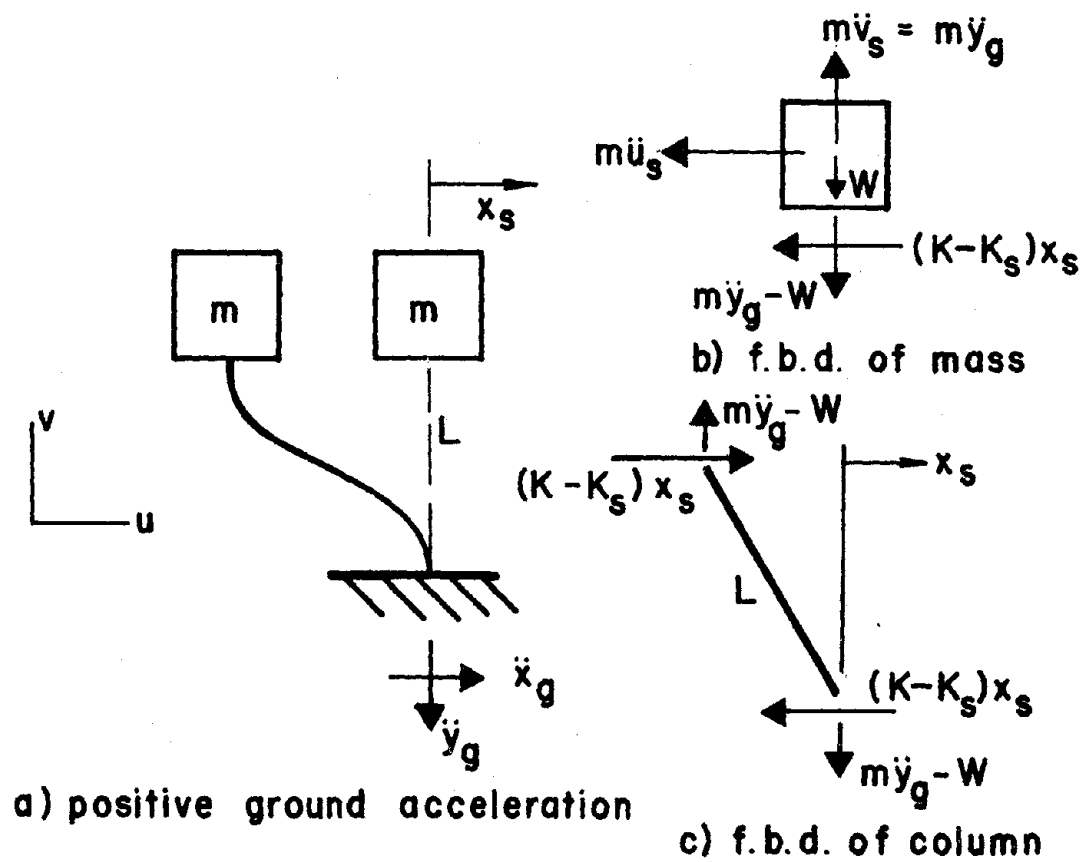


Figure 3.2. Horizontal Plus Vertical Ground Motion Acting on a Single-Degree-of-Freedom System

$$m\Delta\ddot{x}_s + [K - K_s(t+\Delta t)]x_s(t+\Delta t) - [K - K_s(t)]x_s(t) = -m\Delta\ddot{x}_g \quad (3.4)$$

which can be reduced to

$$m\Delta\ddot{x}_s + [K - K_s(t+\Delta t)]\Delta x_s = -m\Delta\ddot{x}_g + \Delta K_s x_s(t) \quad (3.5)$$

where $\Delta\ddot{x}_s = \ddot{x}_s(t+\Delta t) - \ddot{x}_s(t)$,

$\Delta x_s = x_s(t+\Delta t) - x_s(t)$,

$\Delta\ddot{x}_g = \ddot{x}_g(t+\Delta t) - \ddot{x}_g(t)$, and

$\Delta K_s = K_s(t+\Delta t) - K_s(t)$.

Equation 3.5 is the motion equation in incremental form for a single-degree-of-freedom system when considering horizontal and vertical components of an earthquake and including the P-delta effect. Damping is not considered here but is included in the formulation for the multi-degree-of-freedom system in Chapter IV.

Based on the initial values of acceleration, velocity and displacement, a step-by-step numerical integration technique to be discussed in Chapter V is used to solve for the acceleration, velocity and displacement at the end of each time increment during an earthquake. Either elastic, elasto-plastic or bilinear conditions can be assumed for the overall response with the load-deflection relationship taken as constant over each time increment (Δt).

B. COMPARISON OF P-DELTA EFFECT WITH KNOWN SOLUTION

To show the correctness of the formulation for the incremental form of the motion equation when including the P-delta effect, a forced undamped single-degree-of-freedom system of known solution will be used

for comparison. The differential equation of motion for an undamped system subjected to a sinusoidal load is easily formulated from the f.b.d. of Fig. 3.3b:

$$m\ddot{x}_s + Kx_s = F \sin(\omega t + \alpha) \quad (3.6)$$

where F = amplitude of load,

K = stiffness,

m = mass,

\ddot{x}_s = acceleration of mass relative to ground,

x_s = displacement of mass relative to ground,

t = time,

α = phase angle,

ω = forcing frequency.

The solution of this differential equation is well known and is derived in several texts on structural dynamics.^{11,13} Let the initial values of displacement, velocity and acceleration be zero, then the displacement can be expressed as

$$x_s = \frac{F}{p_n(K - m\omega^2)} [p_n \sin(\omega t + \alpha) - \omega \sin(p_n t)] \quad (3.7)$$

where p_n = natural frequency of the system.

When considering the P-delta effect as shown in Fig. 3.2, the above equation for displacement needs to be modified in the following manner.

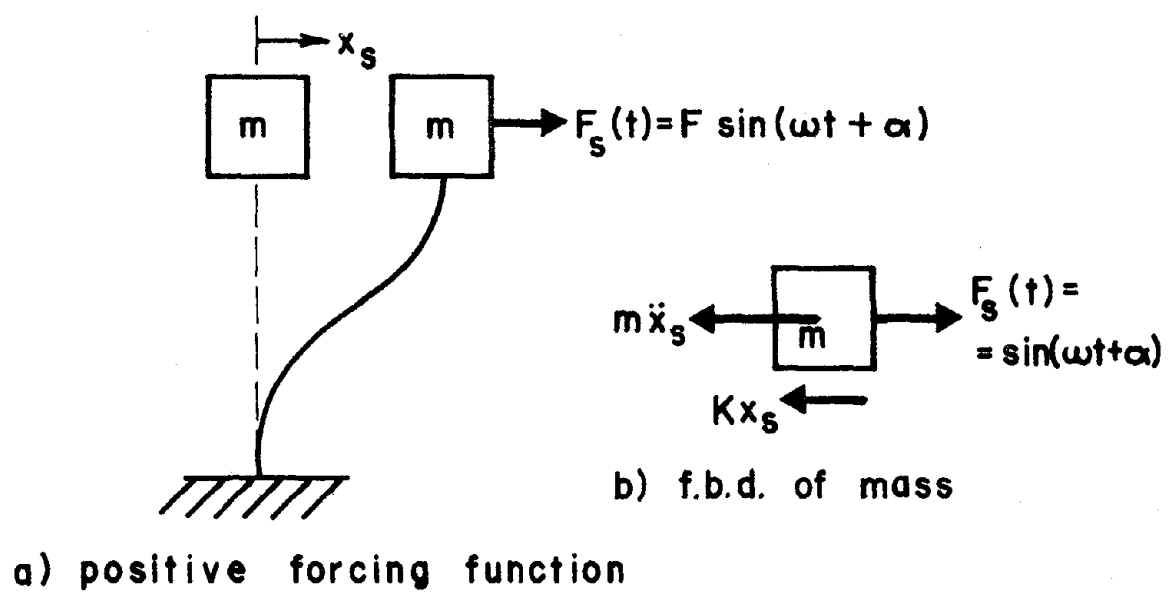


Figure 3.3. Horizontal Forcing Function Acting on a Single-Degree-of-Freedom System

$$x_s = \frac{F}{p_s(K - K_s - m\omega^2)} [p_s \sin(\omega t + \alpha) - \omega \sin(p_s t)] \quad (3.8)$$

where $K_s = (W + F_v)/L =$ geometric stiffness due to constant vertical load,

$W =$ weight of mass m ,

$F_v =$ vertical force,

$L =$ length of supporting column and

$p_s = \sqrt{(K - K_s)/m} =$ natural frequency of system including vertical load.

The system to be used for the comparison is shown in Fig. 3.4. The natural frequency p_n of the structure is 1.0 Hz based on a mass m of 0.31056 kip-sec²/ft (4.62 kg/s²/cm) and a total stiffness K of 12.326 kip/ft (180 N/mm). The vertical load of 100 kip (445 kN) varies stepwise as shown in Fig. 3.5. The total stiffness $(K - K_s)$ of the structure varies from 4.993-18.326 kip/ft (73-267 N/mm) causing the natural frequency p_s to vary from 0.64-1.22 Hz when the vertical force F_v goes from +100 kip (445 kN) to -100 kip (-445 kN). Both the horizontal and vertical loads cease at $t = 3.18$ sec. when considering vertical forces.

The displacement responses of the structure are shown in Fig. 3.5. A plot of the displacement without considering the vertical forcing function is included to show the effect the vertical force has on the response. The horizontal forcing function when considering only horizontal loading is terminated at 3.3 seconds. The curves shown are based on calculations every 0.01 sec. as obtained from a computer solution.

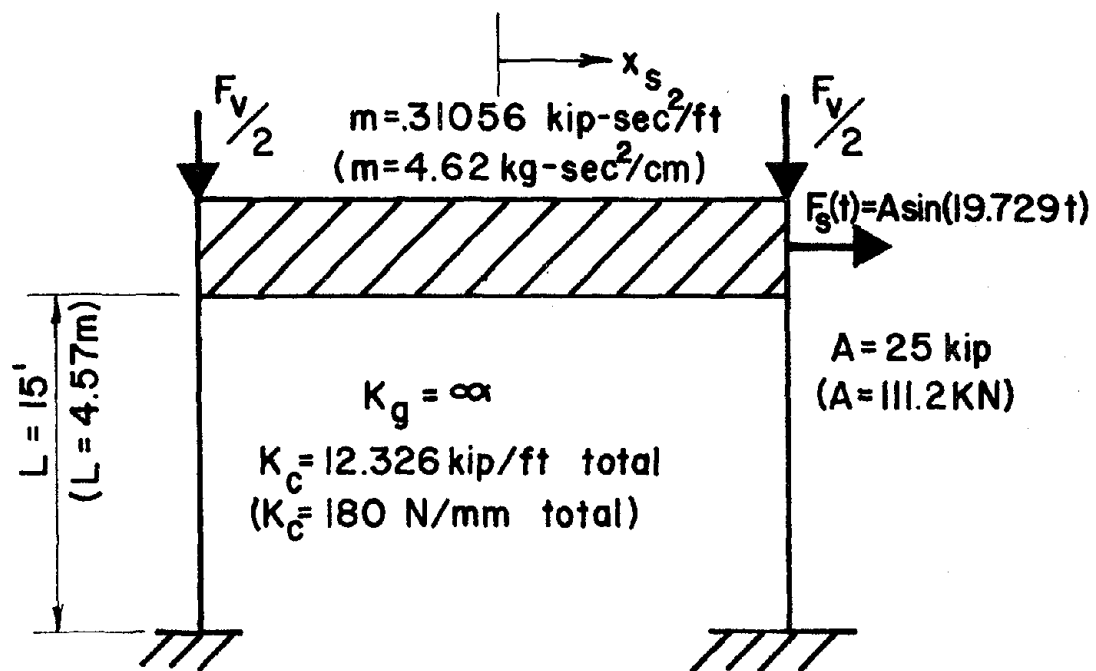


Figure 3.4. Simple Bent with Variable Horizontal Load and Constant Vertical Load

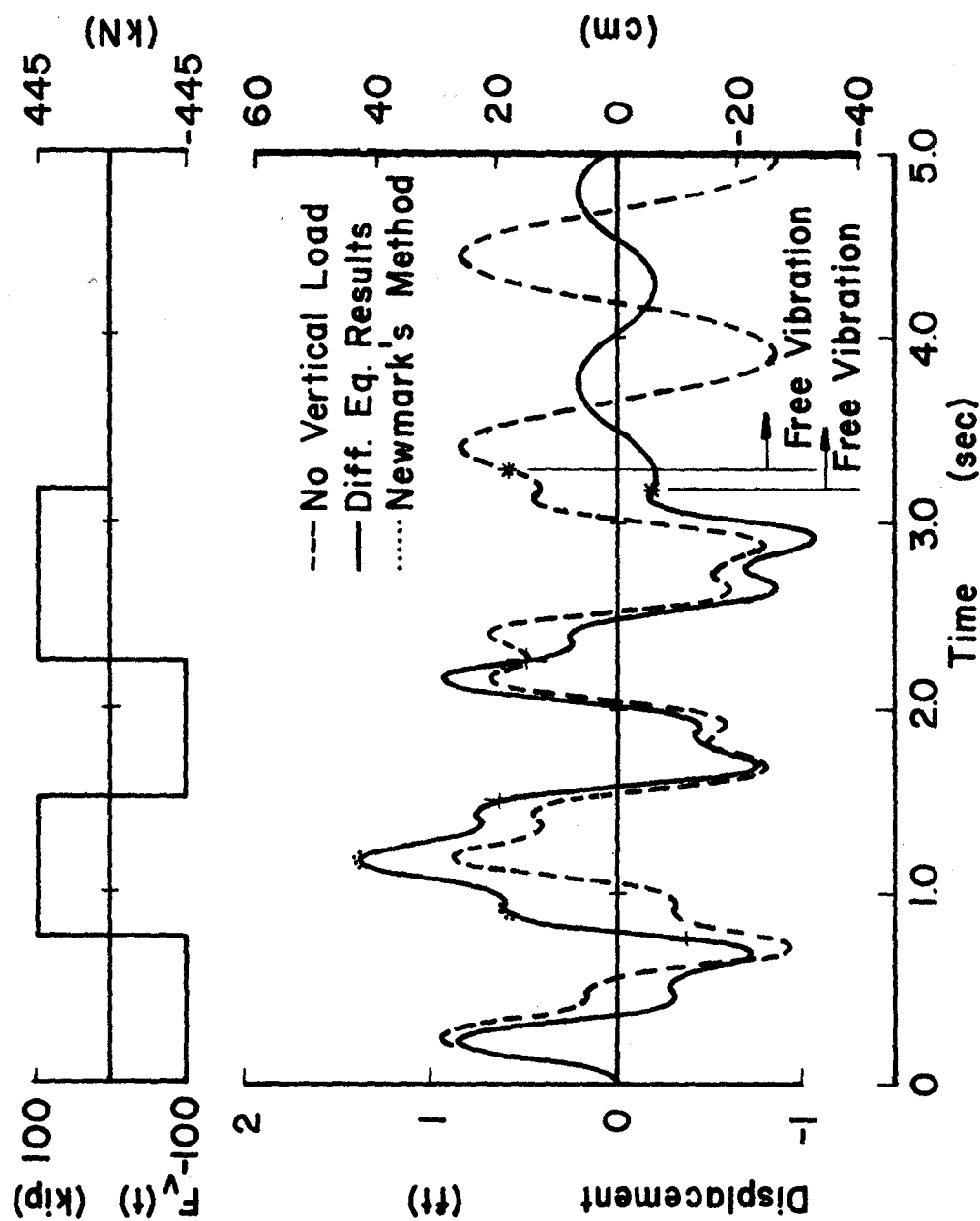


Figure 3.5. Comparison of Methods of Analysis When Considering P-delta Effect on Single-Degree-of-Freedom System

The response obtained using the Newmark Beta method and the solution of the differential equation of motion are identical except for a slight difference at a couple of points as indicated by the dotted lines representing Newmark's method of integration.

C. COMPARISON OF RESPONSES WITH PREVIOUS RESULTS BASED ON MATERIAL BEHAVIOR

Calculations are based on the integration of the motion equation derived in Eq. 3.5 with consideration of elastic, elasto-plastic as well as bilinear material behavior. A comparison will be made with the response curves obtained by Thomaides⁴¹ for an undamped system having a natural period of $T_n = 1.2$ sec. and subjected to the N-S component of the 1940 El Centro earthquake. As shown in Fig. 3.6, the mass of the shear building is lumped on the girder with a yield level of $q_y = 0.24g$ which is the yielding spring force divided by the mass of the system. Since $Q_y = Kx_y$, where K is the stiffness and x_y is the yield displacement, the yield displacement of the structural bent becomes

$$x_y = q_y m / K = 0.28186 \text{ ft (0.0859m)}.$$

Thus the moment-deflection relationship can be expressed as

$$M_p = \frac{6EI_c}{L^2} x_y = 132.12 \text{ kip-ft (179.12 kN-m)}$$

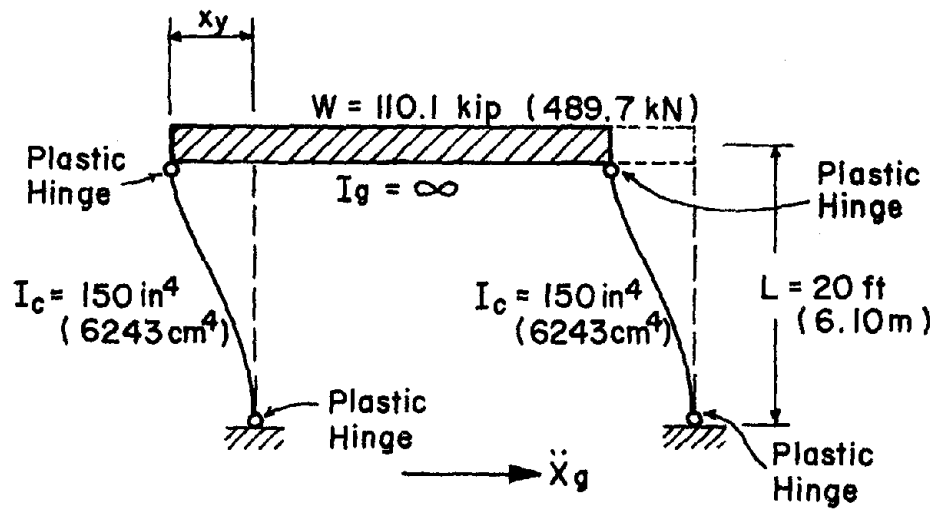


Figure 3.6. Shear Structure for Comparison, $T_n = 1.20 \text{ sec.}$

The moment-rotation relationship of a bilinear material is shown in Fig. 3.7 for which the Bauschinger³⁵ effect due to the reversal of the stress is considered.

The response curves obtained for the single-degree-of-freedom system of Fig. 3.6 are shown in Figs. 3.8-3.10. Figure 3.8 gives the elastic response and Fig. 3.9 shows the bilinear response based on a strain hardening ratio of $p = 0.05$. The elasto-plastic response of the above structure is shown in Fig. 3.10. The nonsymmetry of the two nonlinear responses of Figs. 3.9 and 3.10 is due to the permanent set occurring in the joints containing plastic hinges. All three of the response curves shown in Figs. 3.8-3.10 are the same as those obtained by Thomaides⁴¹.

D. EFFECT OF VERTICAL FORCES ON TOTAL RESPONSE OF A SINGLE-DEGREE-OF-FREEDOM SYSTEM

The contribution of vertical forces to the total response of a single-degree-of-freedom system can be studied by using the motion equation shown in Eq. 3.5:

$$m\Delta\ddot{x}_s + [K - K_{s(t+\Delta t)}]\Delta x_s = -m\Delta\ddot{x}_g + \Delta K_s x_s(t) \quad (3.9)$$

where the notations have been identified previously.

The coefficient of Δx_s represents the following equivalent stiffness:

$$\begin{aligned} K_{eq} &= K - K_{s(t+\Delta t)} \\ &= \frac{12EI_t}{L^3} - [W - m\ddot{y}_{g(t+\Delta t)}]/L \end{aligned} \quad (3.10)$$

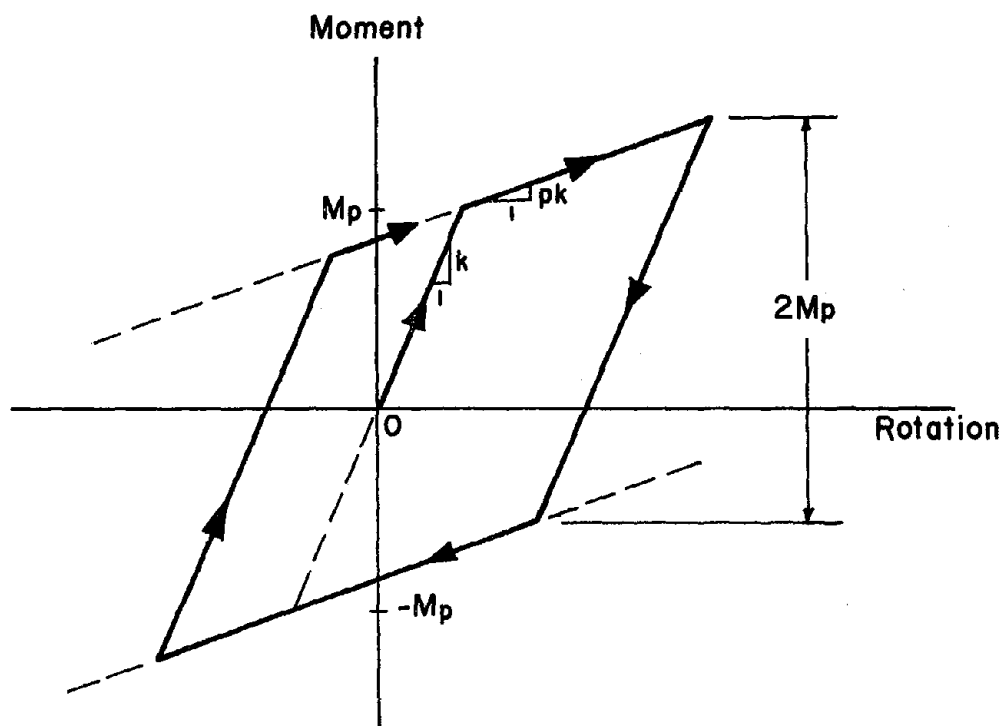


Figure 3.7. Bilinear Response Based on $2M_p$ Stress Range

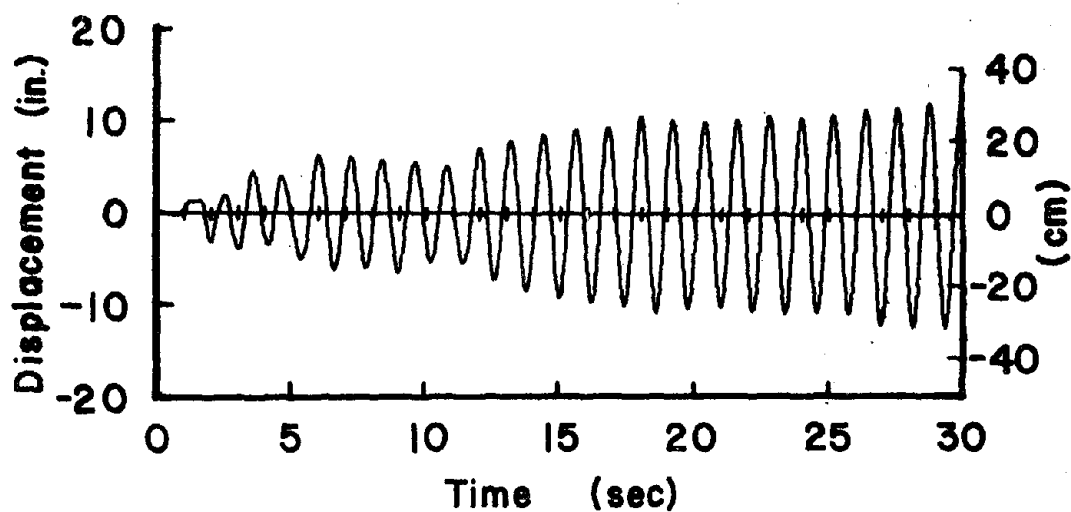


Figure 3.8. Elastic Response of Fig. 3.6, $T_n = 1.20$ sec.

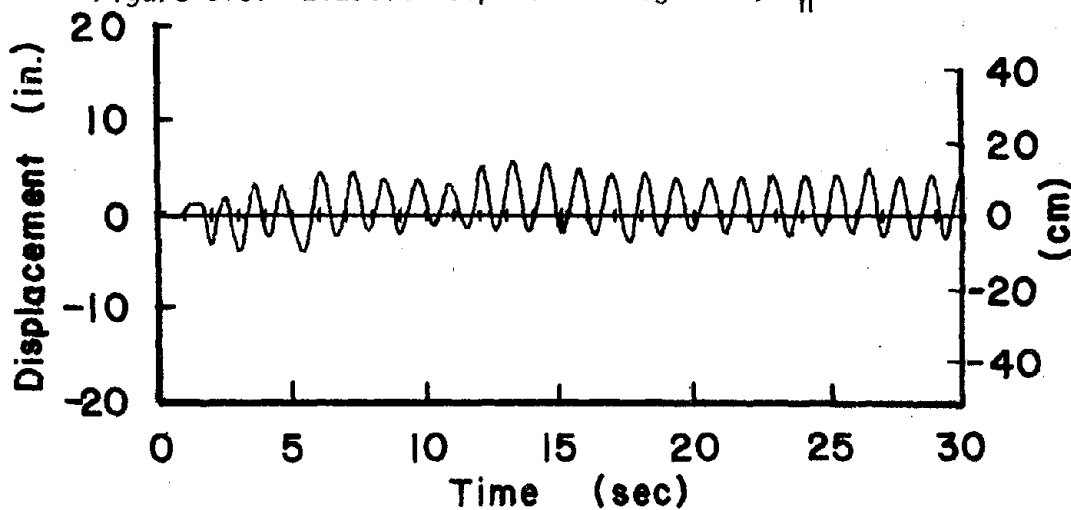


Figure 3.9. Bilinear Response of Fig. 3.6, $T_n = 1.20$ sec.

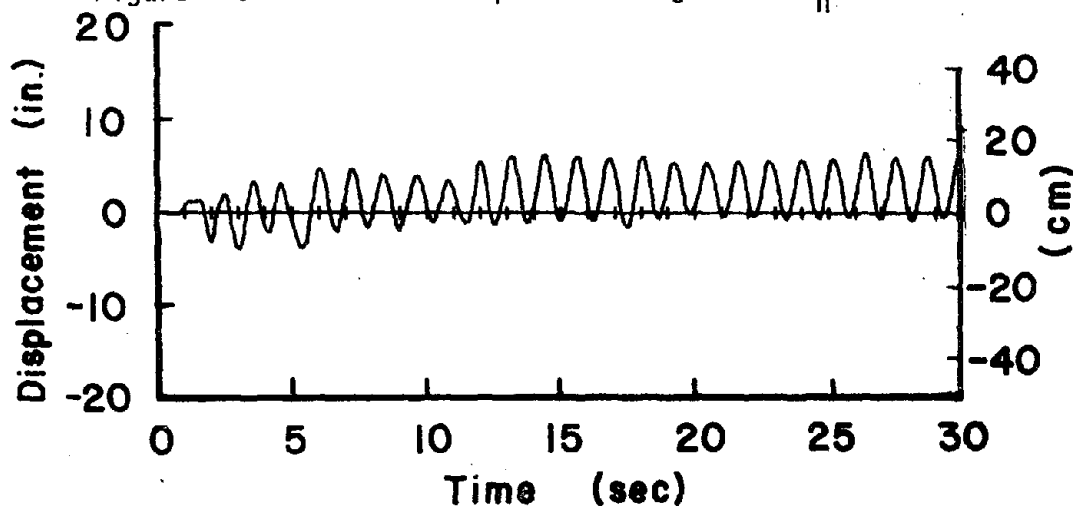


Figure 3.10. Elasto-Plastic Response of Fig. 3.6, $T_n = 1.20$ sec.

The natural frequency of the system is

$$p_s = \sqrt{K_{eq}/m}. \quad (3.11)$$

Apparently, the natural frequency will vary continuously as a function of the vertical motion.

Several examples will be used to illustrate the effect of vertical loads on the displacement responses of the structure shown in Fig. 3.6 with different lumped masses and loading conditions.

The first example will illustrate the effect of interaction of horizontal and vertical components of the 1940 El Centro earthquake on the displacement of the structure having a natural period of $T_n = 2.0$ sec. ($m = 9.494 \text{ kip-sec}^2/\text{ft} = 141.3 \text{ kg-s}^2/\text{cm}$). The resulting horizontal displacement is shown in Fig. 3.11 with and without considering the P-delta effect.

The increase in the response when considering the P-delta effect can be explained from the frequency spectrum of the earthquake loading used. The frequency spectrum of Fig. 2.13 which applies to the earthquake record used here is reproduced in Fig. 3.12 for frequency values between 0.25 and 0.67 Hz. Note that the amplitude corresponding to the natural period of $T_n = 2.0$ sec. is less than that corresponding to the natural period of $T_s = 2.186$ sec. when considering the P-delta effect.

A reduction in response due to considering the P-delta effect can also be realized by having the system with a natural frequency of $T_n = 3.0$ sec. where mass $m = 21.36 \text{ kip-sec}^2/\text{ft}$ ($317.9 \text{ kg-s}^2/\text{cm}$). The inclusion of the P-delta effect causes the natural period to be higher

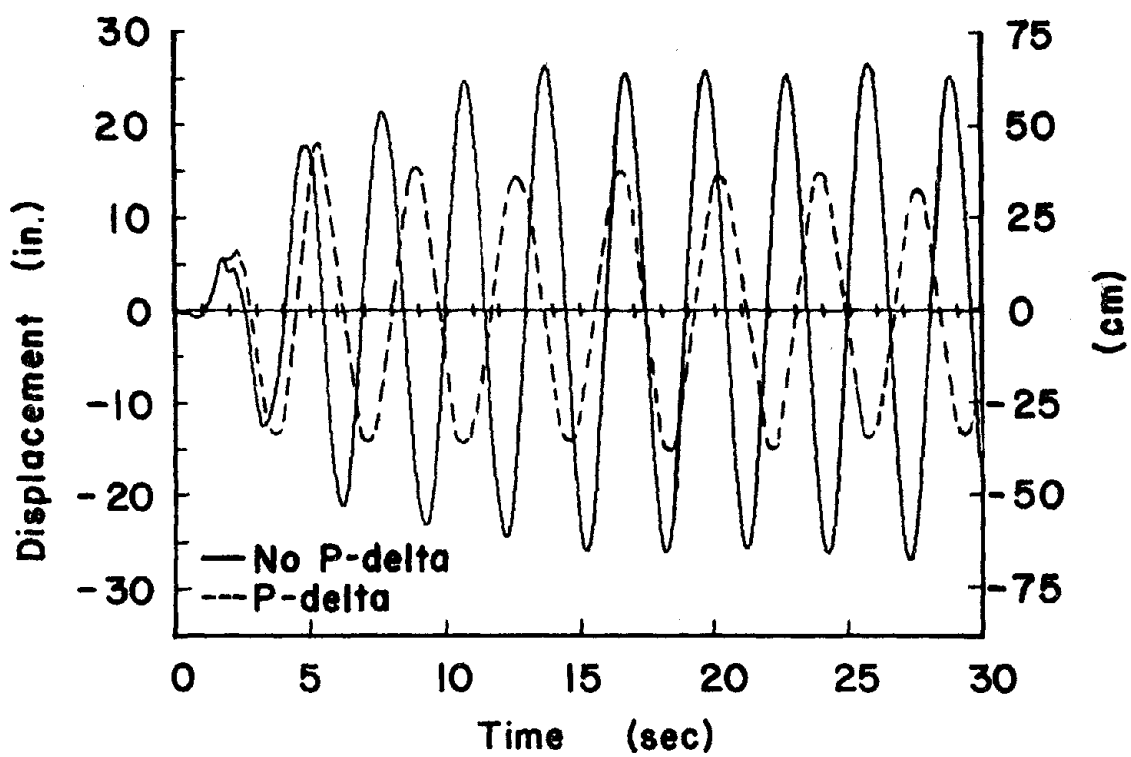


Figure 3.11. Horizontal Displacement of Single-Degree-of-Freedom System, $T_n = 2.0$ sec., 1940 El Centro (N-S)

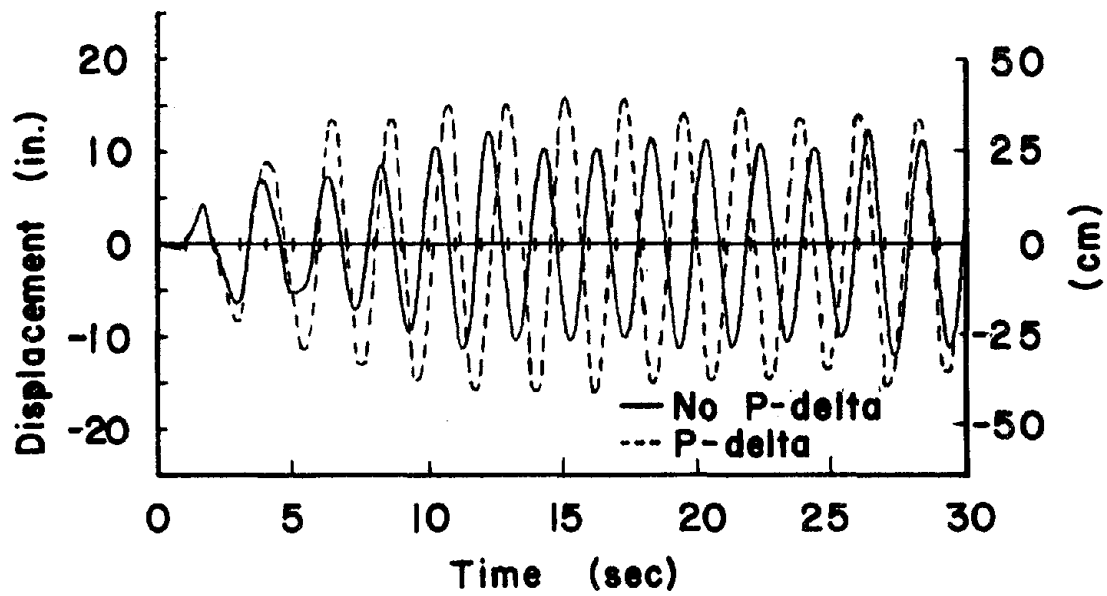


Figure 3.12. Frequency Spectrum (0.25-0.67 Hz),
1940 El Centro Earthquake (N-S)

($T_s = 3.77$ sec) resulting in a lower amplitude from the earthquake frequency spectrum. Therefore, the horizontal displacement of the mass when considering the P-delta effect would be expected to have a lower response as shown in Fig. 3.13.

A second illustration will show the effect of interaction of horizontal and vertical sinusoidal forces on the displacement response of the system having a natural frequency of $p_s = 1.02$ Hz ($m = 0.01$ kip-sec²/ft = 14.88 kg-s²/m). The horizontal and vertical forces may be respectively expressed as $F_h = A_h \sin(\omega_h t + \alpha_h)$ and $F_v = A_v \sin(\omega_v t + \alpha_v)$, where $A_h = 600$ lb (2.67 kN), $\omega_h = 15$ Hz (30π rad/s), $\alpha_h = 0$, $A_v = 1500$ lb (6.67 kN), $\omega_v = 1$ Hz (2π rad/s) and $\alpha_v = 0$. The vertical forcing frequency is the same as the natural frequency of the system.

As shown in Fig. 3.14, the response based on a horizontal force only is represented by the solid line while the dashed line represents the response due to the addition of the vertical forcing function. All loading on the mass is stopped at $t = 6.0$ sec. The horizontal forcing frequency of 15 Hz results in the high frequency displacement as indicated by the spikes in the curves during the loading time of $t = 0-6$ sec.

With the vertical forcing frequency ω_v the same as the natural frequency p_s , there will be a downward vertical force when the horizontal displacement is positive and an upward vertical force when the horizontal displacement is negative. Two significant changes are noted when including the vertical force. First, the downward vertical force produces a somewhat larger response in the positive direction. Second, an increase in the response period is realized over the 6.0 sec. of

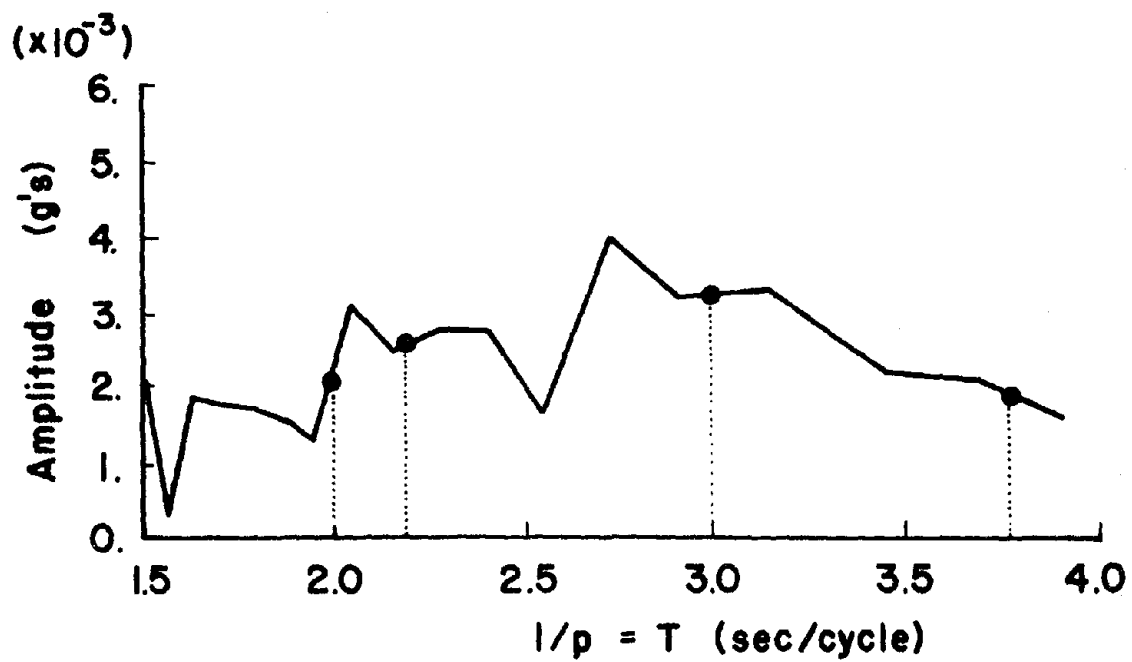


Figure 3.13. Horizontal Displacement of Single-Degree-of-Freedom System, $T_n = 3.0$ sec., 1940 El Centro (N-S)

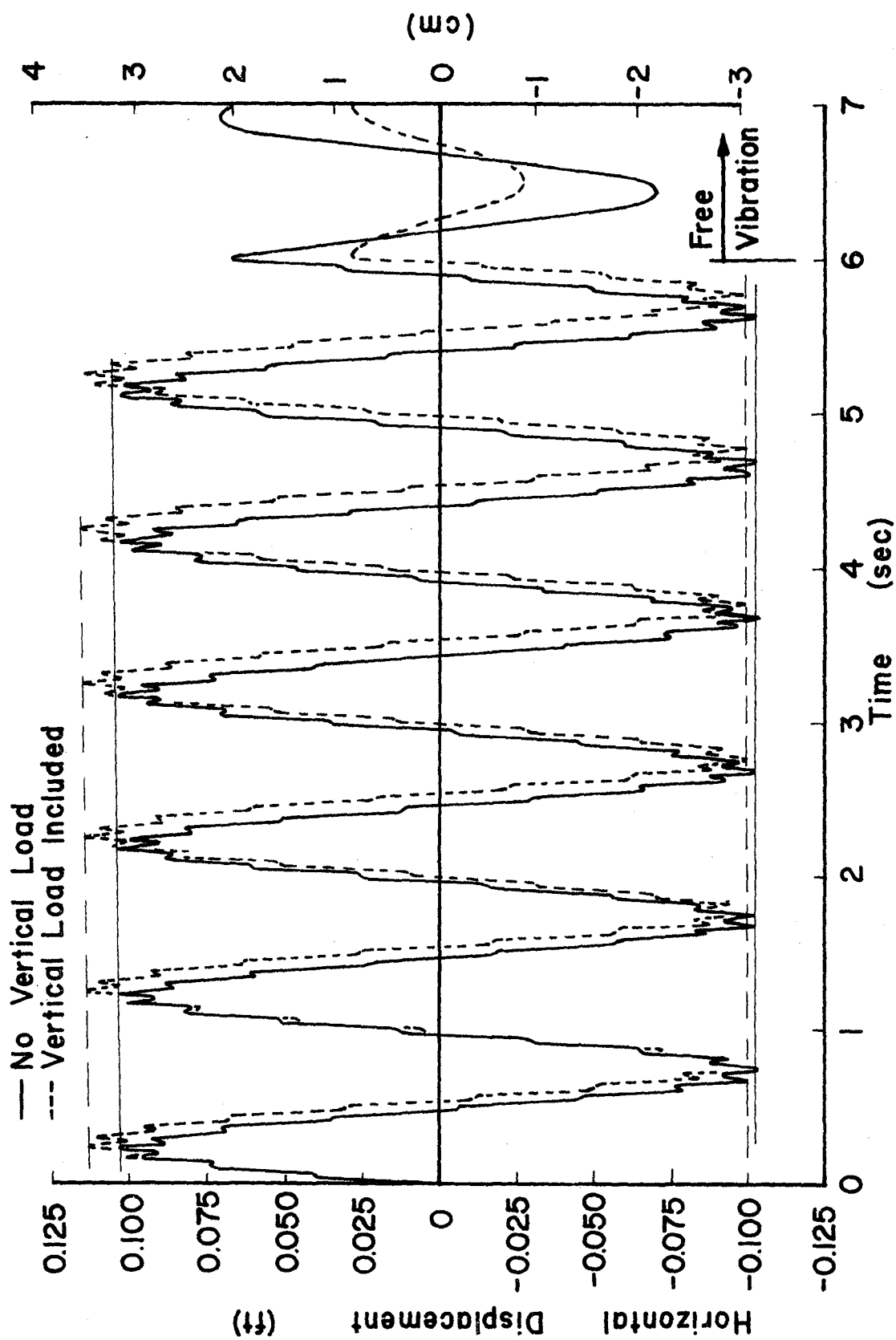


Figure 3.14. Response of Single Mass Subjected to Sinusoidal Loads in the Horizontal and Vertical Directions

loading. The tendency for the downward force to increase the response period and the upward force to decrease the response period is indicated in the response curves.

When the phase angle $\alpha_v = 180^\circ$ (π rad) a different response is obtained. Figure 3.15 shows the comparison of the response with and without the vertical sinusoidal load. The upward force results in a reduced response in the positive horizontal direction while an increase in response is realized in the negative direction.

As shown in Ref. 22 on dynamic instability, the horizontal displacement may increase exponentially when the vertical forcing frequency equals twice the natural frequency. This example will study the influence of phase angle on the dynamic stability case. Let $\omega_v = 2$ Hz (4π rad/s), and $\alpha = \pm 90^\circ$ ($\pm\pi/2$ rad) and the other loading information be the same as given for Fig. 3.15. Figure 3.16 reveals that while the positive phase angle causes an increase in the response frequency the negative phase angle causes a decrease in the response frequency. The increase in the response frequency based on the $\alpha_v = +90^\circ$ ($+\pi/2$ rad) results in the downward force of the vertical forcing function to be more effective in increasing the horizontal response.

A third illustration will be used to show the effect of frequency ω_v and phase angle α_v of the vertical forcing function on the horizontal response when the horizontal displacement is predominantly to one side of its original position. This displacement history may be as a result of a triangular impulse similar to the one shown in Fig. 2.15.

A triangular impulse load in the horizontal direction, having an initial magnitude of $F_s = 160$ lbs (711.7 N) and reducing to zero after

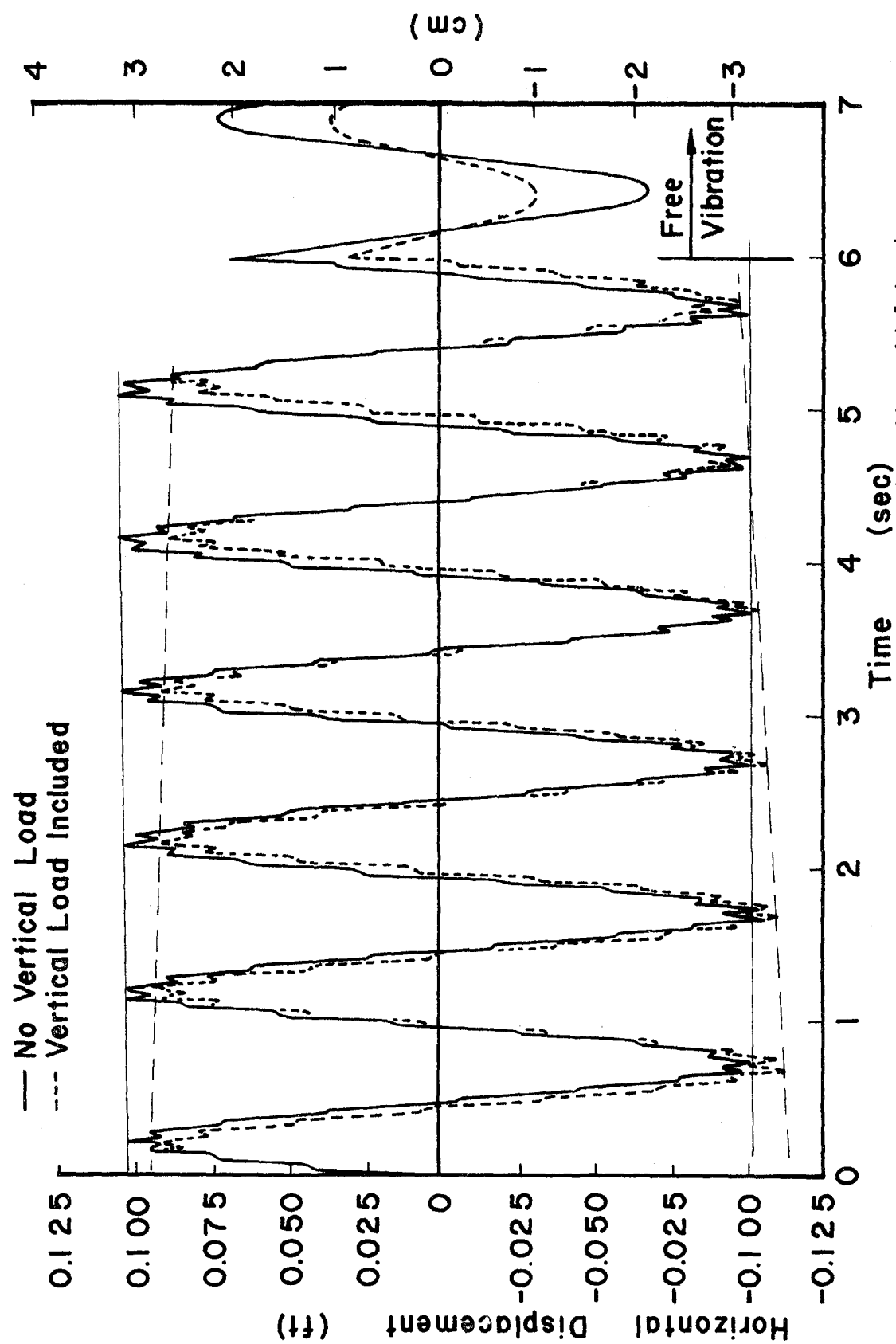


Figure 3.15. Response of Single Mass Subjected to Sinusoidal Loads in the Horizontal and Vertical Directions ($\alpha_v \neq 0$)

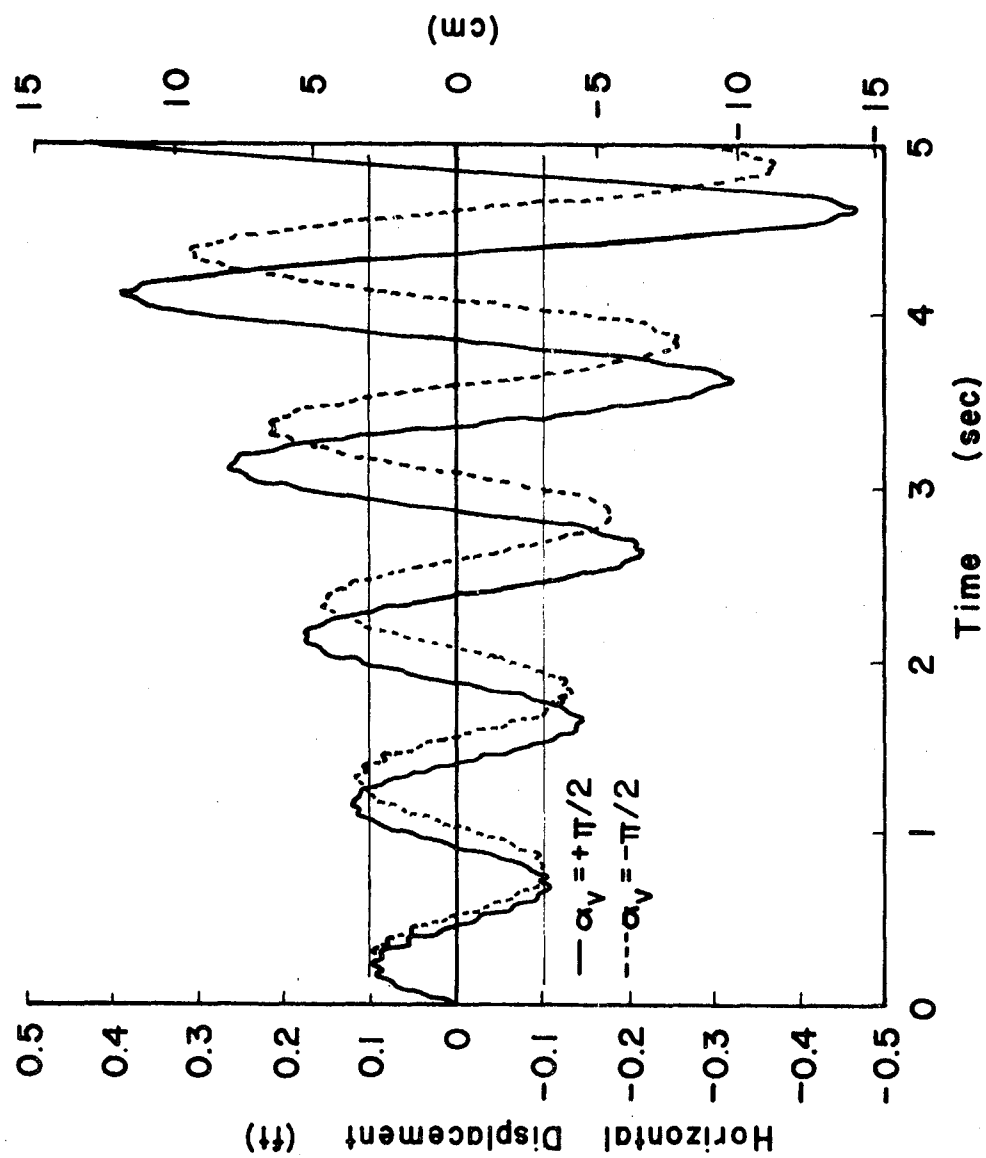


Figure 3.16. Response of Single Mass Subjected to Sinusoidal Loads in the Horizontal and Vertical Directions ($\omega_v = 2p_n$)

6 seconds is used for this study. As indicated in Fig. 3.17, an increase in the horizontal amplitude is realized when the vertical frequency $\omega_v = 1.0$ Hz (2π rad/s). The response curve based on no vertical force is indicated by a solid line. A corresponding decrease in amplitude is realized when the vertical frequency $\omega_v = 2.0$ Hz (4π rad/s). Whereas the critical forcing frequency in the vertical direction for a symmetrical response is shown to be twice the natural frequency, the critical forcing frequency for the unsymmetrical response produced by the impulse load is equal to the natural frequency of the mass. After the impulse of 6 seconds the response becomes free vibration for which the vertical force having $\omega_v = 2$ Hz (4π rad/s) will cause a dynamic instability behavior.

Figure 3.18 illustrates the effect of the phase angle α_v of the vertical forcing function on the horizontal response. Again the structural system is excited by the same horizontal and vertical loads as given in the previous example. By introducing the phase angle $\alpha_v = \pm 180^\circ$ ($\pm\pi$ rad), the amplitudes of the horizontal response become less than that due to horizontal impulse only. An increase in the amplitude of the vertical forcing function with the same phase angle $\alpha_v = \pm 180^\circ$ ($\pm\pi$ rad) results in a larger reduction in the amplitude of the horizontal response. As shown in Fig. 3.18 an increase of the vertical amplitude from 400 lb (1779 N) to 1200 lb (5338 N) results in not only a reduction in the horizontal amplitude response but also causes a change in the response frequency.

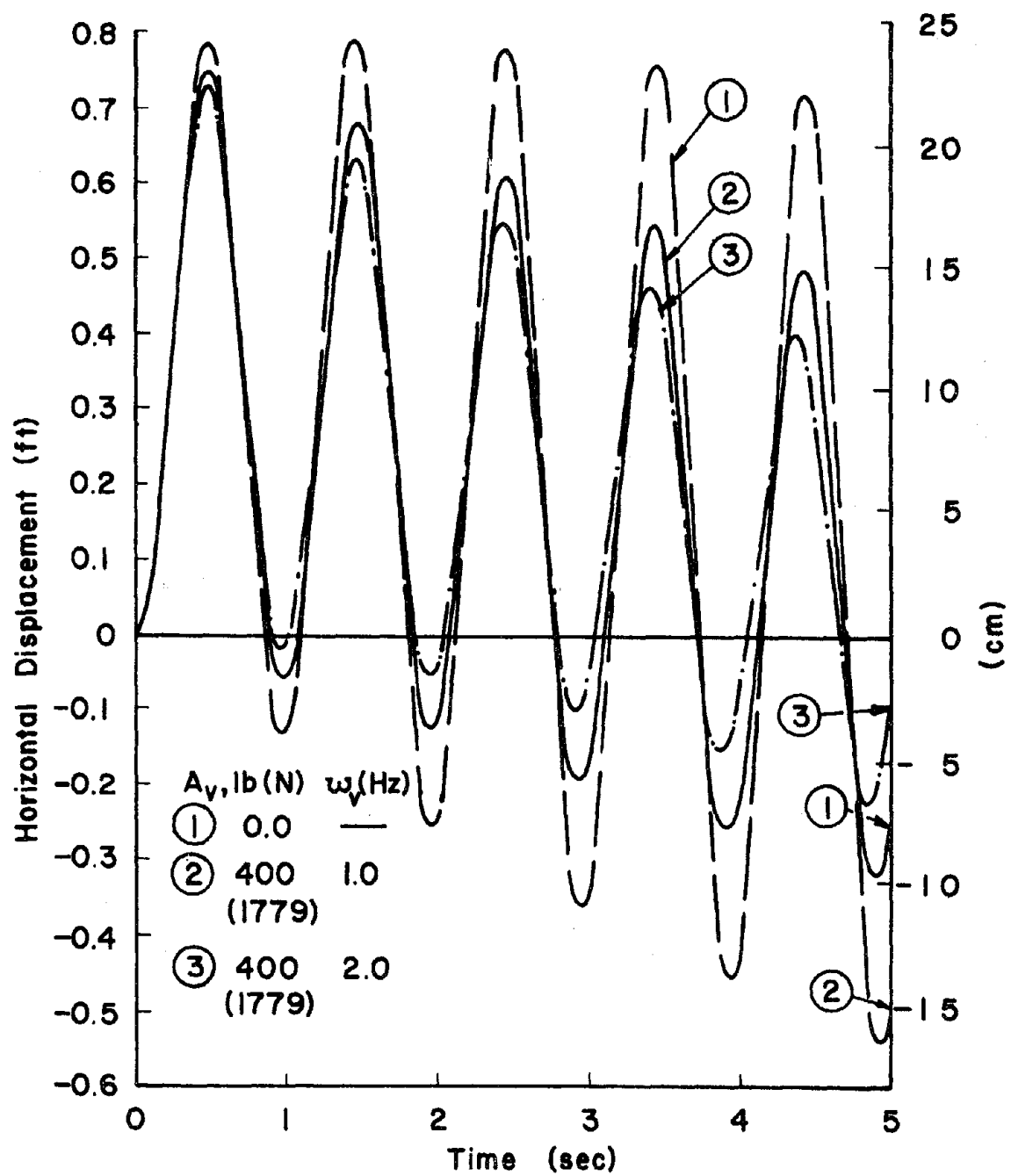


Figure 3.17. Response of a Single Mass Subjected to an Impulse F_s and $F_v = A_v \sin(\omega_v t)$

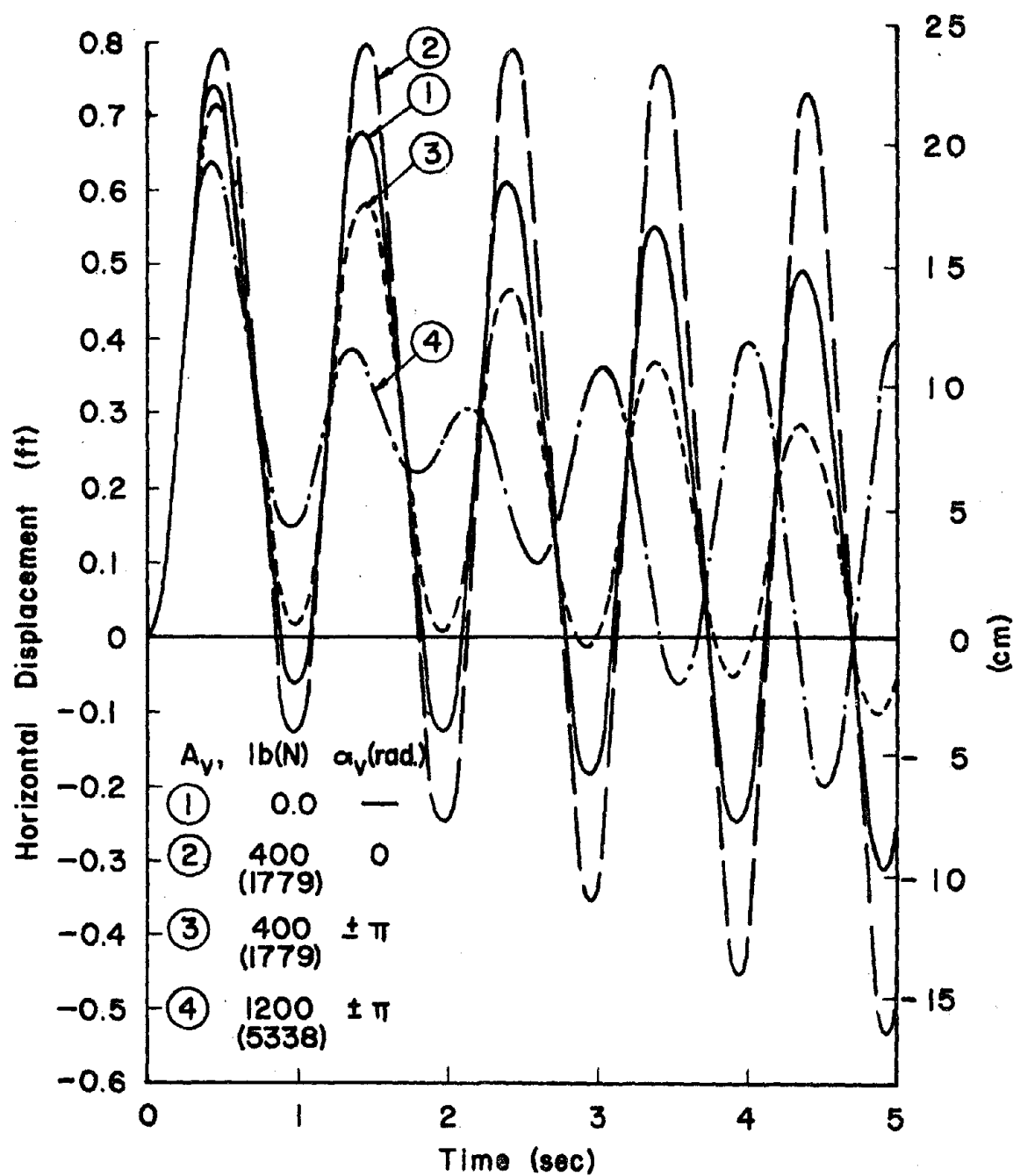


Figure 3.18. Response of a Single Mass Subjected to an Impulse
 F_s and $F_v = A_v \sin(\omega_v t + \alpha_v)$

IV. MATHEMATICAL FORMULATION OF A MULTI-DEGREE-OF-FREEDOM SYSTEM

The mathematical formulation of the motion equation of a multi-degree-of-freedom system consists of generalizing the motion equation for the single-degree-of-freedom system as performed previously in Section III-A. The stiffness matrix of a typical member is given for elastic, bilinear and elasto-plastic materials for which the reduction of plastic moment is formulated from the current specifications of AISC³⁴. Since energy absorption is included in this study, the formulation of the input, stored and dissipated energy is developed. Other considerations include the P-delta effect, interaction between horizontal and vertical earthquake components, viscous damping, and ductility and excursion ratios.

A. MOTION EQUATION

The general differential equation of motion for a multi-degree-of-freedom system may be expressed as follows:

$$[M]\{\ddot{x}\} + [C]\{\dot{x}\} + ([K] - [K_s])\{x\} = -[M]\{\ddot{x}_g\} \quad (4.1)$$

where $[M]$ = mass matrix (NPxNP),

$[C]$ = damping coefficient matrix (NPxNP),

$[K]$ = stiffness matrix (NPxNP),

$[K_s]$ = geometric matrix (NPxNP),

$\{\ddot{x}\}$ = acceleration vector (NPx1),

$\{\dot{x}\}$ = velocity vector (NPx1),

$\{x\}$ = displacement vector (NPx1),

$\{\ddot{x}_g\}$ = ground acceleration vector (NPx1),

NP = total number of degrees of freedom = NPR + NPV + NPH,

NPR = degrees of freedom in rotation,

NPV = degrees of freedom in vertical direction, and

NPH = degrees of freedom in horizontal direction.

The above motion equation in matrix form consists of the following individual motion equations by row. The first NPR equations are the motion equations applicable to the degrees of freedom in rotation. Since rotational inertia forces are negligible, the first NPR rows of matrices $[M]$, $[C]$, $[K_s]$ and $\{\ddot{x}_g\}$ are zero. The next NPV rows are the motion equations applicable to the degrees of freedom in the vertical direction. The last NPH rows are corresponding to the degrees of freedom in the horizontal direction. The acceleration, velocity and displacement vectors of a structural system can be generally written in the form:

$$\{\ddot{x}\} = \begin{Bmatrix} \ddot{x}_\theta \\ \ddot{x}_v \\ \ddot{x}_s \end{Bmatrix}; \quad \{\dot{x}\} = \begin{Bmatrix} \dot{x}_\theta \\ \dot{x}_v \\ \dot{x}_s \end{Bmatrix}; \quad \{x\} = \begin{Bmatrix} x_\theta \\ x_v \\ x_s \end{Bmatrix}$$

where \ddot{x}_θ , \dot{x}_θ , x_θ = angular acceleration, velocity and rotation of a nodal point;

\ddot{x}_v , \dot{x}_v , x_v = vertical acceleration, velocity and displacement of a girder node; and

\ddot{x}_s , \dot{x}_s , x_s = horizontal acceleration, velocity and displacement of a floor level.

1. Incremental Form of Motion Equation. The incremental form of the motion equation can be obtained by considering the motion equations for time t and $t + \Delta t$. These are

$$[M]\{\ddot{x}\}_t + [C]\{\dot{x}\}_t + ([K] - [K_s]_t)\{x\}_t = -[M]\{\ddot{x}_g\}_t, \quad (4.2)$$

$$[M]\{\ddot{x}\}_{t+\Delta t} + [C]\{\dot{x}\}_{t+\Delta t} + ([K] - [K_s]_{t+\Delta t})\{x\}_{t+\Delta t} = -[M]\{\ddot{x}_g\}_{t+\Delta t}. \quad (4.3)$$

Subtracting Eq. 4.2 from Eq. 4.3,

$$[M]\{\Delta\ddot{x}\} + [C]\{\Delta\dot{x}\} + [K]\{\Delta x\} - [K_s]_{t+\Delta t}\{x\}_{t+\Delta t} + [K_s]_t\{x\}_t = \{\Delta F\} \quad (4.4)$$

where $\{\Delta\ddot{x}\} = \{\ddot{x}\}_{t+\Delta t} - \{\ddot{x}\}_t$
 $\{\Delta\dot{x}\} = \{\dot{x}\}_{t+\Delta t} - \{\dot{x}\}_t$
 $\{\Delta x\} = \{x\}_{t+\Delta t} - \{x\}_t$
 $\{\Delta F\} = -[M]\{\ddot{x}_g\}_{t+\Delta t} + [M]\{\ddot{x}_g\}_t$

Since $[K_s]_t = [K_s]_{t+\Delta t} + [K_s]_t - [K_s]_{t+\Delta t}$, and letting $[\Delta K_s] = [K_s]_{t+\Delta t} - [K_s]_t$, Eq. 4.4 can be written

$$[M]\{\Delta\ddot{x}\} + [C]\{\Delta\dot{x}\} + ([K] - [K_s]_{t+\Delta t})\{\Delta x\} = \{\Delta F\} + [\Delta K_s]\{x\}_t \quad (4.5)$$

Matrix condensation is used to reduce the number of equations to the number of vertical and horizontal degrees of freedom. Taking the first NPR equations, those related to the rotational forces, incremental rotations can be solved in terms of the incremental displacements of the system.

$$[K_{11} | K_{12}] \begin{Bmatrix} \Delta x_\theta \\ \Delta x_v \\ \Delta x_s \end{Bmatrix} = 0.$$

where $[K_{11} \ K_{12}]$ are the first NPR rows of $[K]$ related to moment-rotation. Therefore,

$$\{\Delta x_\theta\} = -[K_{11}]^{-1}[K_{12}]\begin{Bmatrix} \Delta x_v \\ \Delta x_s \end{Bmatrix} \quad (4.6)$$

Substituting Eq. 4.6 back into the last NPV + NPH equations of matrix Eq. 4.5, the final incremental form becomes

$$[M]\begin{Bmatrix} \Delta \ddot{x}_v \\ \Delta \ddot{x}_s \end{Bmatrix} + [C]\begin{Bmatrix} \Delta \dot{x}_v \\ \Delta \dot{x}_s \end{Bmatrix} + [K'']\begin{Bmatrix} \Delta x_v \\ \Delta x_s \end{Bmatrix} = \{\Delta F\} + [\Delta K_s]\begin{Bmatrix} x_v \\ x_s \end{Bmatrix}_t \quad (4.7)$$

where $[K''] = [K_{22}] - [K_{12}]^T [K_{11}]^{-1} [K_{12}] - [K_s]_{(t+\Delta t)}$

Based on the initial values of acceleration, velocity and displacement, a step-by-step numerical method discussed in Chapter V is used to solve for the acceleration, velocity and displacement at the end of each time increment during the action of the two components of an earthquake. Consequently, the end moments at each end of a member can then be determined.

2. Mass Matrix. The mass matrix $[M]$ in Eq. 4.7 is a diagonal matrix with girder and floor masses on the diagonal. When a model

without girder nodes is used, only the total mass for each floor is contained in the mass matrix. When girder nodes are assumed, the first N_f rows of the mass matrix will contain half of each floor mass on the diagonal elements.

3. Damping Coefficient Matrix. The damping coefficient matrix $[C]$ in Eq. 4.7 is assumed linearly related to the mass and stiffness matrices⁴² so that

$$[C] = \alpha[M] + \beta[K] \quad (4.8)$$

where α and β are constants depending on the type of damping used. Letting λ equal to the fraction of critical damping and p_n be the estimated fundamental frequency of the structural system in radians per second, the value for α and β are given as follows:

1. Mass plus stiffness proportional damping

$$\alpha = \lambda p_n \quad (4.9a)$$

$$\beta = \lambda/p_n \quad (4.9b)$$

2. Mass proportional damping

$$\alpha = 2\lambda p_n \quad (4.10a)$$

$$\beta = 0 \quad (4.10b)$$

3. Stiffness proportional damping

$$\alpha = 0 \quad (4.11a)$$

$$\beta = 2\lambda/p_n \quad (4.11b)$$

The expressions for α and β are based on the uncoupled equations of motion where displacements are expressed in terms of the normal modes of the system.

4. Geometric Stiffness Matrix. The geometric stiffness matrix $[K_s]$ used for the P-delta effect of a structural system may be derived by generalizing the formulation obtained for a single-degree-of-freedom system as

$$\{F_p\} = [K_s]\{x_s\} \quad (4.12)$$

where $\{F_p\}$ = horizontal force acting at floor levels 1 to N_f due to the P-delta effect,

$\{x_s\}$ = horizontal floor displacements relative to the base, and

$$[K_s] = \begin{bmatrix} (K_{s1}+K_{s2}) & -K_{s2} & & & 0 \\ -K_{s2} & (K_{s2}+K_{s3}) & -K_{s3} & & \\ & & \ddots & \ddots & \\ & & & K_{s(n-1)} & (K_{s(n-1)}+K_{sn}) & -K_{sn} \\ 0 & & & & -K_{sn} & K_{sn} \end{bmatrix} \quad (4.13)$$

The individual elements in Eq. 4.13 may be expressed as

$$K_{si} = \sum_{j=i}^{N_f} \frac{F_j}{L_i}$$

where F_j = vertical loads on floor j ,

L_i = length of columns below floor i , and

N_f = total number of floors also denoted by n .

When considering horizontal plus vertical earthquake motions the expression for F_j can be written in terms of the floor mass m_j , the vertical ground acceleration \ddot{y}_g and the acceleration of gravity g :

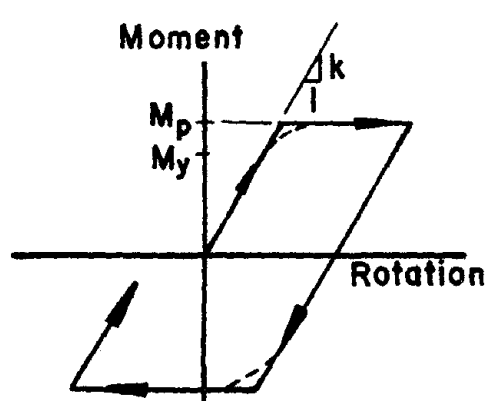
$$F_j = m_j(-\ddot{y}_g + g) \quad (4.14)$$

B. NONLINEAR RESPONSE

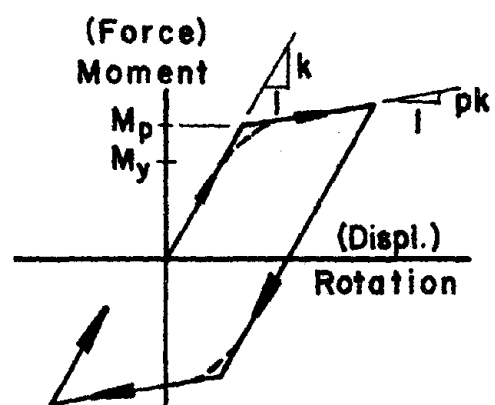
The nonlinear response of a multi-story frame is realized as soon as a point in the frame reaches the yield moment M_y of its cross-section. A yield zone then develops at the member section due to plastification which is the gradual increase of yielding from the outer fiber towards the neutral axis of the section due to an increase in moment. The section of the member acts as if hinged yet is restrained by the plastic moment M_p .

For this study an idealized elasto-plastic or bilinear moment-rotation relationship is assumed. This simplification of the moment-rotation relationship assumes the yield moment to be the same as the plastic moment. The contained plastic flow during plastification as indicated by the dashed lines of Fig. 4.1 is assumed to have a negligible effect on the moment-rotation relationship assumed. The ratio (shape factor) of the plastic moment M_p and the yield moment M_y for wide flange sections ranges from 1.09 to 1.20 as determined from Z/S , the plastic modulus divided by the section modulus of the member. Thus the idealized moment-rotation relationship is based on an assumed shape factor of 1.0.

For the study performed here the maximum moment a section can carry will be based on the idealized moment-rotation relationship.



a) Elasto-Plastic



b) Bilinear

Figure 4.1. Idealized Moment-Rotation Relationship

The moment will be indicated by M_p and will be designated as the plastic moment of the member.

Once a member node becomes plastic the stiffness matrix of the total frame must be modified before the response parameters for the next time increment are calculated. The stiffness matrix must again be modified as soon as one or more nodes become plastic or return to their elastic range.

The formulation of the stiffness matrix for a typical member will be derived in the following articles. The method of Giberson⁴⁵ is used to describe the nonlinear response mechanism and the resulting formulation.

1. Mechanical Equivalent. The equivalent mechanical system for a bilinear response of a typical member node is shown in Fig. 4.2. The system consists of a variable force acting on two parallel components, one containing a spring and the other a spring in series with a coulomb slider. An elasto-plastic system can be realized by the removal of the lower spring.

The total stiffness of a typical bilinear model consists of an elasto-plastic component (spring plus slider) in parallel with an elastic component (spring only). The moment-rotation (force-displacement) relationships for each of the parallel components are shown in Fig. 4.3. Variables included in parentheses in Fig. 4.1 and 4.3 apply to the mechanical system.

The slope of the initial elastic portion of the elasto-plastic component is k_1 while the slope of the elastic component is k_2 . Therefore,

$$k = k_1 + k_2 \quad (4.15)$$

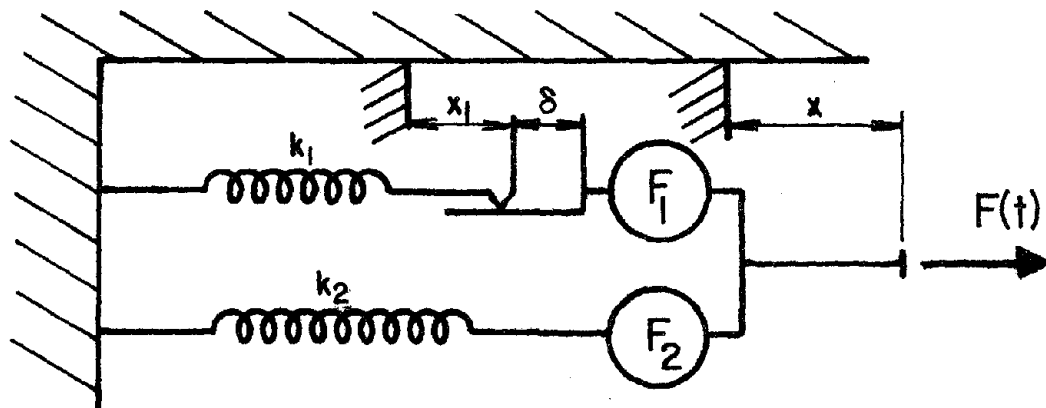


Figure 4.2. Equivalent Mechanical System for Bilinear System

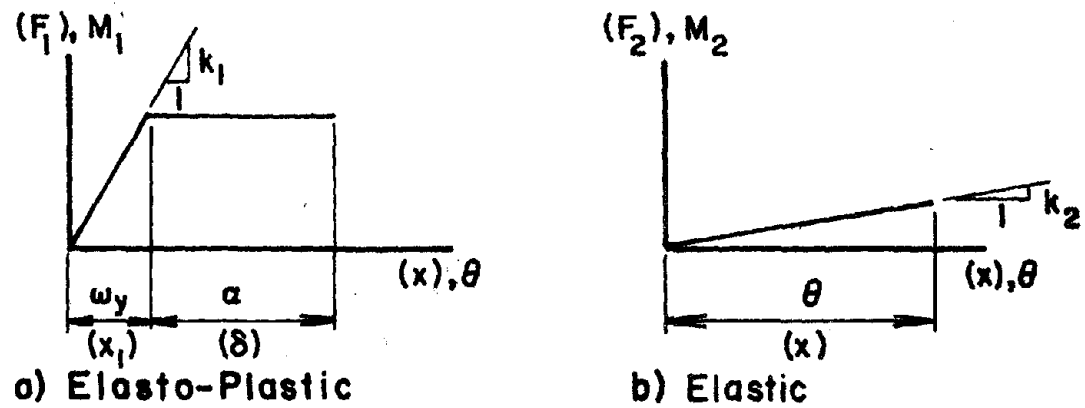


Figure 4.3. M- θ Relationship for Model Components

where k is the elastic stiffness of the member. Let $k_1 = qk$ and $k_2 = pk$, then the elastic stiffness may be expressed as

$$k = qk + pk = k(p + q) \quad (4.16)$$

Therefore, $p + q = 1$.

2. Moment-Rotation Equations. Consider a typical member i shown in Fig. 4.4a containing two possible bilinear hinges, one at each end. The subscripts a (left) and b (right) are used for the member ends $(2i-1)$ and $(2i)$, respectively. The elastic and elasto-plastic beam components are shown in Figs. 4.4b and 4.4c, respectively. The incremental end rotations of the elasto-plastic component of Fig. 4.4c may be obtained as follows:

$$\Delta\omega_a = \Delta\theta_a - \Delta\alpha_a \quad (4.17a)$$

$$\Delta\omega_b = \Delta\theta_b - \Delta\alpha_b \quad (4.17b)$$

where $\Delta\omega_a, \Delta\omega_b$ = incremental end rotation of central beam of elasto-plastic component,

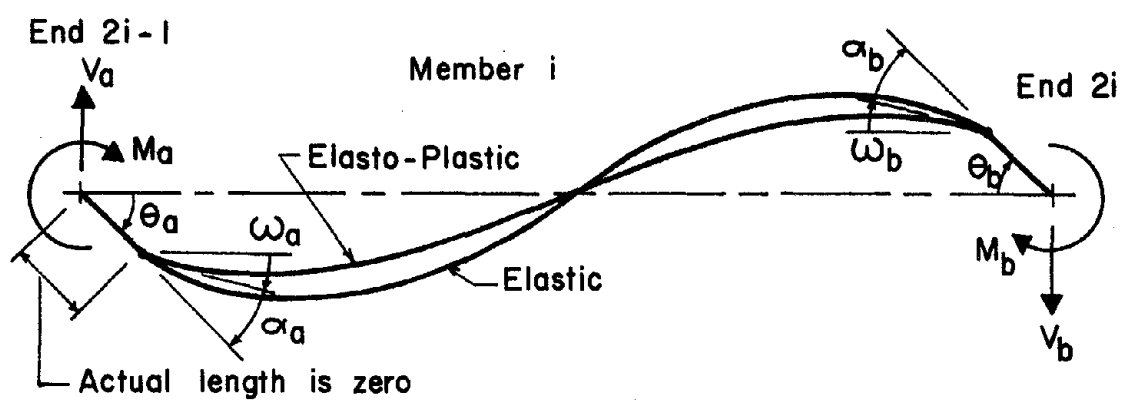
$\Delta\theta_a, \Delta\theta_b$ = incremental end rotation of a member, and

$\Delta\alpha_a, \Delta\alpha_b$ = incremental incurred plastic angle at the ends of elasto-plastic component.

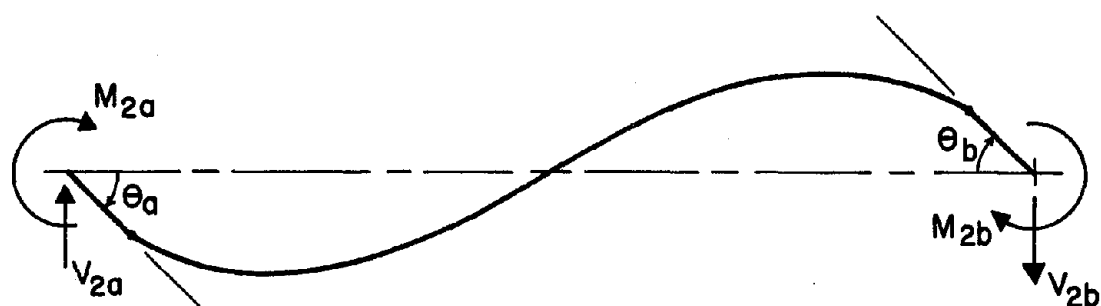
The total incremental end moment values are the sum of the end moment values of the beam components.

$$\Delta M_a = \Delta M_{1a} + \Delta M_{2a} \quad (4.18a)$$

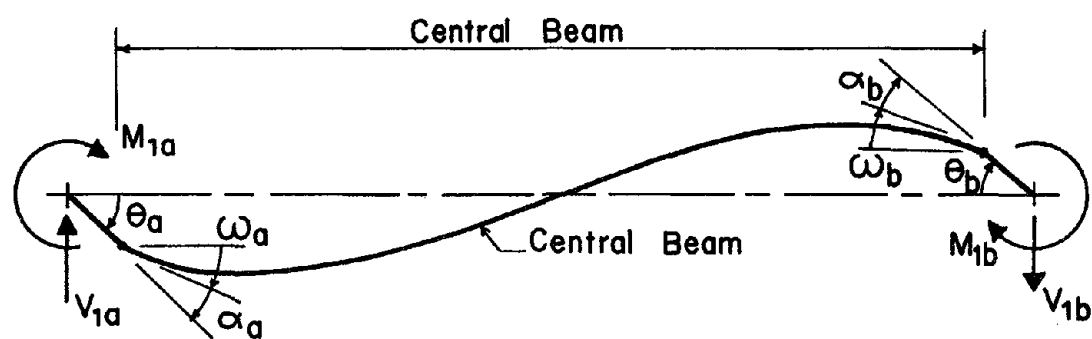
$$\Delta M_b = \Delta M_{1b} + \Delta M_{2b} \quad (4.18b)$$



a) Combined Components



b) Elastic Component



c) Elasto-Plastic Component

Figure 4.4. Two Component Model of Inelastic Member

where $\Delta M_a, \Delta M_b$ = incremental bending moments at ends a and b,

$\Delta M_{1a}, \Delta M_{1b}$ = incremental bending moments at the ends of the elasto-plastic component, and

$\Delta M_{2a}, \Delta M_{2b}$ = incremental bending moments at the ends of the elastic component.

The change in end moments over a time increment Δt can be expressed in terms of the change in member end rotations based on the state of yield for the member during the time increment. Note that either $\Delta \omega_a, \Delta \omega_b$ or $\Delta \alpha_a, \Delta \alpha_b$ in Eqs. 4.17 will be zero depending on whether or not the member node is in the plastic range. In Eqs. 4.18, ΔM_{1a} and ΔM_{1b} will become zero once the node has become plastic. These and other incremental conditions can be realized when one looks at the four possible states of yield for a typical member.

a. Both ends a and b are in the elastic range:

$$\Delta \alpha_a = 0 \quad \Delta \alpha_b = 0$$

b. End a is in plastic range, end b is in elastic range:

$$\Delta M_a = \Delta M_{2a} \quad \Delta \omega_a = 0 \quad \Delta \alpha_b = 0$$

c. End a is in the elastic range, end b is in the plastic range:

$$\Delta \alpha_a = 0 \quad \Delta M_b = \Delta M_{2b} \quad \Delta \omega_b = 0$$

d. Both ends a and b are in the plastic range:

$$\Delta M_a = \Delta M_{2a} \quad \Delta \omega_a = 0$$

$$\Delta M_b = \Delta M_{2b} \quad \Delta \omega_b = 0$$

The fundamental moment-rotation equations in incremental form are derived from the slope-deflection relationships for the components. For the elasto-plastic component in the elastic range,

$$\Delta M_{1a} = qk(\Delta\omega_a + \frac{1}{2}\Delta\omega_b) \quad (4.19)$$

$$\Delta M_{1b} = qk(\frac{1}{2}\Delta\omega_a + \Delta\omega_b) \quad (4.20)$$

and for the elastic component,

$$\Delta M_{2a} = pk(\Delta\theta_a + \frac{1}{2}\Delta\theta_b) \quad (4.21)$$

$$\Delta M_{2b} = pk(\frac{1}{2}\Delta\theta_a + \Delta\theta_b) \quad (4.22)$$

Substituting Eqs. 4.17 into Eqs. 4.19 and 4.20 yields the incremental moments of the elasto-plastic component in terms of the incremental end rotations and plastic angles. The total incremental end moments are obtained from Eqs. 4.18 as follows:

$$\Delta M_a = k[(\Delta\theta_a - q\Delta\alpha_a) + \frac{1}{2}(\Delta\theta_b - q\Delta\alpha_b)] \quad (4.23a)$$

$$\Delta M_b = k[\frac{1}{2}(\Delta\theta_a - q\Delta\alpha_a) + (\Delta\theta_b - q\Delta\alpha_b)]. \quad (4.23b)$$

The above incremental end moments can be expressed in terms of the incremental end rotations alone for the different states of yield. The resulting M- θ relationships in incremental form are given as follows:

a. Both ends a and b are in the elastic range:

$$\Delta M_a = k[\Delta\theta_a + \frac{1}{2}\Delta\theta_b] \quad (4.24a)$$

$$\Delta M_b = k[\frac{1}{2}\Delta\theta_a + \Delta\theta_b] \quad (4.24b)$$

b. End a is in plastic range, end b in elastic range:

$$\Delta M_a = pk(\Delta\theta_a + \frac{1}{2}\Delta\theta_b) \quad (4.25a)$$

$$\Delta M_b = k[\frac{p}{2}\Delta\theta_a + (1 - \frac{q}{4})\Delta\theta_b] \quad (4.25b)$$

c. End a is in elastic range, end b in plastic range:

$$\Delta M_a = k[(1 - \frac{q}{4})\Delta\theta_a + \frac{p}{2}\Delta\theta_b] \quad (4.26a)$$

$$\Delta M_b = pk(\frac{1}{2}\Delta\theta_a + \Delta\theta_b) \quad (4.26b)$$

d. Both ends a and b are in the plastic range:

$$\Delta M_a = pk(\Delta\theta_a + \frac{1}{2}\Delta\theta_b) \quad (4.27a)$$

$$\Delta M_b = pk(\frac{1}{2}\Delta\theta_a + \Delta\theta_b) \quad (4.27b)$$

Using Eqs. 4.24 through 4.27, the incremental rotations can be expressed in terms of the incremental moments for each of the four states of stress. These relationships are used later in the determination of energy absorption as well as ductility ratio.

a. Both ends a and b are in the elastic range:

$$\Delta\theta_a = \frac{4}{3k}(\Delta M_a - \frac{1}{2}\Delta M_b) \quad (4.28a)$$

$$\Delta\theta_b = \frac{4}{3k}(-\frac{1}{2}\Delta M_a + \Delta M_b) \quad (4.28b)$$

b. End a is in the plastic range, end b in the elastic range:

$$\Delta\theta_a = (\frac{1}{p} + \frac{1}{3})\frac{\Delta M_a}{k} - \frac{2}{3k}\Delta M_b \quad (4.29a)$$

$$\Delta\theta_b = \frac{-2\Delta M_a + 4\Delta M_b}{3k} \quad (4.29b)$$

c. End a is in the elastic range, end b in the plastic range:

$$\Delta\theta_a = \frac{4\Delta M_a - 2\Delta M_b}{3k} \quad (4.30a)$$

$$\Delta\theta_b = \frac{-2\Delta M_a}{3k} + (\frac{1}{p} + \frac{1}{3})\frac{\Delta M_b}{k} \quad (4.30b)$$

d. Both ends a and b are in the plastic range:

$$\Delta\theta_a = \frac{4\Delta M_a - 2\Delta M_b}{3pk} \quad (4.31a)$$

$$\Delta\theta_b = \frac{-2\Delta M_a + 4\Delta M_b}{3pk} \quad (4.31b)$$

3. Stiffness of a Member. The derivation of the stiffness of a member is derived here for each of the four states of yield as discussed in the previous section. Let the force-deformation relationships of a typical member be shown in Fig. 4.5. Using the slope-deflection theory

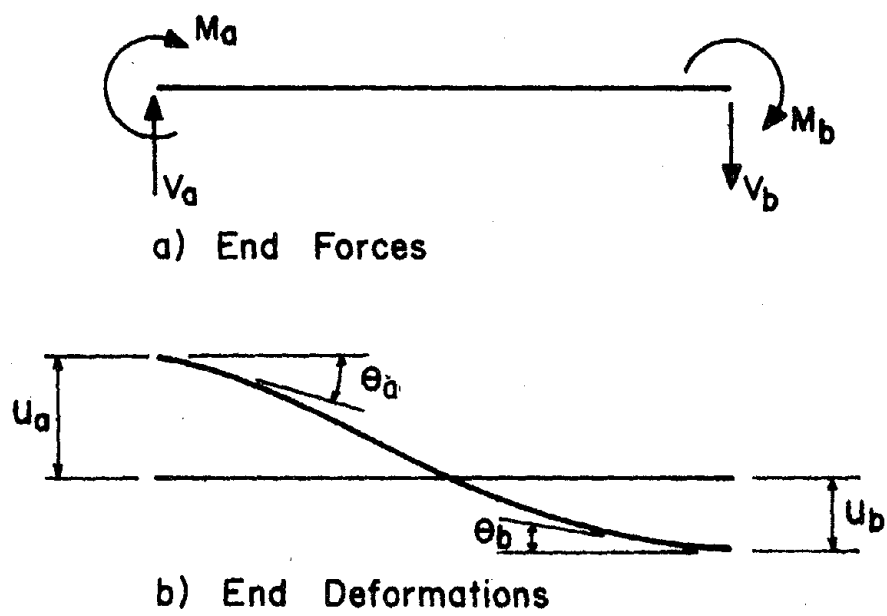


Figure 4.5. Forces and Deformations of a Typical Member

will then yield the following incremental moment equations associated with the elastic state of yield:

$$\Delta M_a = \frac{4EI}{L}(\Delta\theta_a + \frac{1}{2}\Delta\theta_b) - \frac{6EI}{L^2}(\Delta u_a + \Delta u_b) \quad (4.32a)$$

$$\Delta M_b = \frac{4EI}{L}(\frac{1}{2}\Delta\theta_a + \Delta\theta_b) - \frac{6EI}{L^2}(\Delta u_a + \Delta u_b) \quad (4.32b)$$

$$\Delta V_a = \frac{-6EI}{L^2}(\Delta\theta_a + \Delta\theta_b) + \frac{12EI}{L^2}(\Delta u_a + \Delta u_b) \quad (4.32c)$$

$$\Delta V_b = \frac{-6EI}{L^2}(\Delta\theta_a + \Delta\theta_b) + \frac{12EI}{L^2}(\Delta u_a + \Delta u_b) \quad (4.32d)$$

The above equations can also be obtained from the two component members of Fig. 4.4. For the elastic state of yield, $\alpha_a = \alpha_b = 0$, and since $p + q = 1$, the sum of the end forces of the two components will give the same results as shown in Eq. 4.32. Setting $a = 4EI/L$, $b = 2EI/L$, $c = 6EI/L^2$ and $d = 12EI/L^3$, the stiffness matrix of a member for the elastic state of yield will be:

$$\begin{Bmatrix} \Delta M_a \\ \Delta M_b \\ \Delta V_a \\ \Delta V_b \end{Bmatrix} = \begin{bmatrix} a & b & -c & -c \\ & a & -c & -c \\ & & d & d \\ \text{symm.} & & & d \end{bmatrix} \begin{Bmatrix} \Delta\theta_a \\ \Delta\theta_b \\ \Delta u_a \\ \Delta u_b \end{Bmatrix} \quad (4.33)$$

When either one or both ends of a member become plastic, modification of the member stiffness is necessary. Assuming the left end of the member i becomes plastic, the total incremental forces at each end of the member are obtained from the two component members shown in Fig. 4.4. The incremental moment at end a may be expressed as

$$\Delta M_a = \Delta M_{1a} + \Delta M_{2a} \quad (4.34)$$

The incremental moments ΔM_{1a} and ΔM_{2a} refer to the elasto-plastic and elastic components, respectively. Slope-deflection theory is used to derive the incremental moment equations based on the elastic stiffness of each of the components as shown in Fig. 4.3. Therefore,

$$\Delta M_{1a} = q \frac{4EI}{L} (\Delta \omega_a + \frac{1}{2} \Delta \omega_b) - q \frac{6EI}{L^2} (\Delta u_a + \Delta u_b), \text{ and}$$

$$\Delta M_{2a} = p \frac{4EI}{L} (\Delta \theta_a + \frac{1}{2} \Delta \theta_b) - p \frac{6EI}{L^2} (\Delta u_a + \Delta u_b).$$

For this state of yield,

$$\Delta \omega_a = \Delta \theta_a - \Delta \alpha_a \quad (4.35a)$$

$$\Delta \omega_b = \Delta \theta_b \quad (4.35b)$$

$$\Delta M_{1a} = 0 \quad (4.35c)$$

Using $\Delta M_{1a} = 0$ yields

$$0 = q \frac{4EI}{L} (\Delta\theta_a - \Delta\alpha_a + \frac{1}{2}\Delta\theta_b) - q \frac{6EI}{L^2} (\Delta u_a + \Delta u_b)$$

from which

$$\Delta\alpha_a = \Delta\theta_a + \frac{1}{2}\Delta\theta_b - \frac{3}{2L}(\Delta u_a + \Delta u_b) \quad (4.36)$$

Substituting Eqs. 4.35c and 4.36 into Eq. 4.34 gives the resulting moment equation:

$$\Delta M_a = p \frac{4EI}{L} (\Delta\theta_a + \frac{1}{2}\Delta\theta_b) - p \frac{6EI}{L^2} (\Delta u_a + \Delta u_b) \quad (4.37)$$

The incremental moment at right end b may be similarly obtained as:

$$\Delta M_b = \Delta M_{1b} + \Delta M_{2b} \quad (4.38)$$

$$\text{where } \Delta M_{1b} = q \frac{3EI}{L} \Delta\theta_b - q \frac{3EI}{L^2} (\Delta u_a + \Delta u_b)$$

$$\Delta M_{2b} = p \frac{4EI}{L} (\frac{1}{2}\Delta\theta_a + \Delta\theta_b) - p \frac{6EI}{L^2} (\Delta u_a + \Delta u_b)$$

Finally, Eq. 4.38 becomes

$$\Delta M_b = p \frac{2EI}{L} \Delta\theta_a + (p \frac{4EI}{L} + q \frac{3EI}{L}) \Delta\theta_b - (p \frac{6EI}{L^2} + q \frac{3EI}{L^2}) (\Delta u_a + \Delta u_b) \quad (4.39)$$

The incremental shear at end a is

$$\Delta V_a = \Delta V_{1a} + \Delta V_{2a} \quad (4.40)$$

$$\begin{aligned} \text{where } \Delta V_{1a} = & q \frac{-6EI}{L^2} (\Delta \theta_a + \Delta \theta_b) + q \frac{12EI}{L^3} (\Delta u_a + \Delta u_b) \\ & + q \frac{6EI}{L^2} \left[\Delta \theta_a + \frac{1}{2} \Delta \theta_b - \frac{3}{2L} (\Delta u_a + \Delta u_b) \right] \end{aligned}$$

$$\Delta V_{2a} = p \frac{-6EI}{L^2} (\Delta \theta_a + \Delta \theta_b) + p \frac{12EI}{L^3} (\Delta u_a + \Delta u_b)$$

Combining the above equations yields the results of Eq. 4.40 as

$$\Delta V_a = -p \frac{6EI}{L^2} \Delta \theta_a - \left(p \frac{6EI}{L^2} + q \frac{3EI}{L^2} \right) \Delta \theta_b + \left(p \frac{12EI}{L^3} + q \frac{9EI}{L^3} \right) (\Delta u_a + \Delta u_b) \quad (4.41)$$

For the right end b, the shear in incremental form is

$$\Delta V_b = \Delta V_{1b} + \Delta V_{2b} \quad (4.42)$$

where $\Delta V_{1b} = \Delta V_{1a}$ and $\Delta V_{2b} = \Delta V_{2a}$ as shown in Eq. 4.40. Consequently, the final result of Eq. 4.42 becomes

$$\Delta V_b = -p \frac{6EI}{L^2} \Delta \theta_a - \left(p \frac{6EI}{L^2} + q \frac{3EI}{L^2} \right) \Delta \theta_b + \left(p \frac{12EI}{L^3} + q \frac{9EI}{L^3} \right) (\Delta u_a + \Delta u_b) \quad (4.43)$$

Setting $e = 3EI/L$, $f = 3EI/L^2$ and $g = 3EI/L^3$, the member stiffness can be generated from Eqs. 4.37, 4.39, 4.41 and 4.43 as follows:

$$\begin{Bmatrix} \Delta M_a \\ \Delta M_b \\ \Delta V_a \\ \Delta V_b \end{Bmatrix} = \begin{bmatrix} pa & pb & -pc & -pc \\ & pa+qe & -pc-ql & -pc-ql \\ & \text{symm.} & pd+qg & pd+qg \\ & & & pd+qg \end{bmatrix} \begin{Bmatrix} \Delta \theta_a \\ \Delta \theta_b \\ \Delta u_a \\ \Delta u_b \end{Bmatrix} \quad (4.44)$$

The stiffness matrix of a member with end b plastic and end a elastic can be similarly obtained as:

$$\begin{Bmatrix} \Delta M_a \\ \Delta M_b \\ \Delta V_a \\ \Delta V_b \end{Bmatrix} = \begin{bmatrix} pa+qe & pb & -pc-ql & -pc-ql \\ & pa & -pc & -pc \\ & \text{symm.} & pd+qg & pd+qg \\ & & & pd+qg \end{bmatrix} \begin{Bmatrix} \Delta \theta_a \\ \Delta \theta_b \\ \Delta u_a \\ \Delta u_b \end{Bmatrix} \quad (4.45)$$

When both ends become plastic, only the elastic component is considered and the stiffness of the member will be:

$$\begin{Bmatrix} \Delta M_a \\ \Delta M_b \\ \Delta V_a \\ \Delta V_b \end{Bmatrix} = p \begin{bmatrix} a & b & -c & -c \\ & a & -c & -c \\ & \text{symm.} & d & d \\ & & & d \end{bmatrix} \begin{Bmatrix} \Delta \theta_a \\ \Delta \theta_b \\ \Delta u_a \\ \Delta u_b \end{Bmatrix} \quad (4.46)$$

4. Total Stiffness of a Structure. The total stiffness matrix $[K]$ for a structure containing plastic hinges is formulated in the same manner as one containing no plastic hinges.⁴⁴

$$[K] = [A][S][A]^T \quad (4.47)$$

where $[A]$ = static equilibrium matrix

$[S]$ = stiffness matrix of all members

Generation of $[K]$ is accomplished by the computer program without generating the $[S]$ matrix. The member lengths, moment of inertia of their cross-sections and the elastic modulus of the structure in conjunction with the static equilibrium matrix $[A]$ are used to calculate the elements in $[K]$ based on the four states of stress discussed in the previous article. The matrix $[A]$ can be generated in the program by providing a limited amount of input data.

C. REDUCTION OF ALLOWABLE MOMENT IN COLUMNS

Due to the static and dynamic loads applied to a structure as produced by the weight of the structure and earthquake loading, respectively, the axial load in the columns of that structure may be such as to reduce the moment carrying capacity of these members. The interaction formulas of AISC³⁴, used for plastic design of members having combined bending and axial loads,²⁶ are used here to formulate a reduction factor for the M_p values of each column when warranted by the magnitude of the axial load. The interaction formulas are given as follows:

$$\frac{P}{P_{cr}} + \frac{c_m M}{(1 - P/P_e) M_m} \leq 1.0 \quad (4.48)$$

$$\frac{P}{P_y} + \frac{M}{1.18 M_p} \leq 1.0 \quad (M < M_p, \frac{P}{P_y} > 0.15) \quad (4.49)$$

where P = axial load in column, kips;

$$P_{cr} = 1.7AF_a;$$

F_a = allowable axial stress, ksi;

A = gross area of cross section, in.²;

$M = M_{pc}$ = permissible moment based on axial plus bending loads, k-ft;

$$P_e = 1.92AF'_e;$$

$$F'_e = \pi^2 EK_1 [1.92(K\ell_b/r_b)^2];$$

ℓ_b = actual unbraced length in the plane of bending, in.;

r_b = radius of gyration in the plane of bending;

K = effective length factor in plane of bending;

K_1 = earthquake and wind factor = 4/3;

E = modulus of elasticity, ksi;

c_m = coefficient depending on whether braced or unbraced and whether moment is caused by applied end moments or transverse loading;

M = applied moment, k-ft;

$$M_m = M_p;$$

$P_y = F_y A$; and

F_y = yield stress of material, ksi

Assuming all columns are braced in the weak direction results in the above equation for M_m . To be conservative in the determination of the M_p reduction factor, the values $c_m = 0.85$ and $K = 1.0$ are assumed.

Based on the above interaction formulas and the assumed conditions of a member the following equations are derived for determining the required reduction factor for M_p due to large axial compressive loads:

$$\frac{M_{pc}}{M_p} = \left(1 - \frac{P}{P_{cr}}\right) \left(1 - \frac{P}{P_e}\right) \frac{1}{c_m} \quad (4.50)$$

$$\frac{M_{pc}}{M_p} = 1.18 \left(1 - \frac{P}{P_y}\right) \quad \left(\frac{P}{P_y} > 0.15\right) \quad (4.51)$$

The smaller of the two reduction factors that is less than 1.0 is used in determining the reduced moment capacity.

D. ENERGY

There are two reasons for the formulation of energy. First, the overall behavior of a structure can be determined using energy concepts. This will indicate the ability of that structure to successfully respond to a particular earthquake motion. If a structure is able to store the total input energy as the result of an earthquake in the form of elastic strain energy, the integrity of the structure is greater than that for which part of the input energy must be dissipated by strain energy as a result of permanent set. Also, the integrity of one structure would be greater than another if it were necessary to dissipate less strain energy for the one structure when both are subjected to the same earthquake motion.

The second reason for the formulation of energy is to provide a means of checking the accuracy of the step-by-step integration technique used. The law for the conservation of energy states in equation form

$$E_i = E_s + E_d \quad (4.52)$$

where E_i = total input energy up to a certain time,

E_s = total stored energy in the form of kinetic energy and elastic strain energy at that time,

E_d = total dissipated energy in the form of strain energy due to permanent set and energy dissipated due to damping up to that time.

The above energy terms are formulated in the following articles.

1. Input Energy. The total input energy of a structure at the end of a time increment as a result of support motion in both the horizontal and vertical direction is obtained by summing the following terms.

- (1) the product of the average horizontal column shears, V_{ave} , and the incremental horizontal ground displacements, Δx_g ,
- (2) the product of the average vertical column reactions, R_{yave} , and the incremental vertical ground displacements, Δy_g , and
- (3) the product of the average horizontal force, $\{F_p\}$, for each floor due to the P-delta effect and the corresponding incremental values of the absolute horizontal floor displacements, $\{\Delta x_s\}_{ab}$.

In equation form, the input energy at the end of a time increment is

$$E_i = \sum_{t=0}^t (V_{ave}(\Delta x_g) + R_{yave}(\Delta y_g) + \{F_p\}^T \{\Delta x_s\}_{ab}) \quad (4.53)$$

where $\{F_p\}$ is given in Eq. 4.12 and

$$\{\Delta x_s\}_{ab} = \{(\Delta x_s + \Delta x_g)\}$$

2. Stored Energy Due to Elastic Strain. The amount of elastic strain energy stored in a structure is the sum of the elastic strain energy for each member. Since only bending deformations are considered, the elastic strain energy must only be based on bending. The formulation of the elastic strain energy for a typical member can either be found from the basic equation of virtual work³³ or from the moment-rotation curve for each end of the members. Both derivations will be shown here for justification of the use of the moment-rotation relationships when considering a bilinear response.

The basic equation for the elastic strain energy in a member due to bending only is

$$E_{es} = \int_0^L \frac{M^2}{2EI} dx \quad (4.54)$$

For a typical member i the moment varies linearly across the length of the member as shown in Fig. 4.6. The equation for the moment in member i can be written in terms of x , the distance from the left end.

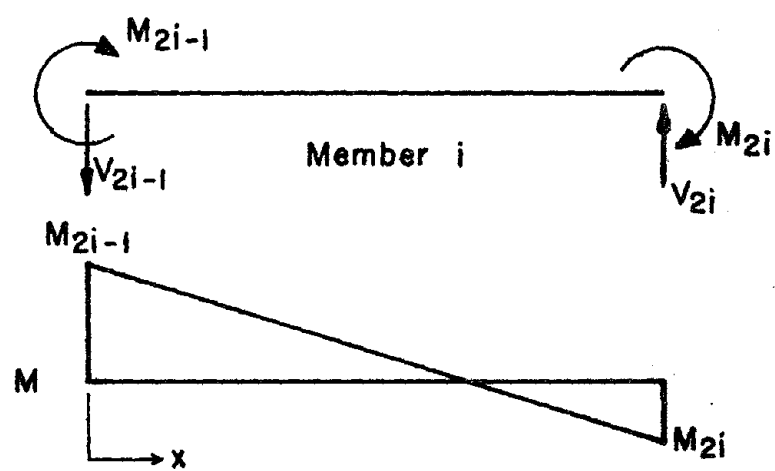


Figure 4.6. Member Moment Diagram

$$M_i = M_{2i-1} - \frac{x}{L}(M_{2i-1} + M_{2i}) \quad (4.55)$$

Substitution of the expression for M_i , Eq. 4.55, into Eq. 4.54 and then performing the integration yields the following equation for the elastic strain energy in member i :

$$E_{esi} = \frac{L_i}{6EI_i} \{M_{2i-1}^2 - M_{2i-1}M_{2i} + M_{2i}^2\} \quad (4.56)$$

The same expression for the elastic strain energy due to bending can be obtained from the moment-rotation curve for each end of member i . The total elastic strain energy for member i is the work produced by the end-moments going through their corresponding end rotations. This is equivalent to the area under the moment-rotation curve for each end of member i .

$$E_{esi} = \frac{1}{2}M_{2i-1}\theta_{2i-1} + \frac{1}{2}M_{2i}\theta_{2i} \quad (4.57)$$

The end moments in terms of rotations are known from slope-deflection equations as

$$M_{2i-1} = \frac{4EI_i}{L_i} \theta_{2i-1} + \frac{2EI_i}{L_i} \theta_{2i} \quad (4.58a)$$

$$M_{2i} = \frac{2EI_i}{L_i} \theta_{2i-1} + \frac{4EI_i}{L_i} \theta_{2i} \quad (4.58b)$$

Solving for rotations in terms of moment, Eqs. 4.58 can be written

$$\theta_{2i-1} = \frac{L_i}{6EI_i} [2M_{2i-1} - M_{2i}] \quad (4.59a)$$

$$\theta_{2i} = \frac{L_i}{6EI_i} [-M_{2i-1} + 2M_{2i}] \quad (4.59b)$$

Substitution of Eqs. 4.59 into Eq. 4.57 results in the Eq. 4.56, the same equation found based on the basic equation for elastic strain energy due to bending.

The total elastic strain energy for the structure is the sum of the elastic strain energies for all the members.

$$E_{es} = \sum_{i=1}^N \frac{L_i}{6EI_i} (M_{2i-1}^2 - M_{2i-1}M_{2i} + M_{2i}^2) \quad (4.60)$$

Since a step-by-step integration method is used, the incremental form for the elastic strain energy is necessary. This formulation is derived from the moment-rotation curve as shown in Fig. 4.7. The change in elastic strain energy of a member over a time increment Δt is the area under the moment-rotation curve for each end of the member when the node at that end is in the elastic range. In equation form this is

$$\Delta E_{esi} = (M_{2i-1})_{ave} \Delta \theta_{2i-1} + (M_{2i})_{ave} \Delta \theta_{2i} \quad (4.61)$$

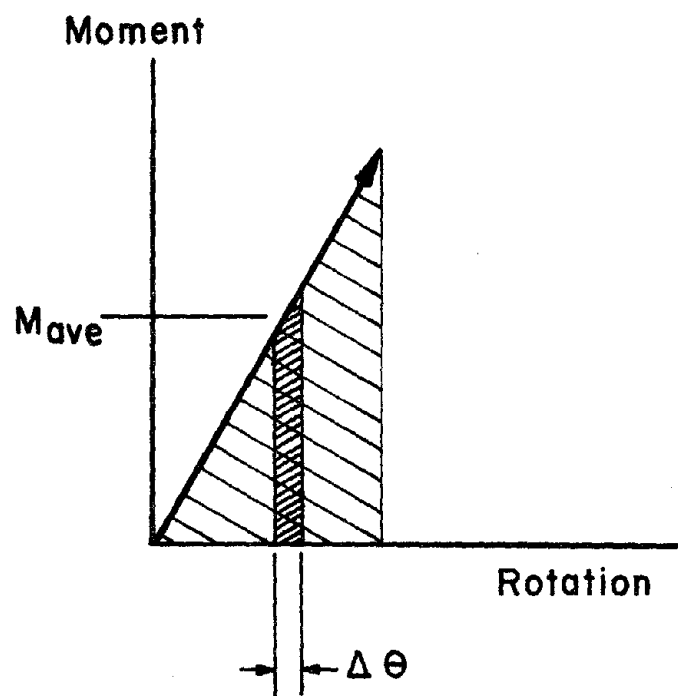


Figure 4.7. Elastic Moment-Rotation Relationship

$$\text{where } (M_{2i-1})_{\text{ave}} = [(M_{2i-1})_t + (M_{2i-1})_{t+\Delta t}]/2$$

$$(M_{2i})_{\text{ave}} = [(M_{2i})_t + (M_{2i})_{t+\Delta t}]/2$$

$$\Delta\theta_{2i-1} = (L/6EI)_i [2\Delta M_{2i-1} - \Delta M_{2i}]$$

$$\Delta\theta_{2i} = (L/6EI)_i [-\Delta M_{2i-1} + 2\Delta M_{2i}]$$

The total increment of the elastic strain energy for the structure is the sum of the elastic strain energies for all the members.

$$\Delta E_{\text{es}} = \sum_{i=1}^N [(M_{2i-1})_{\text{ave}} \Delta\theta_{2i-1} + (M_{2i})_{\text{ave}} \Delta\theta_{2i}] \quad (4.62)$$

3. Kinetic Energy. Kinetic energy is stored in the multi-story structure by virtue of the velocities of the lumped masses as a result of the ground motion. The general equation for kinetic energy of a mass m having a velocity v may be derived as³²

$$\text{kinetic energy} = \frac{1}{2} mv^2 \quad (4.63)$$

When dealing with both horizontal and vertical ground motion, the two components of kinetic energy are obtained in the following form:

$$E_k = \frac{1}{2} \sum_{j=1}^{N_f} m_j (\dot{x}_{sj} + \dot{x}_g)^2 + \frac{1}{2} \sum_{k=1}^m m_k (\dot{x}_{vk} + \dot{y}_g)^2 \quad (4.64)$$

where N_f = number of floors,

N_m = number of lumped masses,

m_j = mass of j th floor,

m_k = lumped mass k ,

\dot{x}_{sj} = velocity in horizontal direction relative to base of mass at floor level j ,

\dot{x}_g = horizontal velocity of ground due to earthquake,

\dot{x}_{vk} = vertical velocity of mass k relative to the ground, and

\dot{y}_g = vertical velocity of ground due to earthquake.

4. Dissipated Energy Due to Damping. The equation for the dissipated energy due to damping is found from the work produced by the damping force going through the relative displacement of the mass. For a one-degree-of-freedom system the damping force equals the damping coefficient times the velocity of the mass. Therefore, the incremental work dissipated due to damping is

$$dW_d = C \dot{x}_s du = C \dot{x}_s (\dot{x}_s + \dot{x}_g) dt \quad (4.65a)$$

and

$$W_d = C \int_0^t \dot{x}_s (\dot{x}_s + \dot{x}_g) dt \quad (4.65b)$$

which is the total energy dissipated by damping up to time t .

When using the incremental approach for the analysis of multi-story structures, the equation for the dissipated energy of a frame due to damping will be:

$$E_{dd} = ([C]^T \{\dot{x}\}_{ave})^T \{\dot{u}_s\}_{ave} \Delta t \quad (4.66)$$

where $[C]$ = damping coefficient matrix,

$\{\dot{x}\}_{ave}$ = average relative velocity vector over Δt for each translation degree of freedom,

$\{\dot{u}_s\}_{ave}$ = average absolute velocity over Δt for each translation degree of freedom, and

Δt = time increment.

5. Dissipated Energy Due to Plastic Rotation. Energy is also allowed to dissipate due to the permanent set caused by the plastic rotation. The amount of energy dissipated for a member node due to this mechanism is found from the moment-rotation curve as shown in Fig. 4.8. For the elasto-plastic condition in Fig. 4.8a the dissipated strain energy during a half cycle of rotation is equal to the area under the curve OABC. Using the step-by-step method of analysis, this is equivalent to

$$E_{ds} = \sum_{i=1}^{N_{\Delta t}} M_p \Delta \theta_i \quad (4.67)$$

where $N_{\Delta t}$ = number of time increments in which the node of a member is in plastic range,

M_p = plastic moment, and

$\Delta \theta_i$ = end rotation during time increment i .

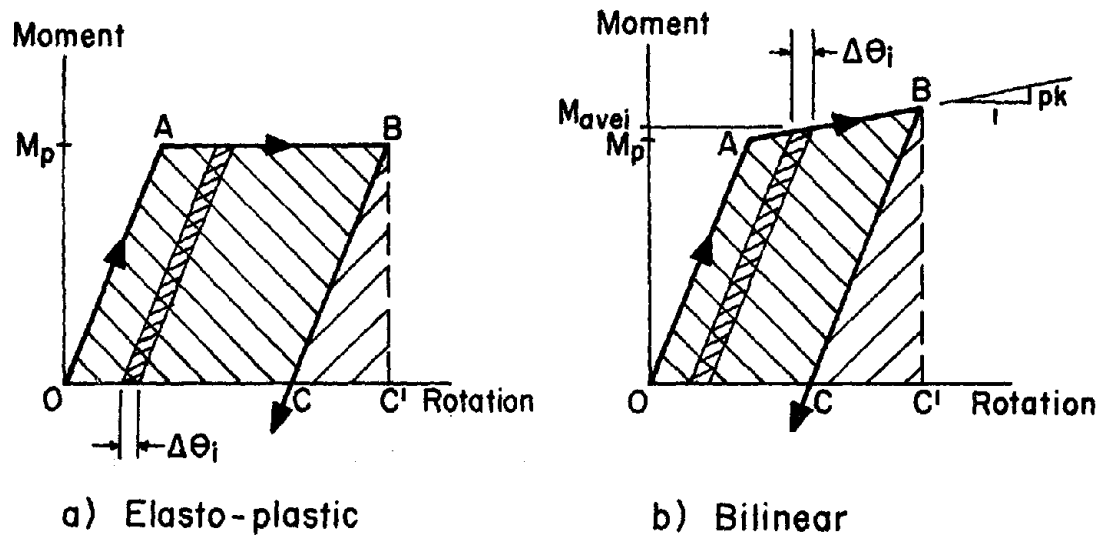


Figure 4.8. Inelastic Moment-Rotation Relationship

When considering a bilinear response, the dissipated strain energy during a half cycle is equal to the area under the curve OABC of Fig. 4.8b which can be expressed in the following form:

$$E_{ds} = \sum_{i=1}^{N_{\Delta t}} M_{avei} \Delta\theta_i (1 - p) \quad (4.68)$$

where $N_{\Delta t}$ = number of time increments in which a joint is in the bilinear range,

M_{avei} = average end moment during time increment i ,

$\Delta\theta_i$ = end rotation during time increment i , and

$p = k_2/k$ = strain hardening ratio.

Note, the above equation reduces to the equation for the dissipated strain energy in a elasto-plastic response when $p = 0$ as given in Eq. 4.67.

The above equations for the dissipated strain energy E_{ds} (Eqs. 4.67 and 4.68) apply to one node of a member. To obtain the total dissipated strain energy of a frame due to strain hardening, the equations are applied to each node of all the constituent members.

6. Elastic Strain Energy For Bilinear Response. The total elastic strain energy during a half cycle of rotation for a member node having bilinear response characteristics is found from the area BCC' of Fig. 4.8b. Introducing a new term, the bilinear strain energy, E_{bl} , defined by area OABC' of Fig. 4.8b, the elastic strain energy during a half cycle of rotation is

$$E_{es} = E_{bl} - E_{ds} \quad (4.69)$$

in which E_{bl} is the total strain energy, stored plus dissipated, during the response of a structure due to earthquake loading. Note, the above equation also applies to the elasto-plastic response of a joint as shown in Fig. 4.8a.

E. DUCTILITY AND EXCURSION RATIO

Three definitions of the ductility ratio for determining the ductility requirement of earthquake structures are formulated in this section. The corresponding excursion ratio is also formulated to indicate the total plastic rotation or dissipated energy of each node of structural members during the loading process.

The three definitions of the ductility ratio are based on symmetrical bending, curvature and strain energy; the ductility ratio based on strain energy seems to have certain advantages for the two-dimensional loading. A numerical comparison using the above three definitions of the ductility ratio and corresponding excursion ratio is made in Section VII-C.

1. Ductility Ratio Based on Symmetrical Bending. The traditional definition^{45,29} of the ductility ratio μ_1 is based on symmetrical bending of a structural member. The half cycle of the moment-rotation curve for either end of such a member is shown in Fig. 4.9 based on a bilinear material response. Both ends of the member become plastic when the end moment reaches the plastic moment, M_p . The ductility ratio based on symmetrical bending is defined as the maximum absolute nodal rotation $|\theta|_{\max}$ divided by the yield rotation θ_y . Using the

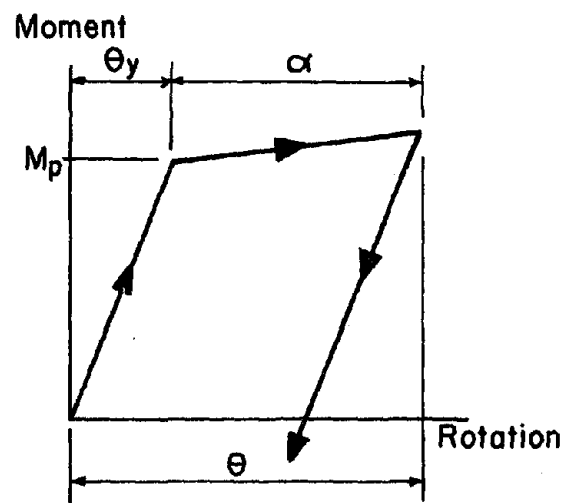


Figure 4.9. Moment-Rotation, Ductility Based on Symmetrical Bending

notation of Fig. 4.8, μ_1 can be written as

$$\mu_1 = \frac{|\theta|_{\max}}{\theta_y} = \frac{\theta_y + \alpha}{\theta_y} = 1 + \frac{\alpha}{\theta_y} \quad (4.70)$$

where α = plastic rotation. Since the yield rotation is based on symmetrical bending, it can be expressed as $\theta_y = M_p L / 6EI$, where L is the length of the member and EI is the member's flexural rigidity.

The excursion ratio ϵ_1 corresponding to the ductility ratio can be defined as the total plastic rotation of a node of a member divided by the yield rotation of the joint. Thus

$$\epsilon_1 = \sum_{i=1}^{N_\mu} \frac{\alpha_i}{\theta_y} \quad (4.71)$$

where N_μ = total number of times the node becomes plastic,

α_i = plastic rotation of the node during a half cycle of rotation i , and

θ_y = yield rotation of symmetric bending.

In terms of the ductility ratios the excursion ratio can be written as

$$\epsilon_1 = \sum_{i=1}^{N_\mu} (\mu_{1i} - 1)$$

where μ_{1i} is the ductility ratio for the half cycle plastic rotation i .

When considering a typical moment-resisting frame subjected to both horizontal and vertical components of an earthquake, symmetrical bending is seldom present in any of the members. Therefore, the use of the yield moment rotation based on symmetrical bending would only normalize the total nodal rotation. An adequate indication of the ductility requirement of the members would only be obtained if all members had the same end moment relationship.

The yield rotation for a typical member is a function of its yield moment, stiffness properties, and the moment conditions at the opposite end of the member. The general equation for the yield rotation can be written as $\theta_y = CM_p L/EI$, where C is the coefficient based on the moment condition at the opposite end of the member. Table 4.1 lists the value of C based on selected end moment conditions for the opposite end.

Table 4.1. Value of C in $\theta_y = CM_p L/EI$ Based on Different Conditions of Opposite End of a Member

Moment at Opposite End (clockwise positive)	Value of C
M_p	1/6
$M_p/2$	1/4
0	1/3
$-M_p/2$	5/12
$-M_p$	1/2

The coefficient C has a minimum value based on symmetrical bending. Therefore, the use of the equation for θ_y based on symmetrical bending will result in larger ductility and excursion ratio values for members not subjected to symmetrical bending.

2. Ductility Ratio Based On Curvature. The second definition of the ductility ratio is based on curvature.^{1,3} The ductility requirement is defined in terms of Fig. 4.10 as follows:

$$\mu_2 = \frac{\phi_{\max}}{\phi_y} = \frac{\phi_y + \phi_o}{\phi_y} = 1 + \frac{\phi_o}{\phi_y} \quad (4.73)$$

where ϕ_{\max} = maximum curvature,

ϕ_y = curvature at yield, and

ϕ_o = plastic curvature.

For members which contain symmetrical bending this equation for μ_2 is the same as for μ_1 .

For bilinear systems this ratio can be expressed in terms of the moment value of Fig. 4.10 as follows:

$$\mu_2 = 1 + \frac{M_{\max} - M_p}{pM_p} \quad (4.74)$$

where M_{\max} = maximum moment at the end of a member,

M_p = plastic moment of the member, and

p = rate of strain hardening.

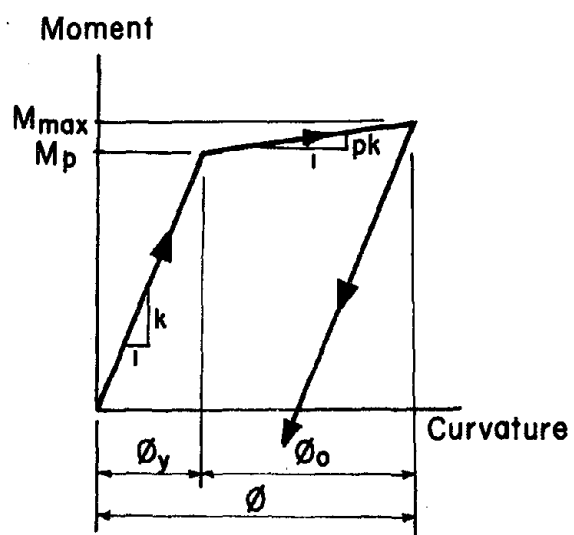


Figure 4.10. Moment-Rotation, Ductility Based on Curvature

The excursion ratio ϵ_2 corresponding to the ductility ratio based on curvature can be defined as

$$\epsilon_2 = \sum_{i=1}^{N_\mu} \frac{\phi_o}{\phi_y} = \sum_{i=1}^{N_\mu} (\mu_{2i} - 1) \quad (4.75)$$

where N_μ = total number of time the node of a member becomes plastic,
 μ_{2i} = ductility ratio for the half cycle plastic rotation i .

The excursion ratio can also be expressed in terms of bending moment or ductility ratio as:

$$\epsilon_2 = \sum_{i=1}^{N_\mu} \frac{(M_{\max})_i - M_p}{pM_p} = \sum_{i=1}^{N_\mu} (\mu_{2i} - 1) \quad (4.76)$$

A couple of advantages of the second definition for ductility over the first can be noted. First, as mentioned above, the ductility requirements based on curvature are applicable to nonsymmetrically loaded members as well as ones loaded symmetrically. Also, when analyzing bilinear systems, both the ductility and excursion ratios using the second definition can be determined from calculated end-moments.

3. Consideration of Stress Reversal. Before going to the third definition of ductility, consideration will be made of the reversal of the stress field occurring in flexural members as related to the ductility ratio. When a member has a stress reversal, the Bauschinger effect³⁵ is present. This consists of the effect of straining a

material in tension beyond its yield point and then reversing the load to obtain a lower yield point in compression than would be obtained if not initially placed in tension. This reduction is the result of residual stresses left in the material due to the tensile deformations. The Bauschinger effect is applicable to flexural members due to the stress reversals present above and below the neutral axis of the member cross-section.

There are several methods one can use to take into consideration the Bauschinger effect. The method used here and by most investigators consists of limiting the stress range or the elastic unloading range to $2M_p$. This causes the total elastic range of the material to remain constant. Figure 4.11 illustrates this method as applied to bilinear systems. A constant $2M_p$ is present in elasto-plastic systems by virtue of no strain hardening.

There are some questions as to the adaptability of the first two definitions of the ductility ratio when the stress range of $2M_p$ is used for bilinear systems. Figure 4.11 illustrates a situation which may result in a misleading ductility ratio. In this situation the first bilinear half cycle of rotation results in a large amount of plastic rotation. With a $2M_p$ stress range, the second half cycle of rotation will have a low absolute magnitude for M_p ; a corresponding low value for θ_y will result. Even though the amount of plastic rotation during the second half cycle of rotation is less than the first, a larger ductility ratio will result in misleading values for both half cycles of rotation.

The third definition of the ductility ratio is presented in an attempt to obtain a more adequate measure of the ductility requirement

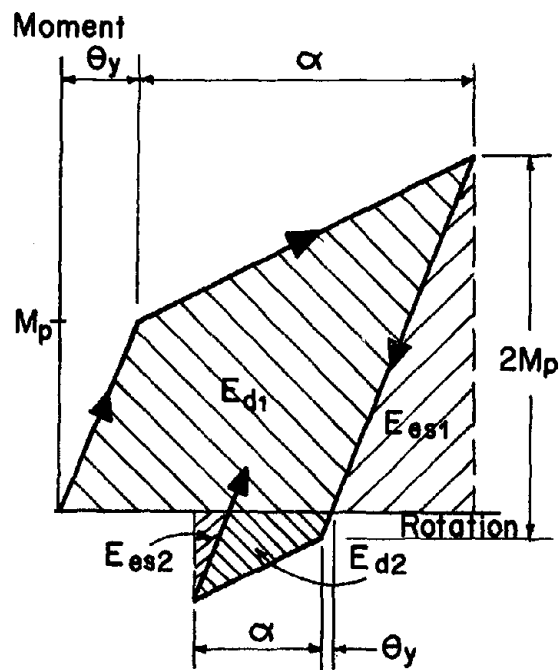


Figure 4.11. Effect of $2M_p$ Stress Range on Ductility

of a structure when considering stress reversals as well as both horizontal and vertical earthquake components.

4. Ductility Ratio Based on Energy. So that an adequate determination can be made of the ductility requirement of a structure, the definition for the ductility ratio should apply for all member end conditions and loading conditions. The ductility ratio should reflect the maximum necessary plastic rotation which a member must withstand as related to its yield condition. The yield condition is a function of the end condition of the member at the time of the plastic rotation.

When plastic rotation of the end of a member occurs, energy is dissipated in the form of strain energy. For an elasto-plastic system the amount of strain energy dissipated during the plastic rotation is directly proportional to the amount of rotation. This relationship between plastic rotation and dissipated strain energy provides ways of formulating the ductility ratio based on dissipated strain energy. This third definition of ductility ratio can be stated as the ratio of the dissipated strain energy of a member end to the total elastic strain energy in the member plus one as

$$\mu_3 = 1 + \frac{E_{ds}}{E_{tes}} \quad (4.77)$$

where E_{ds} = dissipated strain energy of a member end during half cycle of joint rotation as shown in Fig. 4.12, and

E_{tes} = total elastic strain energy in the member under consideration.

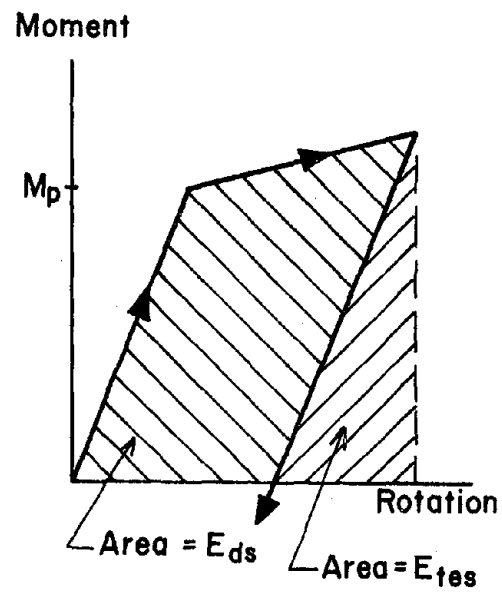


Figure 4.12. Moment-Rotation, Ductility Based on Energy

This third definition is similar to the previous definitions in that the ductility ratio is greater than one when plastic rotation occurs. Also, since the dissipated strain energy is related to the plastic rotation, any increase in the plastic rotation results in an increase in the dissipated strain energy and a corresponding increase in the ductility ratio. The total elastic strain energy in a member is a function of the work produced by the end moments going through the end rotations while in the elastic range. The elastic strain energy of the total member is used so that the yield condition of the member end in question is based on the end conditions of both ends of the member. The elastic strain energy stored in a member by its end moments is independent of the manner in which the end moments are reached. Therefore, the above definition of ductility ratio is especially applicable to structures excited by both horizontal and vertical earthquake components where a nonlinear relationship of end-moment and rotation is present.

A typical example of the moment-rotation curve for a joint in a structure excited by both horizontal and vertical ground motions is shown in Fig. 4.13. The single-bay frame contains a node at the center of the girder where half of the total girder mass is assumed concentrated. The nonlinearity of the response curve is the result of the vertical component of the ground motion acting on the mass at the center of the girder.

The maximum deviation a moment-rotation can have from the usual linear relationship is shown in Fig. 4.14 for an elasto-plastic system. Parallelogram ABCD establishes the boundary to be discussed. Lines OA and OB illustrate the linear paths for a member under symmetrical

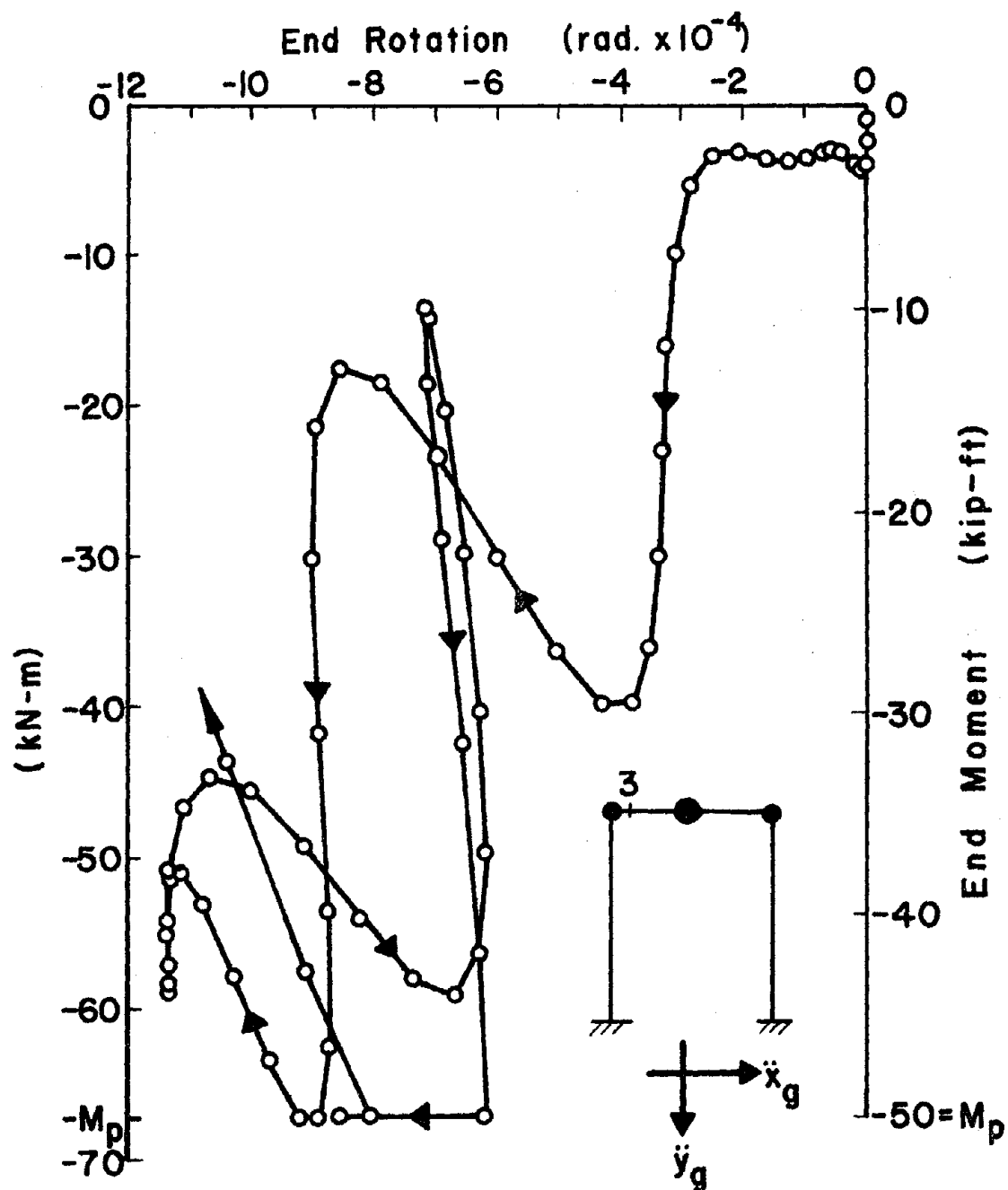


Figure 4.13. M- θ Curve of Node 3 for Horizontal and Vertical Ground Motions of 1940 El Centro

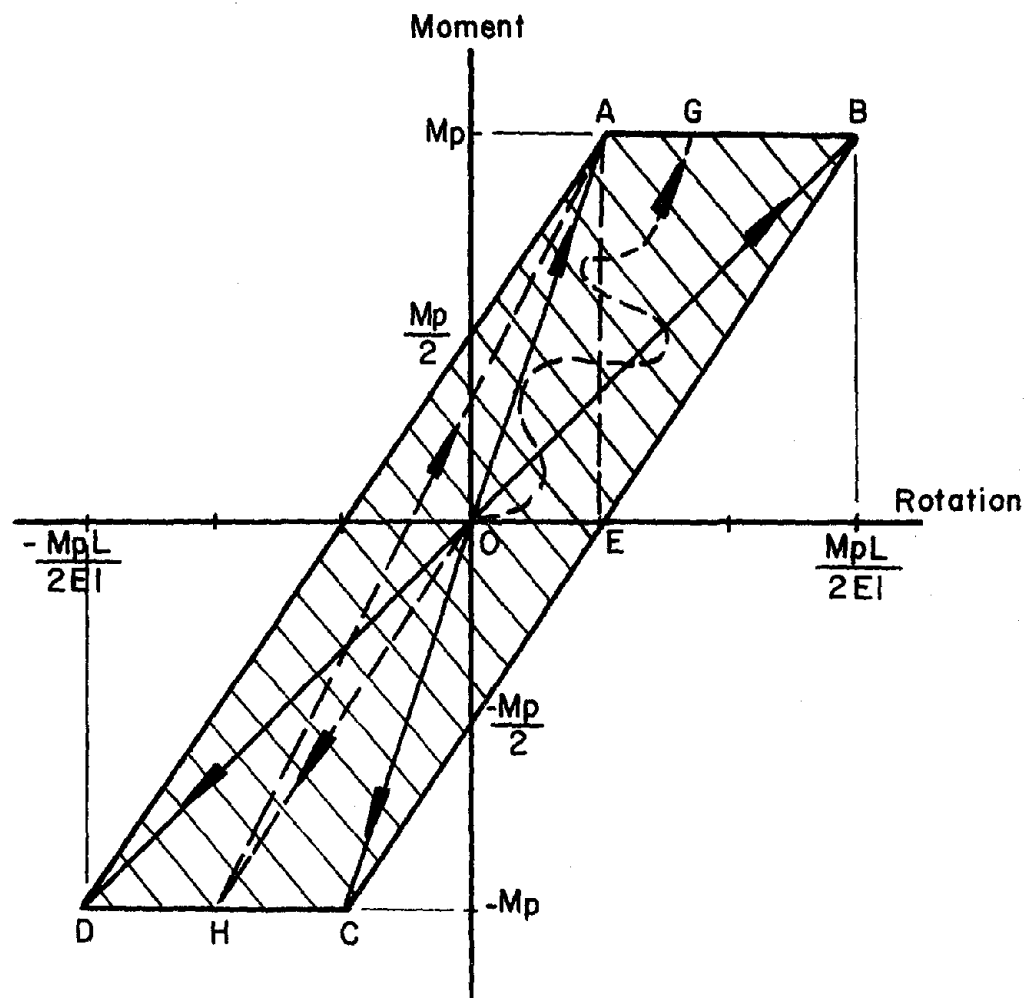
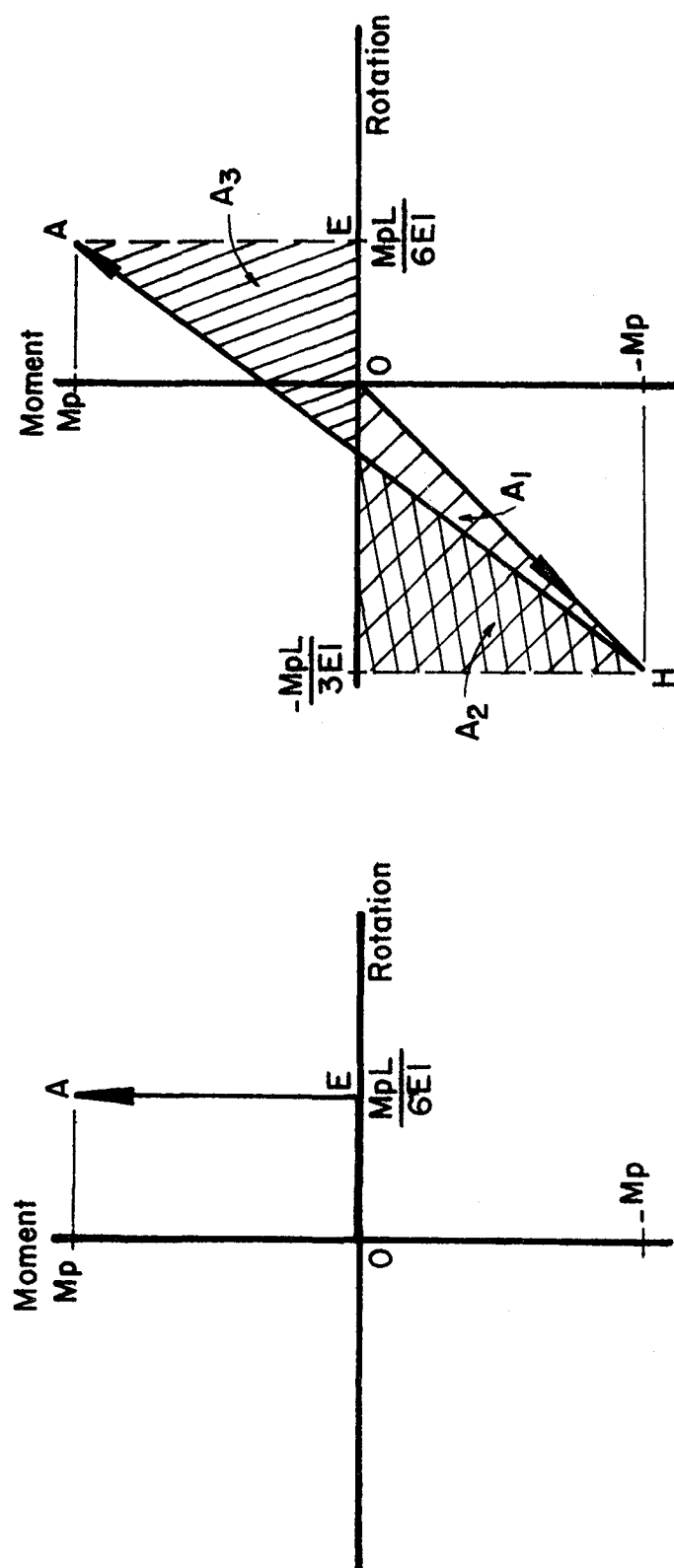


Figure 4.14. Moment-Rotation Boundary for One End of a Member

bending and pure bending, respectively. Lines OC and OD correspond to the negative paths of the same two bending conditions. Curve OG represents a typical curve comparable to the curve in Fig. 4.13 where the moment-rotation relationship is nonlinear.

An example will be shown to illustrate that the elastic strain energy in a member is independent of the manner in which the final end moments are obtained. Assume the final bending condition of a beam consists of symmetrical bending with an end moment of M_p as indicated by point A of Fig. 4.14. This condition is assumed to be reached by two different ways. First, let the member bending condition be reached by symmetrical bending from the unloaded to loaded condition. The moment-rotation curve for each end of the member for this way of loading will be path OA of Fig. 4.14. Second, the moment at the right end of the member is decreased to a negative M_p value while no moment is applied to the left end; a rotation of $-M_p L/3EI$ and $-M_p L/6EI$ will result at the right and left ends of the member, respectively. Now with the simultaneous application of increasing moments of M_p and $2M_p$ to the left and right ends of the member, respectively, the final symmetrical bending case is realized. The moment-rotation paths are also shown in Fig. 4.14. Dashed line OEA represents the left end while dashed line OHA represents the right end of the member.

The resulting elastic strain energy for each of the ways of increasing to the final symmetrical bending are found from the area under the moment-rotation curves. These areas are shown in Fig. 4.15 for the second approach to the symmetrical bending condition.



a) Left End of Member b) Right End of Member

Figure 4.15. Elastic Strain Energy of a Member Based on $M-\theta$ Relationship

(1) Symmetrical increase in end moments

$$E_{es1} = 2 \left[\frac{1}{2} \left(\frac{M_p L}{6EI} \right) \right] M_p = \frac{M_p^2 L}{6EI}$$

(2) Unsymmetrical increase in end moments

$$\begin{aligned} E_{es2} &= 0 + \frac{1}{2} \left(\frac{-M_p L}{3EI} \right) (-M_p) + \frac{1}{2} \left(\frac{M_p L}{4EI} \right) (-M_p) + \frac{1}{2} \left(\frac{M_p L}{4EI} \right) (M_p) \\ &= \frac{M_p^2 L}{6EI} \end{aligned}$$

Therefore, $E_{es1} = E_{es2}$, which illustrates that the elastic strain energy in a member is independent of the manner in which the final end moments are obtained. Apparently, the nonlinearity of the moment-rotation curves, when considering both horizontal and vertical earthquake components in conjunction with girder nodes, does not invalidate the third definition of the ductility ratio.

The advantages of the third definition for ductility ratio based on energy can be stated as follows:

1. Definition is general and applies to nonsymmetrical bending.
2. Definition is independent of the moment-curvature relationship assumed. Elasto-plastic, bilinear as well as the Ramberg-Osgood³⁰ relationships can be used.
3. Definition is more adaptable when considering a bilinear response with a $2M_p$ elastic stress range.
4. No problem results when moment-rotation relationship is non-linear due to inclusion of the vertical earthquake motion.

5. Dissipated and elastic energy values used in definition are easily determined from the area under the M- θ curve for the step-by-step method of analysis.
6. Definition is proportional to the energy dissipated in a node of a member due to plastic rotation.

The only disadvantage to the third definition of the ductility ratio is that the actual nodal rotation in the plastic range cannot be found directly from the ductility ratio for an elasto-plastic or bilinear response.

The excursion ratio based on the third definition for the ductility ratio is given below which indicates the total amount of energy that is dissipated in a node of a member due to plastic rotation:

$$\epsilon_3 = \sum_{j=1}^{N_\mu} \frac{E_{dsj}}{E_{tesj}} = \sum_{j=1}^{N_\mu} (\mu_{3j} - 1) \quad (4.78)$$

where N_μ = total number of times joint becomes plastic during earthquake excitation,

μ_{3j} = ductility ratio during half cycle j ,

E_{dsj} = dissipated strain energy during half cycle j , and

E_{tesj} = total elastic strain energy in member while end-moment is maximum during half cycle j .

Section VII-C will shown numerical comparisons of the ductility and excursion ratios based on the above definitions.

V. NUMERICAL METHODS OF INTEGRATION OF INCREMENTAL MOTION EQUATION

Different techniques are available for the step-by-step integration of the motion equation as formulated in Chapter IV (Eqs. 4.7). These methods are utilized to solve some typical problems to verify adequacy and possible running errors of the computer program. Also, the stability of the solution as well as its accuracy are considered.

A. NEWMARK BETA METHOD

The main technique used here for the step-by-step integration of the motion equation is Newmark's method.³⁶ The velocity and displacement at the end of any time increment is expressed in terms of the displacement, velocity and acceleration at the beginning of the time increment. The change in the acceleration during the time increment Δt can be assumed to have different forms of variation as determined by the coefficient β . The Newmark equations are as follows:

$$\dot{x}_{t+\Delta t} = \dot{x}_t + (\ddot{x}_t + \ddot{x}_{t+\Delta t})(\Delta t)/2 \quad (5.1)$$

$$x_{t+\Delta t} = x_t + \dot{x}_t(\Delta t) + \left(\frac{1}{2} - \beta\right)\ddot{x}_t(\Delta t)^2 + \beta\ddot{x}_{t+\Delta t}(\Delta t)^2 \quad (5.2)$$

where $\ddot{x}_{t+\Delta t}$, $\dot{x}_{t+\Delta t}$, $x_{t+\Delta t}$ = acceleration, velocity and displacement at the end of time increment Δt ,

\ddot{x}_t , \dot{x}_t , x_t = acceleration, velocity and displacement at the beginning of time increment Δt , and

β = coefficient controlling the change in acceleration over the time increment Δt .

A value of $\beta = 1/6$ was found to provide the best accuracy in the solution based on the earthquake loading. This value for β corresponds to assuming a linear variation in the acceleration over the time period Δt .

The incremental form for the velocity and acceleration for a time period Δt are derived from Eqs. 5.1 and 5.2.

$$\Delta \dot{x} = \frac{1}{2\beta(\Delta t)} \Delta x + B \quad (5.3)$$

$$\Delta \ddot{x} = \frac{1}{\beta(\Delta t)^2} \Delta x + A \quad (5.4)$$

where $B = \frac{-1}{2\beta} \dot{x}_t + (1 - \frac{1}{4\beta})\ddot{x}_t(\Delta t)$

$$A = \frac{-1}{\beta(\Delta t)} \dot{x}_t - \frac{1}{2\beta} \ddot{x}_t$$

The above incremental velocity and acceleration, Eqs. 5.3 and 5.4, are substituted into the generalized motion matrix equation given by Eq. 4.7. This results in a system of simultaneous equations containing $\{\Delta x\}$ as the only unknown term. In equation form,

$$\{\Delta x\} = [K^*]^{-1} \{\Delta R\} \quad (5.5)$$

$$\text{where } [K^*] = \frac{1}{\beta(\Delta t)^2}[M] + \frac{1}{2\beta(\Delta t)}[C] + [K'']$$

$$\{\Delta R\} = \{\Delta F\} + [\Delta K_s]\{x\}_t - [M]\{A\} - [C]\{B\}$$

The corresponding change in velocity and acceleration for each mass can be found from Eqs. 5.3 and 5.4, respectively.

The Newmark Beta method of step-by-step integration provides an adequate integration technique when dealing with constant interval lengths of time. The value of β can be changed to increase the accuracy for any given loading and initial value conditions.

The stability limit derived by Newmark³⁶ is the largest value of $(\Delta t)/T$ as based on β resulting in a stable solution. An unstable solution results in oscillations without bounds and does not agree at all with the exact solution. For a β of $1/6$ the stability limit is 0.551. This limit corresponds to a natural period of $T = 0.01815$ sec and a time interval of $\Delta t = 0.01$ sec. Therefore, mode and forcing frequencies of $1/0.01815 = 55.1$ Hz or greater may cause instability in the solution in the form of spurious increasing oscillations in the response output.

The principle of the conservation of energy as discussed in Section IV-D is used to indicate the degree to which the instability condition occurs as well as the amount of roundoff errors introduced in the integration process. Based on the principle of the conservation of energy the total input energy equals the stored energy in the structure plus the dissipated energy as given in Eq. 4.52. The

accuracy of the integration process is indicated by the percent error based on the following equation.

$$\% \text{ Error}_t = \frac{E_i - (E_s + E_d)}{E_i} (100) \quad (5.6)$$

where E_i = total input energy up to time t ,

E_s = total stored energy in the form of kinetic energy and elastic strain energy at time t , and

E_d = total dissipated energy in the form of strain energy due to permanent set and energy dissipated due to damping to the time t .

B. FOURTH-ORDER RUNGE-KUTTA

The quartic Runge-Kutta method for the step-by-step integration of the motion equation is used in the early stages of this research to verify the numerical solution by the Newmark Beta method. This Runge-Kutta method is based on a Taylor's expansion truncated after terms of the fourth order. Therefore, the per-step integration error is Δt^5 , since the terms containing Δt^5 and higher are neglected in the quartic formulation. The necessary equations of numerical integration when using this method are as follows for a single-degree-of-freedom system:

$$x_{t+\Delta t} = x_t + (\Delta t)\dot{x}_t + (\Delta t)(A + B + D)/6 \quad (5.7)$$

$$\dot{x}_{t+\Delta t} = \dot{x}_t + (A + 2B + 2D + E)/6 \quad (5.8)$$

$$\ddot{x}_{t+\Delta t} = m^{-1}[F_{t+\Delta t} - (K - K_s)x_{t+\Delta t} - C\dot{x}_{t+\Delta t}] \quad (5.9)$$

where

$$A = (\Delta t)m^{-1}[F_t - (K - K_s)x_t - C\dot{x}_t],$$

$$B = (\Delta t)m^{-1}[F_{t+\Delta t/2} - (K - K_s)(x_t + (\Delta t)\dot{x}_t/2) - C(\dot{x}_t + A/2)],$$

$$D = (\Delta t)m^{-1}[F_{t+\Delta t/2} - (K - K_s)(x_t + (\Delta t)\dot{x}_t/2 + (\Delta t)A/4) - C(\dot{x}_t + B/2)],$$

$$E = (\Delta t)m^{-1}[F_{t+\Delta t} - (K - K_s)(x_t + (\Delta t)\dot{x}_t + (\Delta t)B/2) - C(\dot{x}_t + D)],$$

$\ddot{x}_{t+\Delta t}$, $\dot{x}_{t+\Delta t}$, $x_{t+\Delta t}$ = acceleration, velocity and displacement at the end of the time increment Δt ,

\ddot{x}_t , \dot{x}_t , x_t = acceleration, velocity and displacement at the beginning of the time period Δt ,

m = mass,

K = stiffness,

K_s = geometric stiffness,

C = damping coefficient, and

F_t , $F_{t+\Delta t/2}$, $F_{t+\Delta t}$ = forcing function for the beginning, middle and end of time increment Δt .

The generalized matrix form of the above Runge-Kutta equations are used for multiple-degree-of-freedom systems. Expressing Eqs. 5.7-5.9 in matrix form yields

$$\{x\}_{t+\Delta t} = \{x\}_t + (\Delta t)\{\dot{x}\}_t + (\Delta t)(\{A\} + \{B\} + \{D\})/6 \quad (5.10)$$

$$\{\dot{x}\}_{t+\Delta t} = \{\dot{x}\}_t + (\{A\} + 2\{B\} + 2\{D\} + \{E\})/6 \quad (5.11)$$

$$\{\ddot{x}\}_{t+\Delta t} = [M]^{-1}(\{F\}_{t+\Delta t} - ([K] - [K_s])\{x\}_{t+\Delta t} - [C]\{\dot{x}\}_{t+\Delta t}) \quad (5.12)$$

where

$$\begin{aligned} \{A\} = (\Delta t)[M]^{-1}(\{F\}_t - ([K] - [K_s])\{x\}_t \\ - [C]\{\dot{x}\}_t), \end{aligned}$$

$$\begin{aligned} \{B\} = (\Delta t)[M]^{-1}(\{F\}_{t+\Delta t/2} - ([K] - [K_s])(\{x\}_t \\ + (\Delta t)\{\dot{x}\}_t/2) - [C](\{\dot{x}\}_t + \{A\}/2)), \end{aligned}$$

$$\begin{aligned} \{D\} = (\Delta t)[M]^{-1}(\{F\}_{t+\Delta t/2} - ([K] - [K_s])(\{x\}_t \\ + (\Delta t)\{\dot{x}\}_t/2 + (\Delta t)\{A\}/4) \\ - [C](\{\dot{x}\}_t + \{B\}/2)), \end{aligned}$$

$$\begin{aligned} \{E\} = (\Delta t)[M]^{-1}(\{F\}_{t+\Delta t} - ([K] - [K_s])(\{x\}_t \\ + (\Delta t)\{\dot{x}\}_t + (\Delta t)\{B\}/2) \\ - [C](\{\dot{x}\}_t + \{D\})), \end{aligned}$$

$\{\ddot{x}\}_{t+\Delta t}$, $\{\dot{x}\}_{t+\Delta t}$, $\{x\}_{t+\Delta t}$ = acceleration, velocity and displacement vectors at the end of time increment Δt ,

$\{\ddot{x}\}_t$, $\{\dot{x}\}_t$, $\{x\}_t$ = acceleration, velocity and displacement vectors at the beginning of time increment Δt ,

$[M]$ = mass matrix,

$[K]$ = stiffness matrix of system,

$[K_s]$ = geometric stiffness matrix of system,

$[C]$ = damping coefficient matrix, and

$\{F\}_t$, $\{F\}_{t+\Delta t/2}$, $\{F\}_{t+\Delta t}$ = forcing function vector for the beginning, middle and end of time increment Δt .

Knowing the magnitudes of the displacement, velocity and acceleration at the beginning of a time increment, the corresponding magnitudes at the end of the time increment are found from the above equations. When considering earthquake loading, the forcing function vector will consist of the inertia forces for each mass in the system as:

$$\{F\}_t = -[M]\{\ddot{x}_g\}_t \quad (5.13)$$

where $\{F\}_t$ = forcing function vector at time t ,

$[M]$ = mass matrix, and

$\{\ddot{x}_g\}_t$ = ground acceleration vector at time t .

Linear interpolation is used to determine the forcing function at the middle of a time increment.

The fourth-order Runge-Kutta method has been proved as a powerful numerical method for earthquake analysis in Cheng's previous work^{22,13} and is used in this research for checking the accuracy of other numerical techniques.

C. WILSON'S θ -METHOD

The third step-by-step integration method considered in this study is Wilson's θ -Method.^{6,7} This method of integration provides a means of eliminating the response to the higher modes as well as producing an unconditionally stable solution. An unconditionally

stable solution is one which is bounded for any time increment Δt . By eliminating the higher mode responses where the $(\Delta t)/T_i$ values are large, $(\Delta t/T_i > 0.01)$, the initial values at each time interval will not have excessive errors and then cause inaccurate integration of the response in the lower modes. The term T_i is the period of mode i . The advantage of this method is that one may use a larger Δt value and still provide for an unconditionally stable solution. The decision as to what Δt value will then be based on the degree of accuracy desired without having to consider stability. Using this method, consideration only of the natural frequencies of the structure and the applied forcing frequencies is needed in determining the most desirable Δt value. Since the higher modes contribute to a lesser degree to the total response, the elimination of these higher modes may not jeopardize the accuracy of the total response and still provide for the desirable unconditionally stable solution.

The elimination of the higher mode responses is obtained in the θ -Method by causing amplitude decay and period elongation to these higher mode responses. Wilson's θ -Method is a modification of the linear acceleration method which is equivalent to Newmark's Beta method with $\beta = 1/6$, as discussed previously. In Wilson's method the acceleration is assumed to be linear during the time interval $\tau = \theta \Delta t$, where $\theta \geq 1.0$. For $\theta = 1$ the method reduces to the linear acceleration method. A magnitude of $\theta = 1.4$ was found by Bathe and Wilson⁷ to result in the best accuracy while still causing amplitude decay and period elongation to occur in the higher mode responses. Wilson had previously shown an unconditionally stable solution could be obtained for $\theta = 2.0$.

The incremental form of the general motion equation for a multi-degree system based on a time increment of τ is

$$[M]\{\Delta\ddot{x}\}_\tau + [C]\{\Delta\dot{x}\}_\tau + [K'']\{\Delta x\}_\tau = \{F\}_{t+\tau} - [M]\{\ddot{x}\}_t - [C]\{\dot{x}\}_t - [K'']\{x\}_t \quad (5.14)$$

where $\{\Delta\ddot{x}\}_\tau$, $\{\Delta\dot{x}\}_\tau$, $\{\Delta x\}_\tau$ = incremental acceleration, velocity and displacement over time period τ ,

$\{\ddot{x}\}_t$, $\{\dot{x}\}_t$, $\{x\}_t$ = acceleration, velocity and displacement at time t , the beginning of the time increment,

$[M]$ = mass matrix,

$[C]$ = damping coefficient matrix,

$[K''] = [K_{22}] - [K_{12}]^T [K_{11}]^{-1} [K_{12}] - [K_s]$, and

$\{F\}_{t+\tau} = \{F\}_t + \theta(\{F\}_{t+\Delta t} - \{F\}_t)$ = projected value of the forcing function at time $t+\tau$.

The projected value of the forcing function is obtained by the linear extrapolation of the value at time t and $t + \Delta t$ to the time $t + \tau$.

Using the linear acceleration approach the velocity and displacement at time $t + \tau$ for a single-degree-of-freedom system is

$$\dot{x}_{t+\tau} = \dot{x}_t + (\ddot{x}_{t+\tau} + \ddot{x}_t)\tau/2 \quad (5.15)$$

$$x_{t+\tau} = x_t + \tau\dot{x}_t + \tau^2(\ddot{x}_{t+\tau} + 2\ddot{x}_t)/6 \quad (5.16)$$

where $\ddot{x}_{t+\tau}$, $\dot{x}_{t+\tau}$, $x_{t+\tau}$ = acceleration, velocity and displacement of mass at time $t + \tau$,

\ddot{x}_t , \dot{x}_t , x_t = acceleration, velocity and displacement of mass at time t , and

$$\tau = \theta(\Delta t).$$

The incremental form of the velocity and acceleration for the time period τ are derived from Eqs. 5.15 and 5.16.

$$\Delta \dot{x}_{\tau} = \frac{3}{\tau} \Delta x + B_{\tau} \quad (5.17)$$

$$\Delta \ddot{x}_{\tau} = \frac{6}{\tau^2} \Delta x + A_{\tau} \quad (5.18)$$

where $B_{\tau} = -3\dot{x}_t - \tau\ddot{x}_t/2$ and

$$A_{\tau} = \frac{-6}{\tau} \dot{x}_t - 3\ddot{x}_t.$$

Thus the incremental velocity and acceleration vectors for a multi-degree-of-freedom system can be similarly derived as shown in Eqs. 5.17 and 5.18. Using Eq. 5.14 will then yield the incremental displacement over the time period τ .

$$\{\Delta x\}_{\tau} = [K^*]_{\tau}^{-1} \{\Delta R\} \quad (5.19)$$

where

$$[K^*]_{\tau} = \frac{6}{\tau^2} [M] + \frac{3}{\tau} [C] + [K] \quad (5.20)$$

$$\{\Delta R\} = \{F\}_{t+\tau} - [M](\{\ddot{x}\}_t + \{A\}_{\tau}) - [C](\{\dot{x}\}_t + \{B\}_{\tau}) - [K]\{x\}_t \quad (5.21)$$

The acceleration at time τ corresponding to the above incremental displacement of Eq. 5.19 can be expressed in the following form based on the linear acceleration approach:

$$\{\ddot{x}\}_{t+\tau} = \frac{6}{\tau^2} \{\Delta x\}_{\tau} - \frac{6}{\tau} \{\dot{x}\}_t - 2\{\ddot{x}\}_t \quad (5.22)$$

The acceleration, velocity and displacement at time $t + \Delta t$ are

$$\{\ddot{x}\}_{t+\Delta t} = \{\ddot{x}\}_t + (\{\ddot{x}\}_{t+\tau} - \{\ddot{x}\}_t)/\theta \quad (5.23)$$

$$\{\dot{x}\}_{t+\Delta t} = \{\dot{x}\}_t + (\Delta t)(\{\ddot{x}\}_{t+\Delta t} + \{\ddot{x}\}_t)/2 \quad (5.24)$$

$$\{x\}_{t+\Delta t} = \{x\}_t + (\Delta t)\{\dot{x}\}_t + (\Delta t)^2(\{\ddot{x}\}_{t+\Delta t} + 2\{\ddot{x}\}_t)/6 \quad (5.25)$$

The values of the above acceleration, velocity and displacement become the initial values for the next time increment.

The amplitude decay and period elongation behavior is illustrated in Fig. 5.1 for an undamped single-degree-of-freedom mass having a natural period of $T_n = 1.2$ sec. An initial displacement of one unit is used to produce the motion. When Δt is equal to 0.012 sec., conditional stability is present, since the $(\Delta t)/T_n$ value is small enough as found by Bathe and Wilson⁷ to have no error in the integration process as measured in terms of amplitude decay and period elongation. The response curve follows the exact solution of $x = \cos pt$ where p is the natural frequency of the single-degree-of-freedom mass. The same response is obtained for any value of $\theta \geq 1.0$.

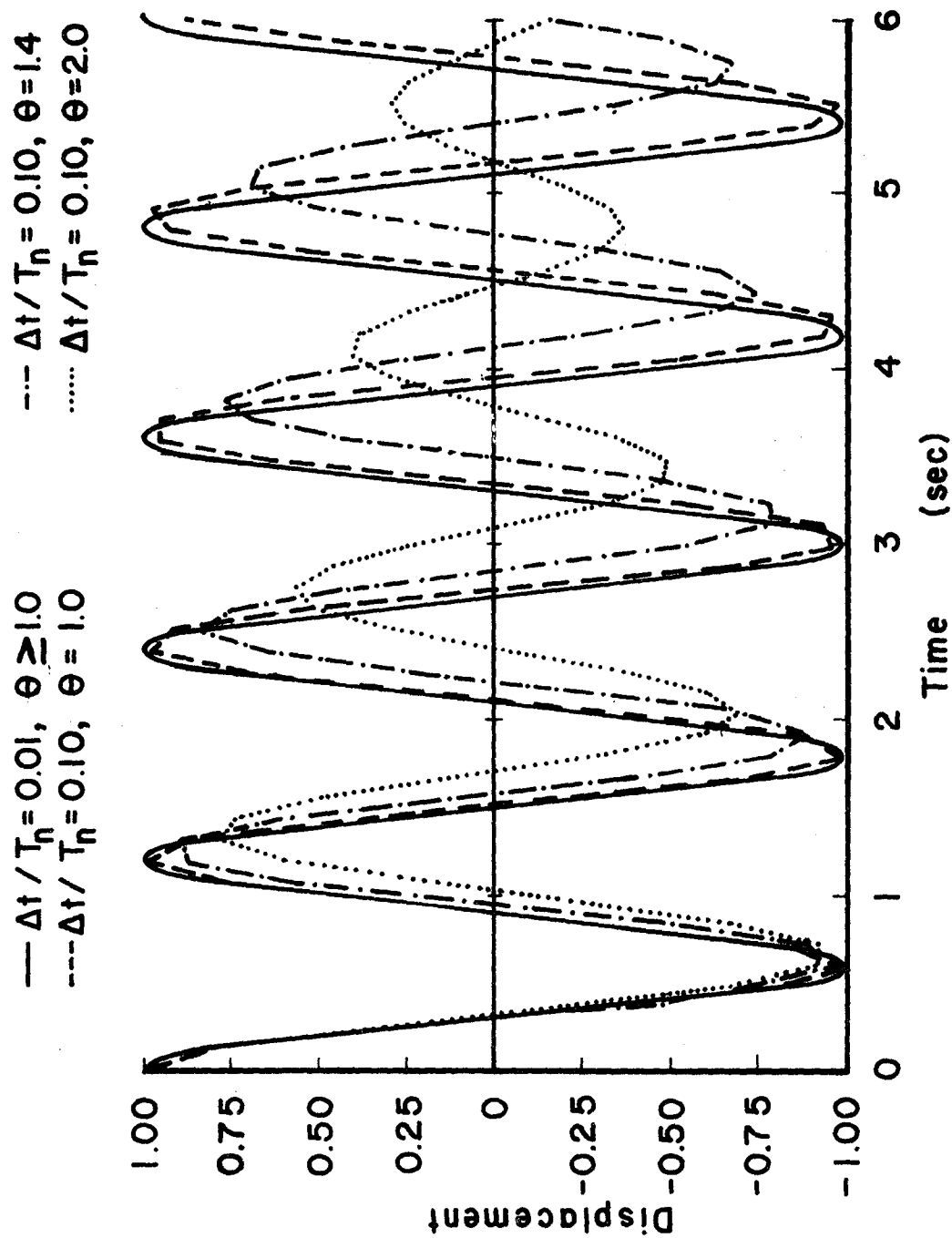


Figure 5.1. Period Elongation and Amplitude Decay of Single Mass Using Wilson's θ -Method

When a Δt of 0.12 sec. is used, the accuracy of the integration is reduced, and the amount of amplitude decay and period elongation increase with the value of θ . For any particular value of θ greater than 1.0 the amount of amplitude decay and period elongation increases with the magnitude of the mode frequency having a $(\Delta t)/T_n$ value greater than approximately 0.01.

VI. ELASTIC RESPONSE OF MULTI-STORY STRUCTURES TO VARIABLE LOADS

The purpose of this section is to relate results obtained in the analysis of linear multi-story frames. Adequacy of the method used in analyzing linear multi-story frames is shown by the analysis of a two-degree-of-freedom system. The free vibration response of a 2-story shear building based on initial values of displacement and velocity are determined and compared with the results obtained from a modal analysis.

Multi-story structures are analyzed to show that some systems are sensitive to the P-delta effect and vertical earthquake motion. Studies include the correlation of the maximum floor displacement and the frequency spectrum of the horizontal ground motion. A frequency spectrum analysis is also included to determine the vertical frequencies most likely to affect the horizontal response of the structure.

A. COMPARISON OF STEP-BY-STEP INTEGRATION TECHNIQUES WITH THEORETICAL RESULTS OF A TWO-DEGREE-OF-FREEDOM SYSTEM

To further verify the validity of the methods used in determining the response of structural systems, the theoretical response of a two-degree-of-freedom system will be compared with numerical solutions. The system consists of a two-story, single bay shear building as shown in Fig. 6.1. The mass of each girder and supporting columns, m_1 and m_2 , are lumped at the floor levels. The total column stiffness for each floor level is K_1 and K_2 . The girders are taken as infinitely rigid resulting in no rotation at the ends of the columns.

The set of motion equations for the two-degree-of freedom can be written from the equivalent spring-mass model shown in Fig. 6.2.

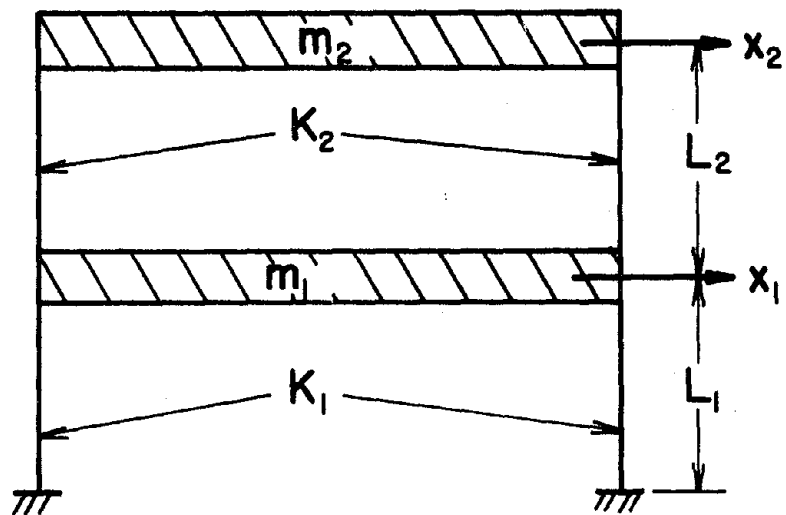


Figure 6.1. Two-Degree System

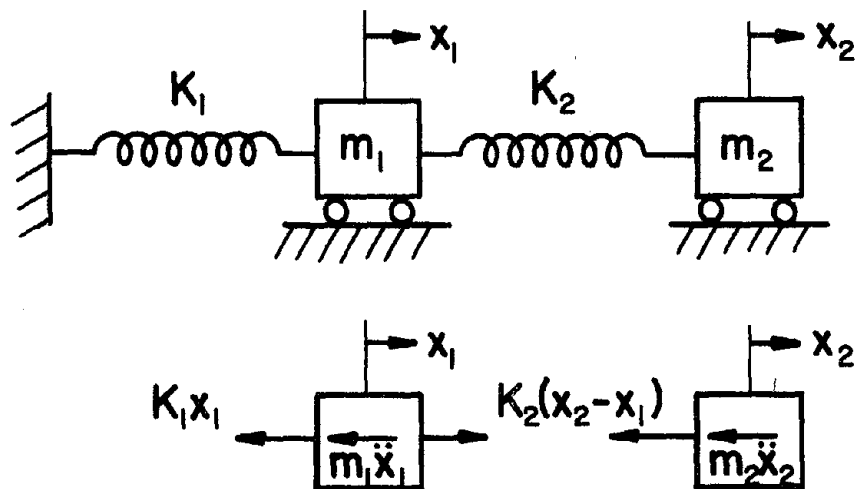


Figure 6.2. Spring-Mass Model for Two-Degree System

$$m_1 \ddot{x}_1 + K_1 x_1 - K_2 (x_2 - x_1) = 0 \quad (6.1a)$$

$$m_2 \ddot{x}_2 + K_2 (x_2 - x_1) = 0 \quad (6.1b)$$

Assume that the mass and stiffness of the system are

$$m = m_1 = m_2 = 100 \text{ kip-sec}^2/\text{ft} \text{ (1488 kg-s}^2/\text{cm)},$$

$$K = K_1 = K_2 = 0.100 \text{ kip/ft (14.6 N/cm)},$$

and that the initial conditions are given as:

$$x_1(0) = 1 \text{ ft (30.5 cm)}, \quad \dot{x}_1(0) = 0, \quad x_2(0) = 0, \quad \dot{x}_2(0) = 0.$$

Then the motion equations can be expressed as

$$x_1 = 0.276 \cos 0.618t + 0.724 \cos 1.618t \quad (6.2a)$$

$$x_2 = 0.447 \cos 0.618t - 0.447 \cos 1.618t \quad (6.2b)$$

Equations 6.2a and 6.2b are derived in Ref. 13 in detail for which the response curves are shown in Fig. 6.3. The same curves are obtained using both Newmark's method and the 4th order Runge-Kutta method in performing a step-by-step integration of the motion equations of Eqs. 6.1a and 6.1b.

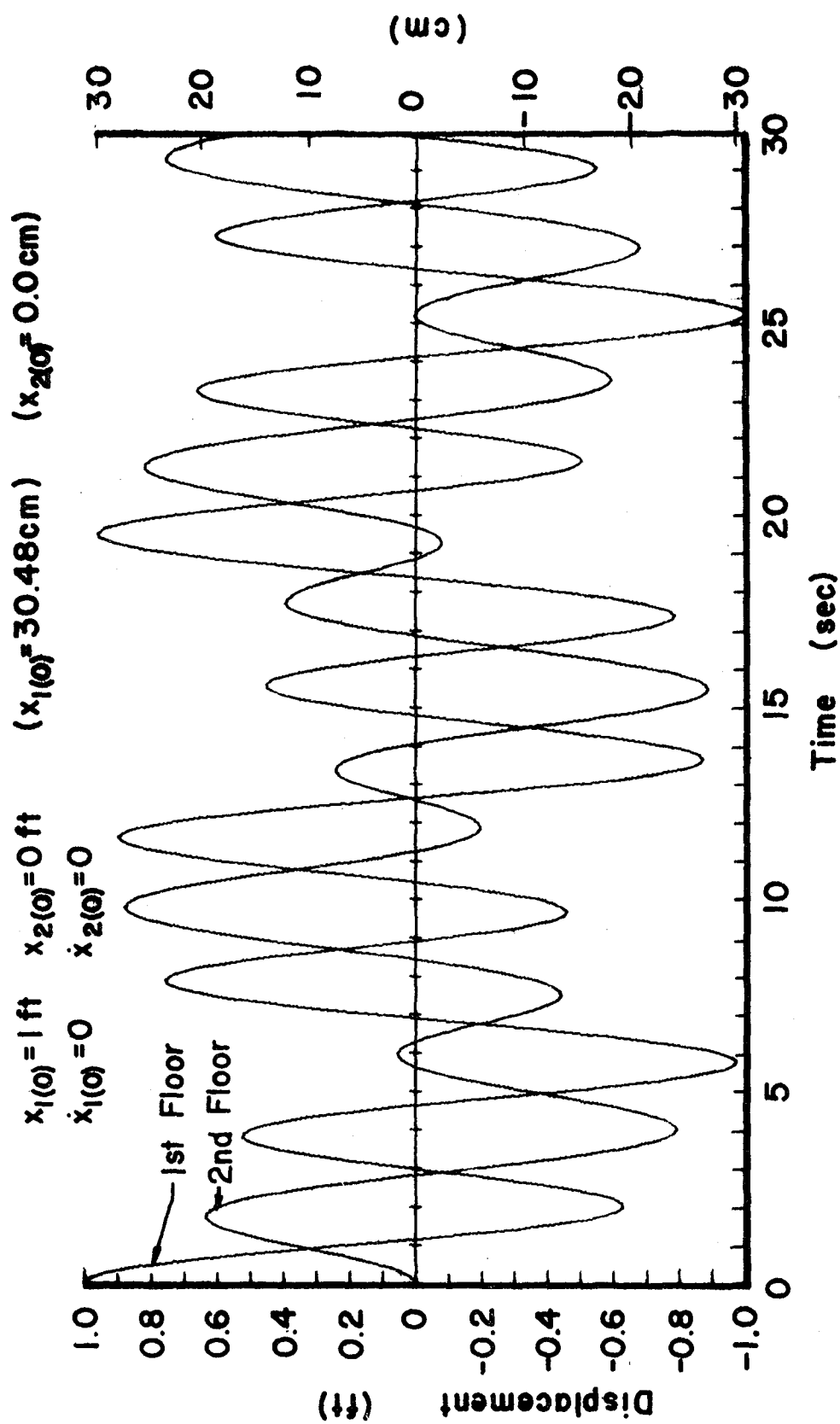


Figure 6.3. Response of Two-Degree System Based on Initial Conditions

B. P-DELTA EFFECT ON DYNAMIC RESPONSE OF A LINEAR SYSTEM DUE TO AN EARTHQUAKE

In Chapter III it is indicated that the change in response of a single-degree-of-freedom system when considering the P-delta effect is due to the change in natural frequency of the system. This change in natural frequency results in a different correlation with the horizontal frequency spectrum of the earthquake loading. For the single-degree-of-freedom system the increase or decrease in response depends on whether the amplitude of the frequency spectrum corresponding to the natural frequency including P-delta is larger or smaller, respectively, than the original amplitude.

The P-delta effect for a multi-degree-of-freedom system will now be studied to see if a similar conclusion can be made. The structure to be studied is a three-story frame as shown in Fig. 6.4. This structure has a total of 9 degrees of freedom, 6 degrees in rotation and 3 degrees in translation. The mass of 1/2 of each girder and its supporting column is lumped at the top of each column.

The top floor response of the 3-story frame based on 30 seconds of the 1940 El Centro earthquake and having floor masses of $m_1 = 14.715 \text{ kip-sec}^2/\text{ft}$ ($219.0 \text{ kg-s}^2/\text{cm}$), $m_2 = 13.749 \text{ kip-sec}^2/\text{ft}$ ($204.6 \text{ kg-s}^2/\text{cm}$) and $m_3 = 6.883 \text{ kip-sec}^2/\text{ft}$ ($102.4 \text{ kg-s}^2/\text{cm}$) is shown in Fig. 6.5 with and without the P-delta effect included. These floor masses result in a first mode natural period of $T_n = 2.426 \text{ sec.}$ without considering the P-delta effect and a natural period of $T_s = 2.731 \text{ sec.}$ when considering the P-delta effect. As shown in Fig. 6.5 the maximum floor displacement is realized when the P-delta effect is included.

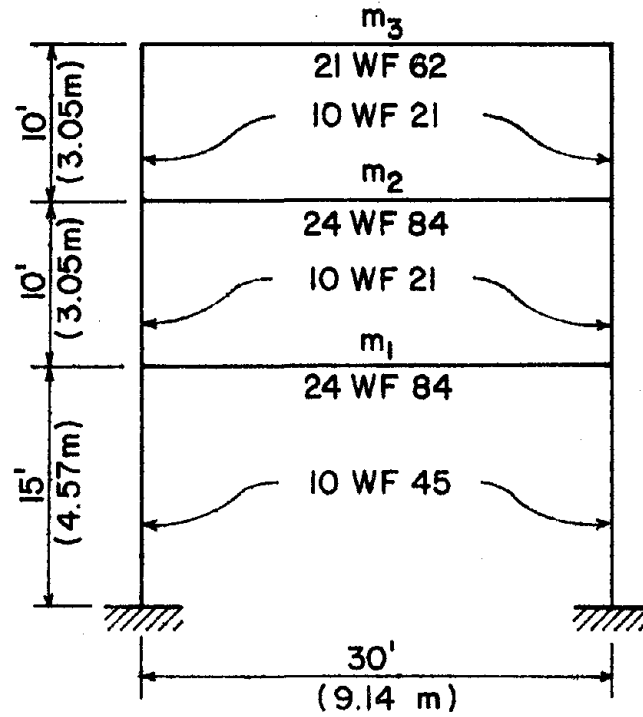


Figure 6.4. Three-Story Frame

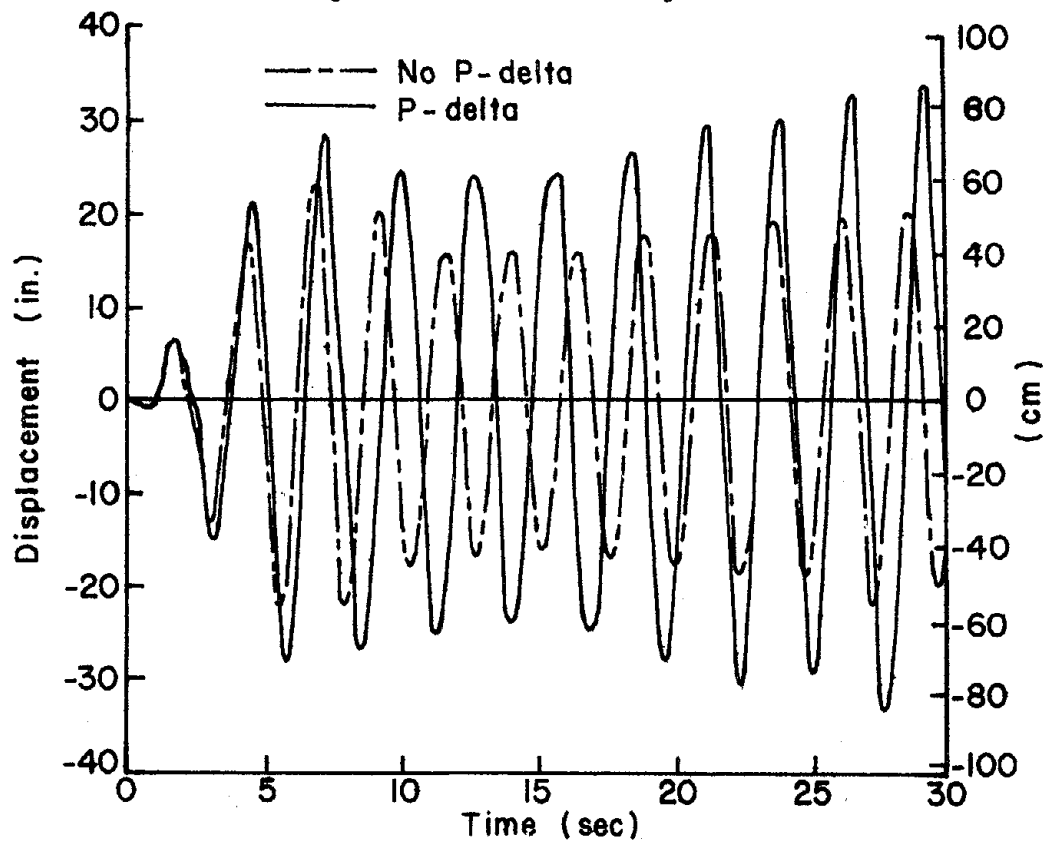


Figure 6.5. Top Floor Response of 3-Story Bldg, 1940 El Centro

The maximum displacements of the top floor of the structure shown in Fig. 6.4 are obtained for different natural frequencies which are evaluated by multiplying each floor mass by equivalent factors. Figure 6.6a shows the variation in the maximum responses with and without the P-delta effect. The natural period, T_n , shown in the figure does not include the P-delta effect in the analysis. As observed from these results the P-delta effect may not always be critical and may cause the displacement response to be decreased or increased as compared with the results of the associated structure without consideration of the P-delta effect.

A comparison of the maximum displacements can be made with the corresponding amplitudes of the horizontal frequency spectrum of the earthquake used to cause the structure to deform. Figure 6.6b shows the variation in amplitude corresponding to each period made up by the 1940 El Centro earthquake's N-S component as determined by the fast Fourier transform discussed in Chapter II. Figure 6.6b is a plot of just a portion of the frequency spectrum shown in Fig. 2.13 with the abscissa being the period T instead of the frequency p where $T = 1/p$. The amplitudes for frequencies $p = 0.25$ - 1.25 Hz are shown in Fig. 6.6b. These frequencies correspond to the range of natural frequencies for the structures being analyzed.

The three-story structure whose response curve is shown in Fig. 6.5 is used to illustrate the influence of natural frequency on response. The displacements shown in Fig. 6.5 corresponding to $T_s = 2.731$ (P-delta included) can be similarly obtained by changing floor masses which will result in a fundamental period of $T_n = 2.731$ sec without the inclusion of the P-delta effect. The response curve

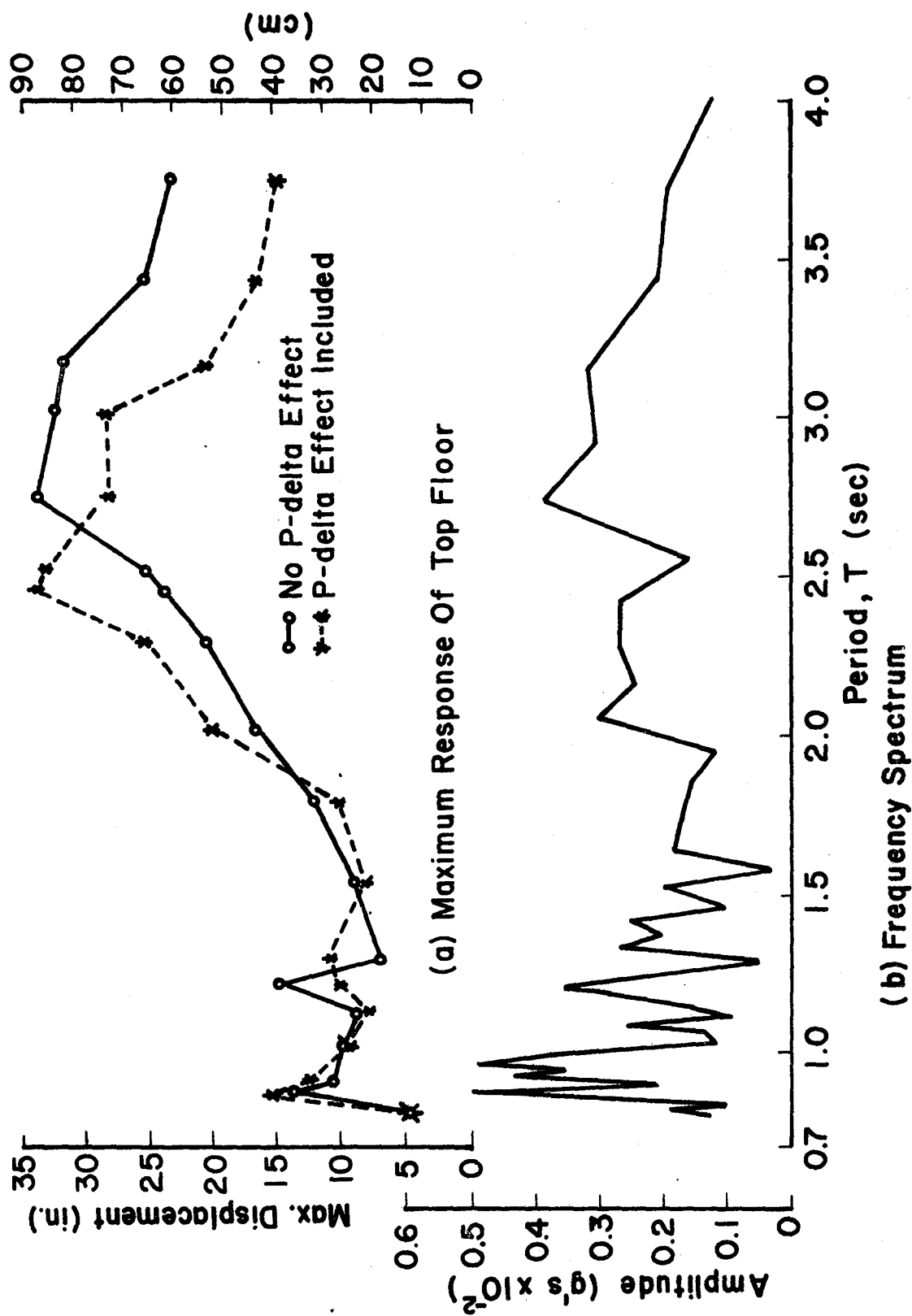


Figure 6.6. Comparison of Maximum Response with Frequency Spectrum of Earthquake (N-S, 1940 El Centro)

for this structure based on the same earthquake loading is shown in Fig. 6.7. Note the similarity in response curves corresponding to these two natural periods.

A comparison of the frequency spectrum amplitudes of Fig. 6.6b corresponding to the fundamental frequencies used above indicates a net increase in amplitude from $A = 0.0026g$ to $A = 0.0040g$ when the fundamental period increases from $T_n = 2.426 \text{ sec}$ to $T_s = 2.731 \text{ sec}$. This increase in amplitude is reflected by the increase in the maximum horizontal displacement of the top floor of the two systems. In other words, the change in fundamental period from $T_n = 2.426 \text{ sec}$ to $T_s = 2.731 \text{ sec}$ results in an increase in the maximum displacement due to the increase in amplitude of the frequency spectrum of the earthquake record used. This result is similar to the results obtained for the single-degree-of-freedom system of Chapter III.

Comparing the curves of Figs. 6.6a and 6.6b indicates the maximum horizontal displacement values for the top floor of a three-story structure when subjected to earthquake ground motions are dependent on several factors. First, the amplitude of the horizontal earthquake frequency spectrum corresponding to the fundamental frequency of the structure determines to a great extent the maximum horizontal displacement. Second, the magnitude of the fundamental period as indicated by Figs. 6.6a and 6.6b governs the magnitude of the maximum response. In other words, for frequencies from the frequency spectrum having the same amplitudes, structures having the lower of these natural frequencies tend to have the larger maximum displacements.

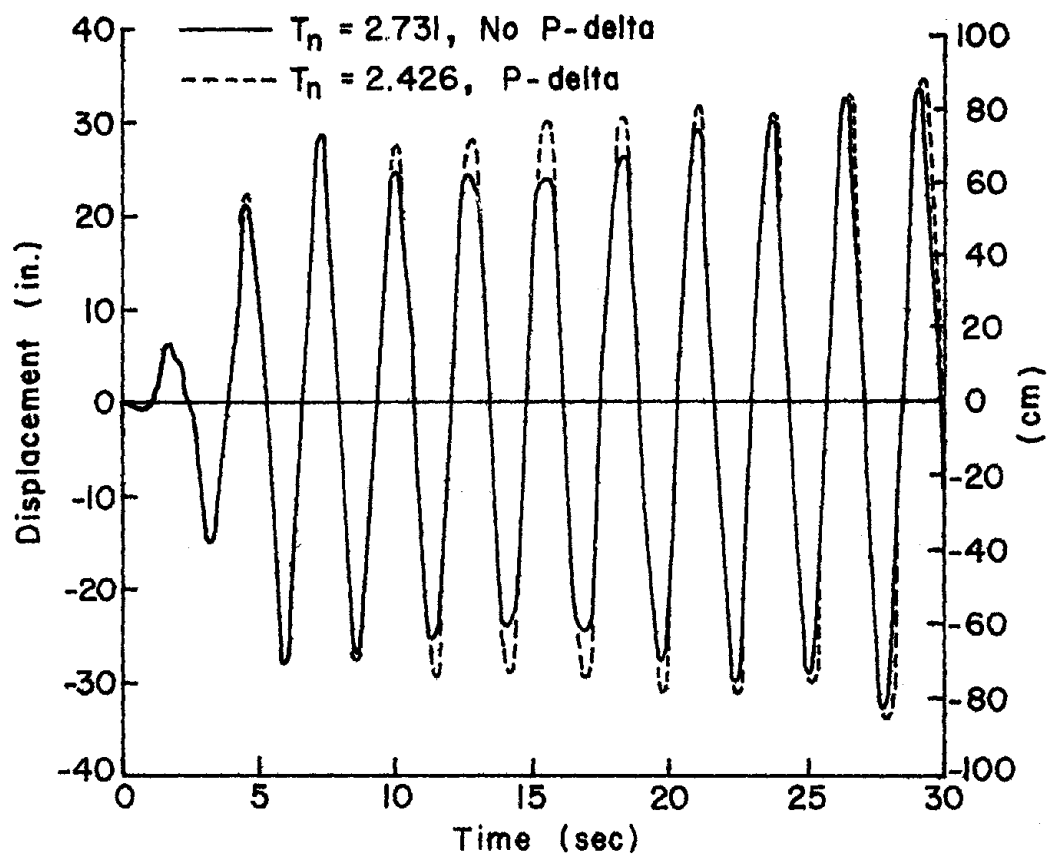


Figure 6.7. Response of 3-Story Bldg, Equal Response Frequencies, 1940 El Centro

A reduction in the maximum horizontal displacement of the top floor due to the inclusion of the P-delta effect can be illustrated by the response curves for a structure having a natural period of $T_n = 2.731$ sec as based on no P-delta effect. Figure 6.8 shows the comparison of maximum response associated with $T_n = 2.731$ sec and $T_s = 3.202$ sec. The natural period, $T_s = 3.202$ sec, of this structure is based on inclusion of the P-delta effect. As shown in Fig. 6.6b the amplitude associated with the natural period of $T_n = 3.202$ sec is less than that corresponding to $T_n = 2.731$ sec.

C. EFFECT OF VERTICAL EARTHQUAKE MOTION ON DYNAMIC RESPONSE

The change in horizontal response of a multi-story structure subjected to horizontal excitation, when the vertical ground motion is included, is to be considered herein.

To reduce the coupling effect of the random motion in the vertical direction with the horizontal excitation, horizontal response of the multi-story structure will be excited by a triangular impulse load on the top floor as shown in Fig. 6.9. The magnitude of the horizontal load is $F_t = 25$ kip (111.2 kN) at $t = 0$ decreasing linearly to zero after 10 seconds.

The structure used in this analysis is the same as shown in Fig. 6.4. The floor masses m_1 , m_2 and m_3 are adjusted equally by a magnification factor to obtain the desired fundamental frequencies.

The horizontal displacement of the three-story structure having a fundamental frequency of $p_n = 3$ Hz is shown in Fig. 6.10 based on the horizontal impulse load only. The 12 second interval of earthquake record is used so that a large scale of response curve can be obtained.

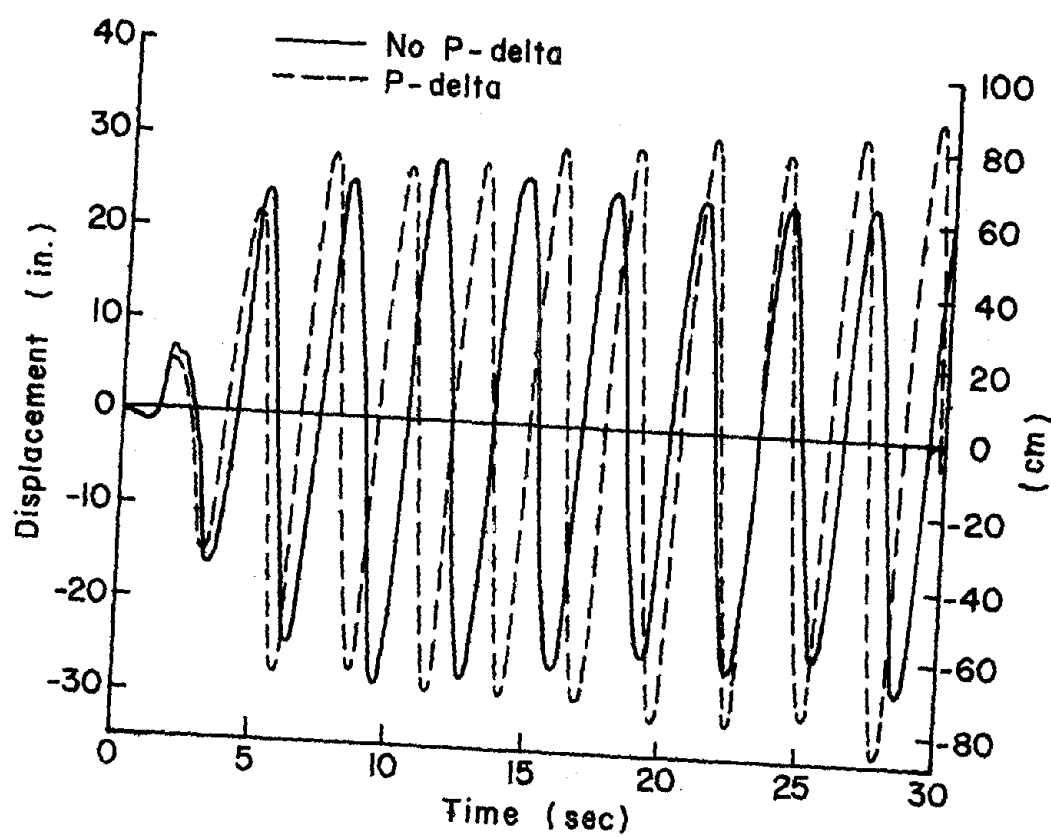


Figure 6.8. Response of 3-Story Bldg, 1940 El Centro

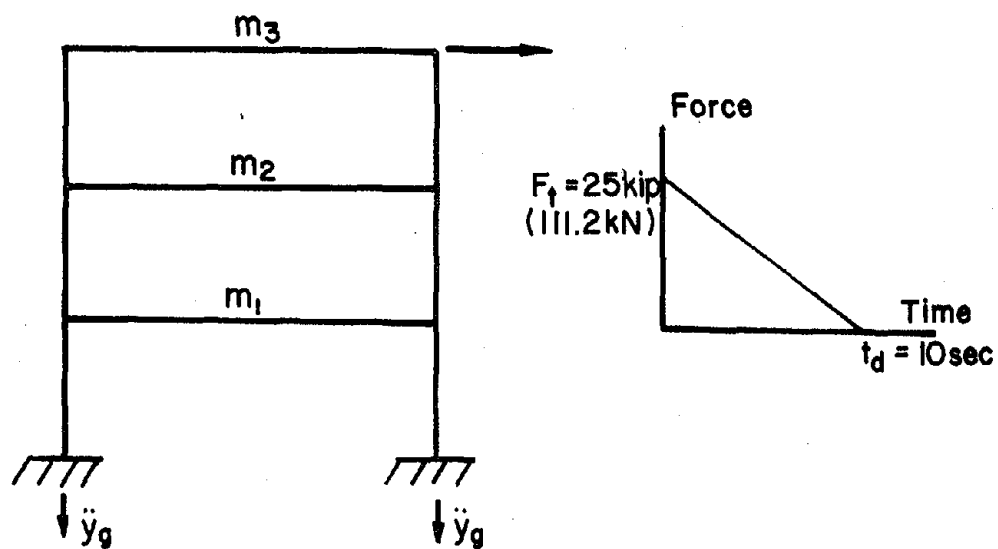


Figure 6.9. Loads on Multi-Story Structure to Study Effect of Vertical Ground Motion

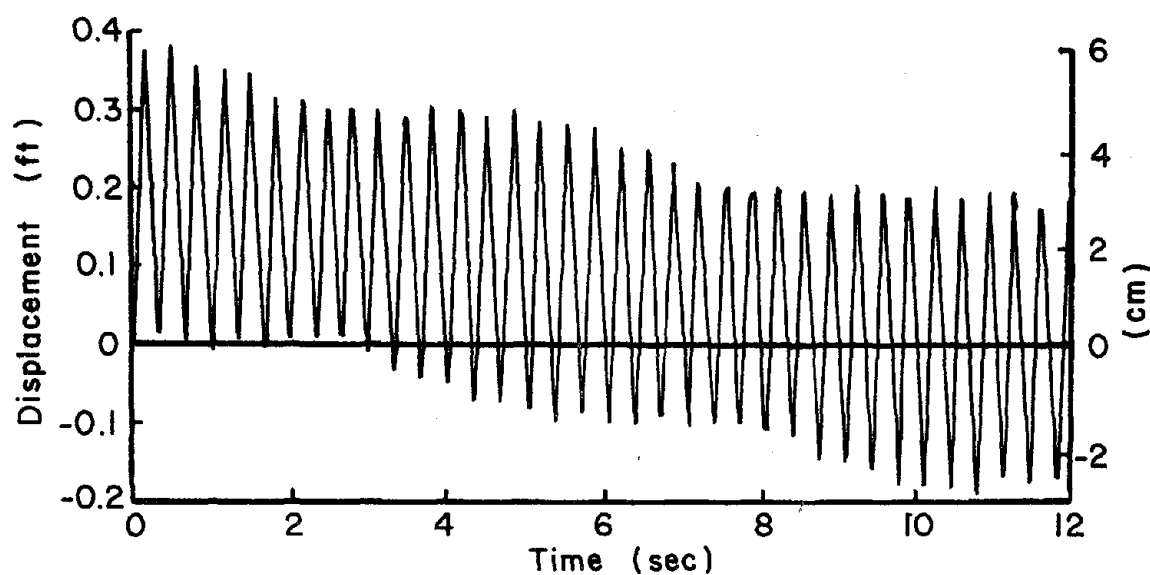


Figure 6.10. Top Floor Displacement, Impulse Only ($p_n = 3.0 \text{ Hz}$)

The magnitude of this portion of the earthquake used is higher than that of the remaining record. No significant change in the response has been found when including the total earthquake record.

When including the vertical component of the 1940 El Centro earthquake multiplied by a factor of 500, the horizontal displacement of the top floor is changed. Figure 6.11 is based on the positive vertical g-loads of the El Centro record being accelerations of the ground in the upward direction while Fig. 6.12 is based on the same positive vertical g-loads being accelerations of the ground in the downward direction. The latter sign convention reflects the situation actually present in the 1940 El Centro earthquake's vertical component as shown in Fig. 2.2.

Figure 6.13 shows the horizontal displacement of the top floor due to the horizontal impulse load only. The fundamental frequency of the structure is $p_n = 4.37$ Hz. When including the same vertical ground motion as in the previous example the response curves of Figs. 6.14 and 6.15 are obtained.

A vertical magnification factor of 141 is used to obtain the response curve shown in Fig. 6.16, based on a structure having a fundamental frequency of 1.22 Hz. These curves illustrate the type of response pattern typical of most of the structures analyzed. An exception is the response pattern obtained for the structure having a fundamental frequency of $p_n = 1.22$ Hz with a magnification factor of 500 applied to the vertical earthquake component of the 1940 El Centro earthquake. The response curves for the first 12 seconds based on this loading is shown in Figs. 6.17 and 6.18. As indicated by the scale used the structure becomes unstable during the 10 seconds

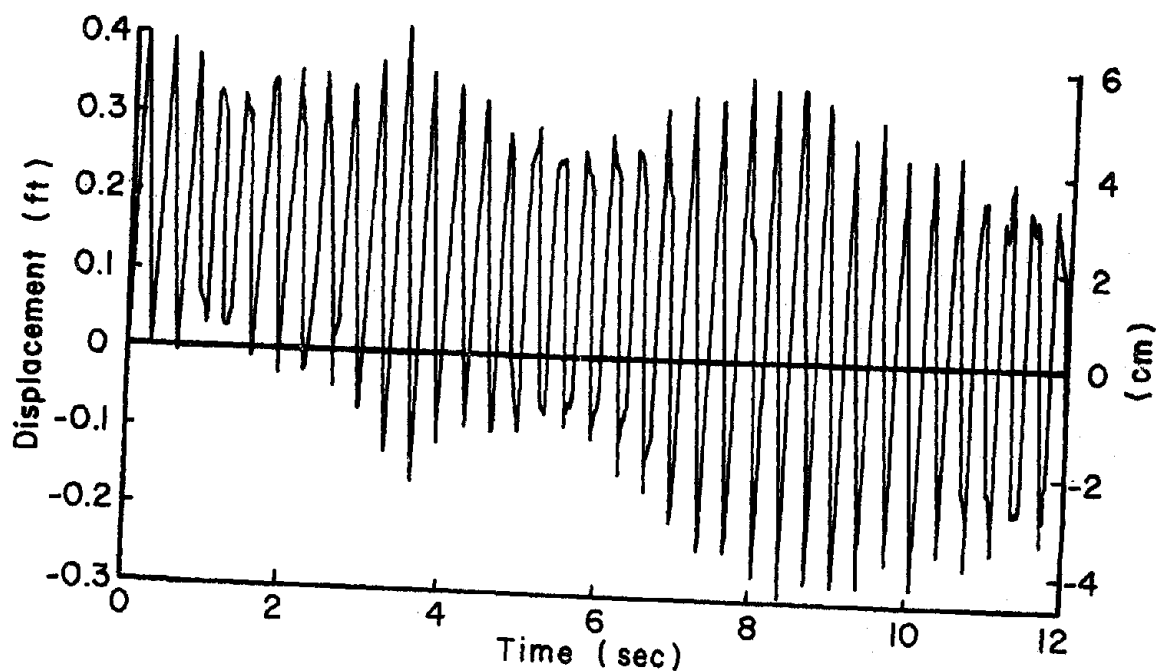


Figure 6.11. Top Floor Displacement, Impulse Plus Vertical Up Positive ($p_n = 3.0$ Hz)

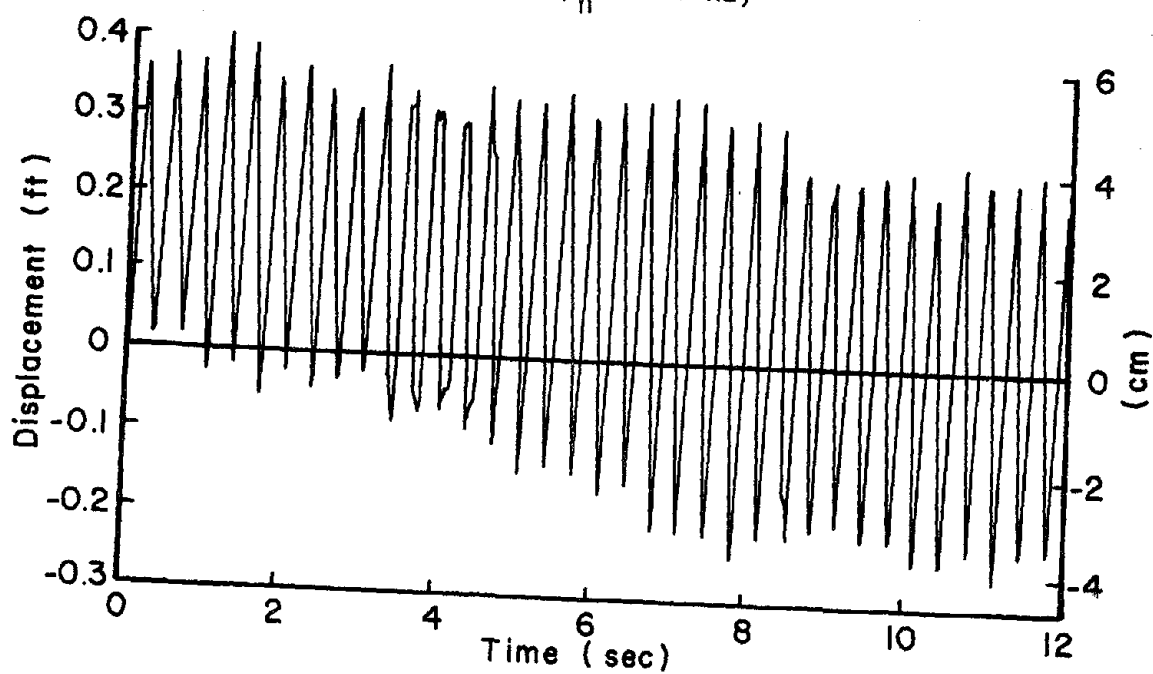


Figure 6.12. Top Floor Displacement, Impulse Plus Vertical Down Positive ($p_n = 3.0$ Hz)

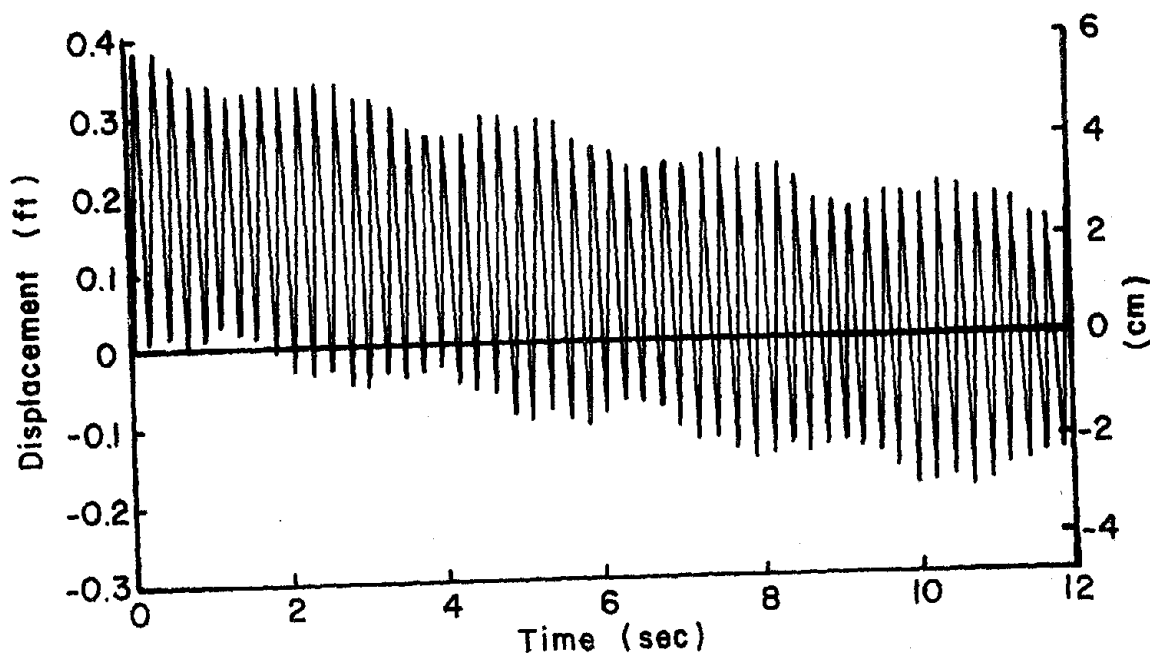


Figure 6.13. Top Floor Displacement, Impulse Only
($p_n = 4.37$ Hz)

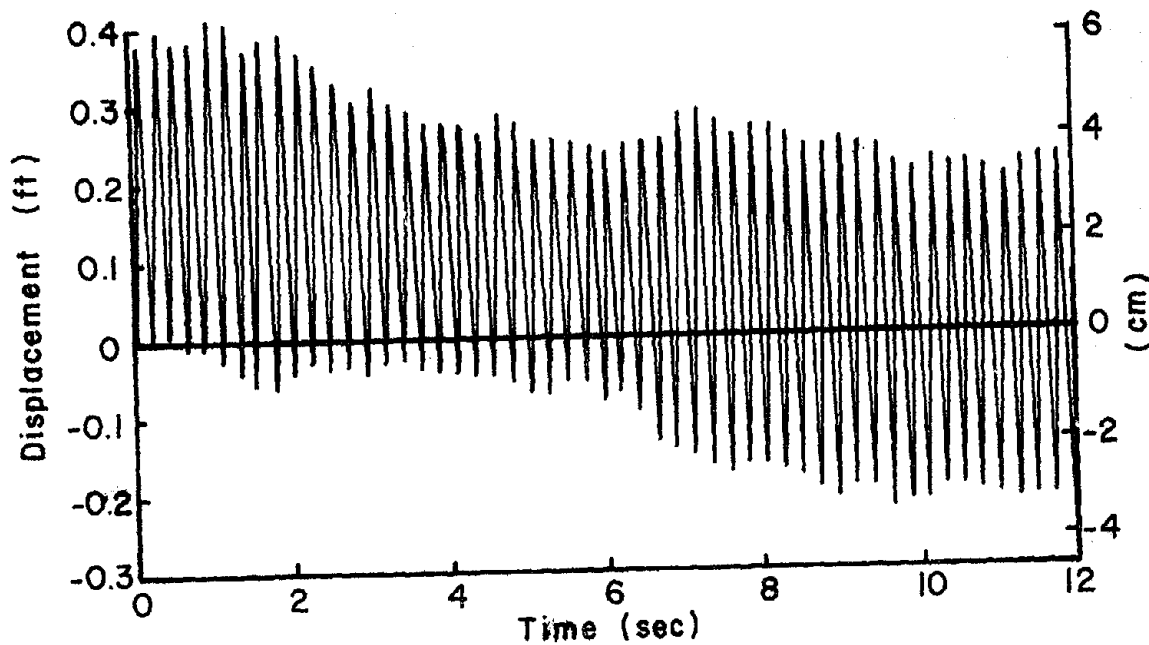


Figure 6.14. Top Floor Displacement, Impulse Plus Vertical
Up Positive ($p_n = 4.37$ Hz)

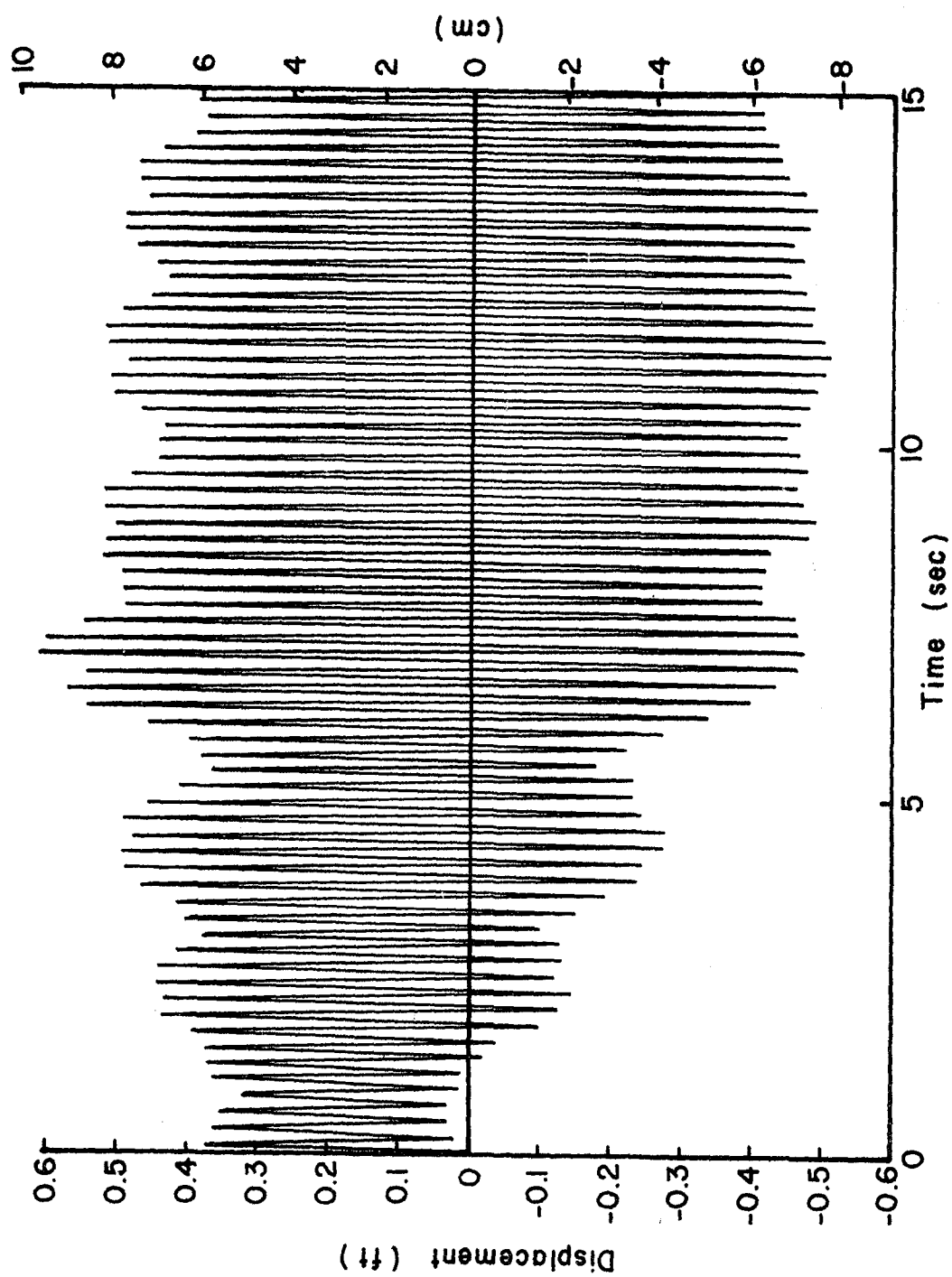


Figure 6.15. Top Floor Displacement, Impulse Plus Vertical Down Positive ($p_n = 4.37$ Hz)

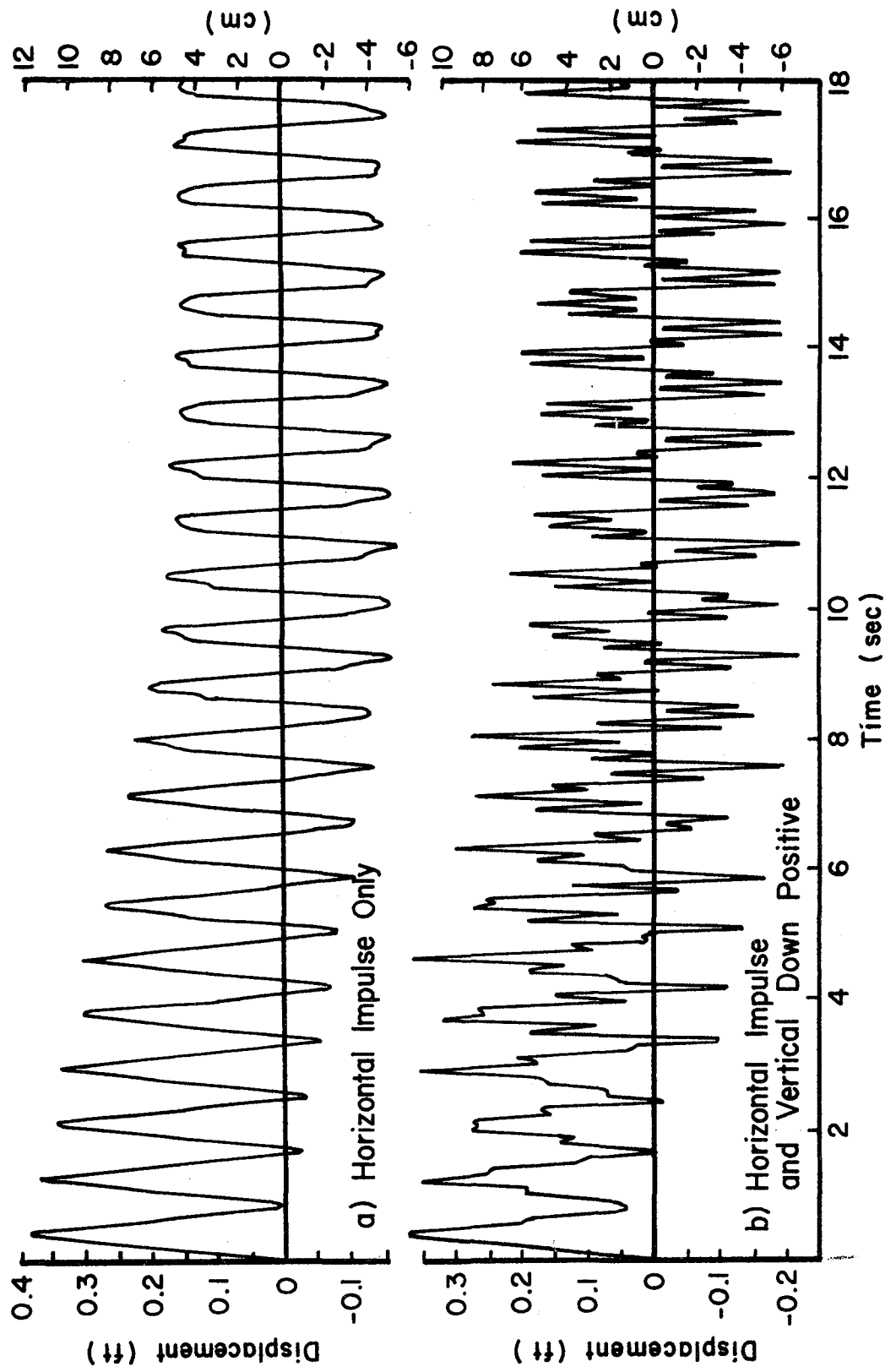


Figure 6.16. Top Floor Displacement ($p_n = 1.22$ Hz)

in which the impulse load is acting. The increase in horizontal displacements of the structures having the lower fundamental frequencies can be partially attributed to the coupling effect of the fundamental frequency with the frequencies made up by the horizontal impulse load. The frequency spectrum for the horizontal impulse used here is similar to the one shown in Fig. 2.16 except the amplitude values are based on 25 kip (111.2 kN) instead of the 1000 units as indicated in Fig. 2.15.

Additional structures having different fundamental frequencies are analyzed to determine the effect of the variable vertical loading on the horizontal response. The responses shown in Figs. 6.10 through 6.18 represent typical results and displacement patterns. Extensive analyses consist of structures having fundamental frequencies ranging from 1.2 Hz to 9.0 Hz. The effect of the variable vertical g-loads on the horizontal response is found to be less prominent in structures having the higher fundamental frequencies.

D. SENSITIVE STRUCTURES TO VERTICAL EARTHQUAKE EXCITATIONS

Two ranges of the fundamental frequency of a structure are found to be sensitive to the application of vertical earthquake components with the horizontal triangular impulse load as studied previously. The first range of the fundamental frequency is less than 3 Hz. Structures having fundamental frequencies in this range are responding to the frequencies of the impulse load. Amplitudes of the frequency spectrum for the impulse load as shown in Fig. 2.16 increase rapidly for values less than 3 Hz. Therefore, structures having this range of fundamental frequency are more sensitive to the horizontal excitation load than to the vertical motion.

The second range of the fundamental frequency of a structure is where the fundamental frequency is half the frequency from the vertical frequency spectrum having the largest amplitude. For the 1940 El Centro earthquake the vertical frequency spectrum (Fig. 2.14) shows a frequency of 8.936 Hz has the maximum amplitude. Therefore, a structure having a fundamental frequency of half this value or 4.468 Hz would be sensitive to the vertical component of the El Centro earthquake. Figures 6.14 and 6.15 illustrate the response of a structure whose fundamental frequency is in the vicinity of the above frequency.

The maximum response of a structure having a fundamental frequency in the sensitive region for vertical excitations is dependent on the phase angles of the vertical excitations in that region. The assumed positive directions for the vertical g-loads in Figs. 6.14 and 6.15 correspond to a difference in phase angle of 180° for each of the sinusoidal loads making up the frequency spectrum for the vertical loading. Therefore, the structure resulting in the maximum horizontal displacement of the top floor may not necessarily have a fundamental frequency value of half the frequency value from the vertical frequency spectrum having the largest amplitude. The fundamental frequency corresponding to the maximum response would be in the vicinity of the sensitive value, its value being dependent on the variation of the vertical frequency spectrum amplitudes and their corresponding phase angles. The effect of the phase angle of a vertical forcing function is studied for a single-degree-of-freedom system and discussed in Section III-E.

The use of a sinusoidal forcing function in the horizontal direction instead of an impulse load results in a coupling of the horizontal forcing frequency with the vertical forcing frequencies in the vicinity of twice the horizontal forcing frequency. The extent to which the vertical frequencies in this region will contribute to the increase or decrease of the horizontal response will depend on their amplitude and phase angle and the extent to which the horizontal forcing frequency controls the response frequency. This coupling of the horizontal forcing frequency with vertical frequencies will be in addition to the coupling of the fundamental frequency of the structure with vertical frequencies of twice their value as discussed in the previous paragraph.

E. FREQUENCIES OF THE VERTICAL FREQUENCY SPECTRUM CONTROLLING THE HORIZONTAL RESPONSE

Three ranges of frequency values from the vertical frequency spectrum contribute substantially to the horizontal response of a multi-story structure when considering the vertical component of an earthquake with a horizontal impulse load initiating the motion. These ranges are: (1) low frequencies that are coupled with frequencies making up the impulse loading, (2) frequencies near the fundamental frequency of the structure, and (3) frequencies in the vicinity of twice the fundamental frequency of the structure. High frequencies not in the above ranges contribute negligibly to the total response due to their low amplitudes.

Since contribution to the response of a multi-story structure by vertical loads is a function of the combined earthquake record, the

total response of a multi-story structure should be based on the total horizontal record plus the total vertical record or a Fourier summation of all frequencies of the horizontal and vertical earthquake components.

VII. INELASTIC RESPONSE OF MULTI-STORY STRUCTURES TO HORIZONTAL AND VERTICAL EARTHQUAKE LOADS

The behavior of inelastic structures will be studied with consideration of damping, structural model, energy absorption, ductility requirements and the interaction of horizontal and vertical earthquake components. The response results will be obtained for various multi-degree-of-freedom systems.

Damping, as formulated in Chapter IV, will be studied as it applies to inelastic structures. The damping coefficient matrix $[C]$ is a function of the fundamental frequency of the structure being analyzed. The change in the fundamental frequency due to plastic hinges occurring in the structure should theoretically necessitate a change in the damping coefficient matrix. The effect of using a constant fundamental frequency based on no plastic hinges is studied in Section VII-A.

The structural model used in an analysis should provide a sufficient means of exemplifying the actual conditions. When considering vertical ground motions, the model should adequately show the effect of this vertical component through its response parameters. The effect of using different lumped mass models is investigated in Section VII-B.

Three definitions of ductility are formulated in Section IV-C. The adaptability of each of these definitions in the determination of the ductility requirement of an inelastic structure is studied in this section. A comparison is made of the ductility and excursion ratios based on these definitions. The structural Model 2 containing girder nodes is used to determine these ratios.

Based on the above considerations of damping, structural models and ductility ratios, the response parameters of several structures are observed by studying maximum horizontal displacements of each floor, maximum relative displacements between floors, maximum vertical displacements of girder nodes, maximum vertical accelerations of girder nodes, ductility and excursion ratios, and the amount of energy stored and dissipated in the structures.

To further describe the inelastic behavior of multi-story structures, two additional studies are made. First, the effect of the reduction in the plastic moment on the response parameters is determined. Second, the effect of structural damping on the response parameters is shown.

A total of three different structures are analyzed in this chapter. They consist of the 3-story, 1-bay frame, the 4-story, 3-bay frame, and the 10-story, 1-bay frame.

The 3-story, 1-bay framed structure designated as Frame A is used to exemplify a small multi-story building. The frame is basically a strong column-weak girder structure with the major portion of the plastic rotations occurring in the girder members. The columns for this structure are assumed elastic by increasing the plastic moment capacity in the study pertaining to the definitions of ductility (Section VII-C); however, they are considered elasto-plastic based on actual M_p values in determining response parameters (Section VII-D). The fundamental period of this frame is $T_s = 1.20$ sec. including the P-delta effect.

The 4-story, 3-bay framed structure designated as Frame B has a fundamental period of $T_n = 2.01$ sec. and represents a typical multi-bay frame structure.

The 10-story, 1-bay framed structure designated as Frame C has floor weights equal to 249.4 kip/floor (1109 kN/floor) for which the fundamental period is $T_s = 2.731$ sec. Based on the results obtained in Section VI-B pertaining to the frequency spectrum of the El Centro earthquake, this fundamental period represents a critical value with regard to the maximum top floor displacement. To limit the amount of permanent set due to plastic deformation in the frame, the plastic moment is increased by a factor of 2.5. A material yield stress of 36 ksi (248.4 MN/m^2) and a modulus of elasticity of 30,000 ksi ($207,000 \text{ MN/m}^2$) are assumed.

A. FUNDAMENTAL FREQUENCY IN DAMPING FORMULATION OF INELASTIC STRUCTURES

When considering viscous damping of a structure it is necessary to determine or estimate the fundamental frequency of the system. The formulation of the damping coefficient $[C]$ in Eqs. 4.8-4.11 includes the fundamental frequency p_n . The purpose of this section is to show the effect of misestimating the fundamental frequency. Also included is the effect of the change in the fundamental frequency due to a member or members becoming plastic. In the study the damping formulation is based on mass, stiffness or a combination of mass and stiffness.

1. Effect of Misestimating Fundamental Frequency. The equation for the damping coefficient $[C]$ is given in Eq. 4.8 and is repeated here.

$$[C] = \alpha[M] + \beta[K] \quad (7.1)$$

The constants α and β are a function of the fraction of critical damping λ being considered and the fundamental frequency p_n of the structural system. The equation for α and β are dependent on the type of damping formulation.

For mass proportional damping the constants, $\beta = 0$ and $\alpha = 2\lambda p_n$, are given in Eqs. 4.10a and 4.10b. Therefore, the damping coefficient $[C]$ is directly proportional to the fundamental frequency p_n . It is apparent that an underestimation of the fundamental frequency for a structure will result in a corresponding decrease in the damping of the system and vice versa.

For stiffness proportional damping the constants, $\alpha = 0$ and $\beta = 2\lambda/p_n$, are given in Eqs. 4.11a and 4.11b. Therefore, the damping coefficient $[C]$ is inversely proportional to the fundamental frequency p_n . For this type of damping an underestimation of the fundamental frequency for a structure will result in a corresponding increase in the damping of the system and vice versa.

For damping proportional to a linear combination of mass and stiffness, the constants, $\alpha = \lambda p_n$ and $\beta = \lambda/p_n$, are given in Eqs. 4.9a and 4.9b. Therefore, the damping coefficient will be neither fully proportional nor inversely proportional to the natural frequency p_n .

To illustrate the use of a misestimated fundamental frequency a comparison is made in the response of a three-story frame with the three different types of damping considered. The 3-story structure,

Frame A of Fig. 7.1, is subjected to the N-S component of the 1940 El Centro earthquake. The P-delta effect and 5% critical damping are considered in this study.

Misestimated values of half and double the correct natural frequency of 0.833 Hz are used for comparison. Table 7.1 gives a tabular comparison of response parameters. The expected increase and decrease in damping due to misestimated values of p_n , are reflected in the maximum and minimum horizontal displacements of the top floor. The change in the damping is also reflected by the change in the maximum input energy per mass. Misestimation of the fundamental frequency of the system causes only a change in the amount of damping and does not result in an unstable solution as indicated by the small percent errors based on the law of the conservation of energy.

The elastic response of the top floor of the three-story structure based on the N-S component of the 1940 El Centro earthquake and 5% damping is shown in Figs. 7.2 and 7.3. When a linear combination of mass and damping is assumed on the basis of either double or half the actual fundamental frequency, the difference in response is shown in Fig. 7.2. The solid line illustrates the response obtained based on the correct value of p_n . An overall reduction of the amplitude without a change in the response frequency is indicated.

For either mass or stiffness proportional damping, the response curves are shown in Fig. 7.3. The response curve when using the correct value of the fundamental frequency is shown as the solid line. An overestimated value of p_n ($2p_n$) based on mass proportional damping results in the same response as when underestimating p_n ($p_n/2$) for stiffness proportional damping. This response is represented by the

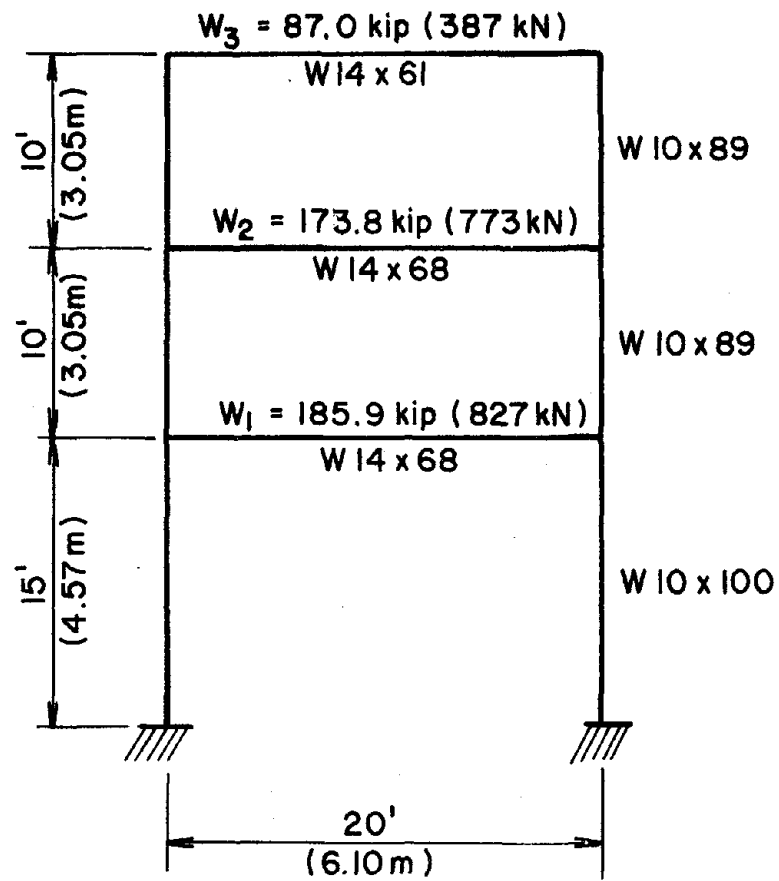


Figure 7.1. 3-Story, 1-Bay Frame (Frame A)

Table 7.1. Linear Response of Frame A Using Different Damping Formulation and Estimated Fundamental Frequency (1940 El Centro, P-delta Included, 5% Damping)

Type of Proportional Damping	$\frac{p_{est}}{p_{act}}$	x_{max} in. (cm)	x_{min} in. (cm)	Max. Input Energy per Unit Mass $\frac{in^2}{sec^2}$ ($\frac{cm^2}{s^2}$)	Largest % Error Based on Energy Eq. 5.6	Time of Largest Error
Mass	0.5	6.126 (15.56)	-5.163 (-13.11)	1052 (6787)	0.6853	2.27
	1.0	4.808 (12.21)	-3.942 (-10.01)	830 (5255)	0.6205	2.27
	2.0	3.541 (8.99)	-3.319 (-8.43)	737 (4755)	0.5199	2.27
Stiffness	0.5	3.584 (9.10)	-3.424 (-8.70)	751 (4845)	0.6581	27.83
	1.0	4.702 (11.94)	-3.979 (-10.11)	843 (5439)	0.7116	2.27
	2.0	5.929 (15.06)	-5.185 (-13.17)	1065 (6871)	0.7505	2.27
Mass Plus Stiffness	0.5	4.275 (10.86)	-3.807 (-9.67)	799 (5155)	0.5470	2.27
	1.0	4.700 (11.94)	-3.932 (-9.99)	838 (5406)	0.6157	2.27
	2.0	4.256 (10.81)	-3.754 (-9.54)	792 (5110)	0.5332	2.27

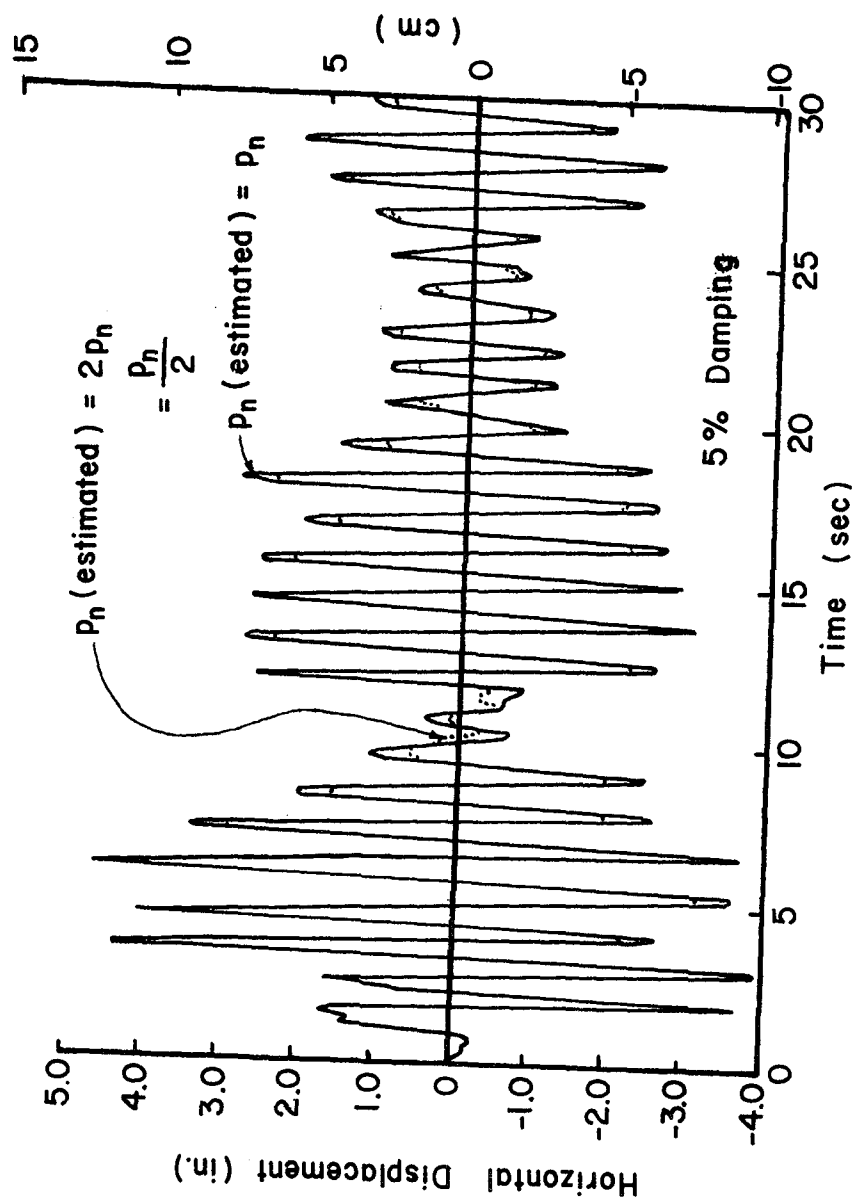


Figure 7.2. Linear Combination of Mass and Stiffness Damping, Top Floor Displacement, Frame A ($p_n = 0.833$ Hz)

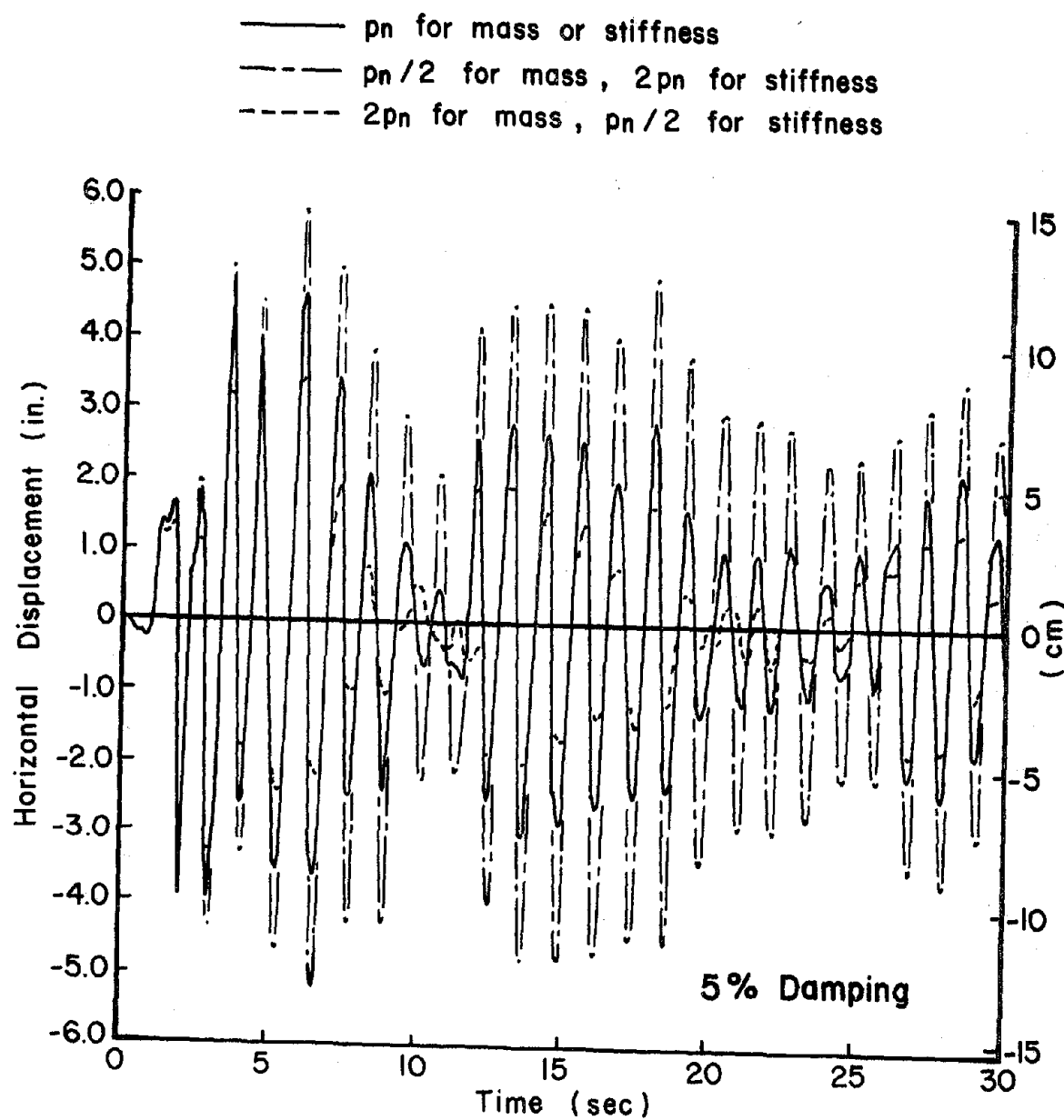


Figure 7.3. Mass and Stiffness Proportional Damping, Top Floor Displacement, Frame A ($p_n = 0.833$ Hz)

dashed line and has the most reduction in amplitude due to damping. Accordingly, an underestimated value of p_n ($p_n/2$) for mass proportional damping results in the same response as when overestimating the value of p_n ($2p_n$) for stiffness proportional damping. This response is represented by the curve (dash-dot) having the largest amplitude.

2. Effect of Change in Fundamental Frequency Due to Plastic Deformations. Due to the relaxation of a structure when a member or members become plastic, a corresponding decrease in the stiffness of the structure occurs. This reduction in stiffness results in a reduction in the fundamental frequency p_n during the short time a member or members are plastic. When damping is included in an inelastic structural analysis, the natural frequency of the structure during the times of plastic deformation should theoretically be changed according to the actual stiffness. Table 7.2 gives a tabular comparison of the elasto-plastic response for the same three-story frame subjected to the N-S component of the 1940 El Centro earthquake with 5% damping.

Mass proportional damping is the only one of the three types of damping resulting in an error less than 1%. Due to the change in stiffness during plastic deformations, the stiffness proportional damping and the mass plus stiffness proportional damping result in errors of 8.73% and 5.74%, respectively. The difference in response between considering mass proportional damping and stiffness proportional damping is shown in Fig. 7.4. The largest error in the stiffness proportional damping response occurs at $t = 3.48$ seconds. A remarkable difference in response is noted at this time in Fig. 7.4.

Table 7.2. Elasto-Plastic Response of Frame A Using Different Damping Formulation (1940 El Centro, P-delta Included, 5% Damping)

Type of Proportional Damping	$\frac{p_{est}}{p_{act}}$	x_{max} in. (cm)	x_{min} in. (cm)	Max. Input Energy per Unit Mass $\frac{in^2}{sec^2}$ ($\frac{cm^2}{s^2}$)	Largest % Error Based on Energy Eq. 5.6	Time of Largest Error
Mass	1.0	2.370 (6.02)	-4.440 (-11.28)	1269 (8187)	0.2975	1.85
Stiffness	1.0	3.924 (9.97)	-4.353 (-11.06)	1364 (8800)	8.7343	3.48
Mass Plus Stiffness	1.0	3.640 (9.25)	-4.358 (-11.07)	1316 (8490)	5.7415	4.24

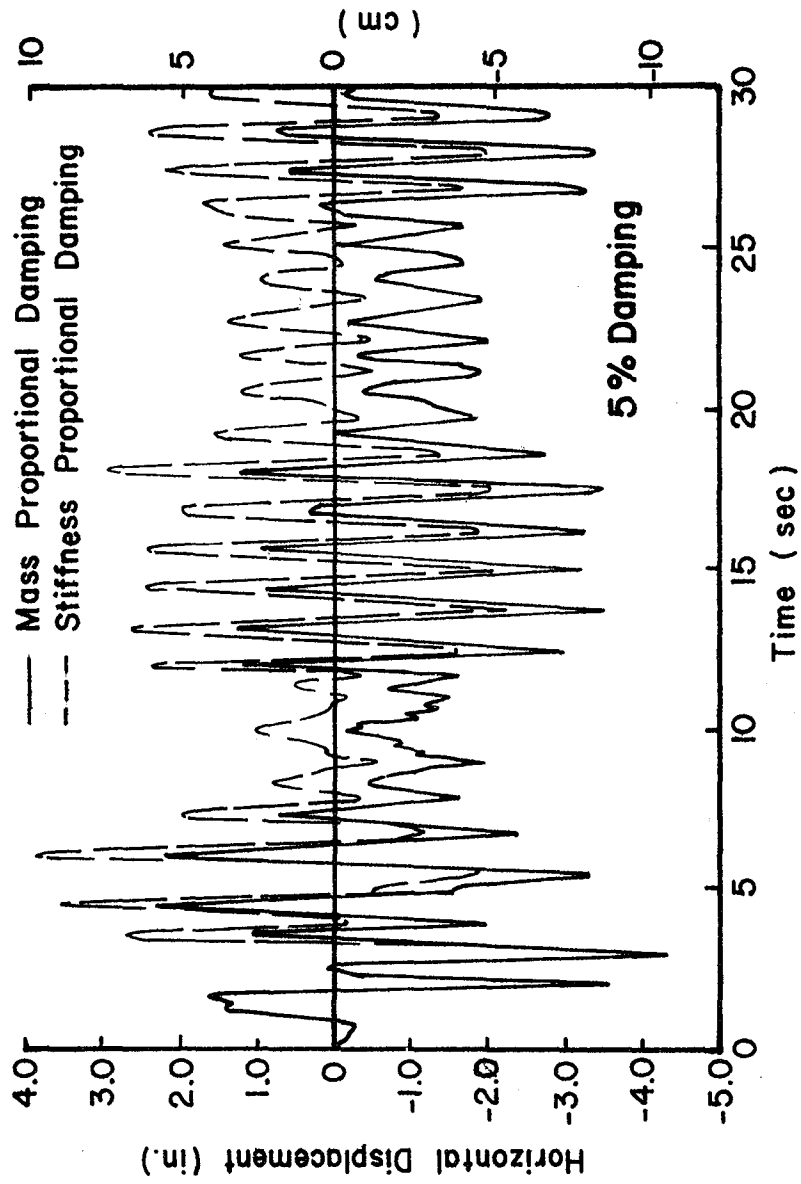


Figure 7.4. Comparison of Elasto-Plastic Responses, Frame A, ($p_n = 0.833$ Hz)

Even though a change in the fundamental frequency occurs during the presence of plastic hinges in a structure, the time duration of the occurrence is usually short compared with the total time of loading. Since mass proportional damping of nonlinear structures results in a low error level, this type of damping will result in the best solution without recalculating the fundamental frequency each time a member or members become plastic or return to their elastic range. Since a reduction in the fundamental frequency of a structure results from plastic deformations, the mass proportional damping will cause a reduction in damping. This will consequently provide a more conservative analysis with a larger displacement response.

Therefore, mass proportional damping will be used in the determination of the behavior of nonlinear structures when damping is considered.

B. BEHAVIOR COMPARISONS BASED ON STRUCTURAL MODEL

When including the coupling of the horizontal and vertical earthquake motions in the analysis of structural systems, selection of an appropriate model is important. The structural model should provide a sufficient means for adapting the effects of these coupling motions. The purpose of this section is to show the effect of the coupling earthquake motions on two lumped mass models. The response parameters used for comparison are the maximum horizontal floor displacements, maximum vertical floor displacements, energy absorptions, and ductility and excursion ratios.

Model 1 is the traditional spring-mass system in which the mass of each floor is lumped at nodes located at the intersection of column and girders. The total floor mass for each floor consists of girder

weight, superimposed mass, and the half weight of the columns located above and below the floor level. Model 2 is similar to Model 1 except part of the floor mass is lumped at an additional node at the center of each girder. The mass lumped at the girder node is half the floor mass distributed on the member.

1. 4-Story, 3-Bay Frame (Frame B). The first structure to be analyzed using the two different models is the 4-story, 3-bay rigid frame shown in Fig. 7.5. The 1940 El Centro earthquake is used to provide the ground motion for this structure.

The P-delta effect and the reduction in the plastic moment capacity are included for determining response parameters of the structure. The P-delta effect as formulated in Article IV-A-4 results from the structural weight as well as the vertical earthquake component. The reduction in the plastic moment capacity of columns due to axial loads is formulated in Section IV-C based on AISC specifications.

The top floor displacement of the structure is shown in Fig. 7.6 for the two models based on an elasto-plastic response. Viscous damping of 3% critical is assumed. The difference in displacement can be attributed to the larger amount of permanent set taking place in the initial plastic rotations of the lower floor column joints of Model 2.

The effect of the vertical component on the energy absorption of the two models in the elastic range is shown in Figs. 7.7 and 7.8. Though the energy curves are the same for the two models when only horizontal ground motion is considered, an increased amount of energy is absorbed when the vertical ground motion is included. For the same structure having elasto-plastic behavior, the energy absorption curves

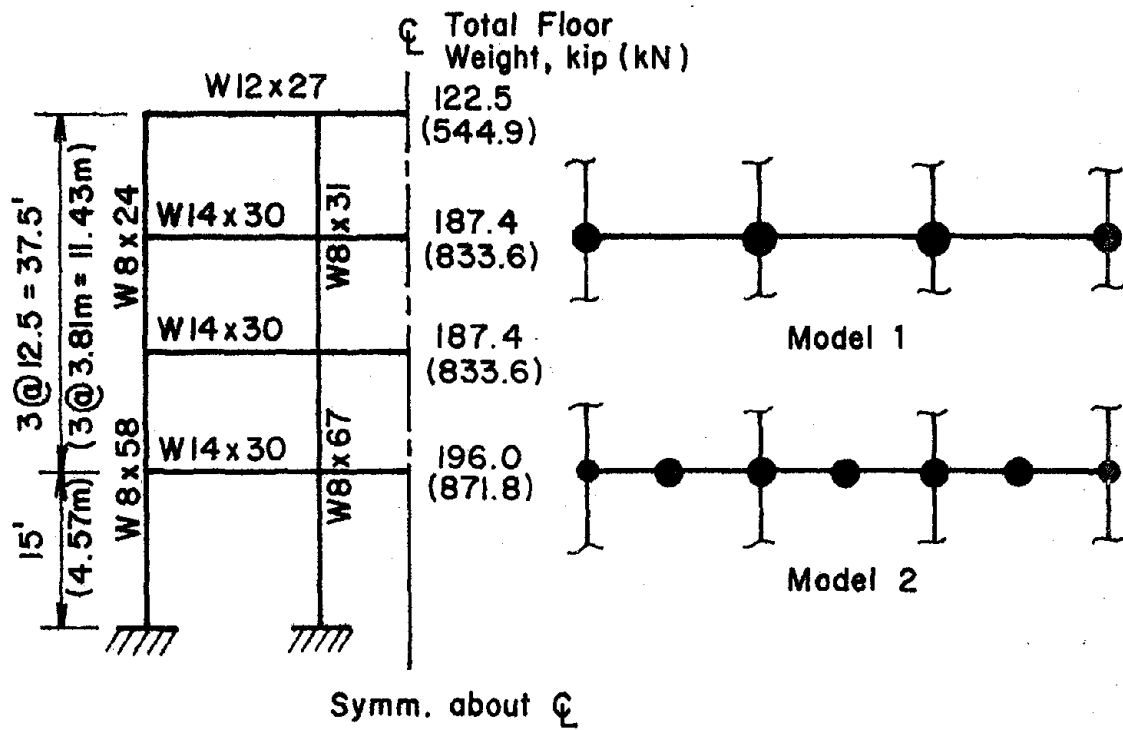


Figure 7.5. 4-Story, 3-Bay Frame (Frame B)

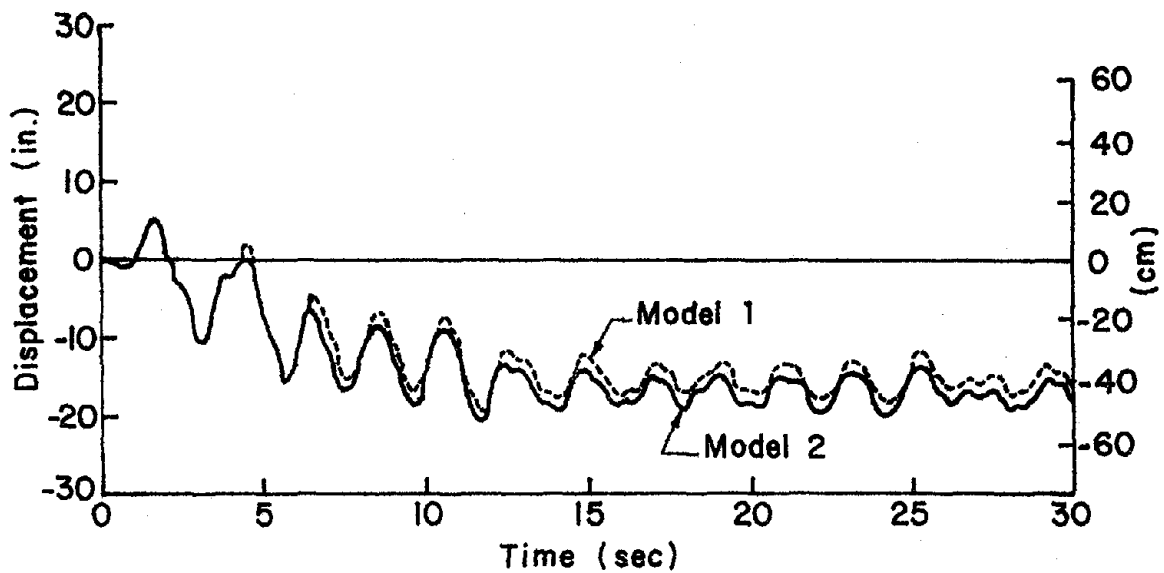


Figure 7.6. Models 1 and 2, Top Floor Displacement of Frame B, Elasto-Plastic System, 3% Damping, 1940 El Centro

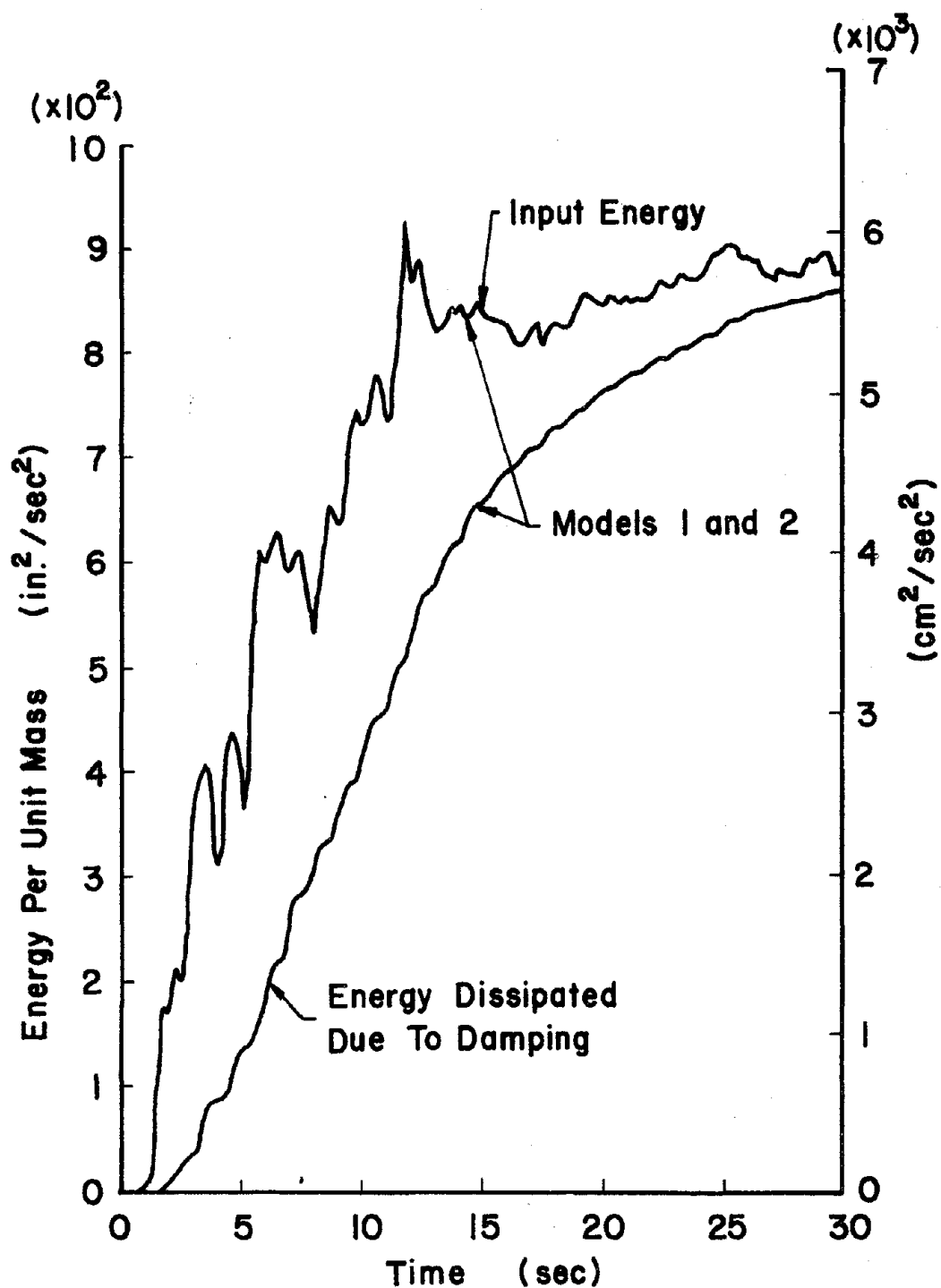


Figure 7.7. Models 1 and 2, Energy Plot of Frame B, Elastic System, 3% Damping, 1940 El Centro, N-S Component Only

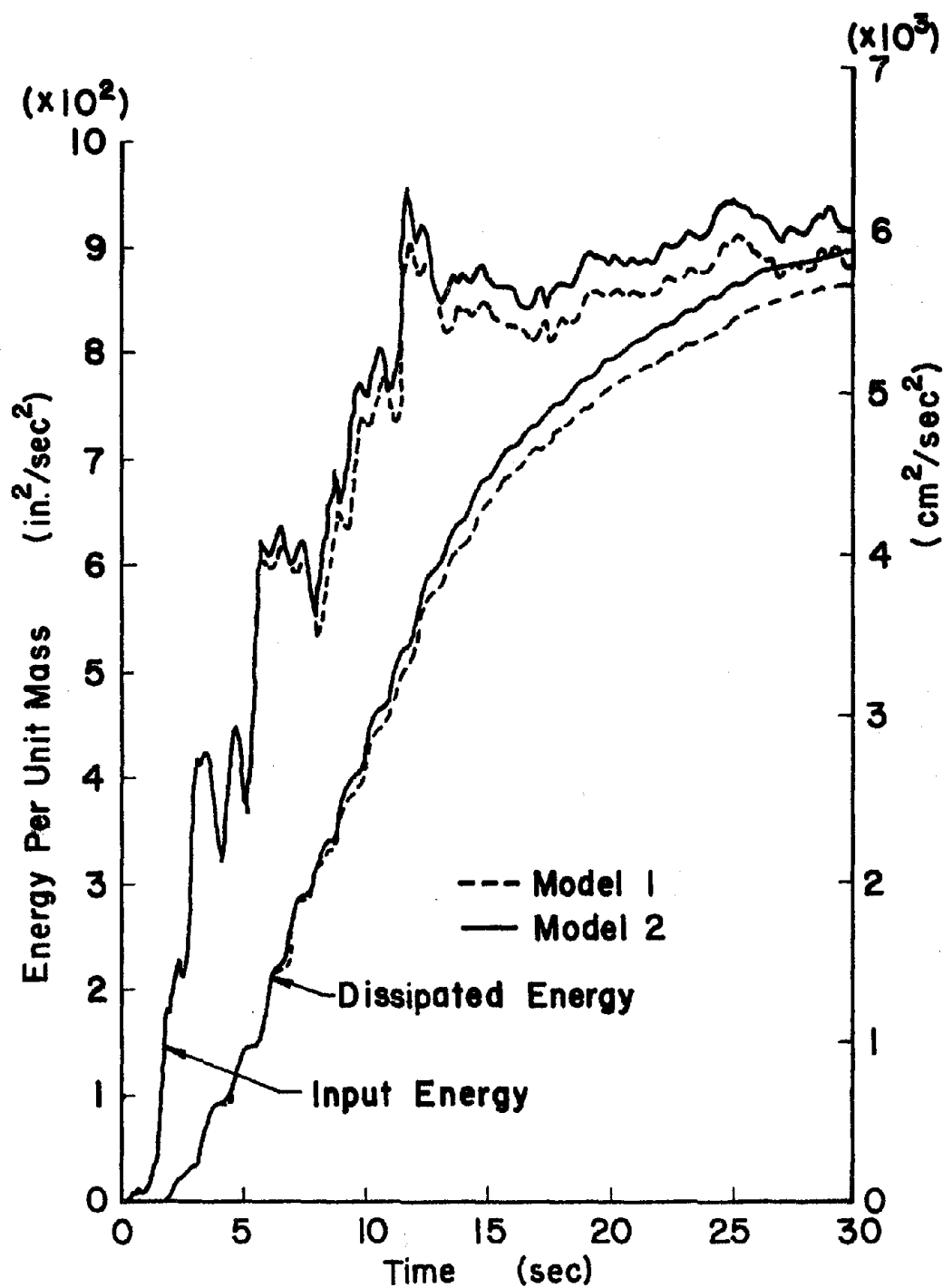


Figure 7.8. Models 1 and 2, Energy Plot of Frame B, Elastic System, 3% Damping, 1940 El Centro, N-S Plus Vertical

are shown in Figs. 7.9 and 7.10. One may observe that less energy is absorbed into Model 2 with only the horizontal component acting; however, with the addition of the vertical ground motion, the amount of input and dissipated energy is larger for Model 2.

The ductility and excursion ratios of the columns and girders of the two models for the elasto-plastic system are shown in Fig. 7.11. The largest difference in the girder ductility ratio and corresponding excursion ratio between the models occurs in the lower girders. This difference is more pronounced when the vertical earthquake component is included. The third floor columns have the largest difference in ductility and excursion ratios. The inclusion of the vertical ground motion results in the largest value for both ratios.

The maximum vertical displacement at the girder nodes for Model 2, when the vertical earthquake component is included, is shown in Fig. 7.12. These maximum displacements occur at the girder nodes of the center bay of the 3-bay structure. The vertical displacement of the girder nodes without including the vertical earthquake motion, though negligible, are found in the outer bays.

2. 10-Story, 1-Bay Frame (Frame C). The second structure to be analyzed using the two different models is the 10-story, 1-bay rigid frame as shown in Fig. 7.13. The 1940 El Centro earthquake is used to provide the ground motion for this structure.

As in the previous example, the P-delta effect due to vertical loads and the reduction in the plastic moment of columns due to axial loads are included for determining response parameters of the structure.

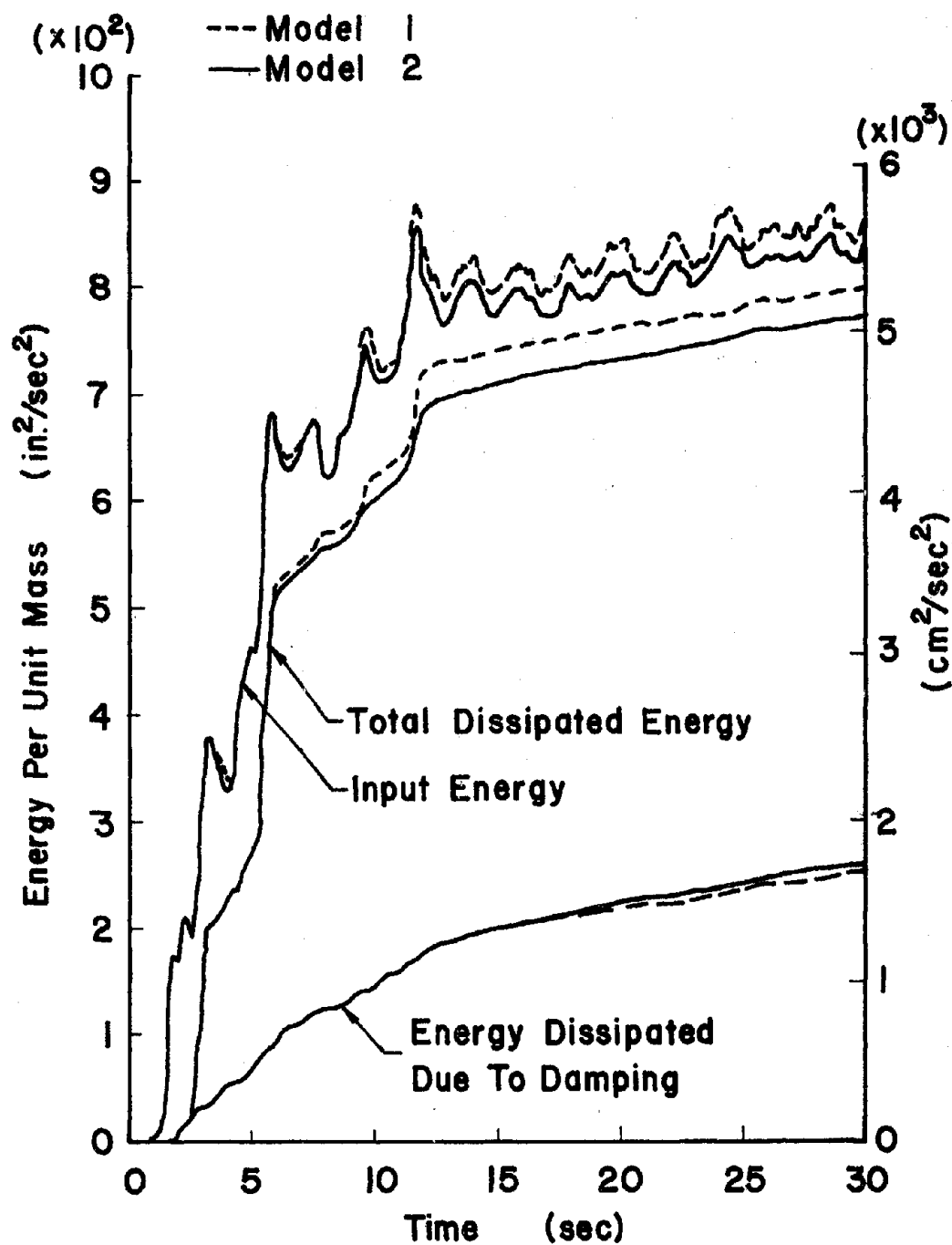


Figure 7.9. Models 1 and 2, Energy Plot of Frame B, Elasto-Plastic System, 3% Damping, 1940 El Centro, N-S Component Only

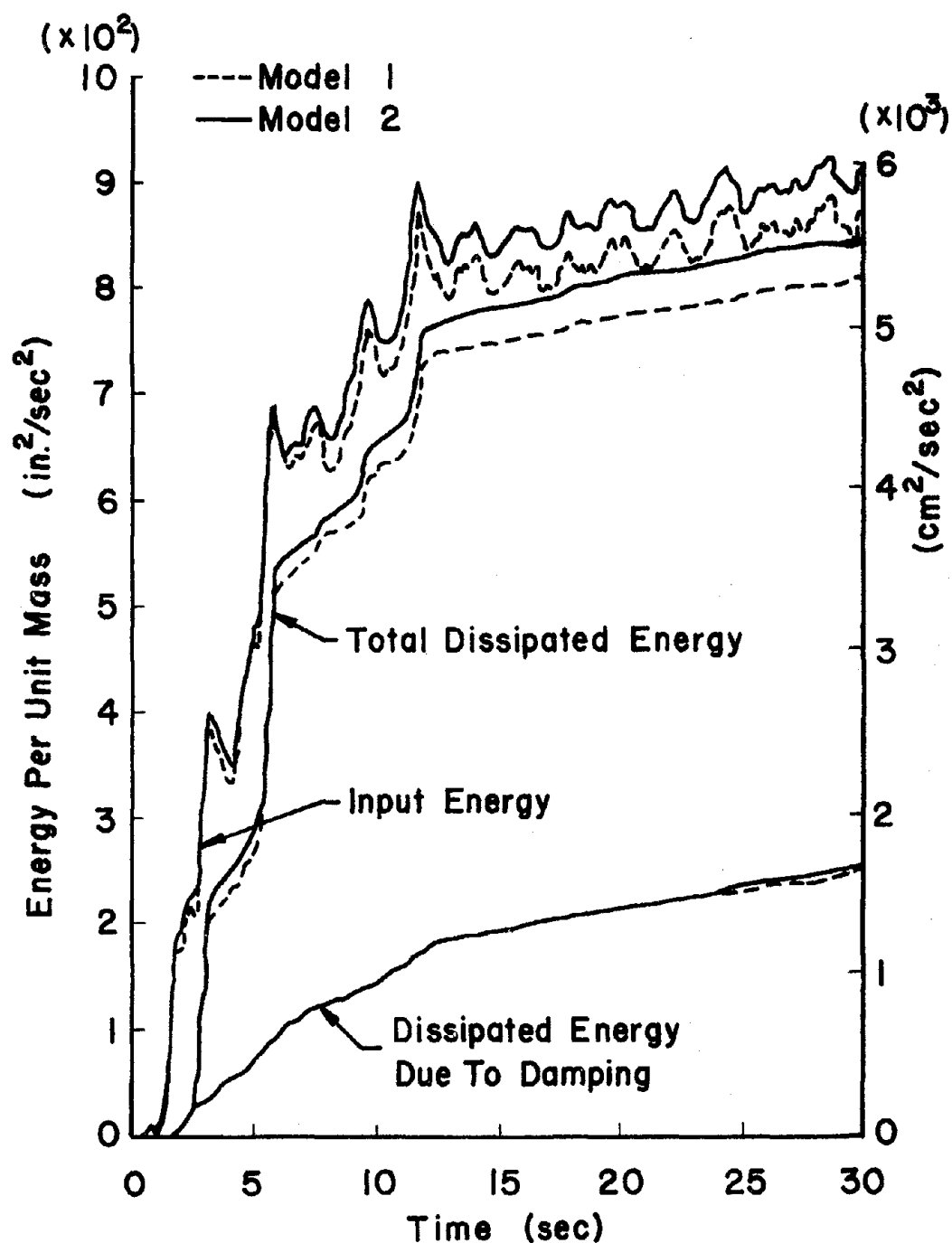


Figure 7.10. Models 1 and 2, Energy Plot of Frame B, Elasto-Plastic System, 3% Damping, 1940 El Centro, N-S Plus Vertical

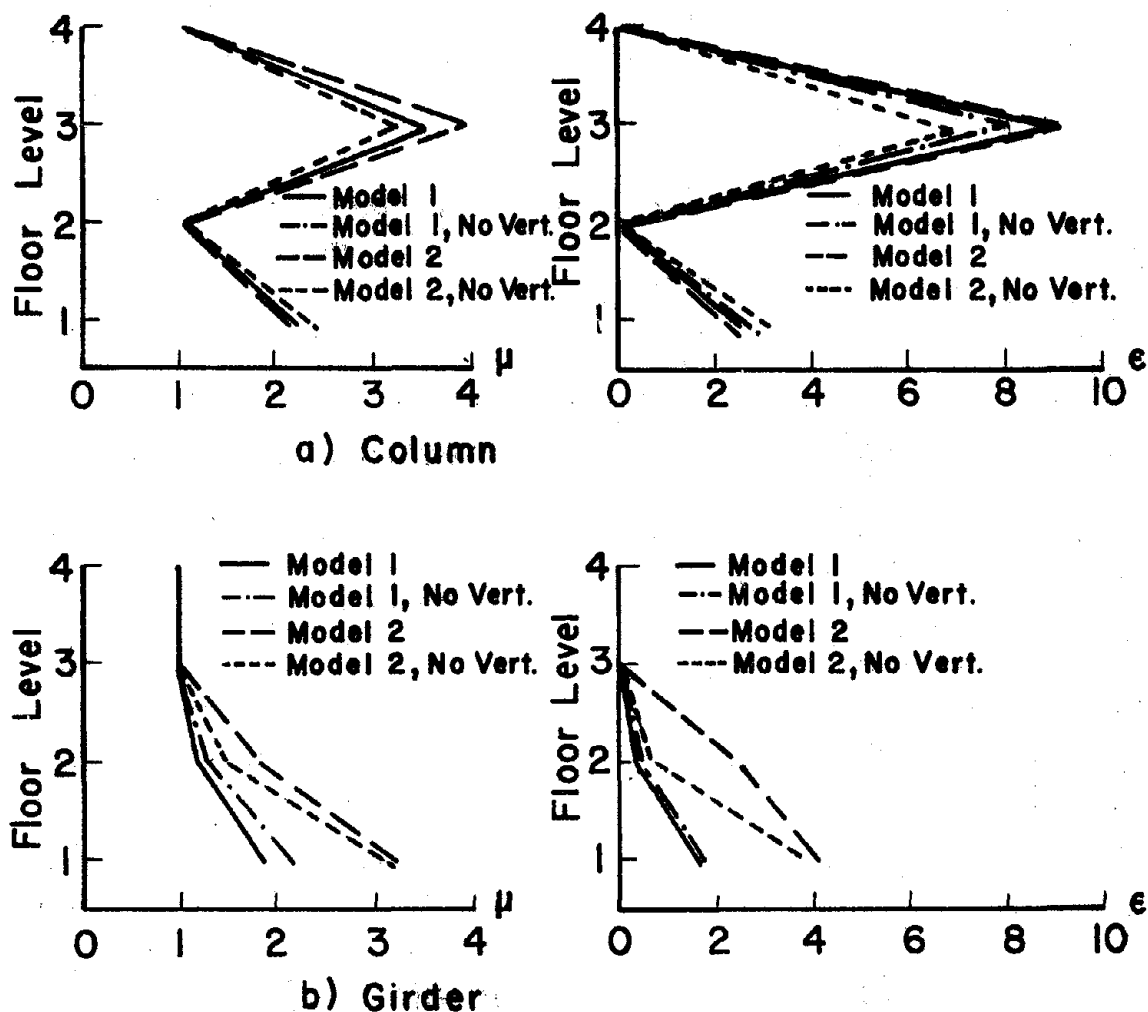


Figure 7.11. Models 1 and 2, Ductility Requirement of Frame B, Elasto-Plastic System, 1940 El Centro (cm)

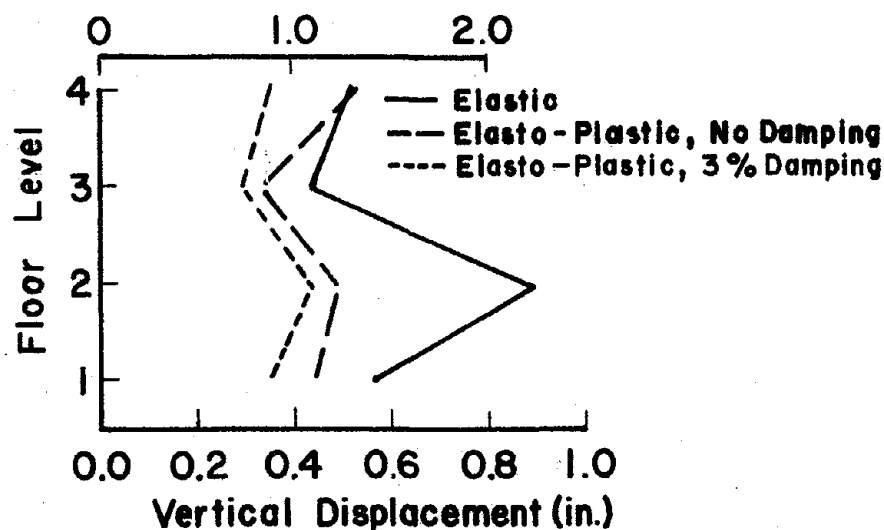


Figure 7.12. Maximum Vertical Displacement at Center of Girders, Model 2 of Frame B, 1940 El Centro, N-S Plus Vertical

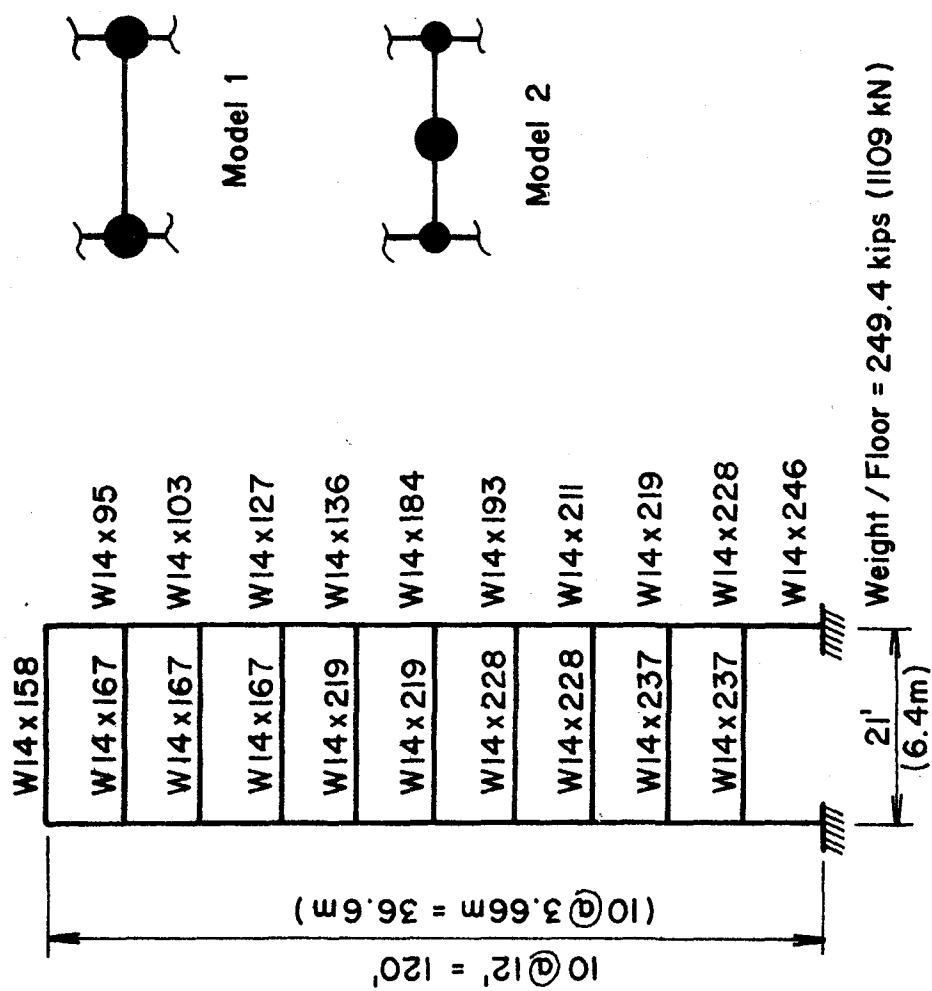


Figure 7.13. 10-Story, 1-Bay Frame (Frame C)

For Frame C the difference in the horizontal displacement of the top floor is found to be negligible between Model 1 and 2 when all members remain elastic. A small difference in horizontal displacement between the two models is realized for elasto-plastic systems with or without damping (3%). The fact that this structure has strong columns that have only plastic hinges developed at the supporting base justifies these small differences in displacement.

The vertical displacement response at the girder centers is shown in Fig. 7.14 based on Model 2 with the vertical ground motion included. Due to symmetry of the structure about the center of the bay, no vertical displacements result when considering only the horizontal component of the earthquake.

The maximum relative horizontal floor displacement is indicated by Δ/H , where Δ is the horizontal displacement of a floor relative to the floor below and H is the vertical distance between these floors. Figure 7.15 illustrates the difference in the maximum value of the relative floor displacements for the two models based on different response systems. These values reflect the small differences in the maximum horizontal displacements stated above.

The ductility and excursion ratios for the girders of Models 1 and 2 are shown in Fig. 7.16. Model 2 results in the larger ductility and excursion ratios for the floor girders having a more significant ductility requirement. The inclusion of the vertical ground motion results in an increase in the ductility requirement for the upper floor girders.

As would be expected from the small difference in horizontal displacement and the larger ductility ratios for floors 2 and 7, the

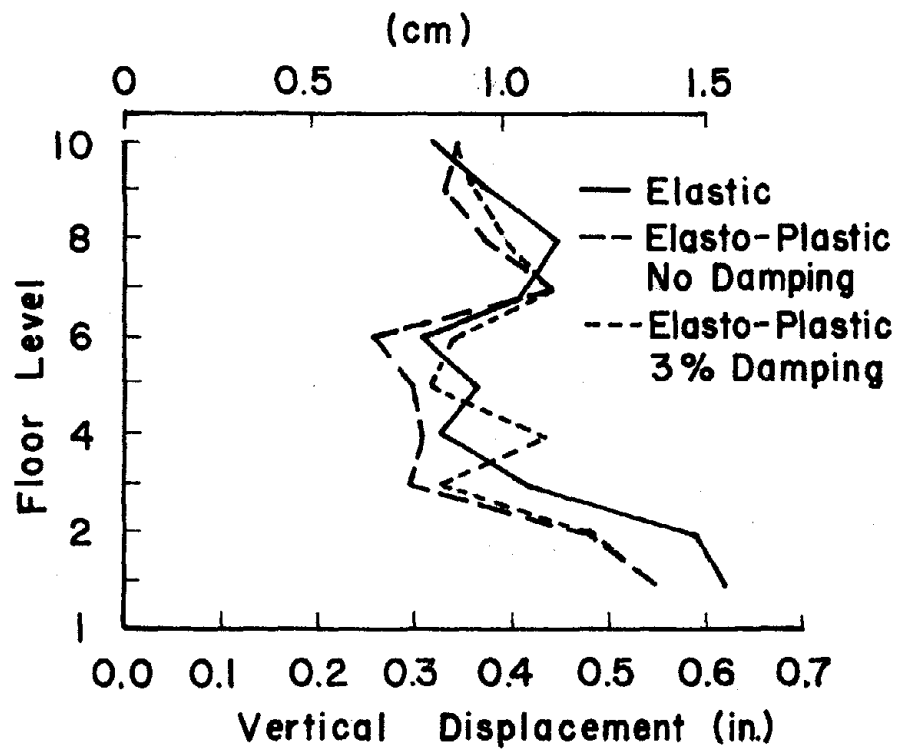


Figure 7.14. Maximum Vertical Displacement at Center of Girders, Model 2 of Frame C, 1940 El Centro, N-S Plus Vertical

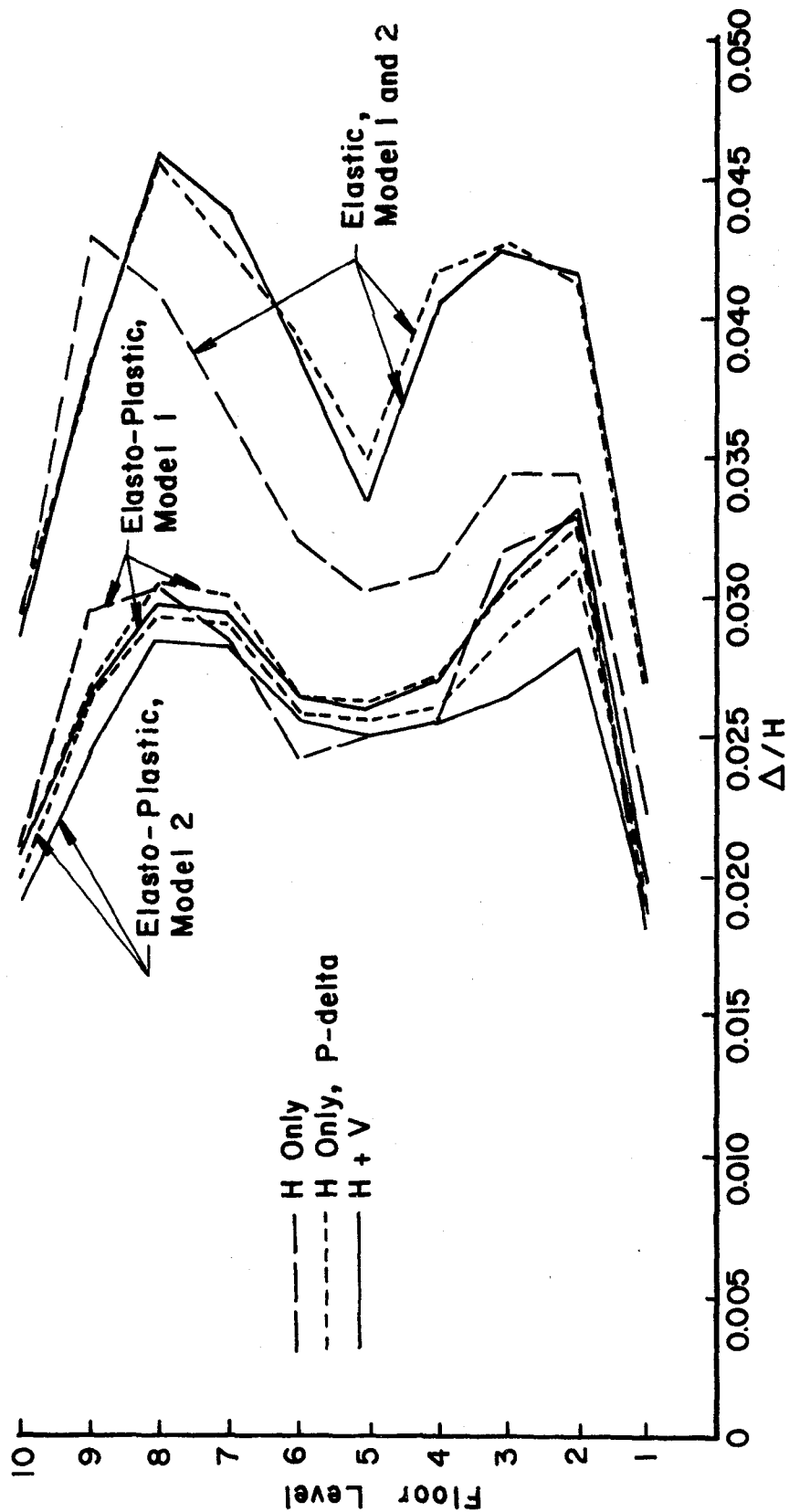


Figure 7.15. Models 1 and 2, Maximum Relative Floor Displacement of Frame C, 1940 El Centro

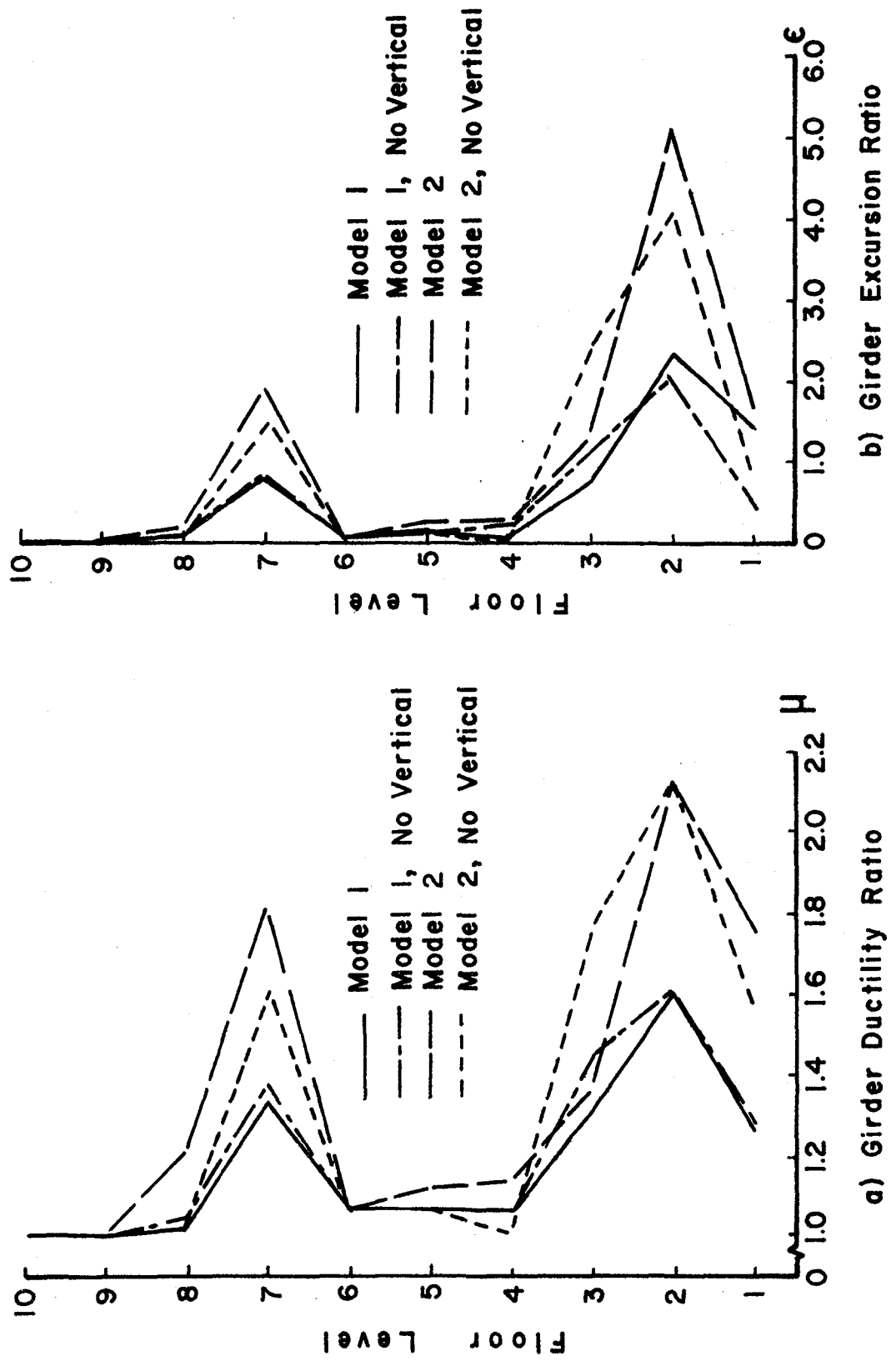


Figure 7.16. Models 1 and 2 Ductility Requirement of Frame C, 1940 El Centro

difference in energy absorption between Model 1 and 2 is negligible except for a slightly larger amount of strain energy being dissipated for Model 2.

3. Conclusions of Model Study. Based on the results obtained in the study of the lumped mass models the following conclusions are made.

- 1) Model 2 provides a better simulation of a structural system by allowing possible plastic hinges to occur at the center of girders.
- 2) The inclusion of girder nodes of Model 2 provides a means for a structural system to respond to the energy produced by the vertical ground motion.
- 3) Vertical ground motion affects the response parameters more for Model 2 than Model 1 particularly on structures with weaker columns.
- 4) Ductility requirements of girders are greater when vertical ground motion is reacted by the Model 2 structure.
- 5) Vertical ground motion significantly affects all response parameters.

C. COMPARISON OF DUCTILITY AND EXCURSION RATIOS BASED ON DEFINITION

The purpose of this section is to provide numerical examples for comparison of the three definitions of the ductility and excursion ratios as formulated in Section IV-E, Eqs. 4.70-4.78.

The equations for the three ductility ratio definitions are repeated as follows.

Based on symmetrical bending,

$$\mu_1 = 1 + \frac{\alpha}{\theta_y} \quad (7.2)$$

Based on curvature,

$$\mu_2 = 1 + \frac{M_{\max} - M_p}{pM_p} \quad (7.3)$$

Based on strain energy,

$$\mu_3 = 1 + \frac{E_{dse}}{E_{tese}} \quad (7.4)$$

The equation for the excursion ratio corresponding to each of these definitions can be written as:

$$\epsilon_i = \sum_{j=1}^{N_\mu} (\mu_{ij} - 1) \quad (7.5)$$

where ϵ_i = excursion ratio corresponding to definition i,

μ_{ij} = ductility ratio based on definition i during the half cycle of rotation j, and

N_μ = total number of times the node of a member becomes plastic during earthquake excitation.

As shown in Eq. 7.3, the ductility ratio based on curvature is expressed in terms of end moments. This equation is applicable to bilinear systems and results in ductility ratios of infinity for a

truly elasto-plastic system. The ductility ratio formulation for an elasto-plastic system may be found in Ref. 1. For a numerical analysis a small number of $p = 0.00001$ has been used satisfactorily in the computer program for elasto-plastic systems.

The ground acceleration records of the 1940 El Centro and the 1952 Taft earthquakes are used to produce the ground motion for this investigation. Observations based on the resulting ductility and excursion ratios are made.

1. 3-Story, 1-Bay Frame (Frame A). The first structure analyzed is Frame A shown in Fig. 7.1. The N69°W component of the 1952 Taft earthquake along with its vertical component is used to produce the ground motion. To obtain a sufficient amount of plastic joint rotation, a magnification factor of 2.0 and 3.0 is applied to the horizontal and vertical earthquake components, respectively. Model 2 which includes girder nodes is used so that the ductility effect of the vertical earthquake component is realized. The P-delta effect is included, and the initial conditions of the dynamic response at time $t = 0$ are based on a static analysis. Both elasto-plastic ($p = 0.00001$) and bilinear ($p = 0.05$) response systems are considered. Mass proportional damping is included with 5% of critical damping.

The variation in the ductility and excursion ratios for each girder based on an elasto-plastic condition is shown in Figs. 7.17 and 7.18, respectively. Curves corresponding to the bilinear response condition for the same structure are shown in Figs. 7.19 and 7.20. The results are based on the definitions of curvature, energy and symmetrical bending due to the horizontal earthquake component as well as the interaction of horizontal and vertical components.

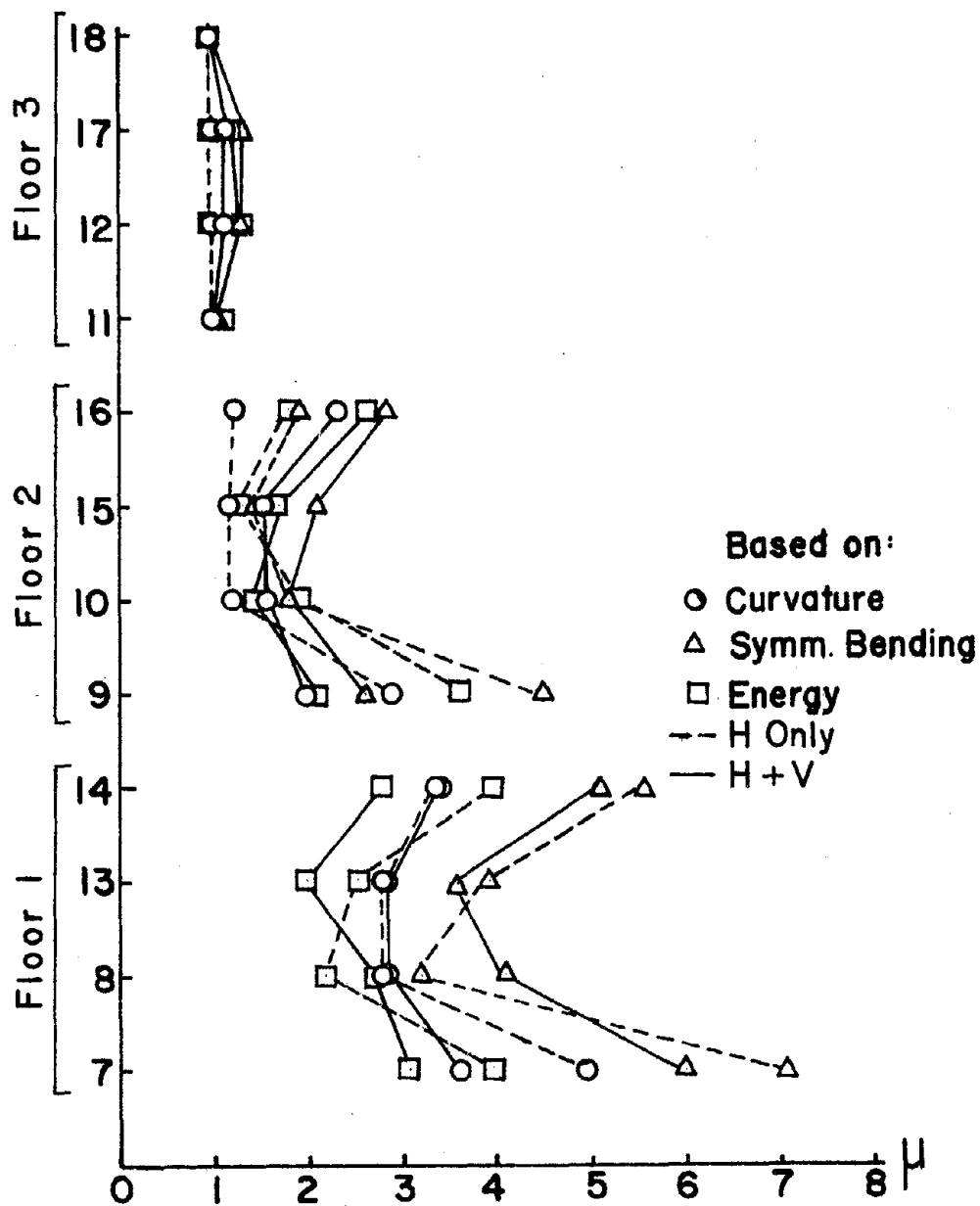


Figure 7.17. Elasto-Plastic Ductility Ratios for Girders of Frame A, 1952 Taft

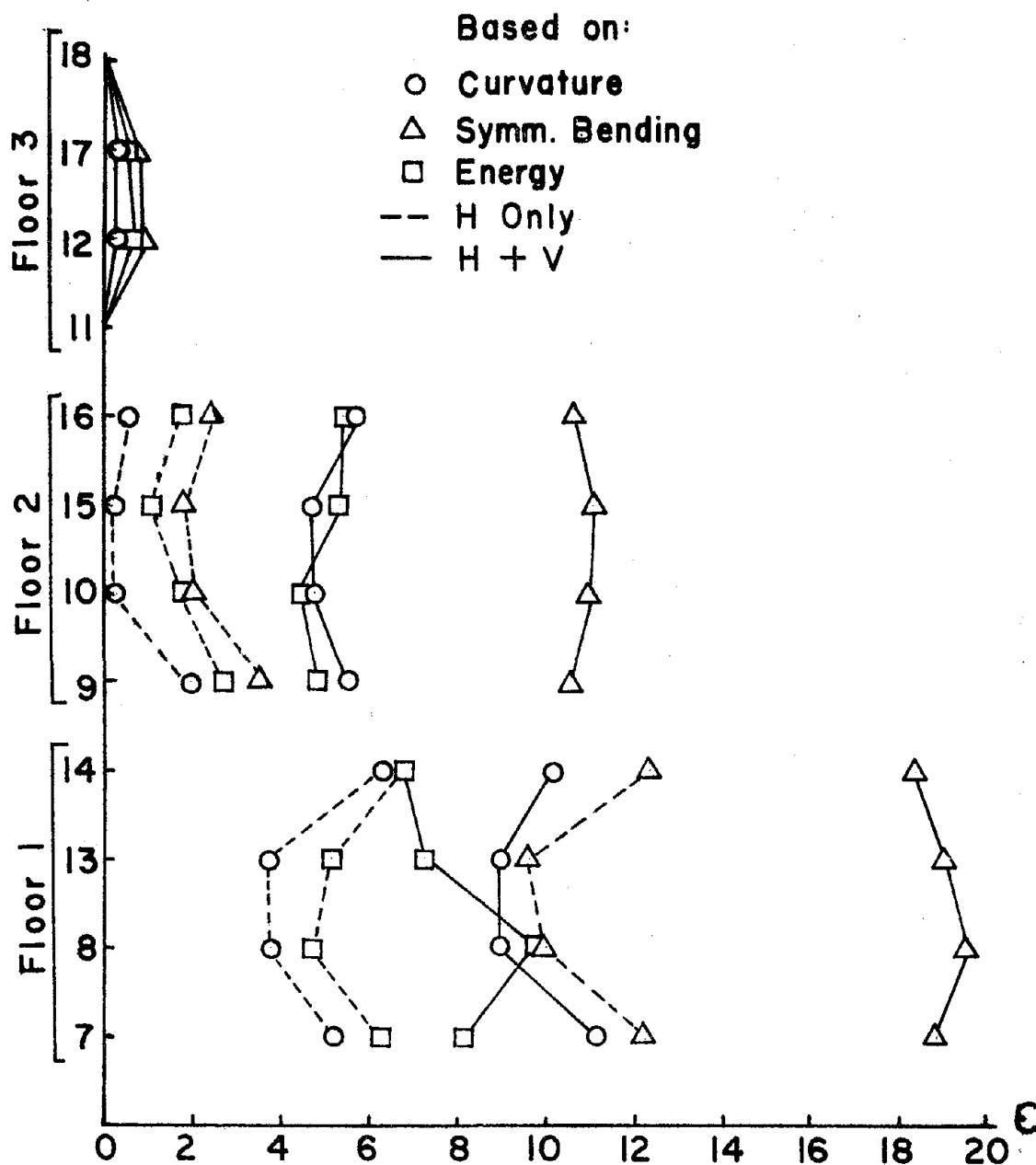


Figure 7.18. Elasto-Plastic Excursion Ratios for Girders of Frame A, 1952 Taft

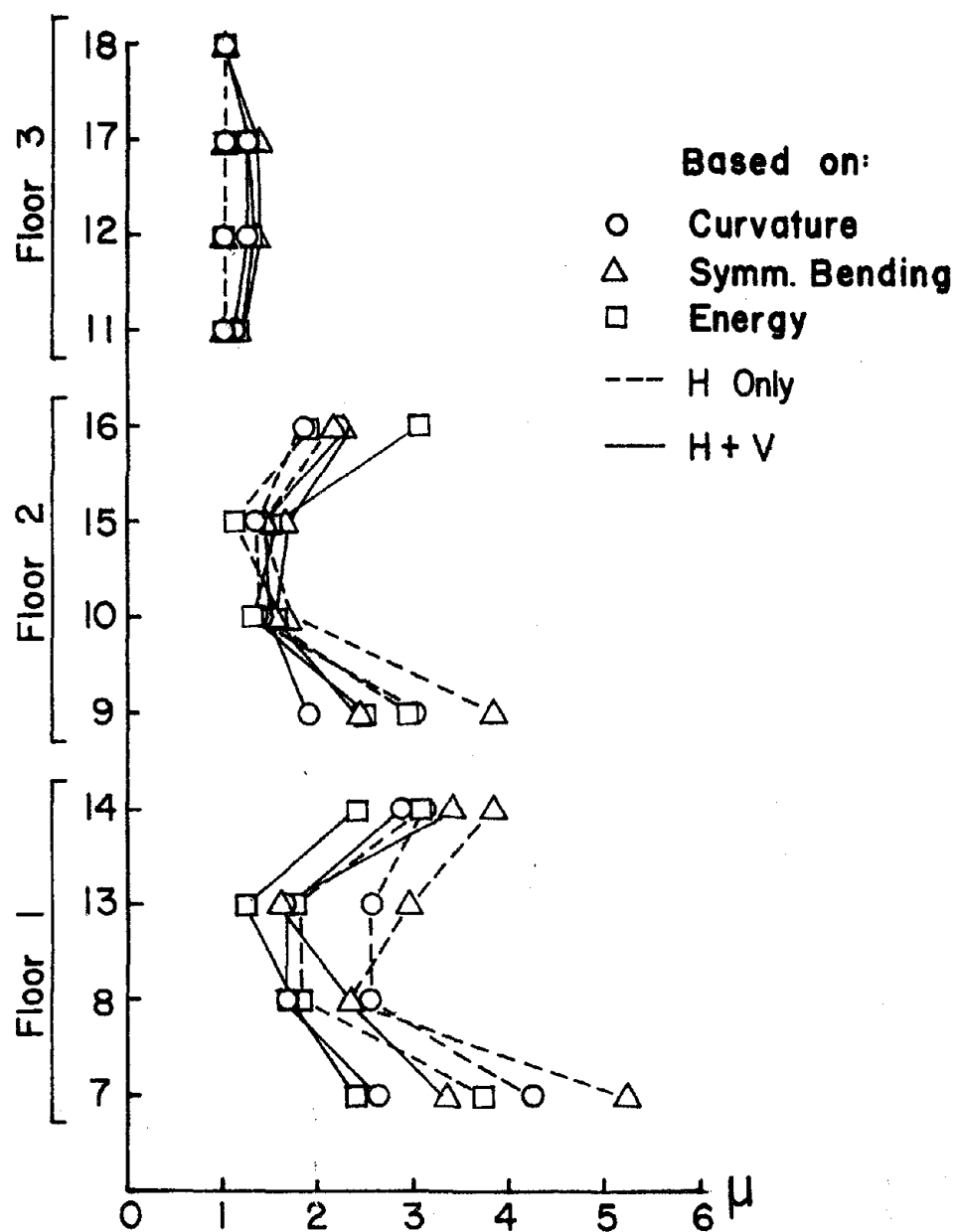


Figure 7.19. Bilinear Ductility Ratios for Girders of Frame A, 1952 Taft

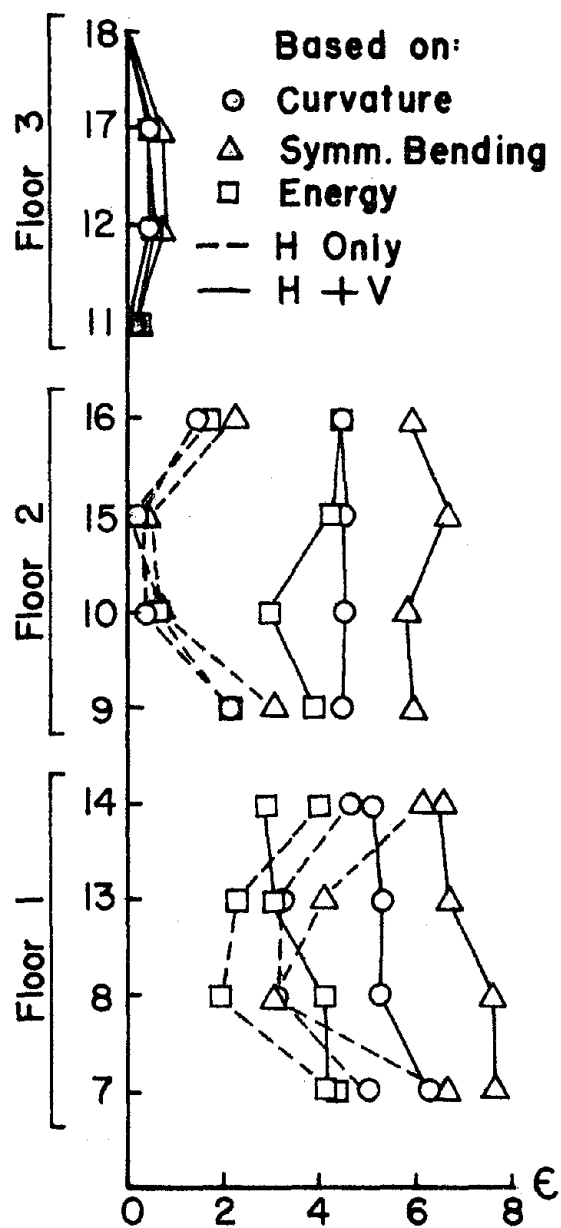
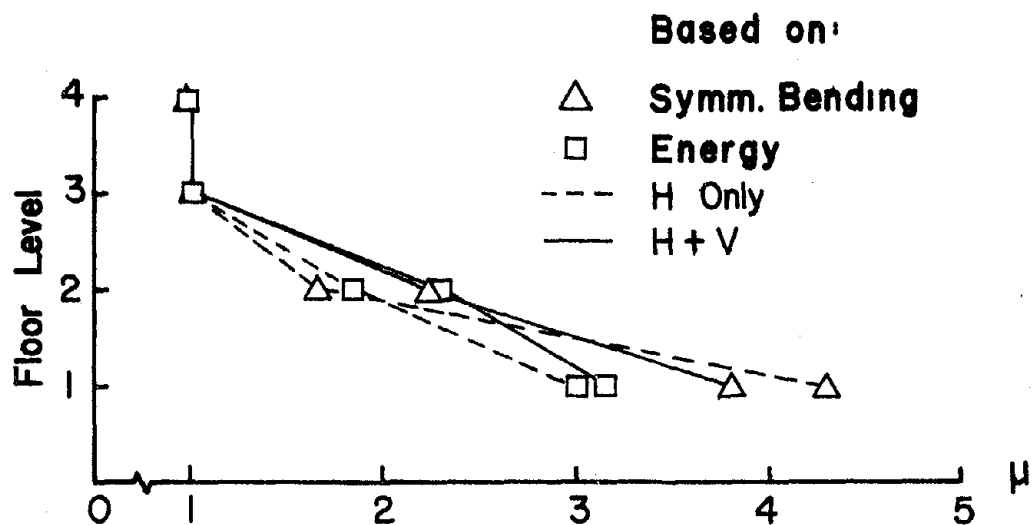


Figure 7.20. Bilinear Excursion Ratios for Girders of Frame A, 1952 Taft

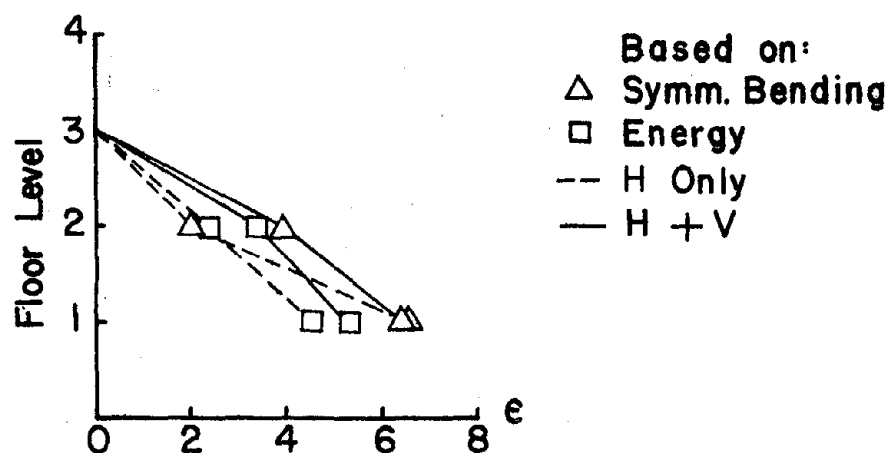
2. 4-Story, 3-Bay Frame (Frame B). The second structure analyzed is the 4-story, 3-bay frame as shown in Fig. 7.5. The N-S component of the 1940 El Centro earthquake along with its vertical component is used to produce the ground motion without magnification factor. Reduction of the allowable bending moment M_p in each column is performed based on the AISC specifications as formulated in Section IV-C. Model 2 with girder nodes is used so the influence of the vertical earthquake component on ductility requirement can be observed. The P-delta effect is included with no damping or initial static analysis. An elasto-plastic response in Figs. 7.21 and 7.22 for the girders and columns, respectively. As in the first structure, curves represent the ratios with and without the vertical ground motion.

3. 10-Story, 1-Bay Frame (Frame C). The third structure analyzed is Frame C as shown in Fig. 7.13 subjected to the N-S component of the 1940 El Centro earthquake along with its vertical component. No magnification factor is included in the loading. Reduction of the allowable bending moment M_p in each column is considered on the basis of the AISC specifications. Girder nodes are assumed with inclusion of the P-delta effect. Initial moments in the structure due to static loads are not included. The maximum ductility and excursion ratios for each girder of the elasto-plastic system are shown in Figs. 7.23 and 7.24 for each definition of ductility considered. Plastic hinges only occur in the columns at the supports; consequently, the ductility and excursion ratios are not shown.

4. Observations Based on Ductility Studies. The following observations can be made from the comparisons of the ductility definitions as illustrated in Figs. 7.17 through 7.24.

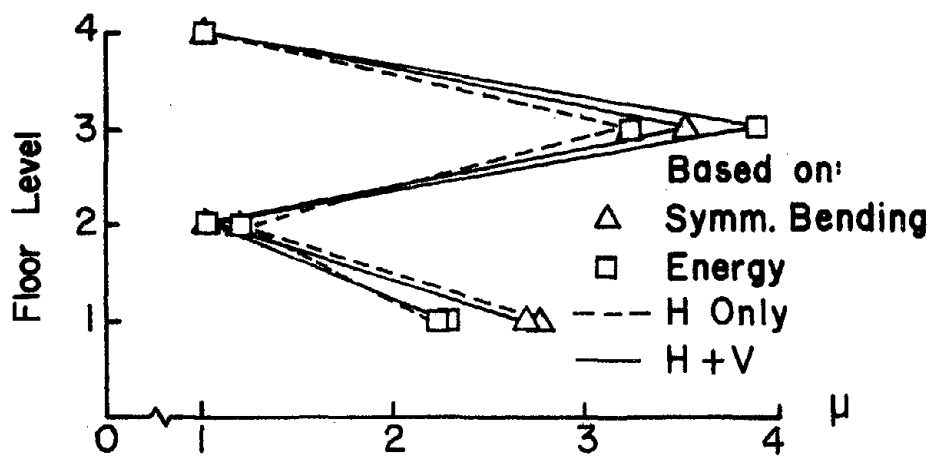


(a) Girder Ductility Ratio

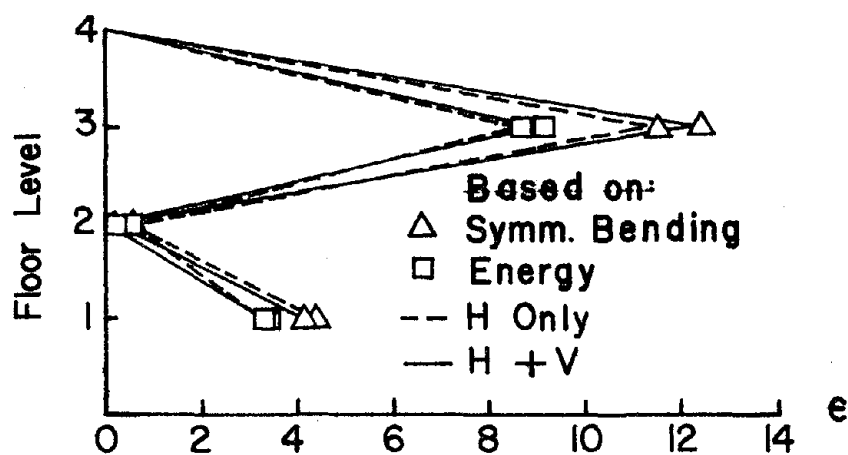


(b) Girder Excursion Ratio

Figure 7.21. Elasto-Plastic Girder Ductility and Excursion Ratios of Frame B, 1940 El Centro



(a) Column Ductility Ratio



(b) Column Excursion Ratio

Figure 7.22. Elasto-Plastic Column Ductility and Excursion Ratios of Frame B, 1940 El Centro

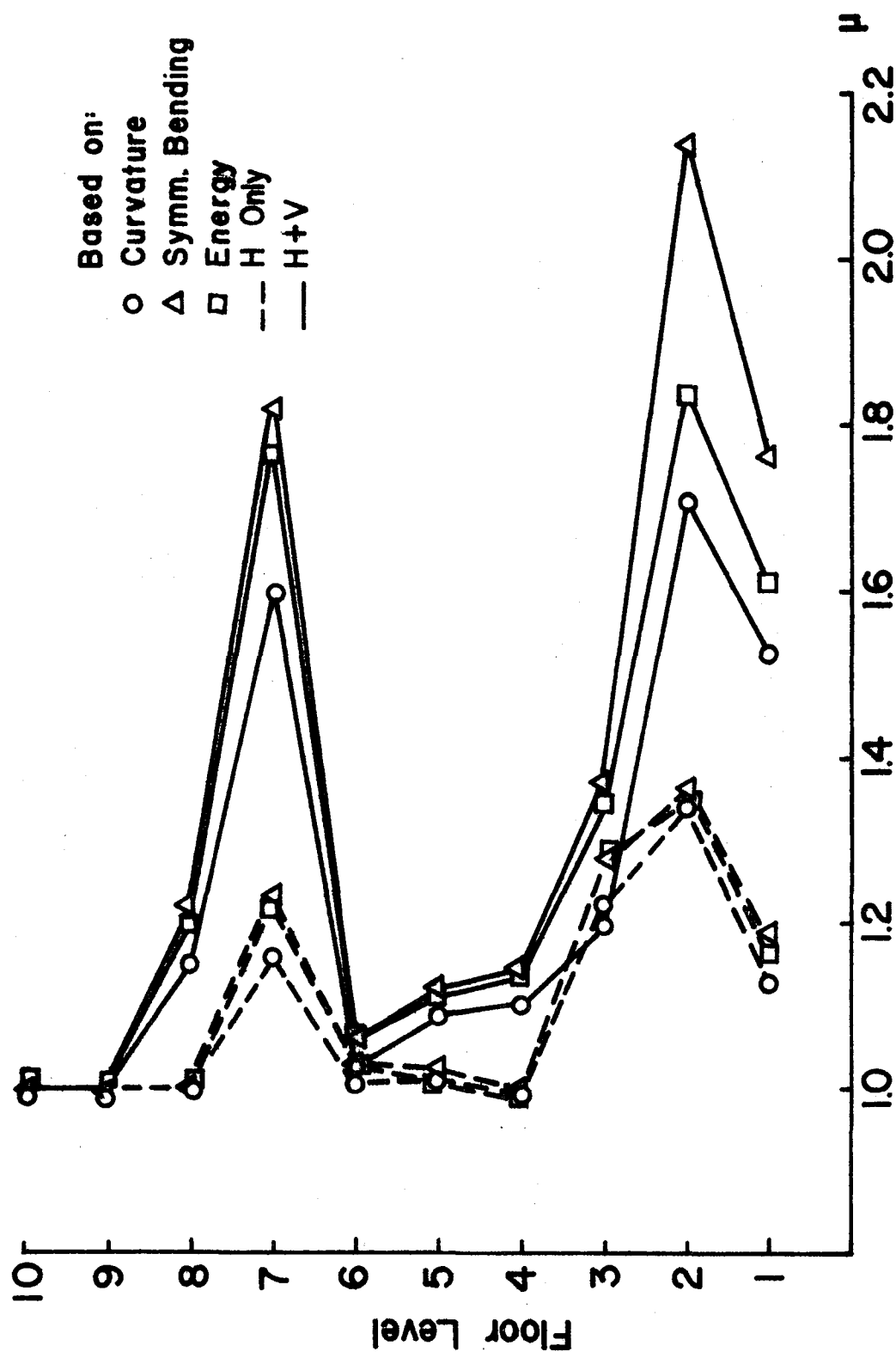


Figure 7.23. Elasto-Plastic Girder Ductility Ratios of Frame C, 1940 E1 Centro

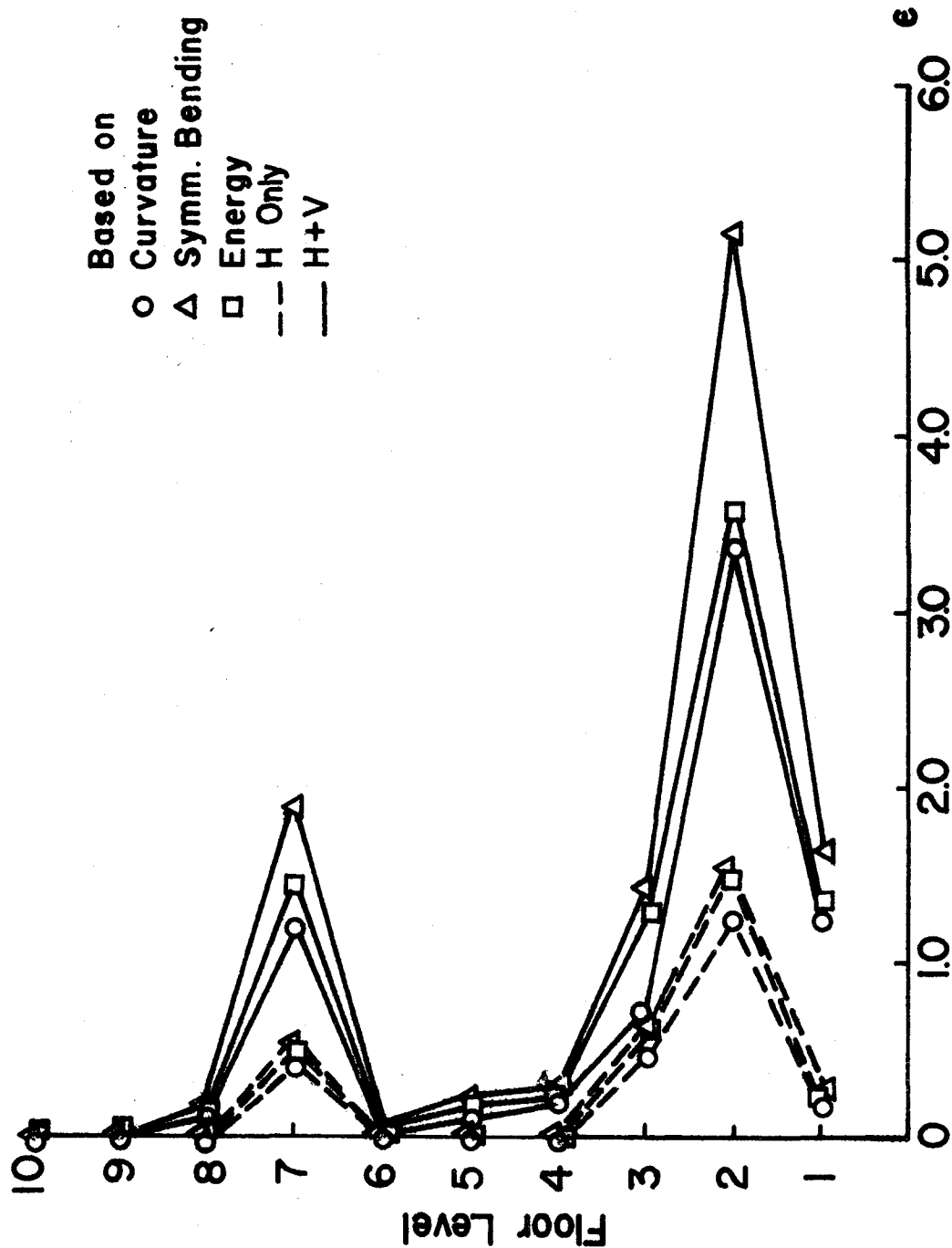


Figure 7.24. Elasto-Plastic Girder Excursion Ratios of Frame C, 1940 E1 Centro

- 1) A similar pattern in the variation of the girder ductility ratios based on the three definitions is realized for the structures studied. A qualitative determination of the ductility requirements could be made by either of the three definitions.
- 2) The ductility ratio based on symmetrical bending always yields a higher ratio than that obtained on the basis of curvature and energy. The ductility ratio based on energy seems higher than that defined by curvature.
- 3) Due to the lower value of the ductility ratios for the 10-story frame, the difference in the ductility definitions are not as significant as in the other two frames, especially when the vertical ground motion is not included.
- 4) The use of the ductility ratio based on energy provides a reasonable estimator of the ductility requirement of a structure containing members having unsymmetrical bending and a constant stress range.

Additional observations can be made on the basis of the behavior of individual structures.

- 1) The inclusion of the vertical earthquake component for Frames A and B results in the girders of the upper floors to have an increase in ductility requirement. This can be said of both the elasto-plastic and bilinear response systems.
- 2) For Frame A, the inclusion of the vertical component causes a reduction in the ductility ratio for the lower girders, especially at the nodes adjacent to the columns.

- 3) An increase in the total plastic rotation of the lower girder nodes due to the inclusion of the vertical component is revealed in the increase in the excursion ratios.
- 4) The largest amount of plastic rotation for Frame B occurs in the lower floor girders and the 1st and 3rd floor columns.
- 5) The effect of the inclusion of the vertical component is less prominent for structures having strong columns such as Frame A.
- 6) The inclusion of the vertical earthquake component for Frame C results in almost all definitions of ductility to have an increase in their value.
- 7) The maximum ductility requirements for Frame C occur approximately at the quarter points in its height.

D. EFFECT OF INELASTIC ACTION ON RESPONSE PARAMETERS

The purpose of this section is to show the effect of both horizontal and vertical ground motions on the response parameters of inelastic systems having elasto-plastic and bilinear material characteristics. The response parameters of the 3-story, 1-bay (Frame A), the 4-story, 3-bay (Frame B), and the 10-story, 1-bay (Frame C) framed structures as shown in Figs. 7.1, 7.5 and 7.13, respectively, are used for illustration.

For each of the structures analyzed the following response parameters are included:

- 1) maximum horizontal displacement of each floor relative to the ground,
- 2) maximum horizontal displacement of each floor relative to the floor below,

- 3) response history of top floor,
- 4) maximum vertical displacement of girder nodes relative to the ground,
- 5) maximum vertical acceleration of girder nodes relative to the ground,
- 6) ductility requirement of member nodes based on symmetrical bending, and
- 7) energy in the form of input, stored and dissipated.

To further illustrate the effect of vertical ground motion on the above response parameters, the following load conditions are considered:

- 1) The horizontal component of the earthquake is applied without considering the P-delta effect.
- 2) The horizontal component of the earthquake is applied with inclusion of the P-delta effect due to structure's weight.
- 3) Both horizontal and vertical earthquake components are applied with the P-delta included.
- 4) The 1940 El Centro earthquake is used in the analyses.

The following damping formulation, structural model and ductility ratio are selected for this investigation:

- 1) Mass proportional damping is used since it provides a very low percent error based on Eq. 5.6 for the nonlinear response.
- 2) Model 2 containing girder nodes is used since it has been shown to provide an excellent model when considering vertical ground motions.
- 3) The ductility ratio based on symmetrical bending is used to provide a qualitative comparison of the ductility requirement of structural joints.

The response parameters of the individual structures are illustrated first with comments as to the results obtained. A comparison of the response parameters of the three structures are made after the response parameters of each structure are obtained.

1. 3-Story, 1-Bay Frame (Frame A). In the analysis of Frame A, damping is not considered and a reduction in the plastic moment M_p of the columns is not included. An initial static analysis is based on half the floor weight being concentrated at the girder node. The effect of including the M_p reduction in column members for this frame is discussed in Section VII-E.

A comparison of the maximum floor displacements for Frame A is shown in Figs. 7.25 and 7.26. Elastic, elasto-plastic and bilinear ($p = 0.05$) systems are compared for the loading conditions stated above. Both the elasto-plastic and bilinear systems result in a reduced horizontal displacement. The response history of the top floor is shown in Fig. 7.27 for the elastic and elasto-plastic systems.

Figure 7.28 illustrates the difference in the top floor displacement over the 30 second time period of the earthquake record with and without including the initial static analysis. The response is reduced when the initial static load is included in the analysis.

The maximum relative floor displacement is indicated in Figs. 7.29 and 7.30 by the term Δ/H where Δ is the floor displacement relative to the floor below and H is the floor height between floors. The same reduction in response is realized for the elasto-plastic and bilinear systems as indicated in the maximum floor displacements of Fig. 7.25.

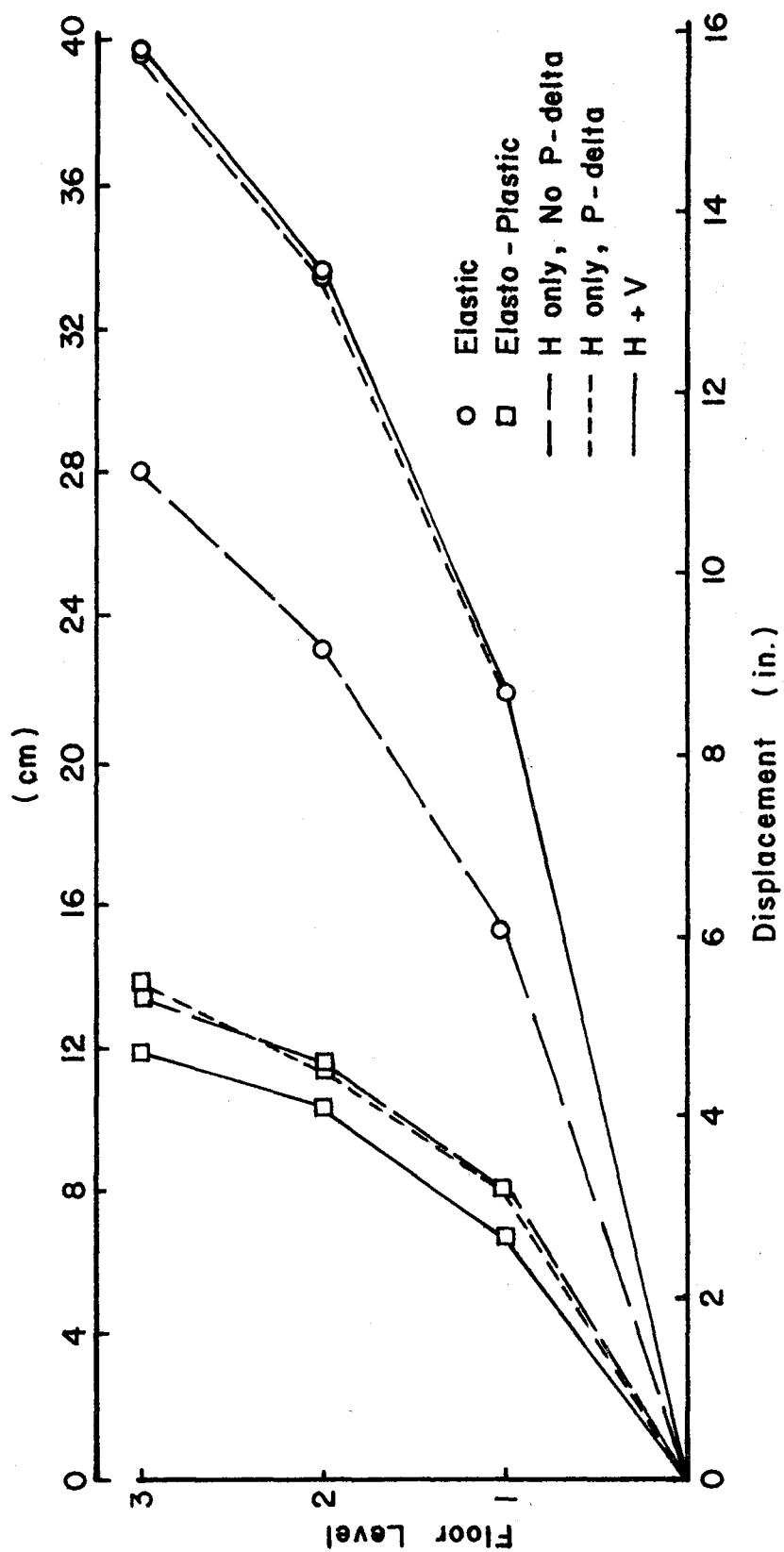


Figure 7.25. Maximum Floor Displacement, Frame A, Elastic and Elasto-Plastic Systems, 1940 E1 Centro

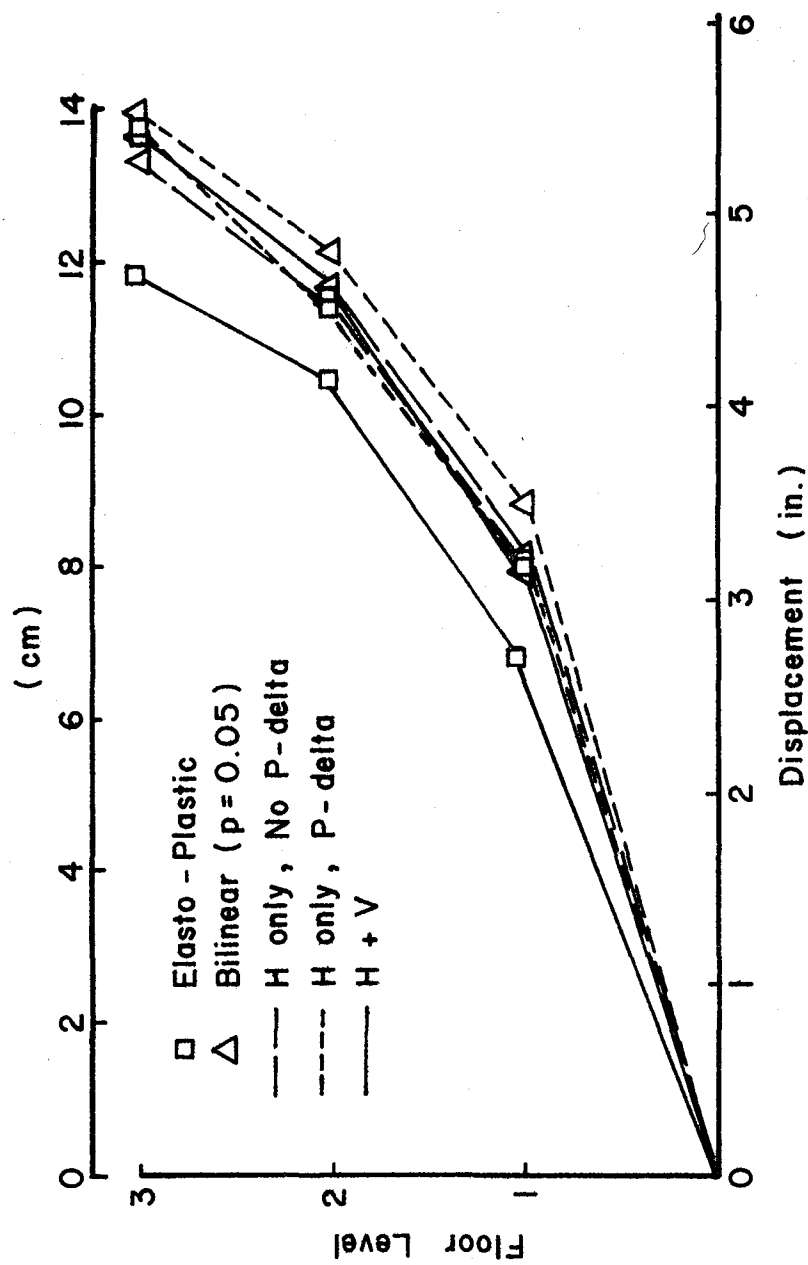


Figure 7.26. Maximum Floor Displacement, Frame A, Elasto-Plastic and Bilinear ($p = 0.05$) Systems, 1940 El Centro

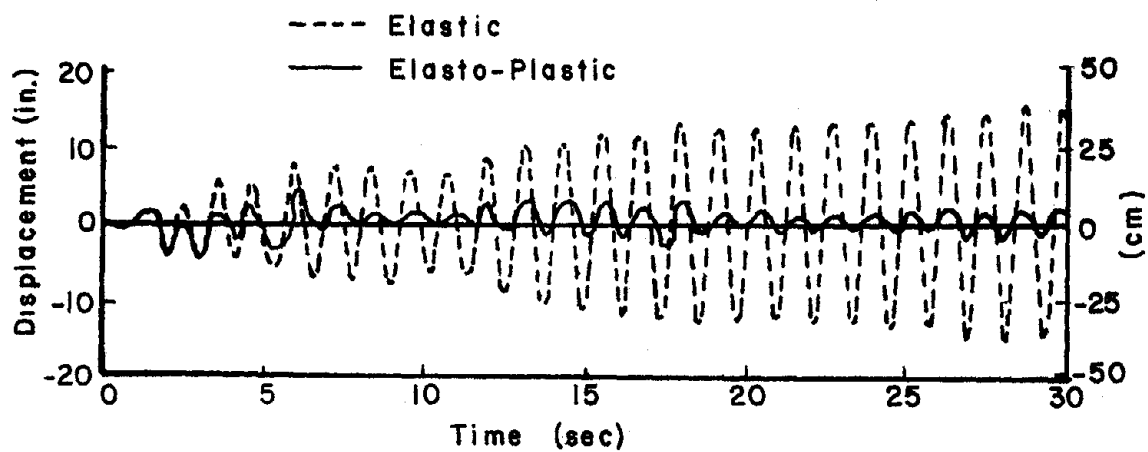


Figure 7.27. Top Floor Displacement of Frame A, Elastic and Elasto-Plastic Systems, 1940 El Centro

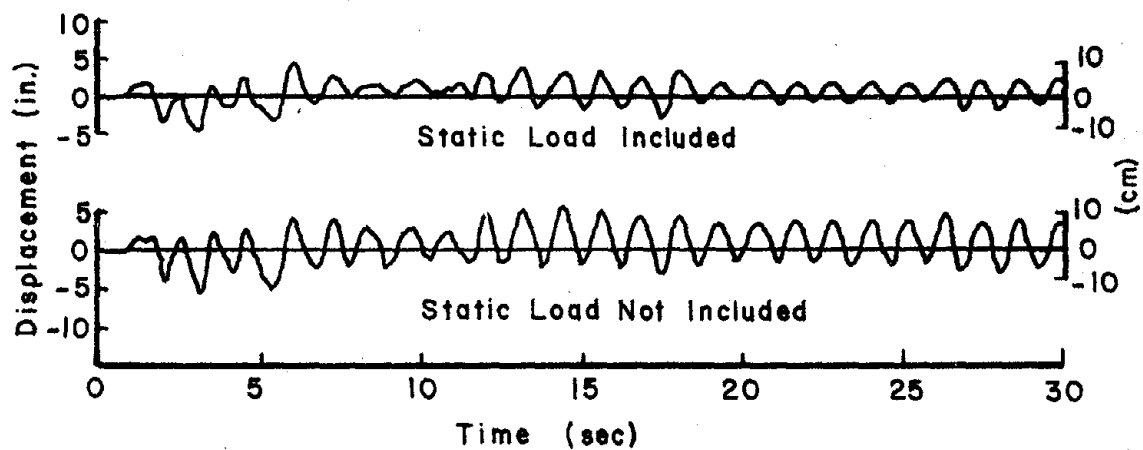


Figure 7.28. Top Floor Displacement of Frame A With and Without Static Loads, Elasto-Plastic System, 1940 El Centro

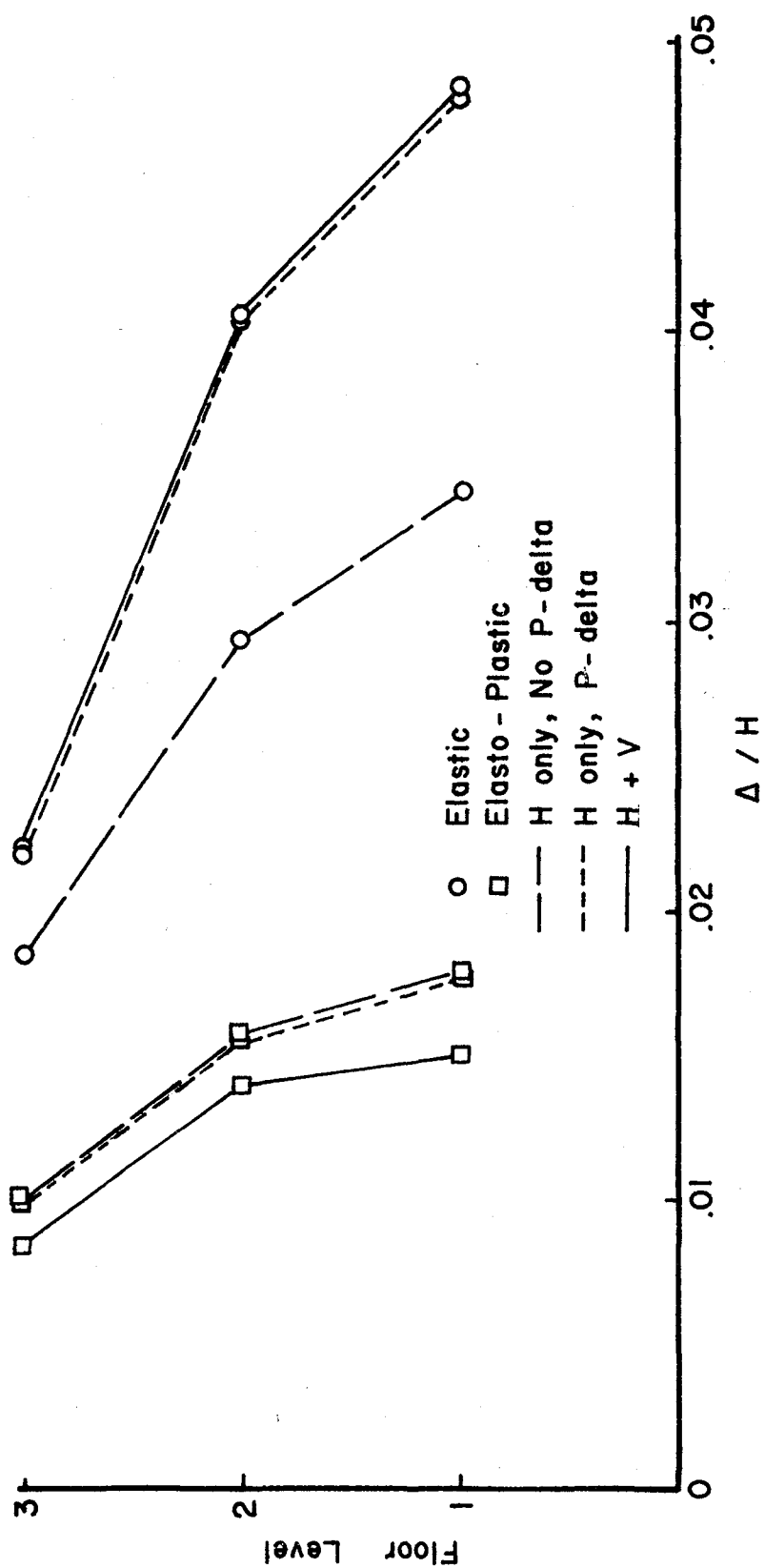


Figure 7.29. Maximum Relative Floor Displacements, Frame A, Elastic and Elasto-Plastic Systems, 1940 El Centro

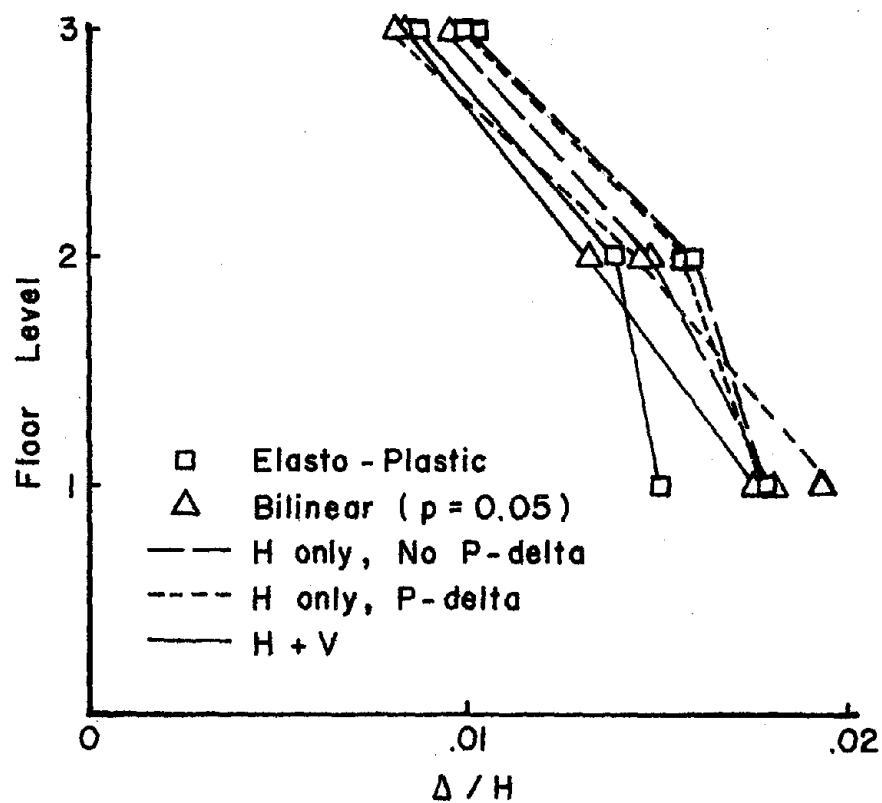


Figure 7.30. Maximum Relative Floor Displacement, Frame A, Elasto-Plastic and Bilinear ($p = 0.05$) Systems, 1940 El Centro

The maximum vertical displacement of the girder nodes when including vertical ground motion is shown in Fig. 7.31. Though the larger horizontal displacements occur under elastic conditions, the larger vertical displacements occur under the elasto-plastic conditions. As shown in Fig. 7.32, the maximum vertical acceleration, when including the vertical component of ground motion, occurs in the top floor for all the response conditions. The behavior shown in Figs. 7.31 and 7.32 is consistent in that the larger displacements are associated with the smaller accelerations. For the case of plastic hinges developing in the lower members of the system, the ductility ratios for the girder and column members are shown in Fig. 7.33, in which the small column ductility ratios indicate the frame having strong columns.

Figures 7.34 and 7.35 show the variation in the ductility ratio between the ends and center of each girder member. Even though plastic hinges occur at both locations, the ductility requirement is greater for the nodes adjacent to the columns.

2. 4-Story, 3-Bay Frame (Frame B). For the analysis of Frame B, damping is not considered in the response analysis except in the evaluation of energy. A reduction of the plastic moment M_p for all column members is included. however, no static analysis is initially performed.

The variation in the time history of the top floor displacement for Frame B is shown in Fig. 7.36 for elastic, bilinear ($p = 0.05$) and elasto-plastic systems. The nonsymmetrical response curves for both the bilinear and elasto-plastic systems are due to the permanent set in some of the columns.

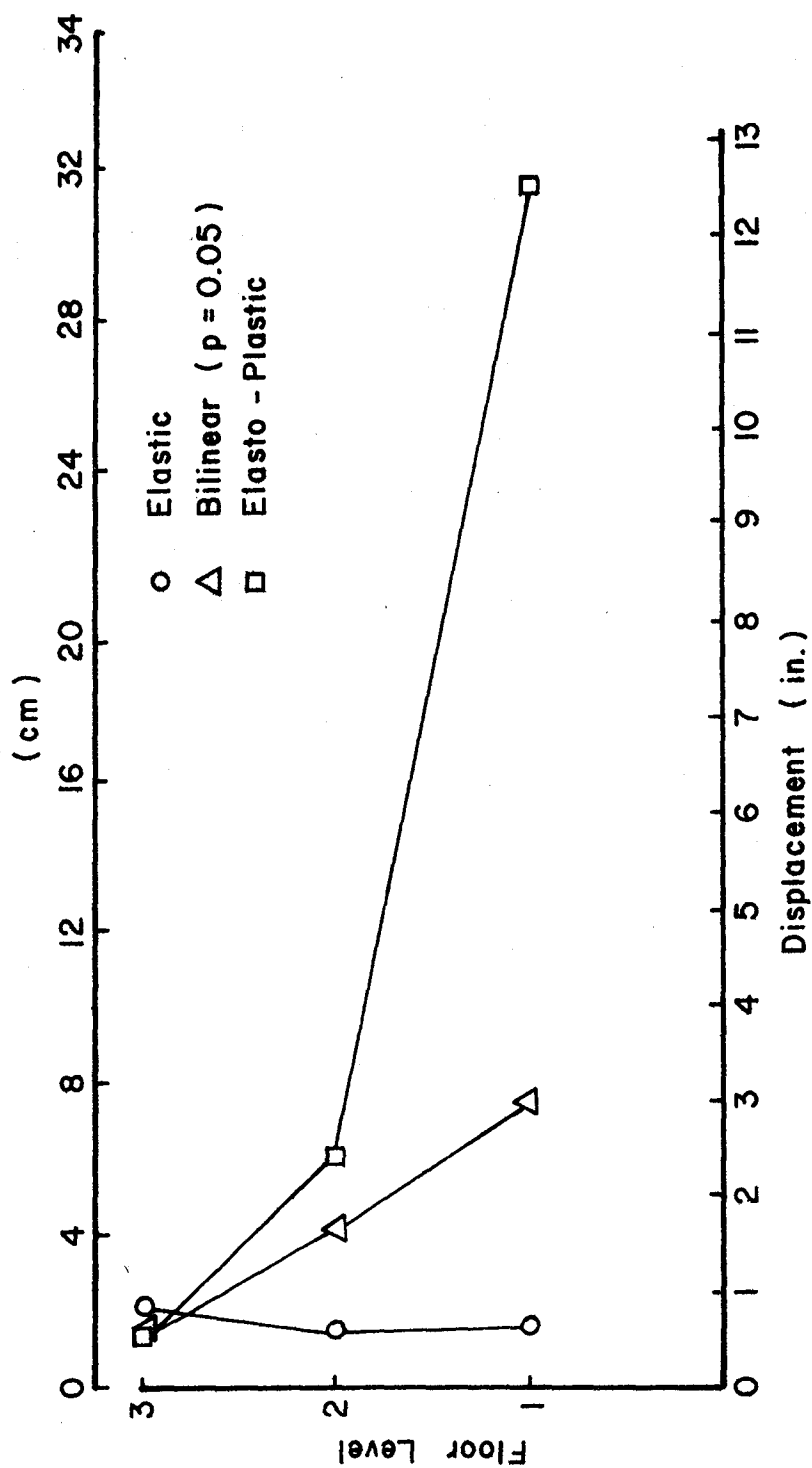


Figure 7.31. Maximum Vertical Displacement at Center of Girder, Frame A, 1940 El Centro, N-S Plus Vertical

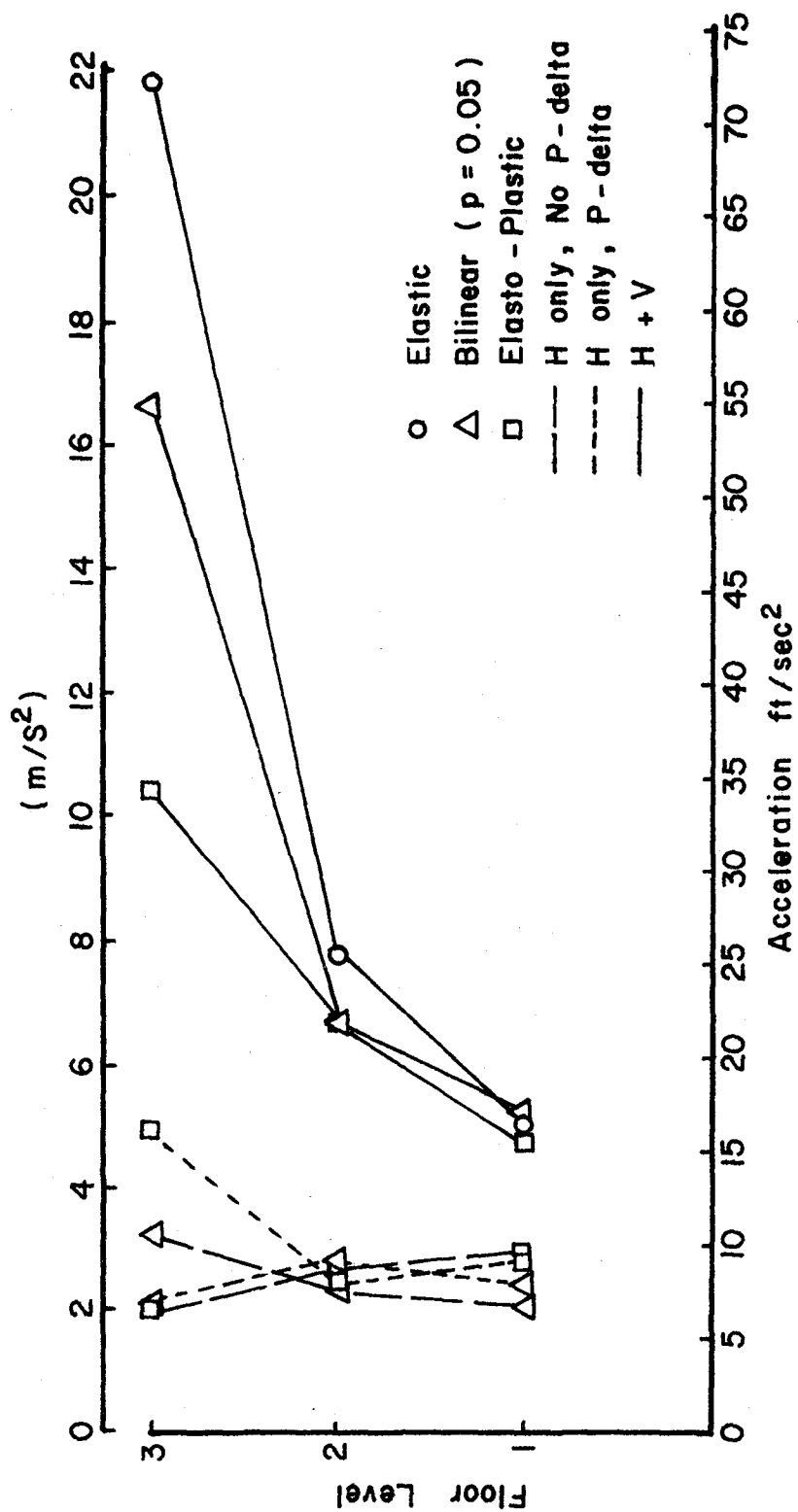
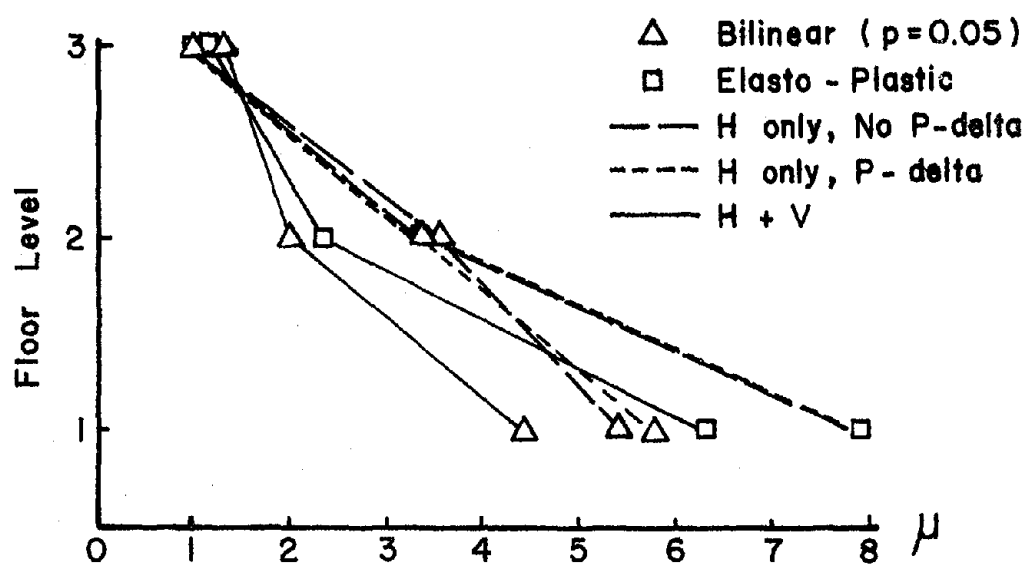
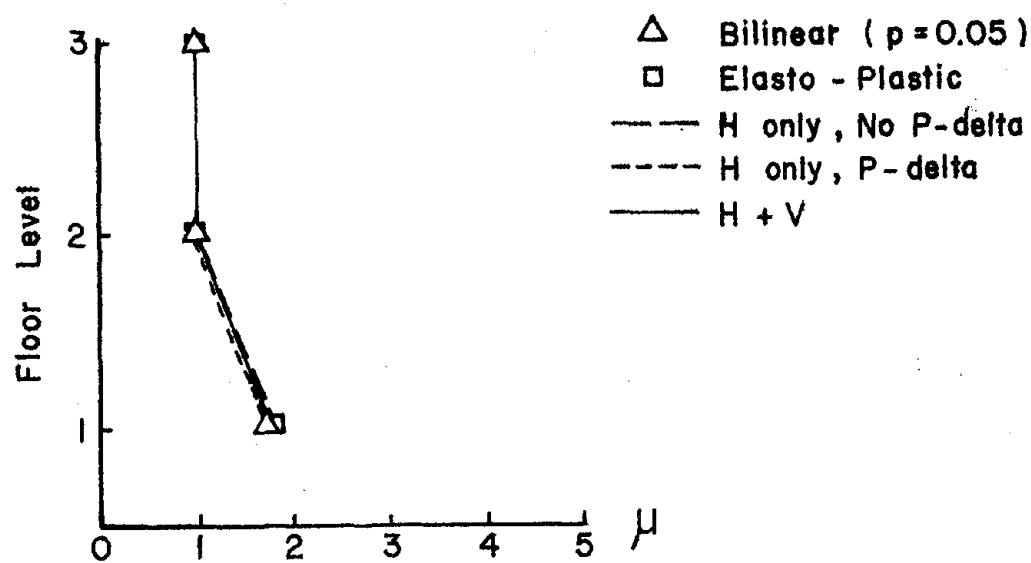


Figure 7.32. Maximum Vertical Acceleration at Center of Girder, Frame A, 1940 El Centro, N-S Plus Vertical



a) Girder



b) Column

Figure 7.33. Maximum Ductility Ratios, Frame A, 1940 El Centro

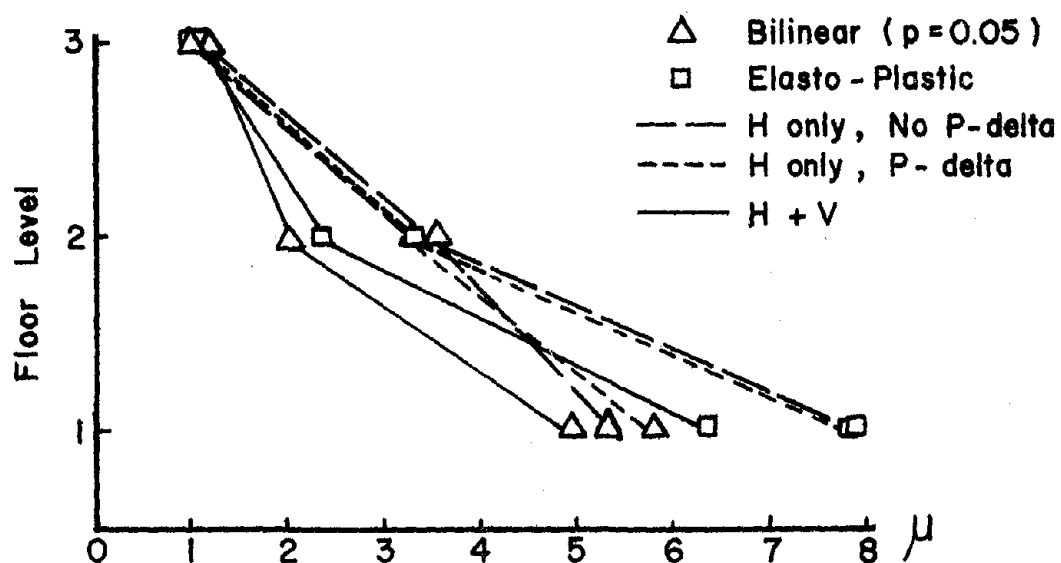


Figure 7.34. Maximum Girder Ductility Ratios at Face of Column, Frame A, 1940 El Centro

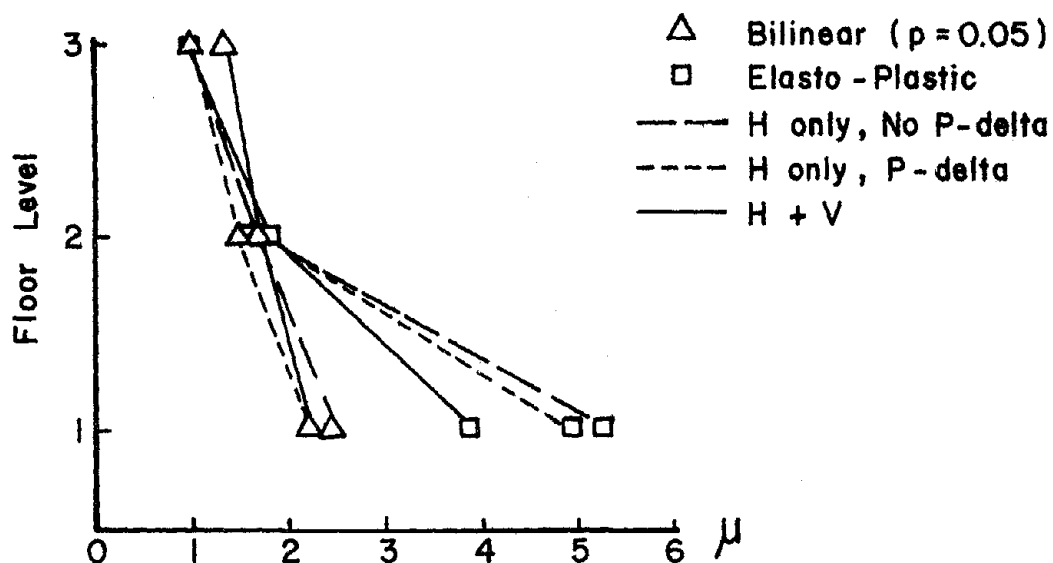


Figure 7.35. Maximum Girder Ductility Ratios at Center of Span, Frame A, 1940 El Centro

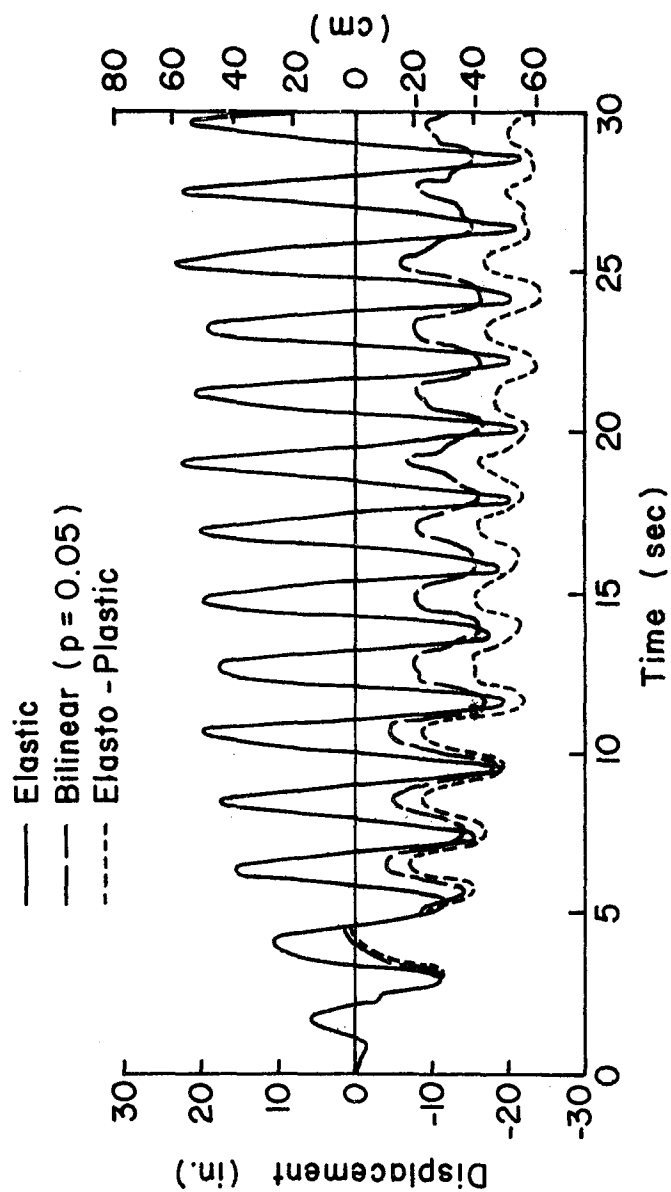


Figure 7.36. Top Floor Displacement of Frame B, 1940 El Centro, N-S Plus Vertical

The maximum floor displacement of each floor is illustrated in Fig. 7.37 and the maximum relative floor displacement is shown in Fig. 7.38. Only the maximum values of displacement, when considering both horizontal and vertical components, are shown for the bilinear system. A significant increase in the horizontal displacement is noted for the elasto-plastic system above the 2nd floor.

The maximum vertical displacement and acceleration of the girder nodes are shown in Figs. 7.39 and 7.40, respectively. These maximum values are present in the inner girder nodes when both the horizontal and vertical components are included. When the vertical component is not included in the analysis, the outer girder nodes have the larger values. This is due to the unsymmetrical bending present in the outer girder members even when no vertical load is included.

The ductility and excursion ratios for the girder members are shown in Fig. 7.41 for the bilinear and elasto-plastic systems. All the plastic hinges of girders occur in the first two floors adjacent to columns. Similar variations for the two systems are apparent. Inclusion of the vertical component of ground motion results generally in an increase in the ductility requirement of the girder members.

The corresponding column ductility and excursion ratios are shown in Fig. 7.42. Less difference in the ductility requirements between the two systems is apparent for the columns. Also, the inclusion of the vertical component of ground motion results in an insignificant change in the ductility requirement of the column members. The maximum column ductility requirement occurs in the 3rd floor as previously indicated by the relative floor displacements of Fig. 7.38.

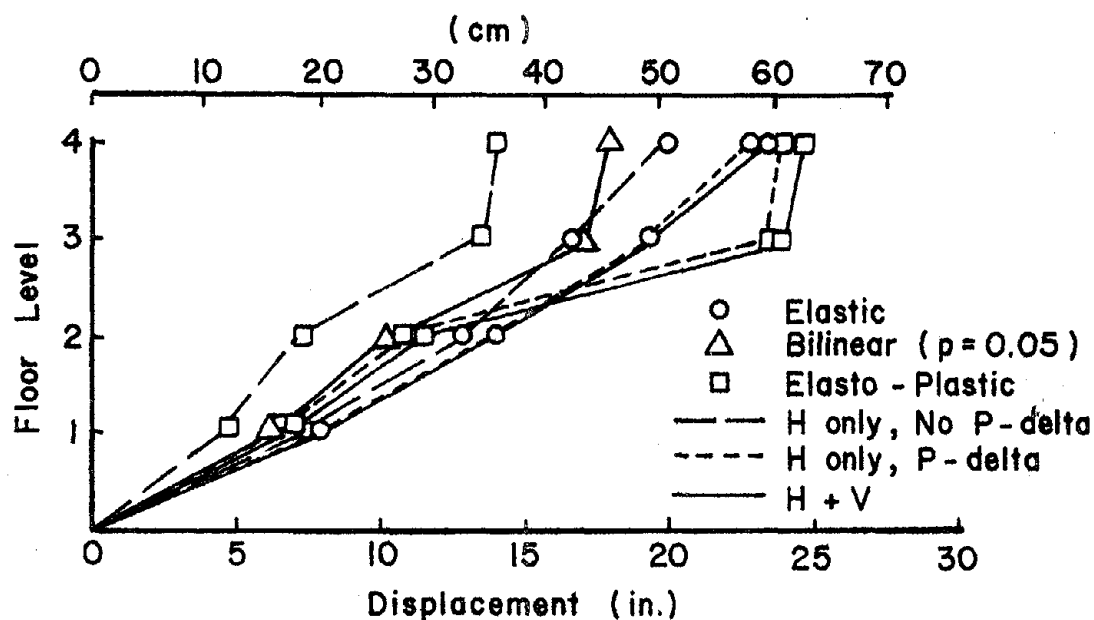


Figure 7.37. Maximum Floor Displacements, Frame B, 1940 El Centro

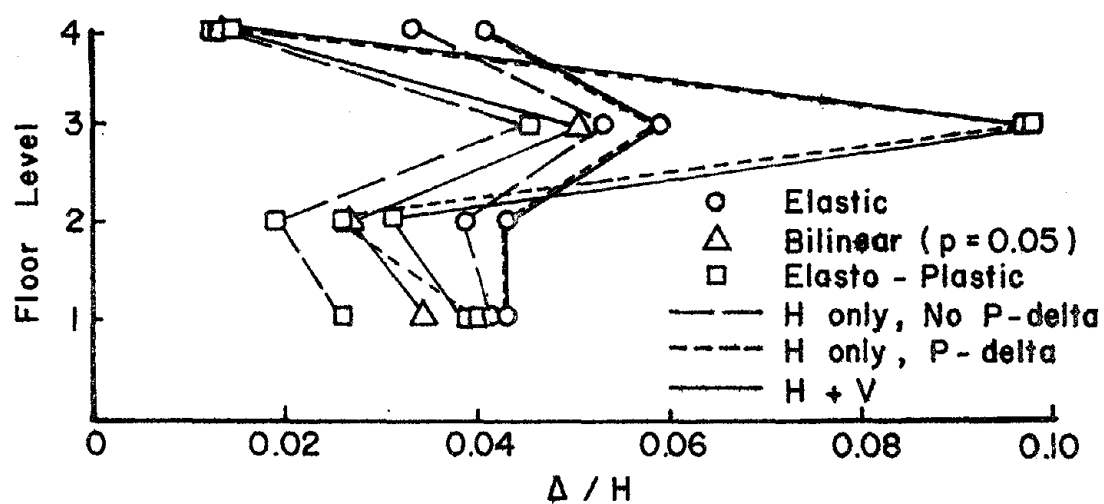


Figure 7.38. Maximum Relative Floor Displacements, Frame B, 1940 El Centro

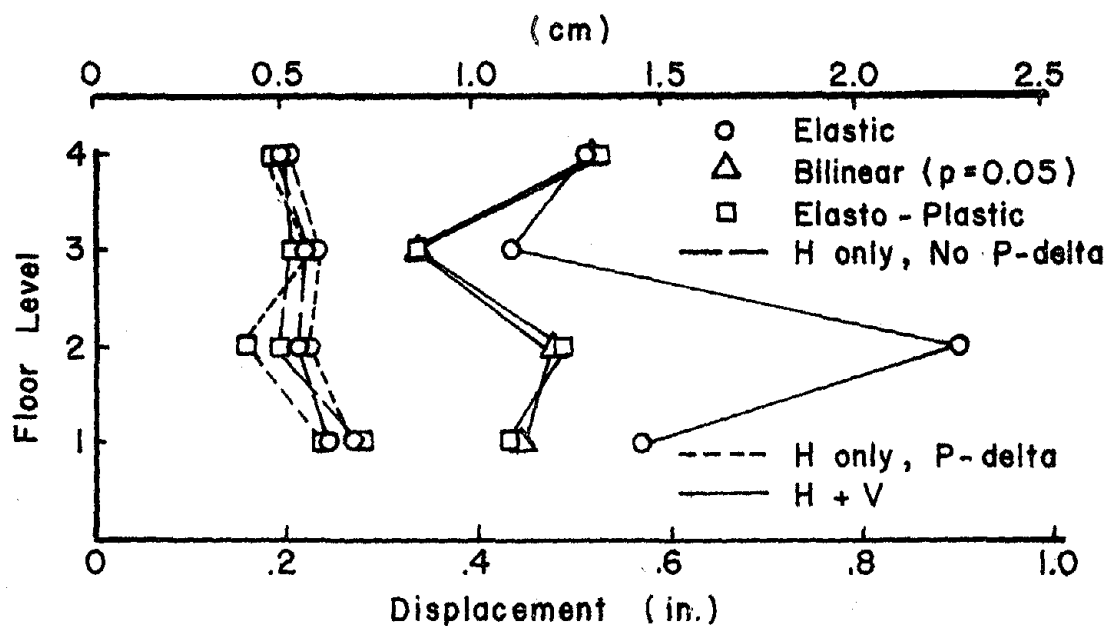


Figure 7.39. Maximum Vertical Displacement at Center of Girders, Frame B, 1940 El Centro

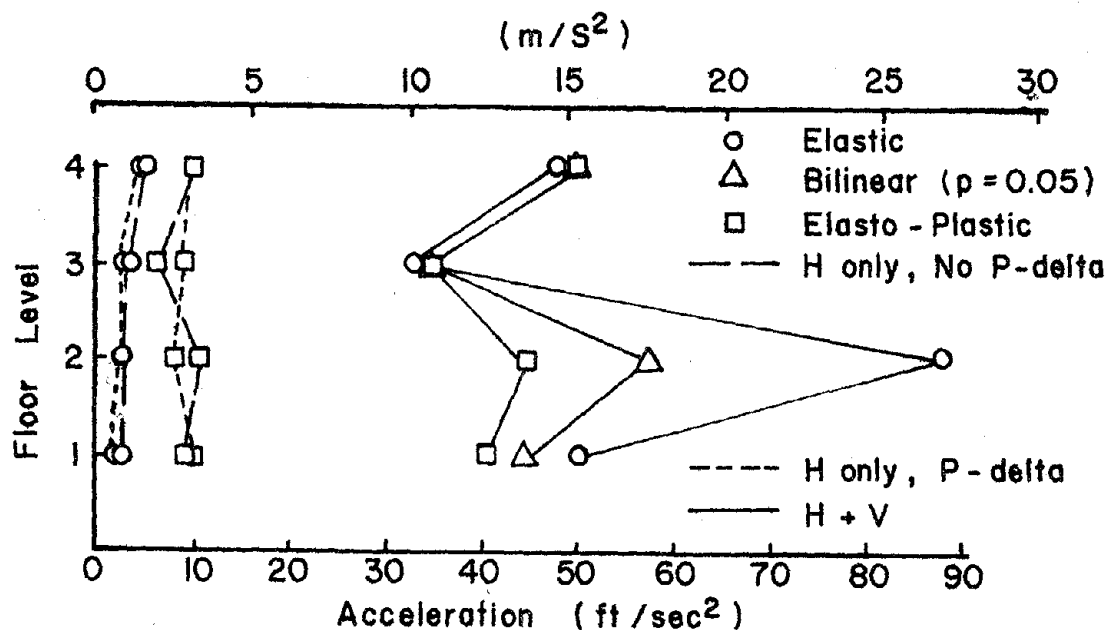
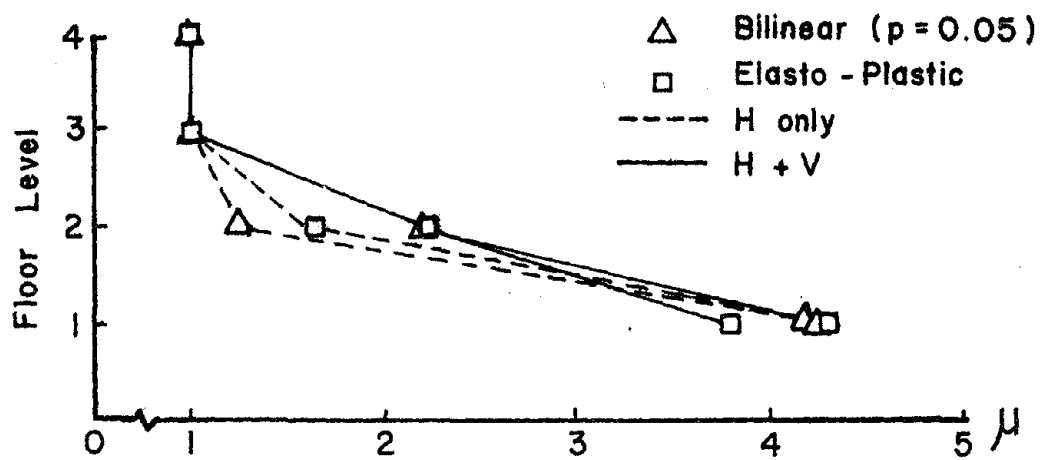
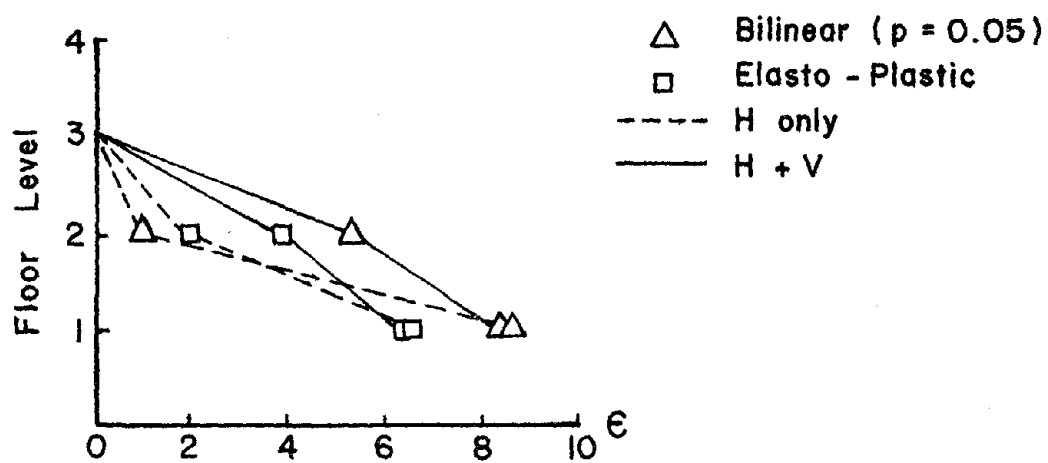


Figure 7.40. Maximum Vertical Acceleration at Center of Girders, Frame B, 1940 El Centro

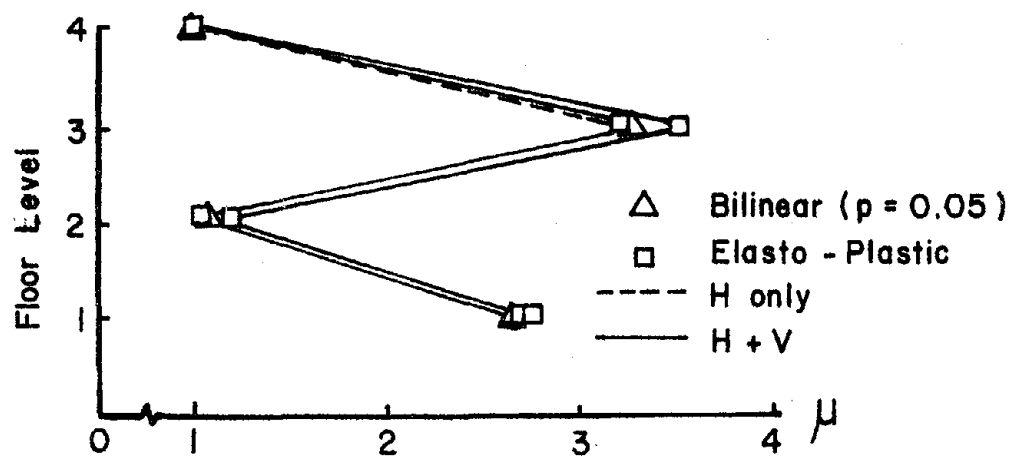


a) Ductility Ratio

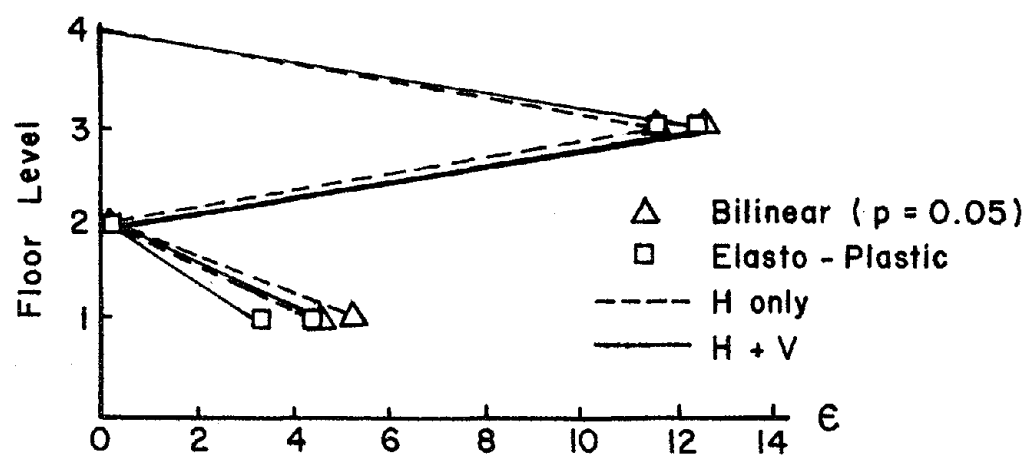


b) Excursion Ratio

Figure 7.41. Maximum Girder Ductility and Excursion Ratios, Frame B, 1940 El Centro



a) Ductility Ratio



b) Excursion Ratio

Figure 7.42. Maximum Column Ductility and Excursion Ratios, Frame B, 1940 El Centro

Five energy plots in terms of energy per unit mass are used to compare the energy absorption for the different loading and response conditions of Frame B.

Figure 7.43 shows the change in energy absorption when including the P-delta effect. Though an increase in the amount of input and dissipated strain energy is realized, the total stored energy remains approximately the same. The stored energy is the difference between the input and dissipated energy.

An increase in both the input and dissipated strain energy is realized in Fig. 7.44 when considering an elasto-plastic system. A less amount of energy is dissipated by strain hardening when assuming a bilinear behavior with $p = 0.05$. A slightly larger amount of stored energy is indicated for the bilinear system.

To further illustrate the energy absorption of Frame B, 3% damping is included for comparisons as shown in Figs. 7.45-7.47. Figure 7.45 shows the effect on energy absorption when the vertical component of ground motion is included for an elastic system. Figure 7.46 illustrates the difference in energy absorption between an elastic and an elasto-plastic response system when there is 3% damping. Even though the total amount of input energy is the same at 30 seconds, the amount of energy dissipated by damping is much greater for the elastic system. The final energy plot in this section is shown in Fig. 7.47. The effect of including the vertical ground motion component on an elasto-plastic system is illustrated. An increase is realized in the total input energy due to the vertical earthquake component.

3. 10-Story, 1-Bay Frame (Frame C). As in the other two example structures, damping is not considered in comparing the significant

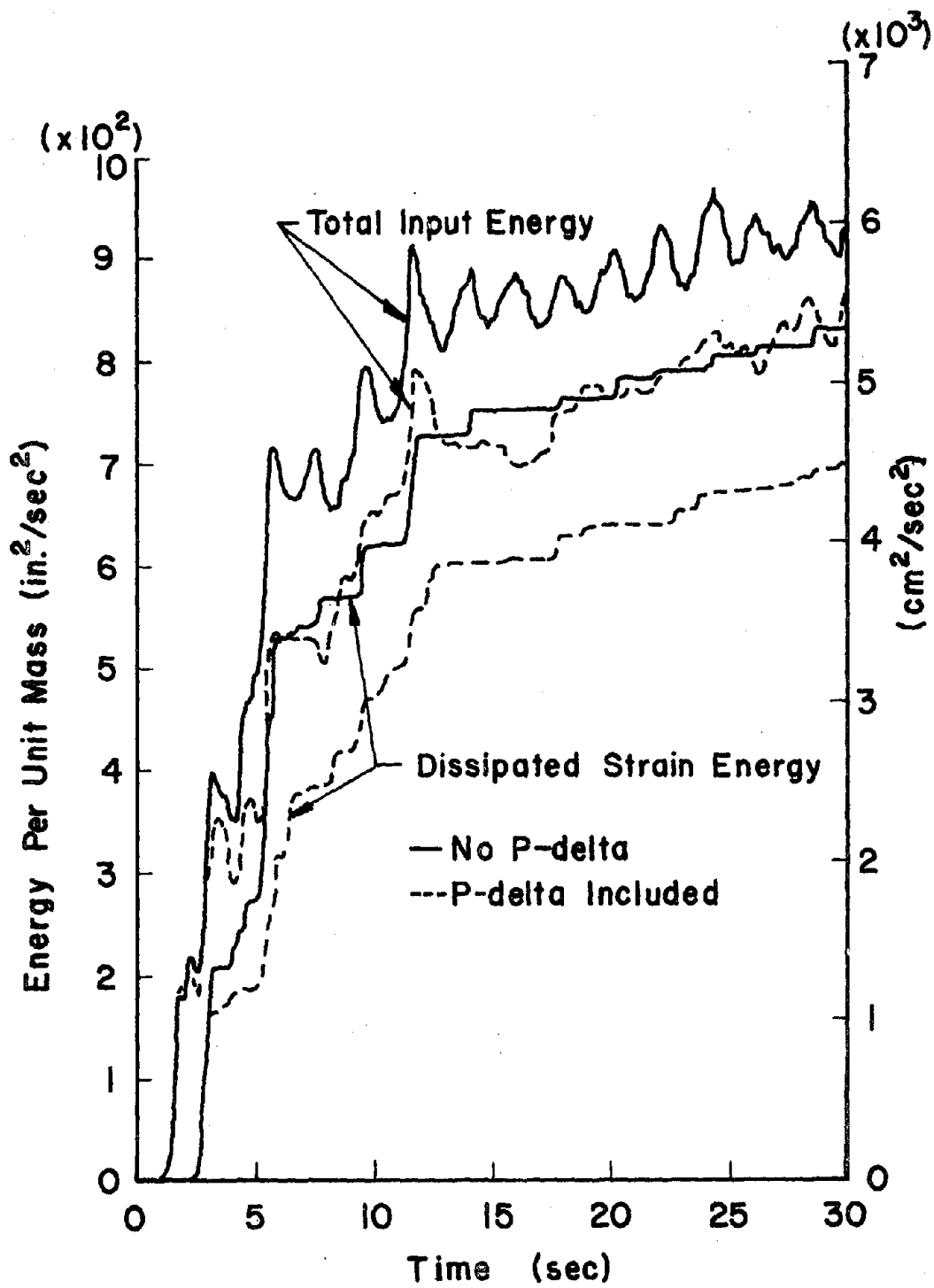


Figure 7.43. Effect of P-delta on Energy, Frame B, Elasto-Plastic System, 1940 El Centro, N-S Only

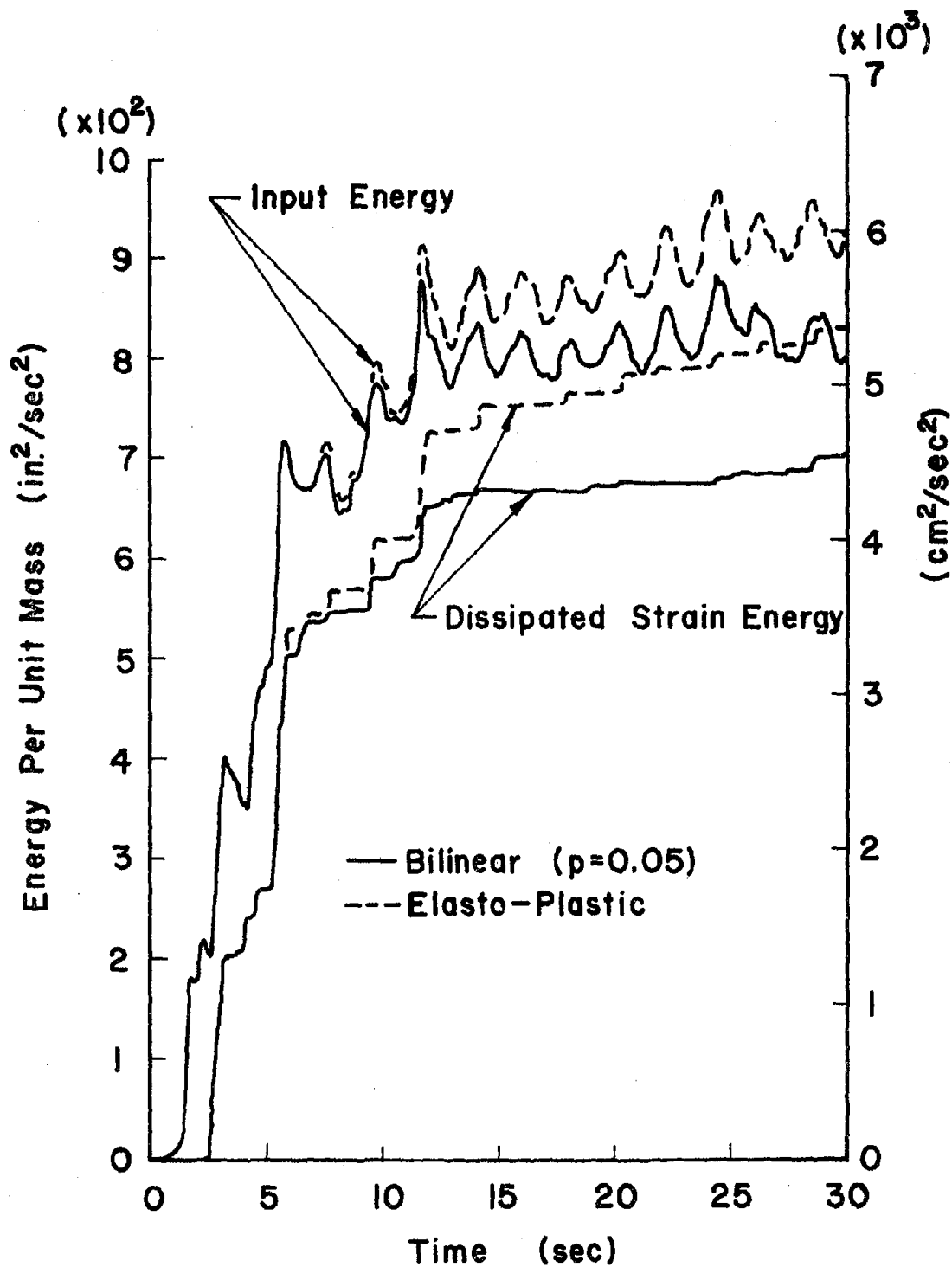


Figure 7.44. Effect of Response Condition on Energy, Frame B, N-S Only

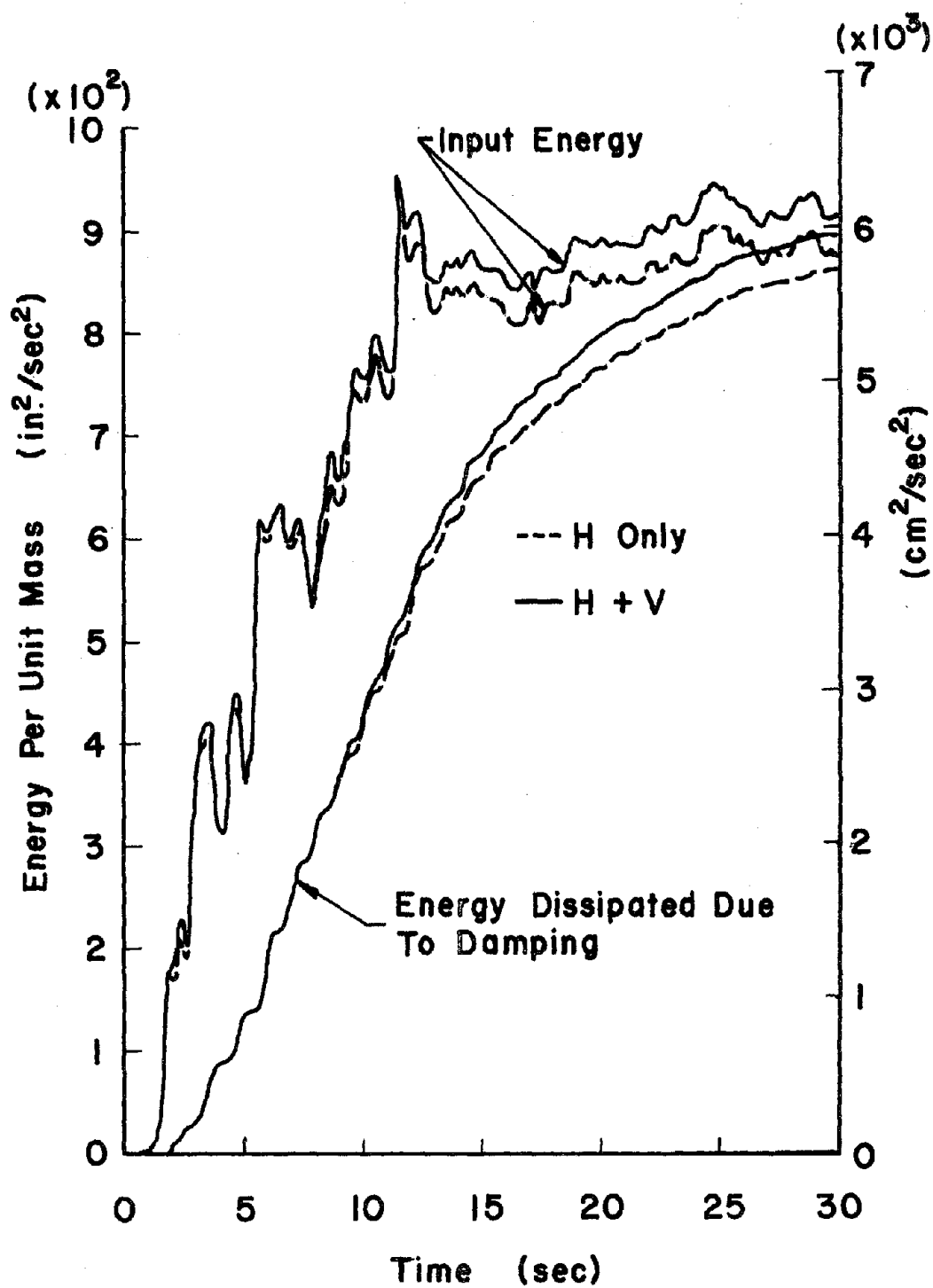


Figure 7.45. Effect of the Vertical Ground Motion on Energy, Frame B, 3% Damping, Elastic System, 1940 El Centro

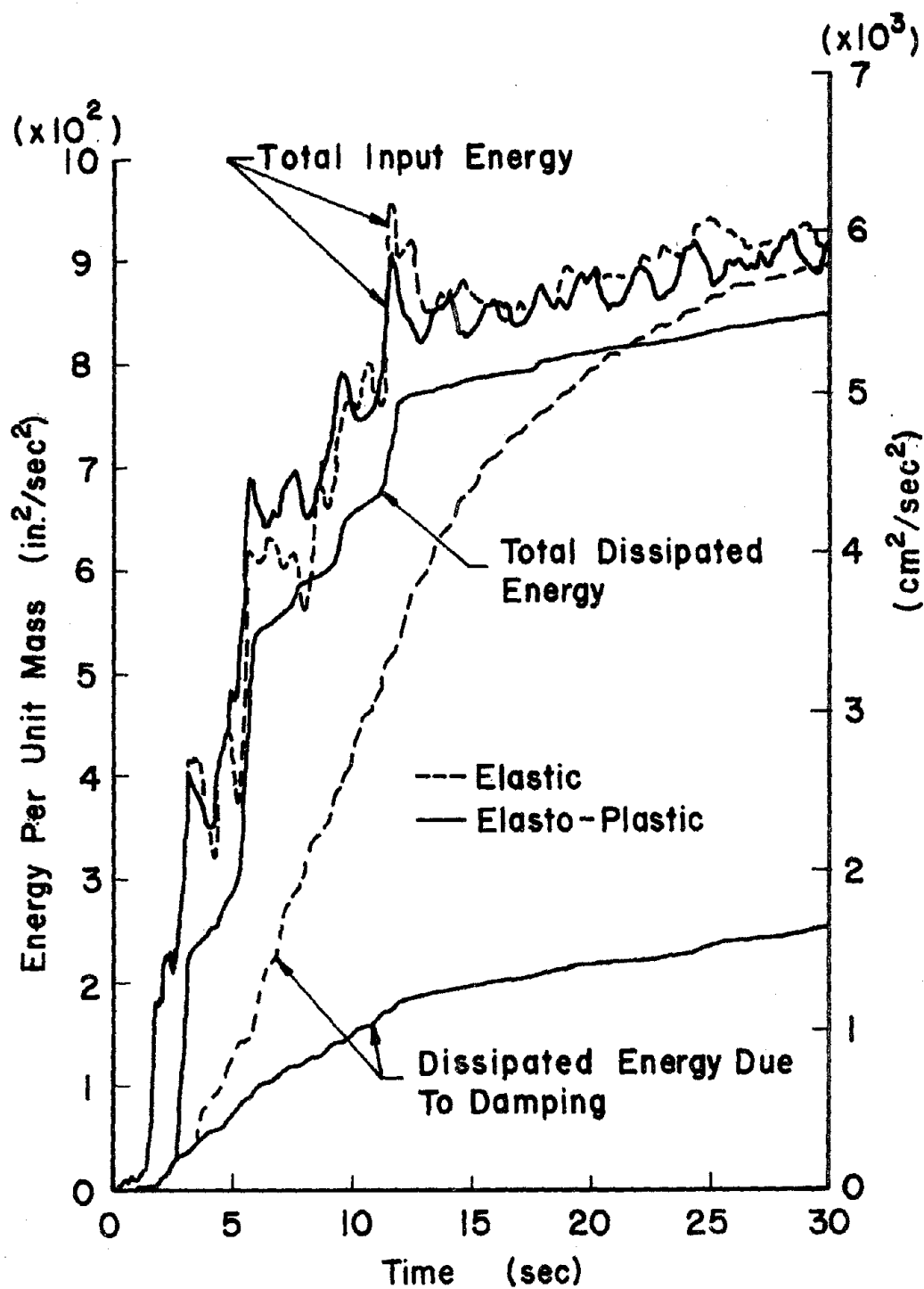


Figure 7.46. Elastic and Elasto-Plastic Energy, Frame B, 3% Damping, 1940 El Centro, N-S Plus Vertical

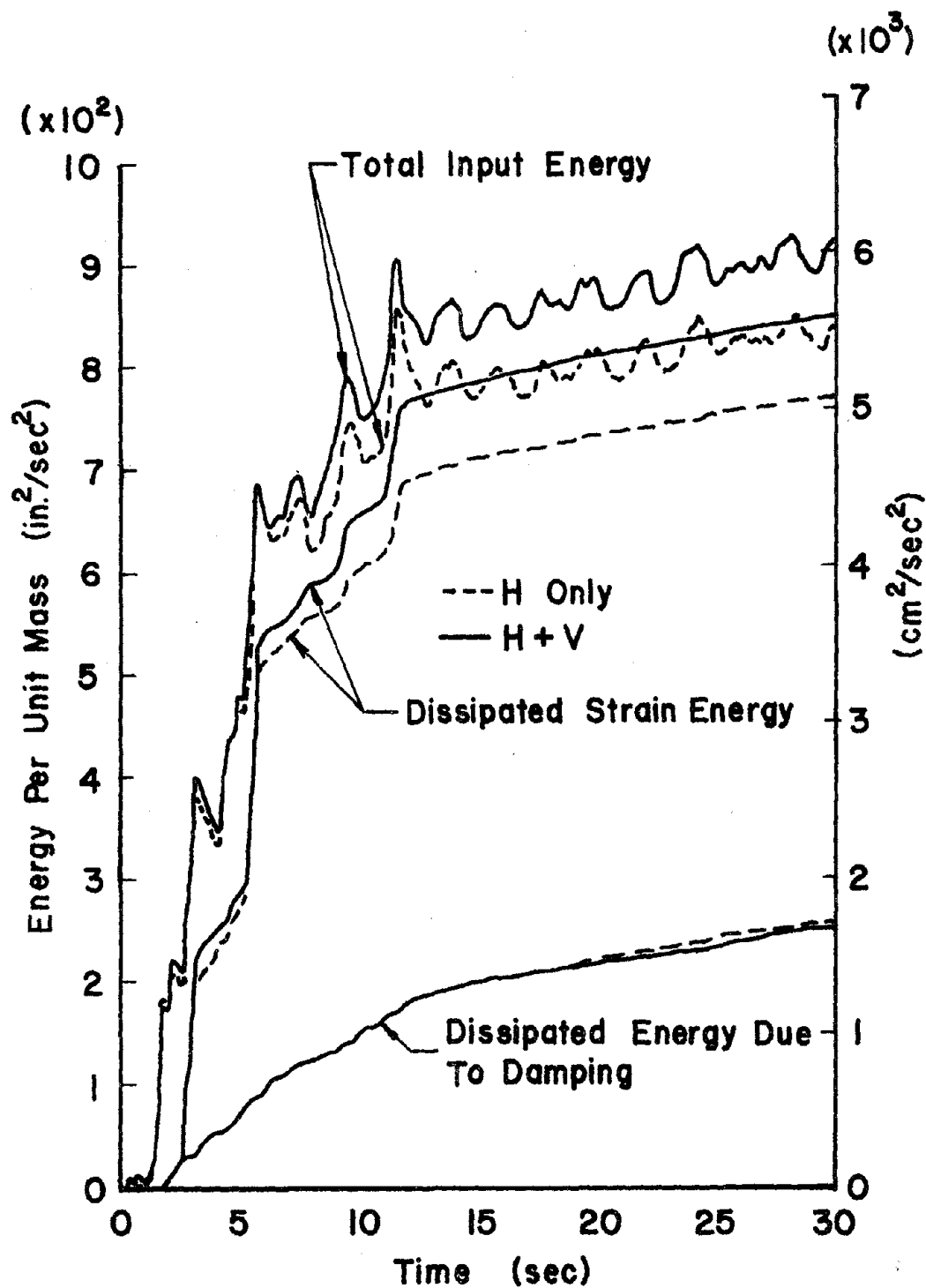


Figure 7.47. Effect of the Vertical Ground Motion on Energy, Frame B, 3% Damping, Elasto-Plastic System, 1940 El Centro

response parameters of Frame C. Reduction of the plastic moment in columns based on axial loads is included. An initial static analysis is not considered.

The maximum horizontal floor displacement of each floor is shown in Fig. 7.48 for the elastic, bilinear ($p = 0.05$) and elasto-plastic response systems. The maximum values shown for the bilinear and elasto-plastic systems are those due to both earthquake components.

The change in the response history for Frame C based on the total earthquake record between the elastic and elasto-plastic response systems is shown in Fig. 7.49. The symmetrical elasto-plastic response curve indicates the structure to have strong columns.

The maximum relative floor displacement for the frame is shown in Fig. 7.50 for the elastic, bilinear, and elasto-plastic systems. Increased values of relative displacement occur at the approximate quarter points in the structures height. The maximum vertical displacement and acceleration of the girder nodes are shown in Figs. 7.51 and 7.52.

The girder ductility and excursion ratios of the structure are shown in Figs. 7.53 and 7.54, respectively. The larger relative floor displacements indicated in Fig. 7.50 are reflected by the higher ductility requirements for floors 2 and 7. Though plastic hinges do occur in the 1st and 2nd floor columns of the frame during the ground motion, the major part of the dissipated strain energy occurs in the girder members. All the plastic hinges in the girder members occur adjacent to the column face.

Figure 7.55 shows the comparison of energy absorption for an undamped elasto-plastic system with that of an undamped elastic system.

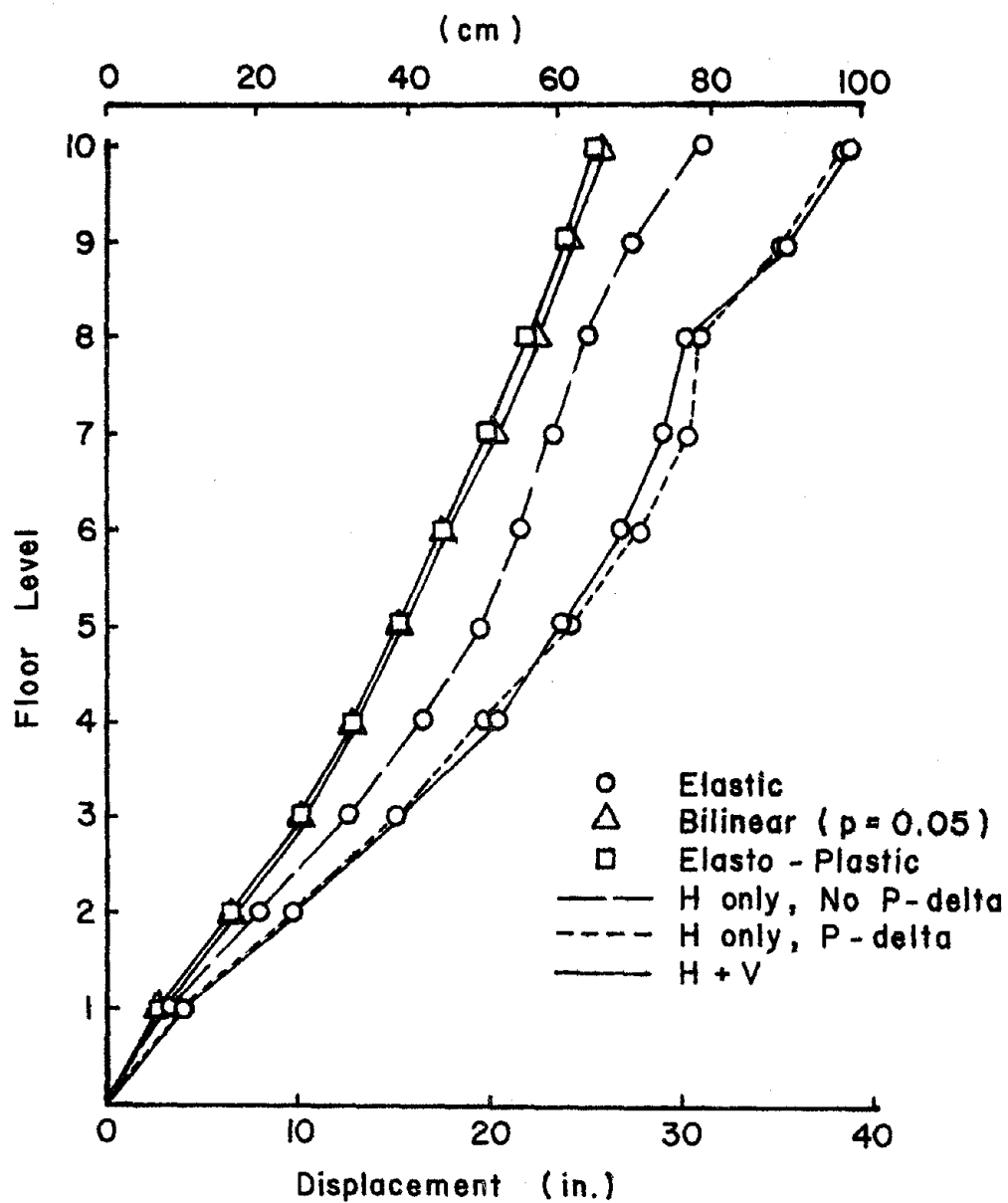


Figure 7.48. Maximum Floor Displacement, Frame C, 1940 El Centro

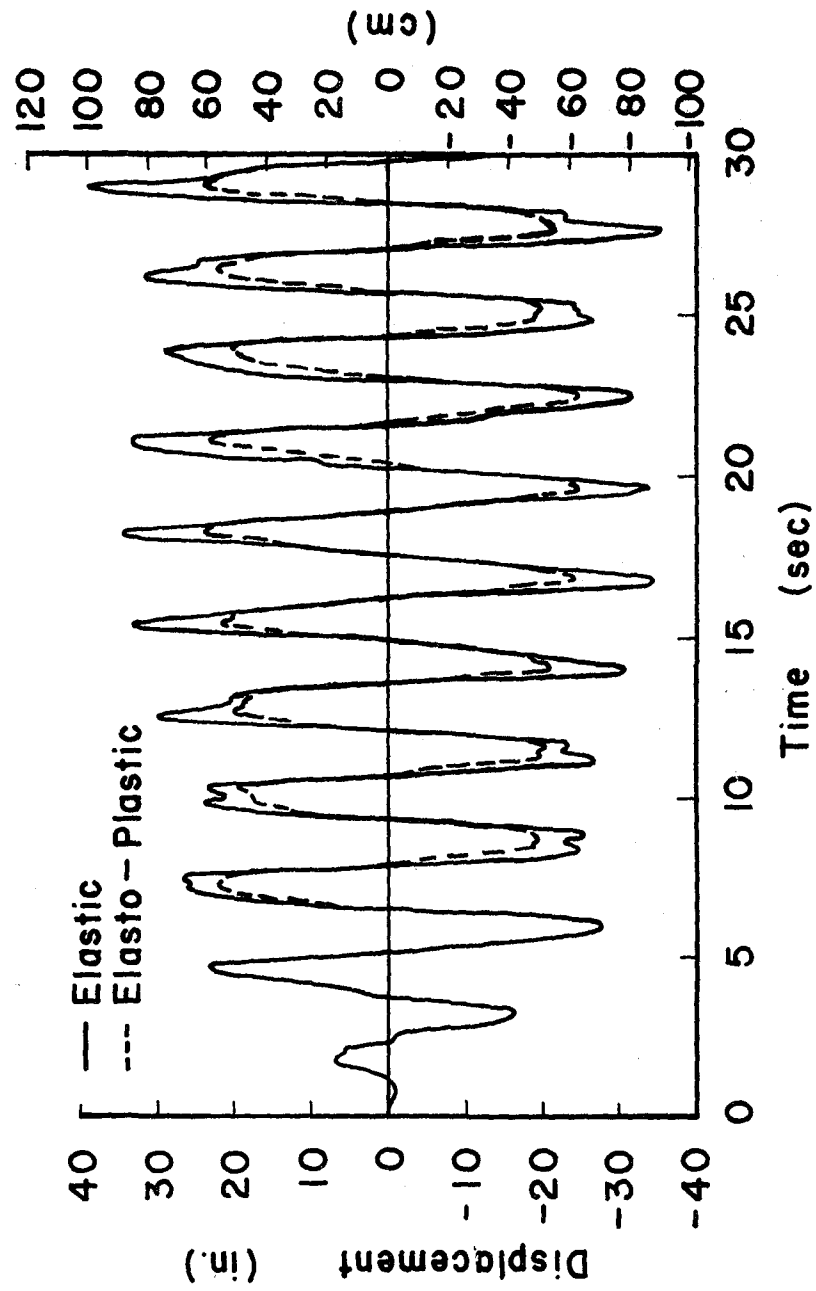


Figure 7.49. Top Floor Displacement, Frame C, 1940 El Centro, N-S Plus Vertical

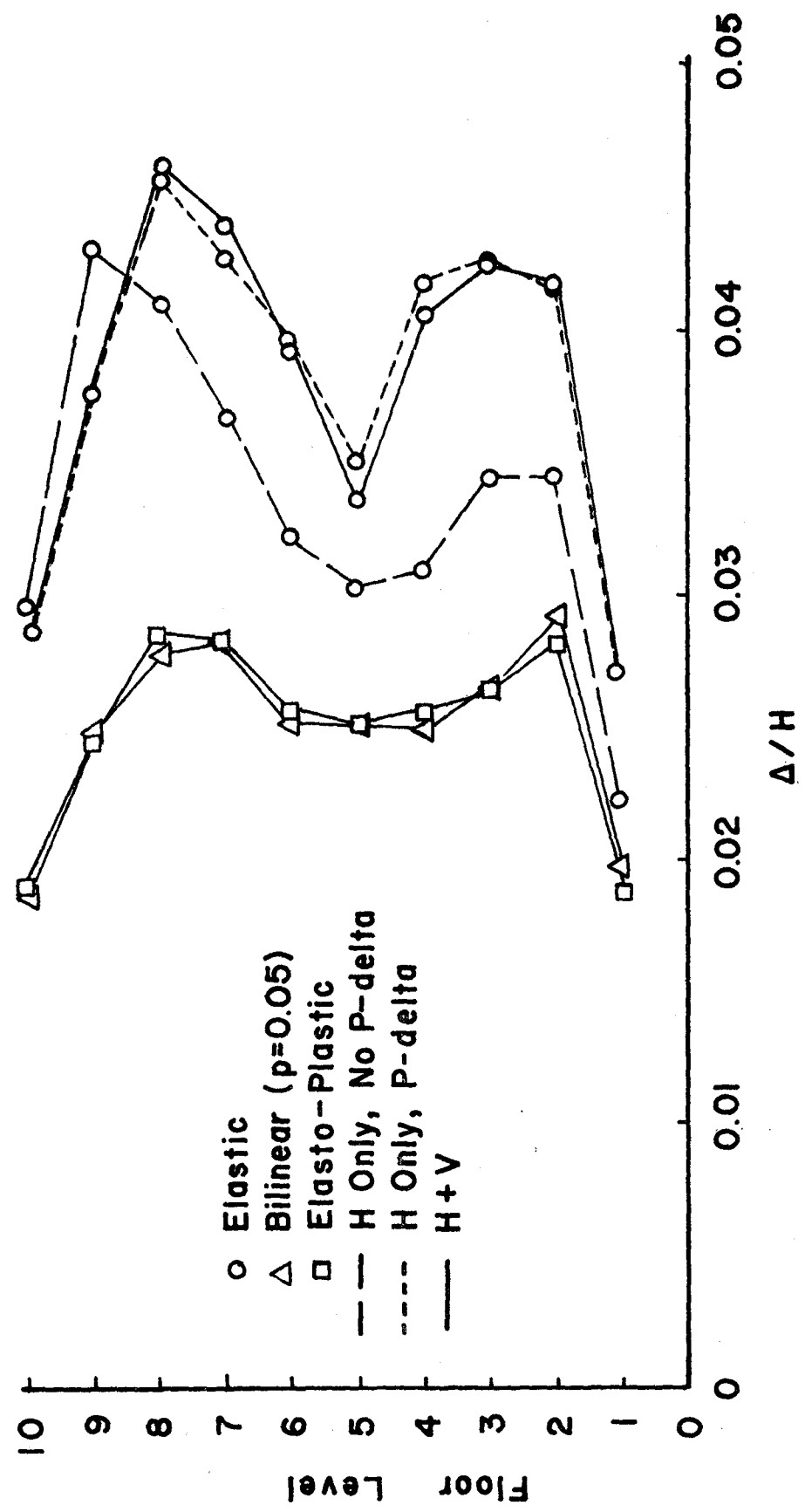


Figure 7.50. Maximum Relative Floor Displacements, Frame C, 1940 El Centro

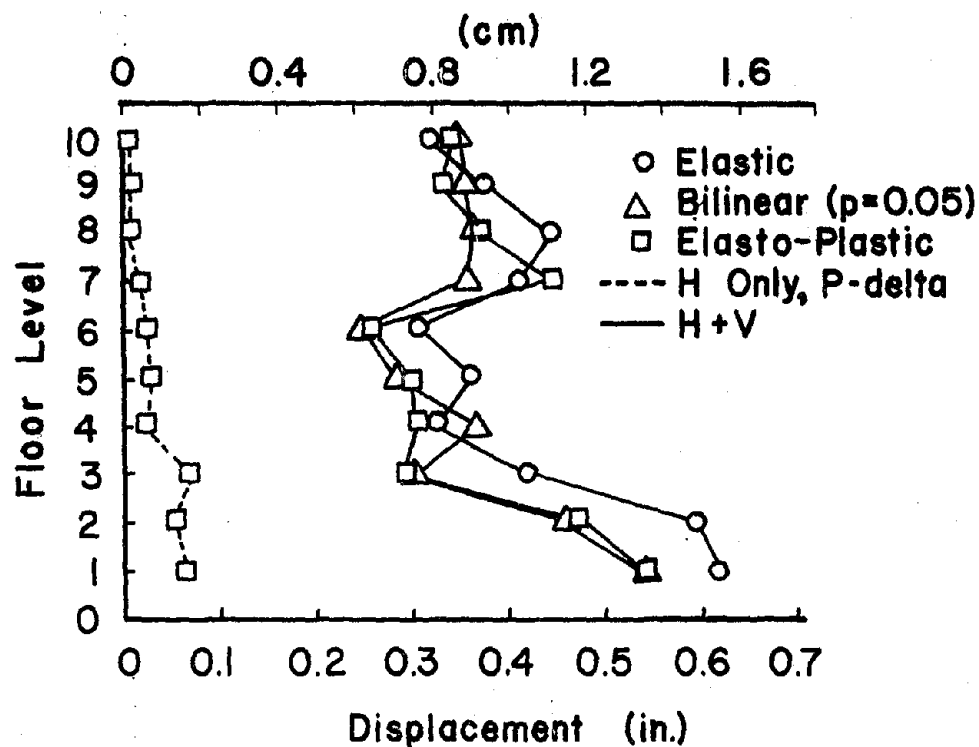


Figure 7.51. Maximum Vertical Displacement, Frame C, 1940 El Centro

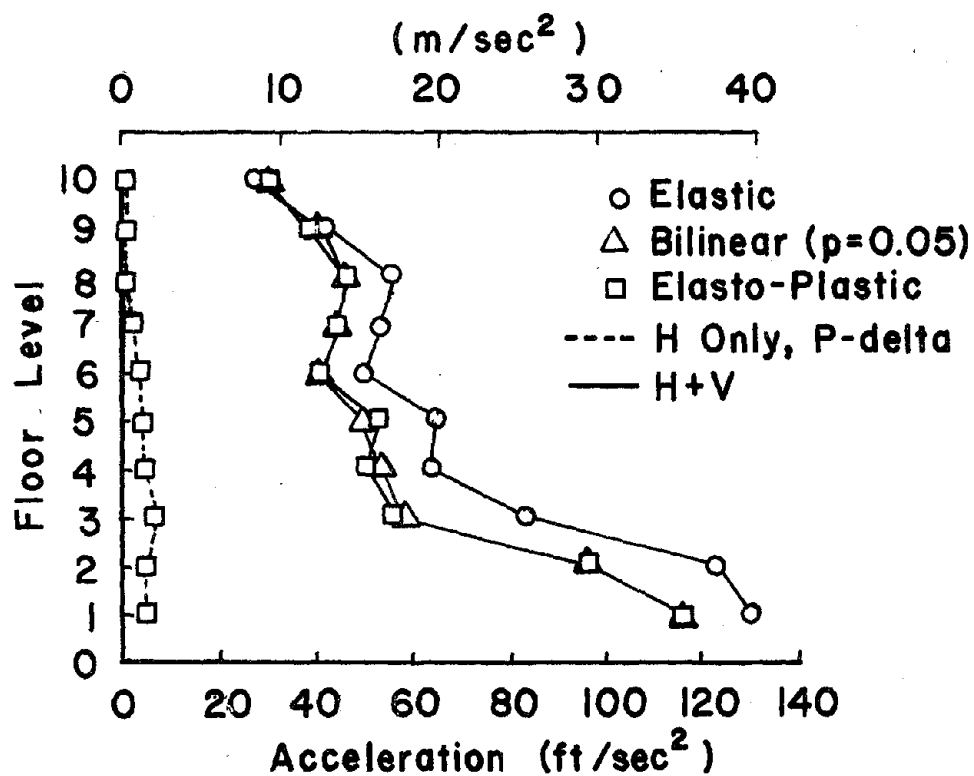


Figure 7.52. Maximum Vertical Acceleration, Frame C, 1940 El Centro

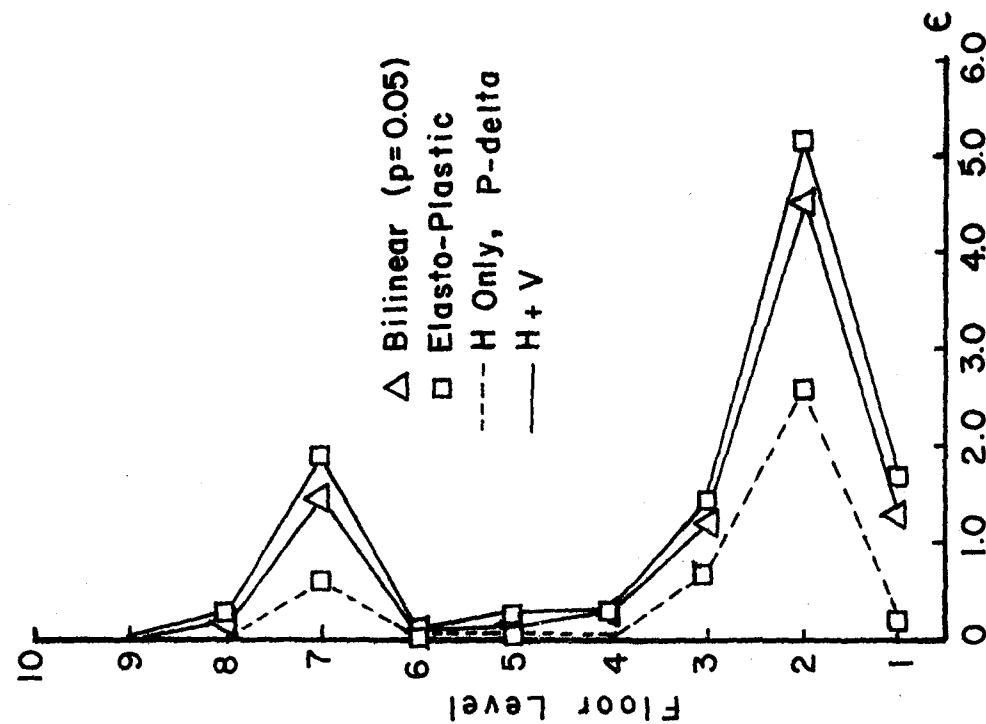


Figure 7.53. Girder Ductility Ratios, Frame C, 1940 El Centro

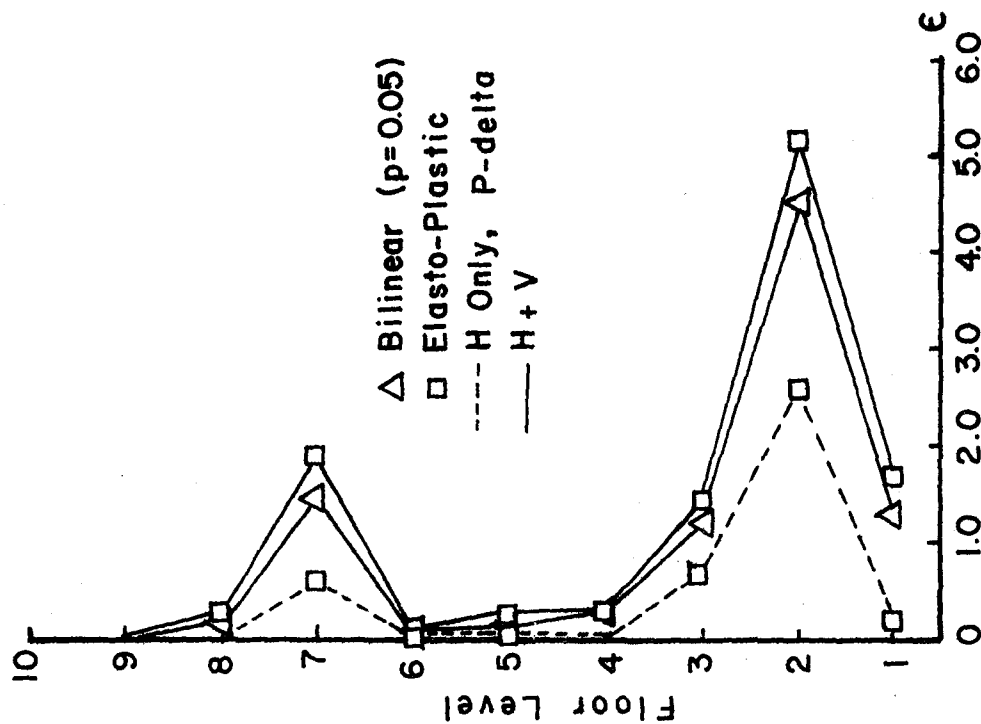


Figure 7.54. Girder Excursion Ratios, Frame C, 1940 El Centro

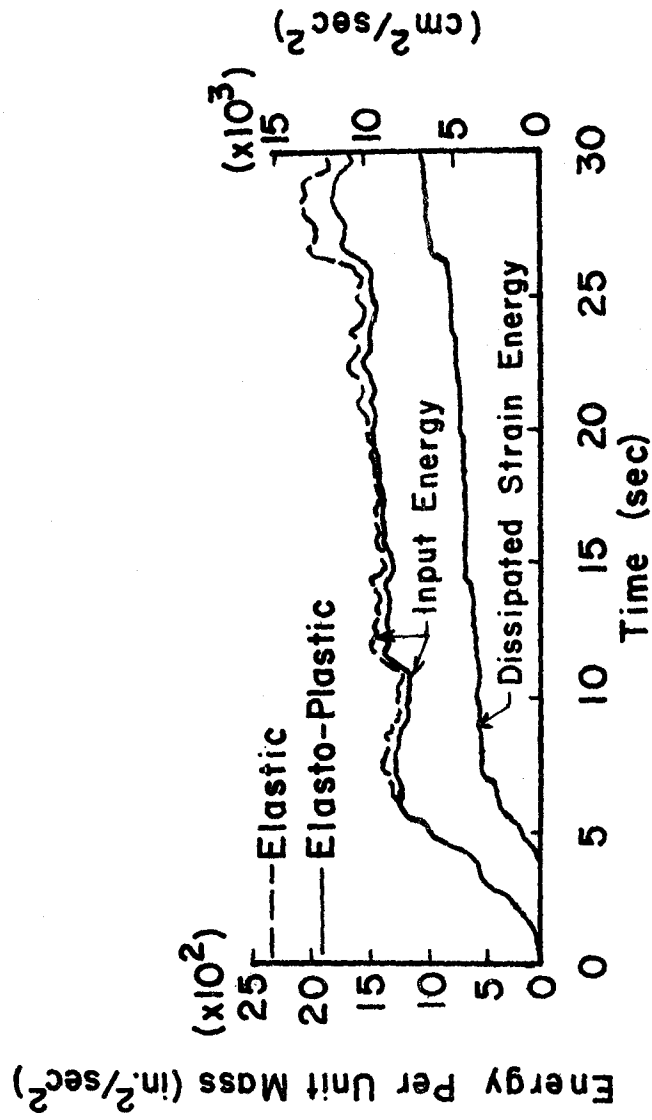


Figure 7.55. Effect of Response Condition on Energy, Frame C, 1940 E1 Centro, N-S Plus Vertical

4. Observations Based on Response Parameter Studies. Based on the response parameter studies of the three framed structures, Frames A, B and C, the following overall observations can be made:

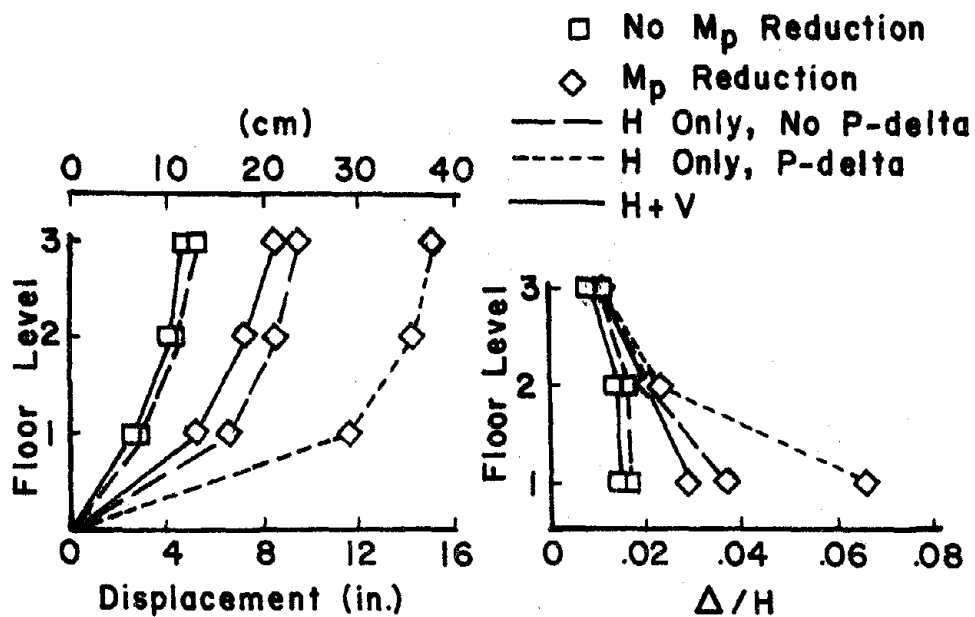
- 1) Except when excessive plastic rotation in columns occurs as in the case of Frame B, the maximum horizontal floor displacements take place when assuming an elastic response condition.
- 2) The difference in the maximum horizontal floor displacements for the elasto-plastic and bilinear systems is negligible with the exception as stated in 1 above. This is because Frames A and C have strong columns.
- 3) The reduction in the top floor displacement from the elastic to the elasto-plastic condition is reflected in the amount of input energy that is dissipated by inelastic strain.
- 4) The inclusion of the vertical earthquake component results in an increase in the ductility requirement of girder members.
- 5) The ductility requirement of columns when including the vertical earthquake component depends on whether the structural system has strong columns or not.
- 6) When the P-delta effect is included, there results an increase in the input energy and dissipated strain energy.
- 7) Assuming a frame to be elasto-plastic results in more energy being dissipated by plastic rotation than for a bilinear system with $p = 0.05$.

- 8) Even though the total amount of input energy is approximately the same for damped elastic and elasto-plastic systems based on the same earthquake loading, the amount of energy dissipated by damping is much less in the elasto-plastic system. The remainder is dissipated by inelastic joint rotations.
- 9) The amount of input energy is increased for an elasto-plastic system when the vertical component of ground motion is included. Though the variation in stored energy remains the same, the dissipated strain energy increases when including the vertical component.

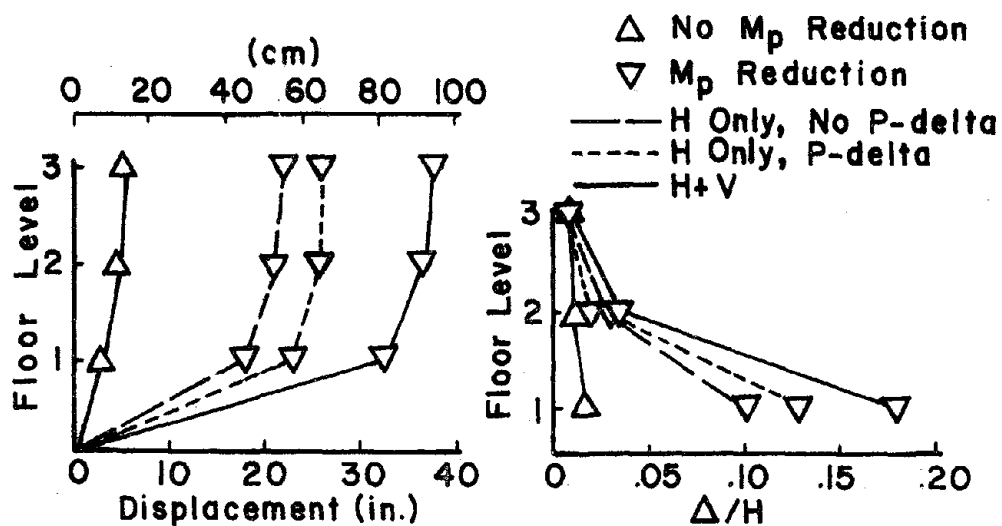
E. EFFECT OF M_p REDUCTION ON RESPONSE PARAMETERS

The purpose of this section is to illustrate by example frames the effect of the reduction of the plastic moment of columns on structural response. Frames A and B are used for this illustration. As in the previous study, the 1940 El Centro earthquake is used to produce the necessary ground motion in the horizontal and vertical directions. The structural Model 2 is used to fully reveal the effect of the vertical component.

1. 3-Story, 1-Bay Frame (Frame A). The horizontal response in the maximum horizontal and maximum relative floor displacements is compared for the elasto-plastic and bilinear response conditions in Fig. 7.56. The inclusion of the M_p reduction is characterized by an increase in the maximum horizontal floor displacement as a result of an increase in the maximum relative floor displacements of the lower floors.



a) Elasto-Plastic Response

b) Bilinear Response ($p=0.05$)Figure 7.56. Effect of M_p Reduction on Horizontal Response, Frame A, 1940 El Centro

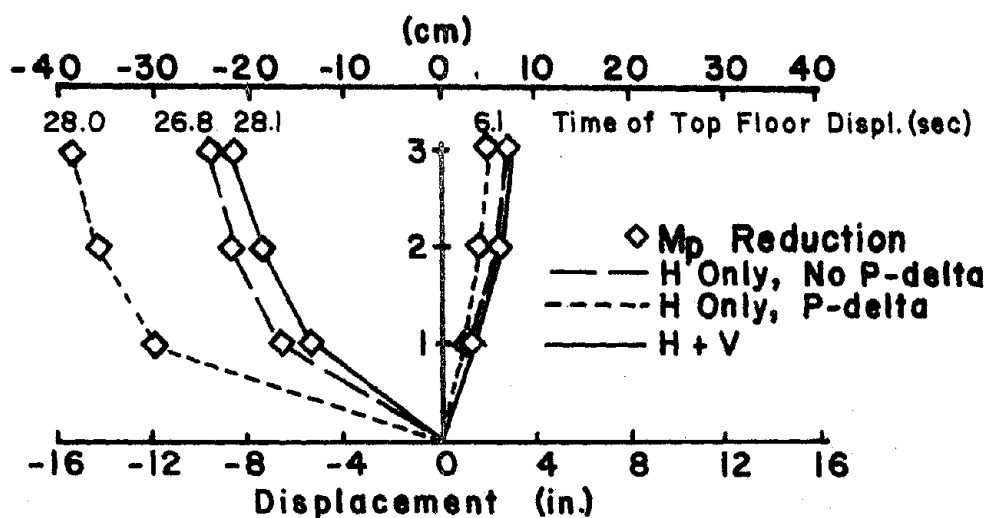
The maximum positive and negative floor displacements are shown in Fig. 7.57 for the two response systems. The curve associated with the maximum positive displacement for the bilinear response system of Fig. 7.57b is for all loading conditions. As indicated by the maximum negative displacement for the elasto-plastic response, the inclusion of the vertical earthquake component does not always result in an increase in the horizontal response. The nonsymmetry of these extreme displacements is due to plastic hinges occurring in the support columns.

The difference in the vertical response of the girder nodes due to the inclusion of the M_p reduction is considered negligible based on the maximum displacement and acceleration values of Fig. 7.58. However, the vertical earthquake motion can significantly influence both displacements and accelerations at girder nodes.

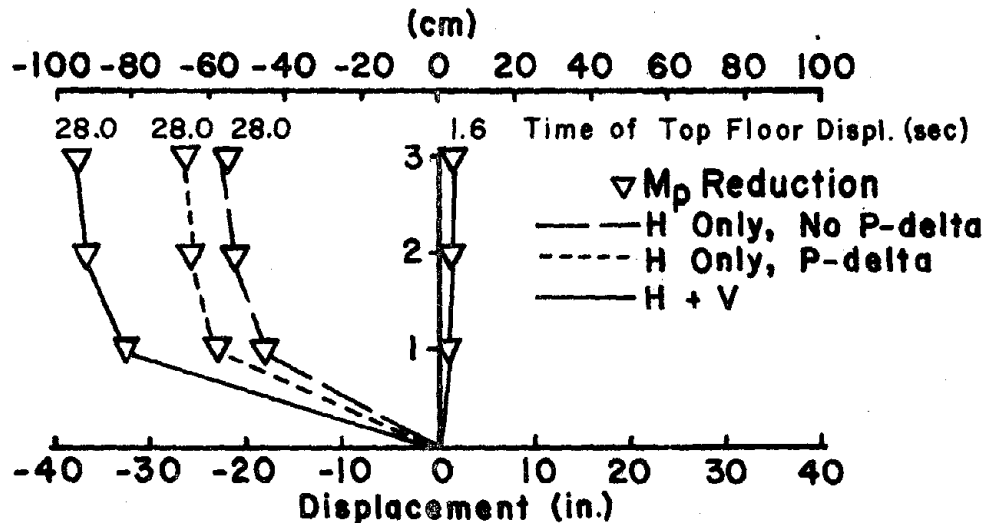
Only a slight increase in the ductility requirement of the lower girder members is realized for the elasto-plastic system as shown in Fig. 7.59a. Increases in the ductility requirement of lower column members are realized for both the elasto-plastic and bilinear systems.

2. 4-Story, 3-Bay Frame (Frame B). For the analysis of this structure, 3% viscous damping is assumed. A comparison of the response parameters based on both horizontal and vertical components is made with and without assuming the M_p reduction due to axial loads.

Figure 7.60 shows the change in the maximum horizontal floor displacement and the maximum relative floor displacement when including the M_p reduction. The increase in the maximum top floor displacement is reflected in the response shown in Fig. 7.61.



a) Elasto-Plastic Response

b) Bilinear Response ($p=0.05$)Figure 7.57. Maximum and Minimum Floor Displacements, Frame A, Elasto-Plastic and Bilinear ($p = 0.05$) Systems, 1940 El Centro

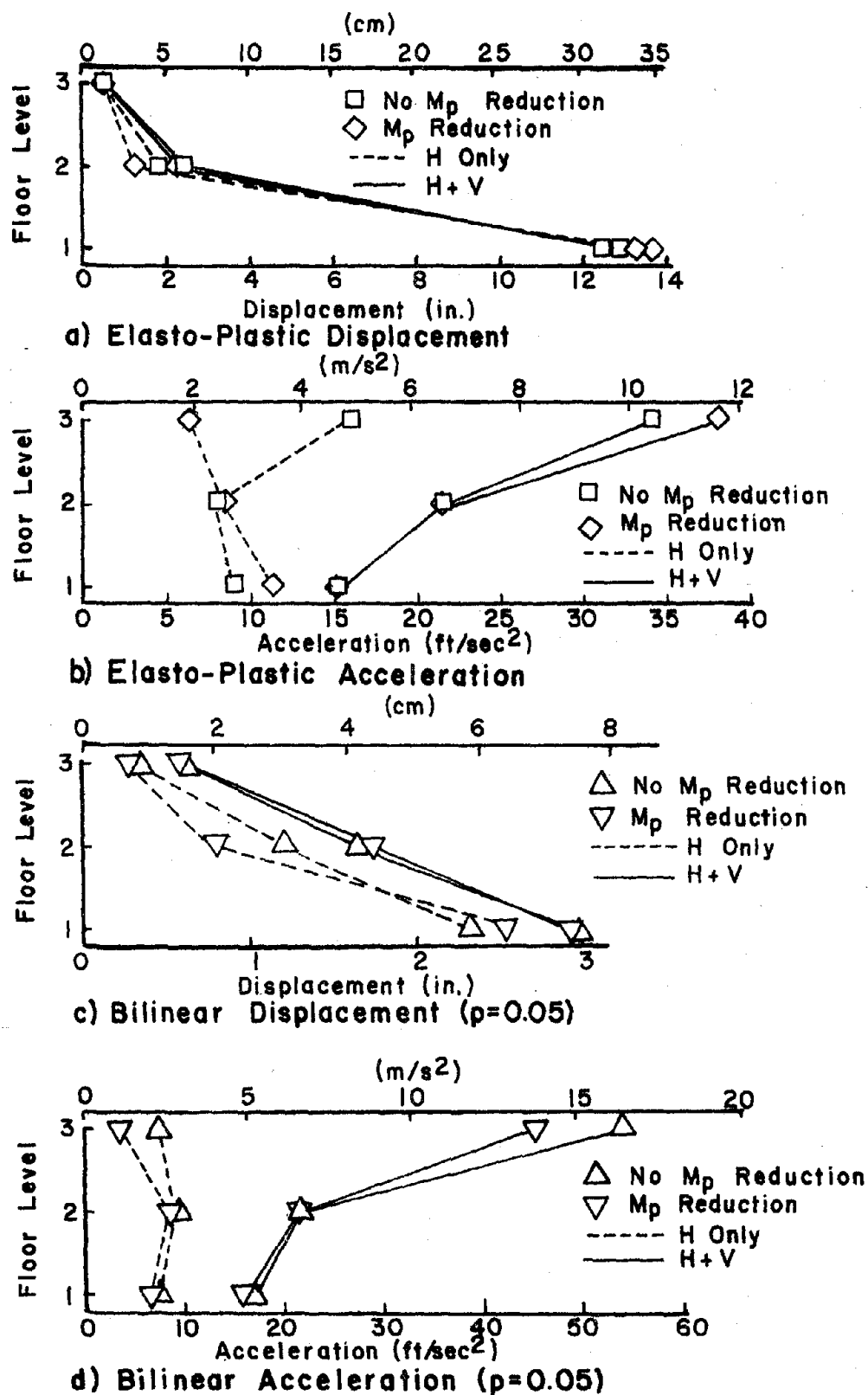
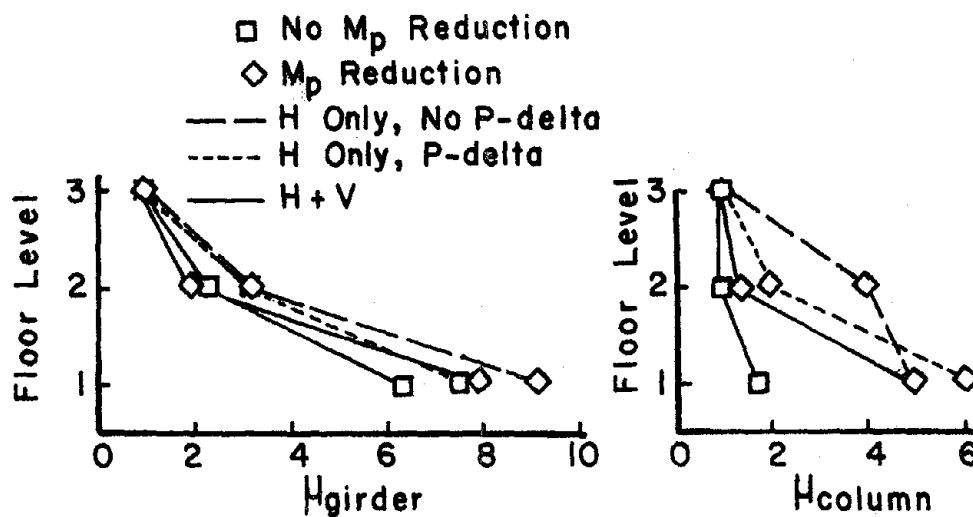
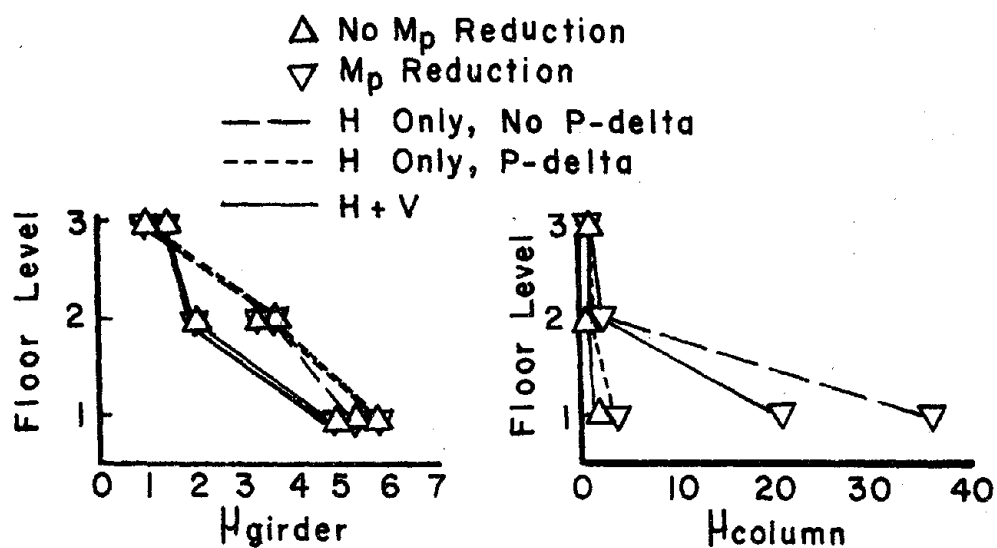


Figure 7.58. Effect of M_p Reduction on Vertical Response, Frame A, 1940 El Centro

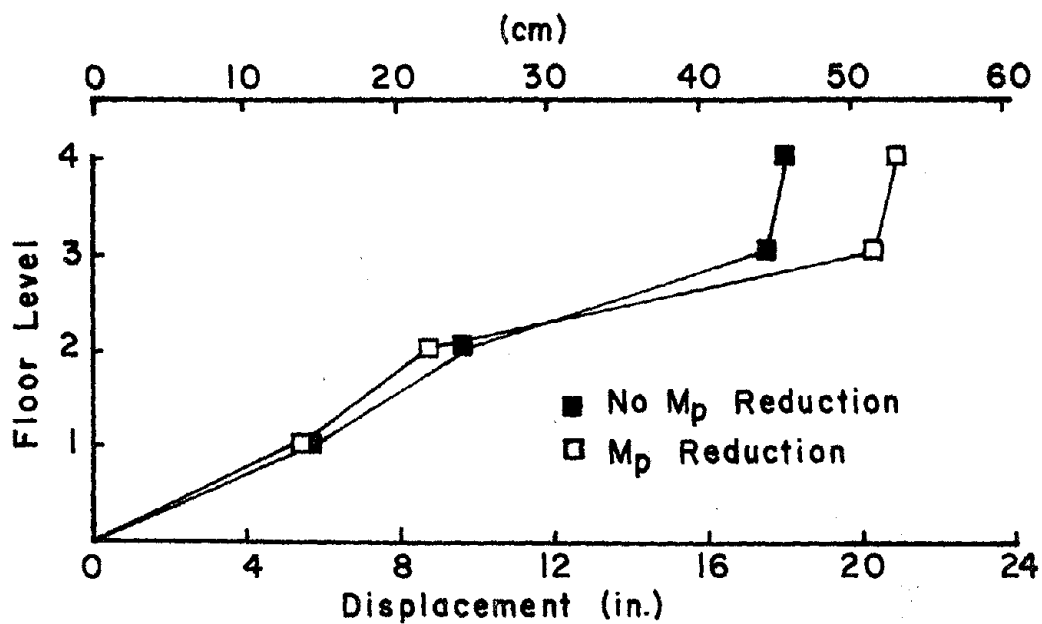


a) Elasto-Plastic Response

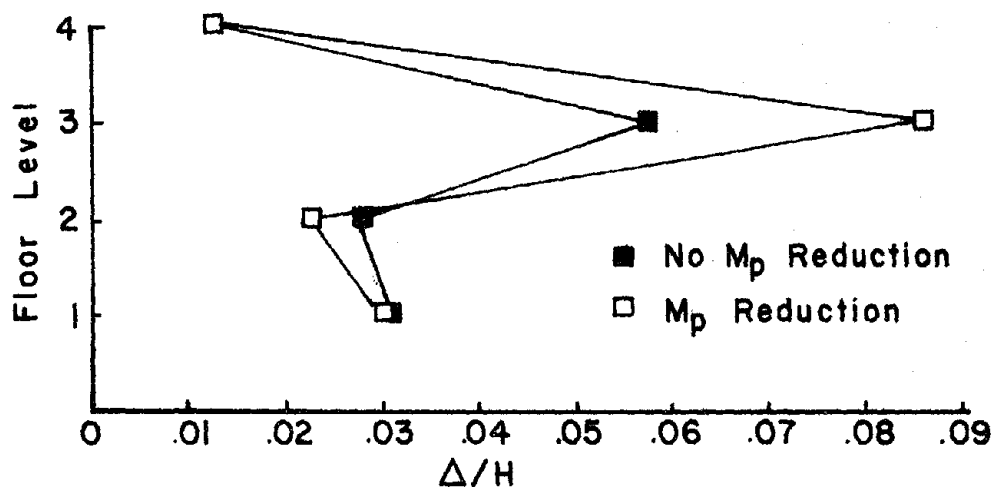


b) Bilinear Response ($p=0.05$)

Figure 7.59. Effect of M_p Reduction on Ductility, Frame A, 1940
El Centro P



a) Maximum Floor Displacement



b) Maximum Relative Floor Displacement

Figure 7.60. Effect of M_p Reduction on Horizontal Response, Frame B, 3% Damping, Elasto-Plastic System, 1940 El Centro, N-S Plus Vertical

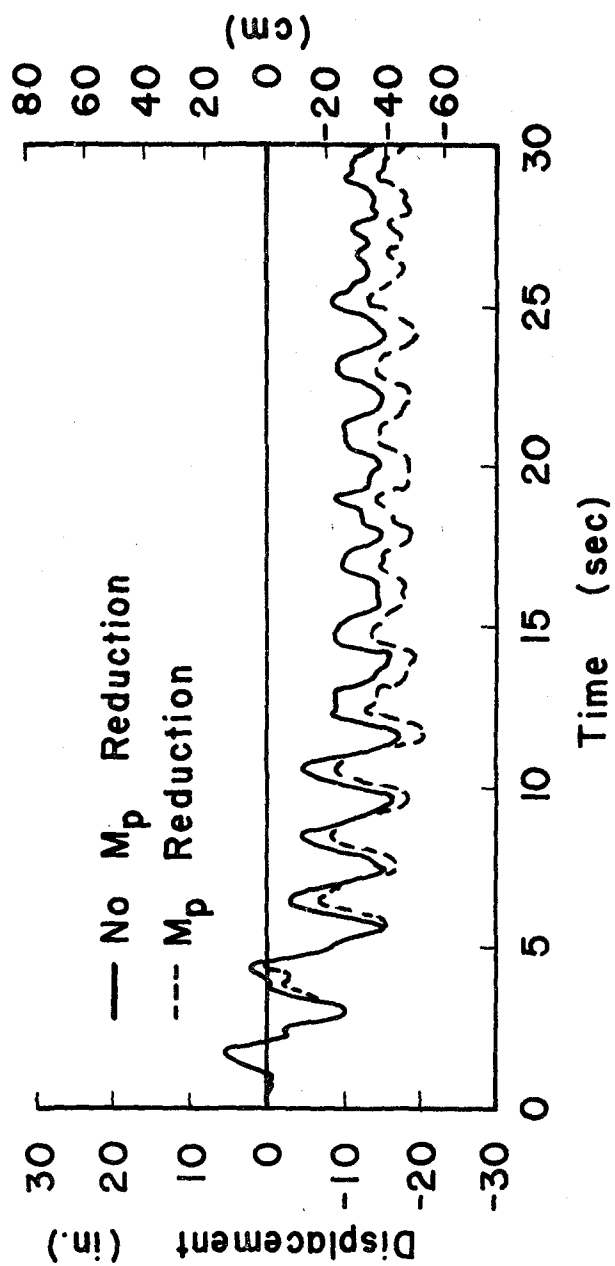


Figure 7.61. Effect of M_p Reduction on Top Floor Displacement, Frame B, 3% Damping, Elasto-Plastic System, 1940 El Centro, N-S Plus Vertical

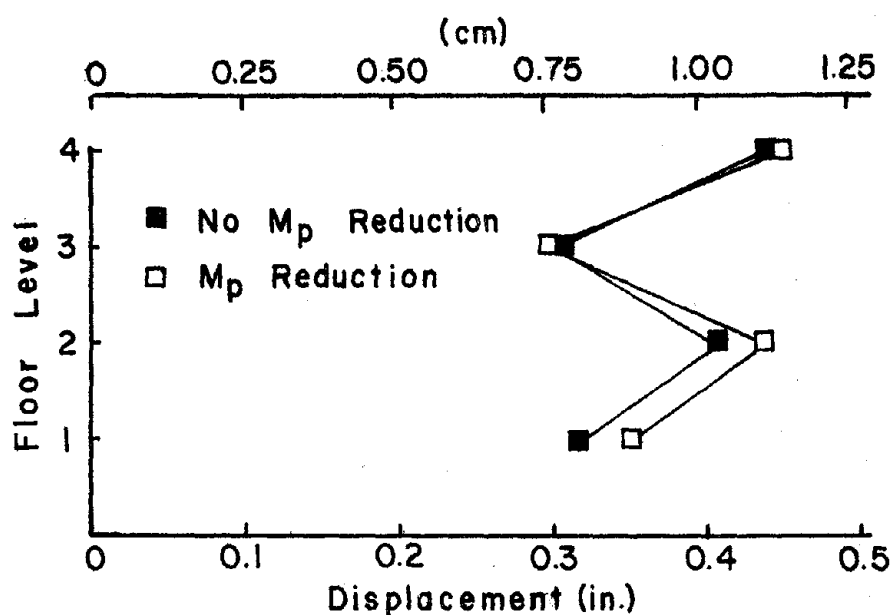
The change in the vertical response of girder nodes is shown in Fig. 7.62. The effect of the M_p reduction is more significant on Frame B than on Frame A.

Ductility and excursion ratios for the girder and column members of Frame B are shown in Fig. 7.63 with and without the M_p reduction. A decrease in the ductility requirement of the lower girder members and an increase in the ductility requirement of column members are observed.

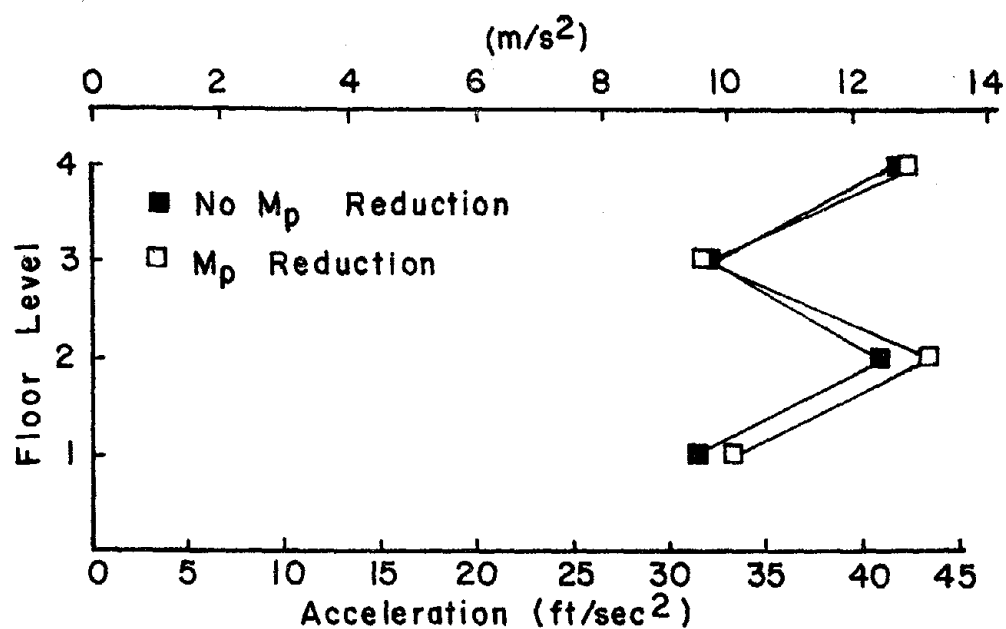
Figure 7.64 illustrates the increase in the input energy when including the M_p reduction. Even though its inclusion reduces the energy dissipated by damping, an increase in the dissipated strain energy due to additional inelastic rotation is observed.

3. Conclusions on the Effect of M_p Reduction. Based on the two example frames studied the following conclusions are made concerning the M_p reduction due to axial loads:

- 1) An increase in the horizontal response occurs for structures containing columns of reduced M_p values.
- 2) The effect on the vertical response at girder nodes varies for different frames. The M_p reduction combined with the vertical earthquake motion can greatly influence the response behavior.
- 3) An increase in the ductility requirement of columns is realized with a negligible difference for girders.
- 4) The amount of input energy increases due to the increased amount of dissipated strain energy.

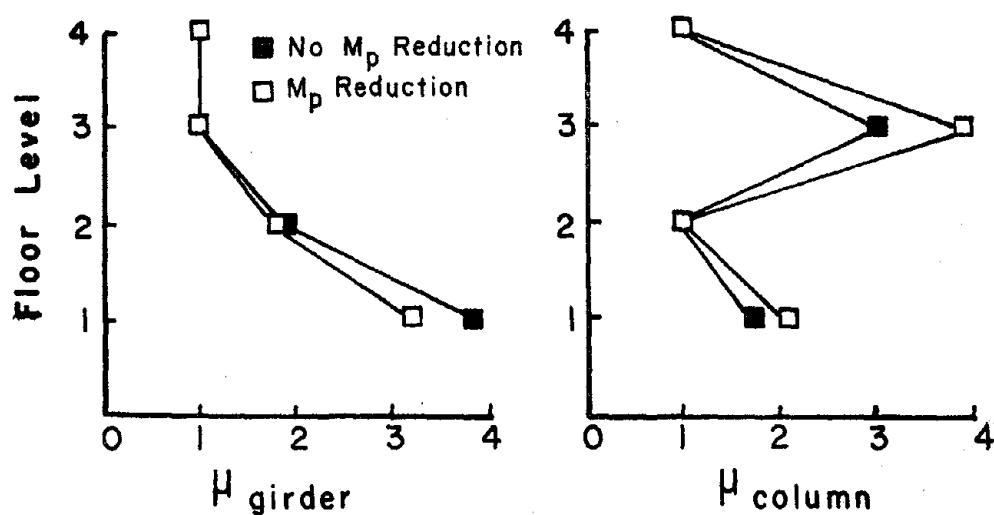


a) Maximum Vertical Displacement

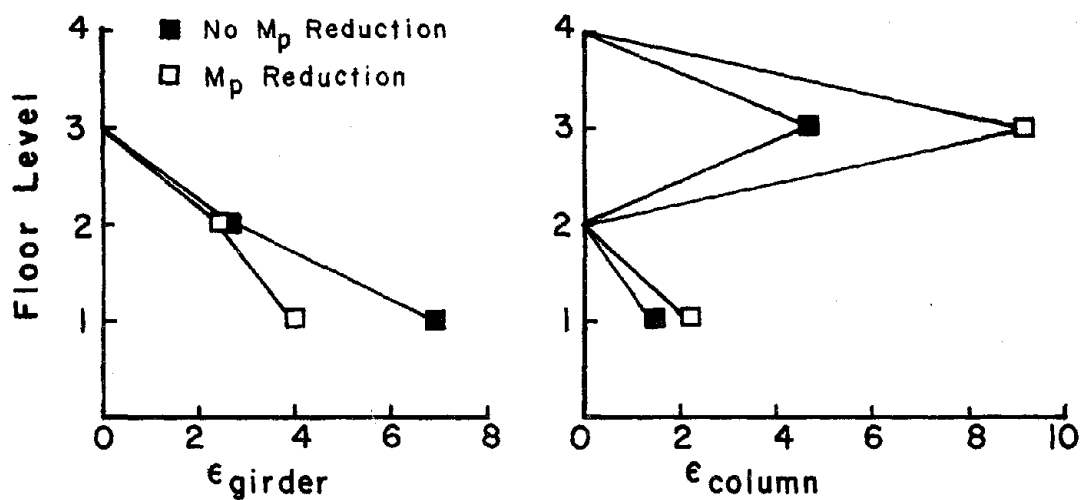


b) Maximum Vertical Acceleration

Figure 7.62. Effect of M_p Reduction on Vertical Response, Frame B, 3% Damping, Elasto-Plastic System, 1940 El Centro, N-S Plus Vertical



a) Ductility Ratio



b) Excursion Ratio

Figure 7.63. Effect of M_p Reduction on Ductility Requirement, Frame B, 3% Damping, Elasto-Plastic System, 1940 El Centro, N-S Plus Vertical

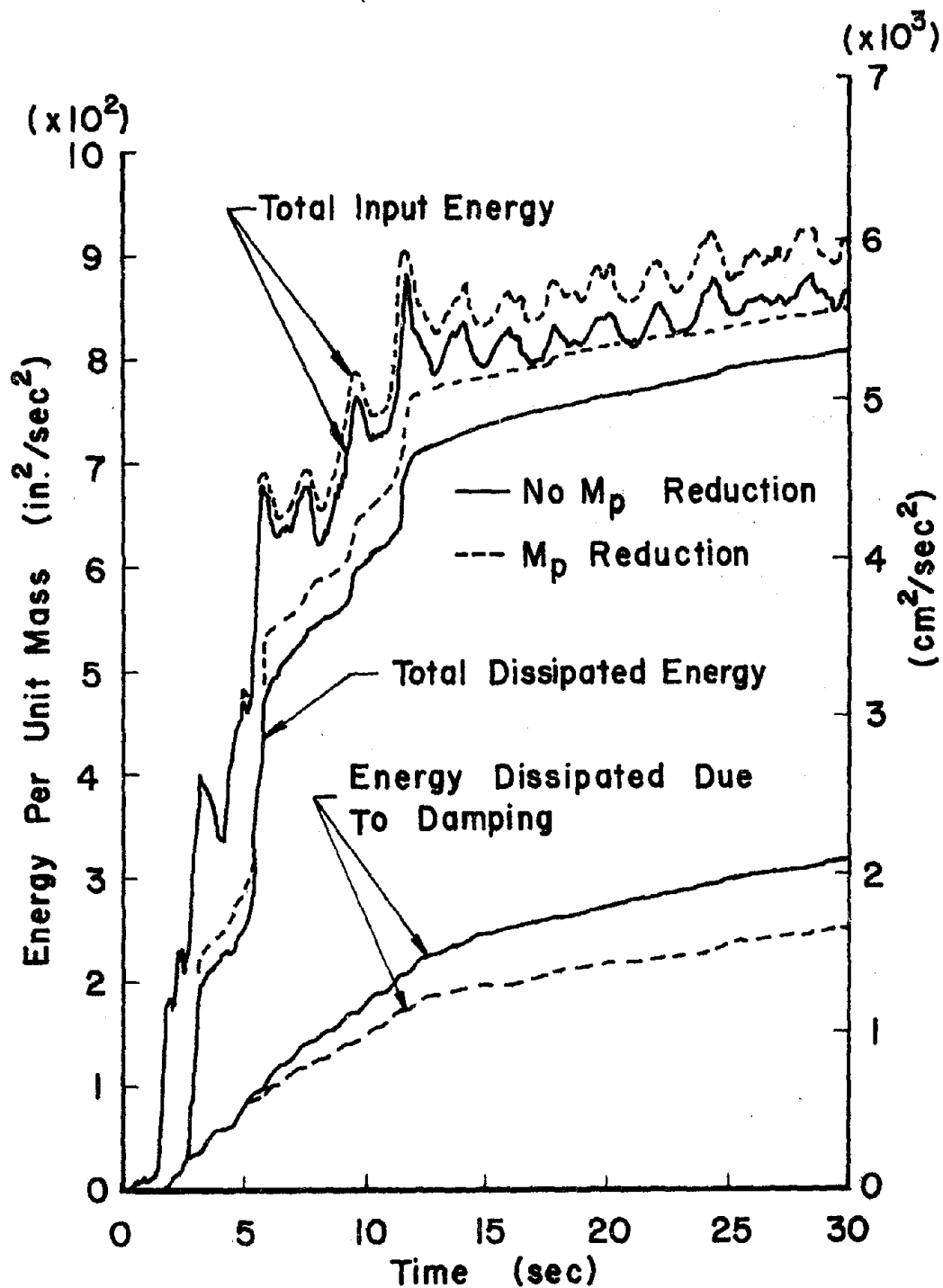


Figure 7.64. Effect of M_p Reduction on Energy, Frame B, 3% Damping, Elasto-Plastic System, 1940 El Centro, N-S Plus Vertical

F. EFFECT OF VISCOUS DAMPING ON RESPONSE PARAMETERS

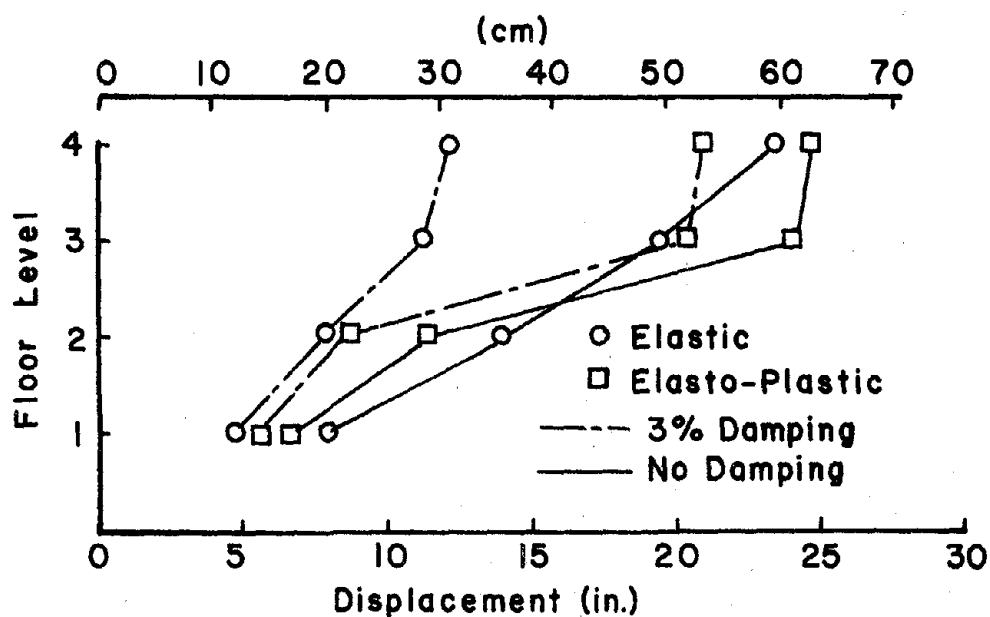
This section is to show the effect that damping has on the response parameters of multi-story structures when including the vertical ground motion. Mass proportional damping at 3% of critical is used in this study. The 4-story, 3-bay frame (Frame B) and the 10-story, 1-bay frame (Frame C) illustrate the response parameter studies.

1. 4-Story, 3-Bay Frame (Frame B). The overall effect of damping on the elastic and elasto-plastic response of Frame B is a reduction in both the maximum floor displacement and maximum relative floor displacement as shown in Fig. 7.65. This reduction in elasto-plastic response of the top floor is shown in Fig. 7.66 for the total time history. A reduction in the vertical response is shown in Fig. 7.67 for the elastic and elasto-plastic conditions.

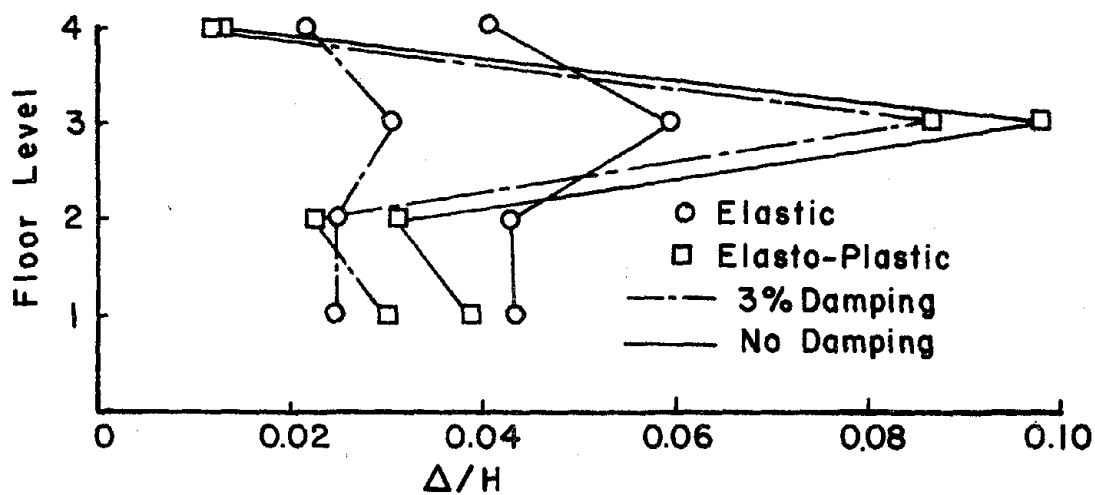
Ductility requirements are reduced for both the column and girder members when including damping as shown in Fig. 7.68, except for the 3rd floor column ductility ratio. The maximum excursion ratio corresponding to this floor is reduced for the damped case indicating less total inelastic rotation.

Figure 7.69 illustrates the effect that damping has on the energy consumption of the structural system of Frame B. Even though additional energy is dissipated due to damping, the reduced amount of dissipated strain energy for the damped system results in a net reduction in the total input energy as compared to the undamped system.

2. 10-Story, 1-Bay Frame (Frame C). The same damping effect on the horizontal and vertical response parameters is found for Frame C as found for Frame B. Reduction in the maximum floor displacement,



a) Maximum Floor Displacement



b) Maximum Relative Floor Displacement

Figure 7.65. Effect of Damping on Horizontal Response, Frame B, 1940 El Centro, N-S Plus Vertical

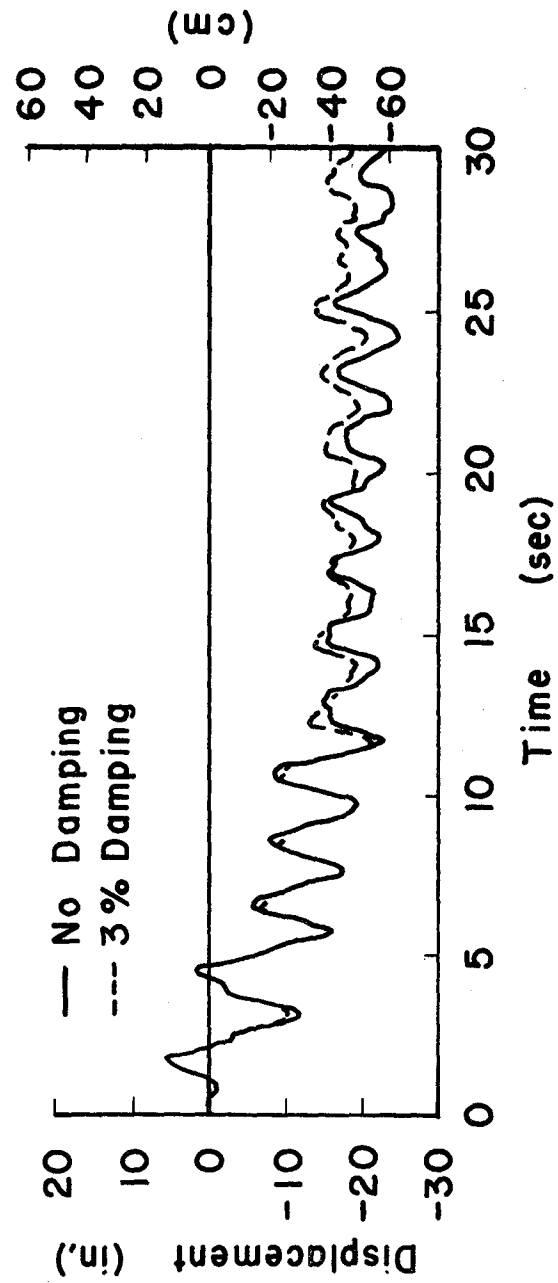
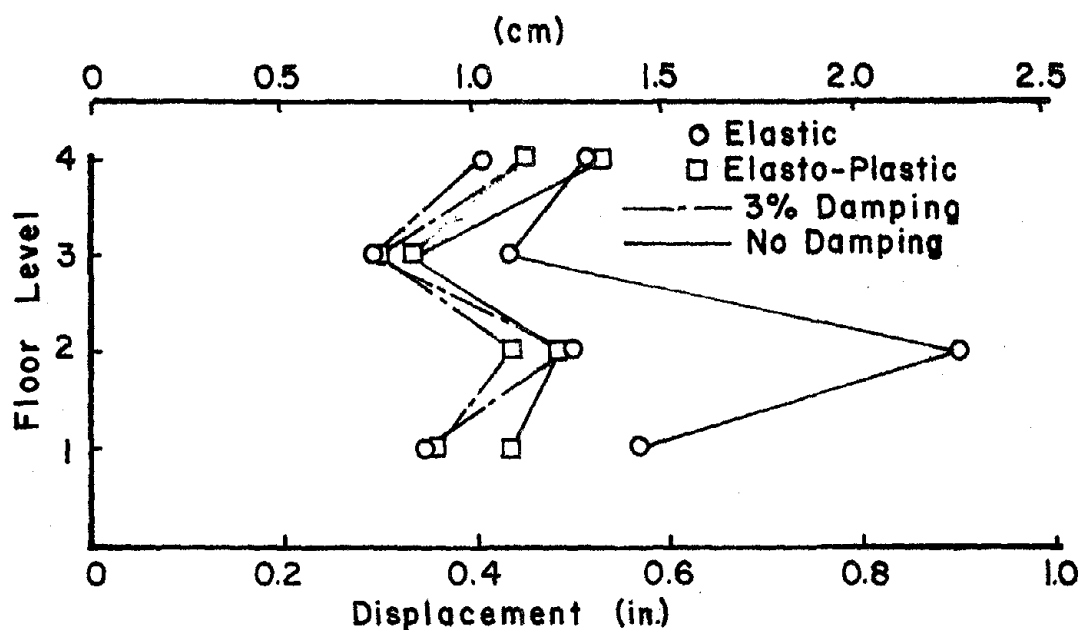
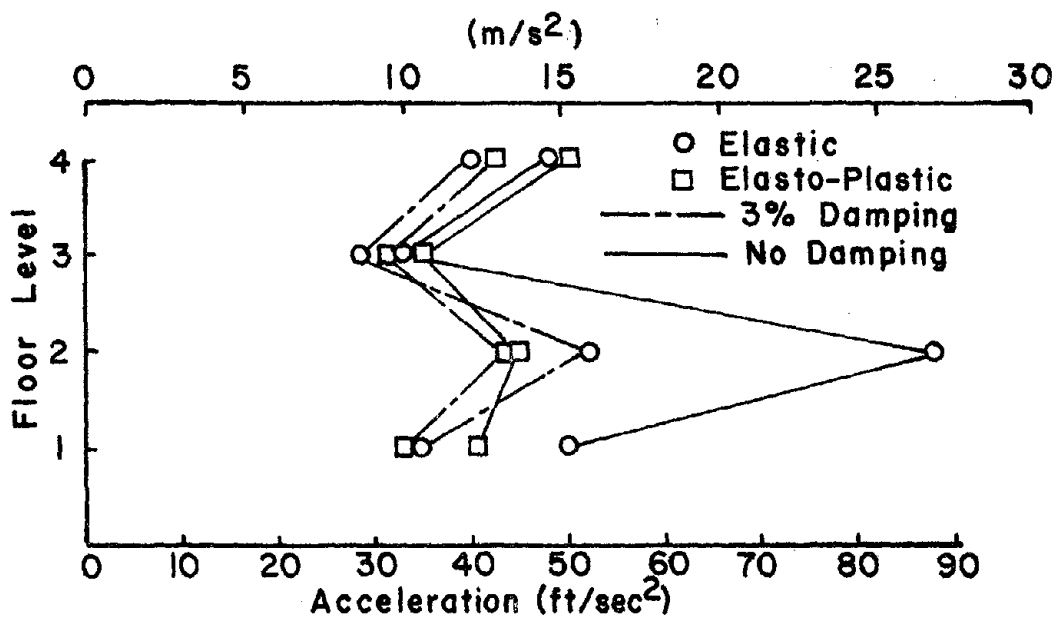


Figure 7.66. Effect of Damping on Displacement of Top Floor, Frame B, Elasto-Plastic System, 1940 El Centro, N-S Plus Vertical



a) Maximum Vertical Displacement



b) Maximum Vertical Acceleration

Figure 7.67. Effect of Damping on Vertical Response, Frame B, 1940 El Centro, N-S Plus Vertical

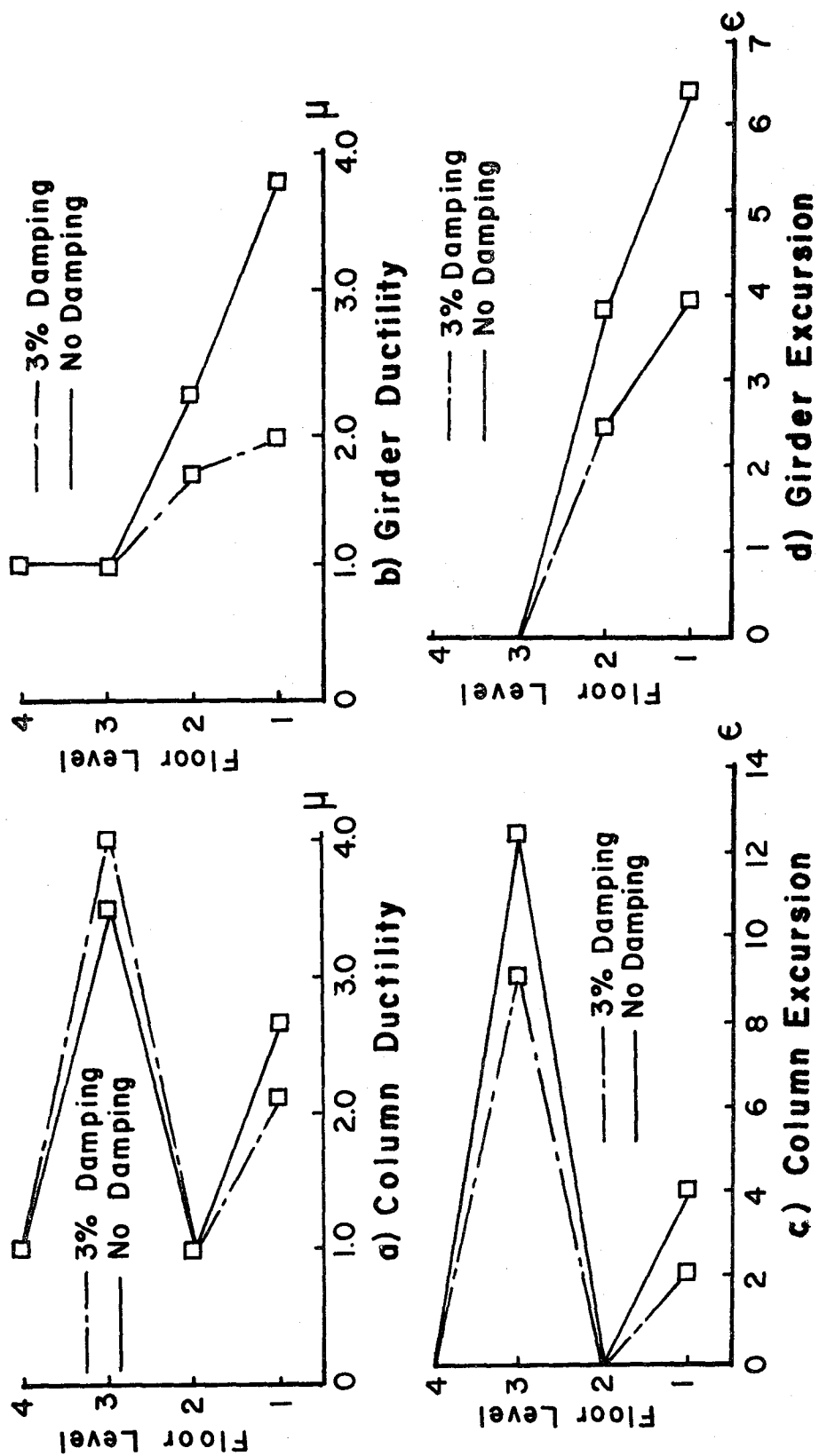


Figure 7.68. Effect of Damping on Ductility Requirements, Frame B, Elasto-Plastic System, 1940 El Centro, N-S Plus Vertical

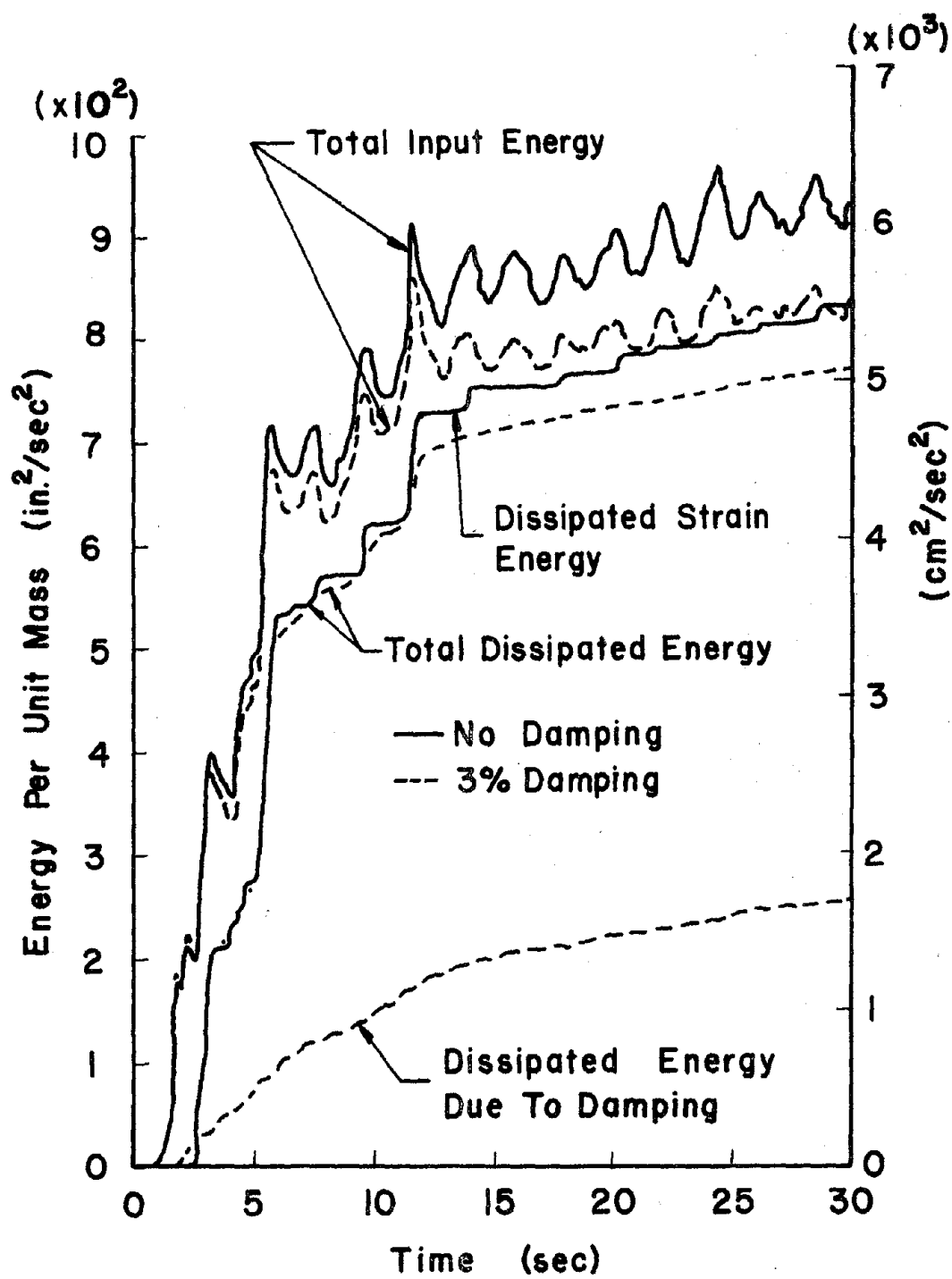
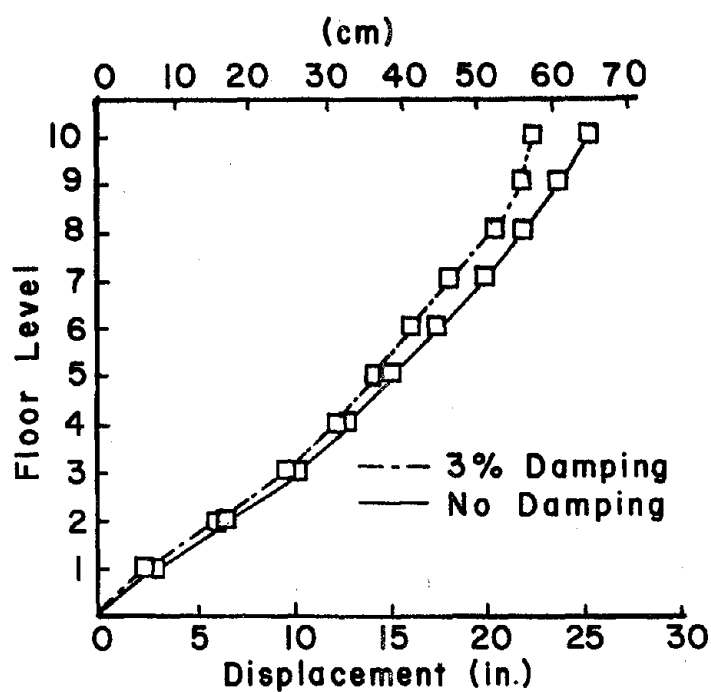


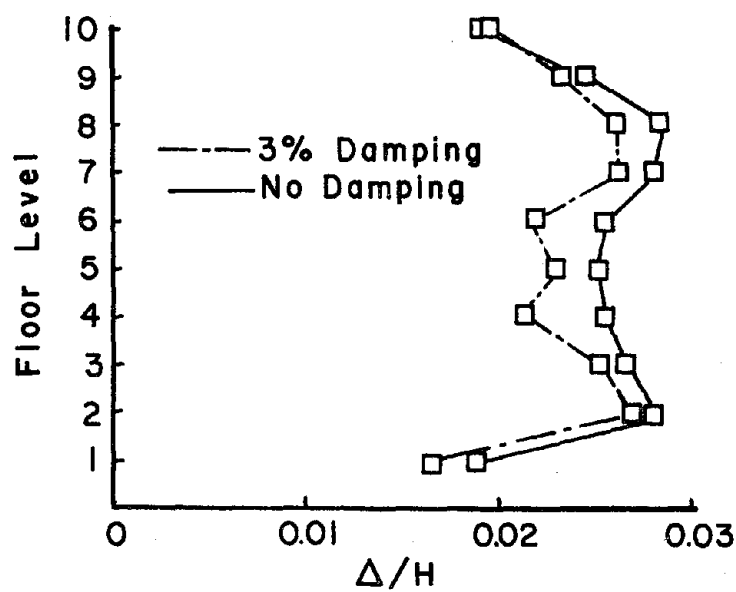
Figure 7.69. Effect of Damping on Energy, Frame B, Elasto-Plastic System, 1940 El Centro, N-S Plus Vertical

maximum relative floor displacement, top floor response, and the maximum vertical displacement and acceleration of the girder nodes is shown in Figs. 7.70-7.72 for the elasto-plastic system. The 3% damping results in a reduction of the inelastic rotations as illustrated by the reduced ductility and excursion ratios of Fig. 7.73. Several plastic hinges which originally develop in the undamped system do not occur when damping is included. A corresponding reduction in the total input energy due to damping may be observed from Fig. 7.74.

3. Conclusions on the Effect of Damping. This study has clearly shown that although the consideration of damping in an elastic or inelastic analysis results in a reduction in the response as expected, the general behavior of the significant influence of vertical earthquake motion on response parameters remains the same as previously shown for undamped systems.



a) Maximum Floor Displacement



b) Maximum Relative Floor Displacement

Figure 7.70. Effect of Damping on Maximum Horizontal Response, Frame C, Elasto-Plastic System, 1940 El Centro, N-S Plus Vertical

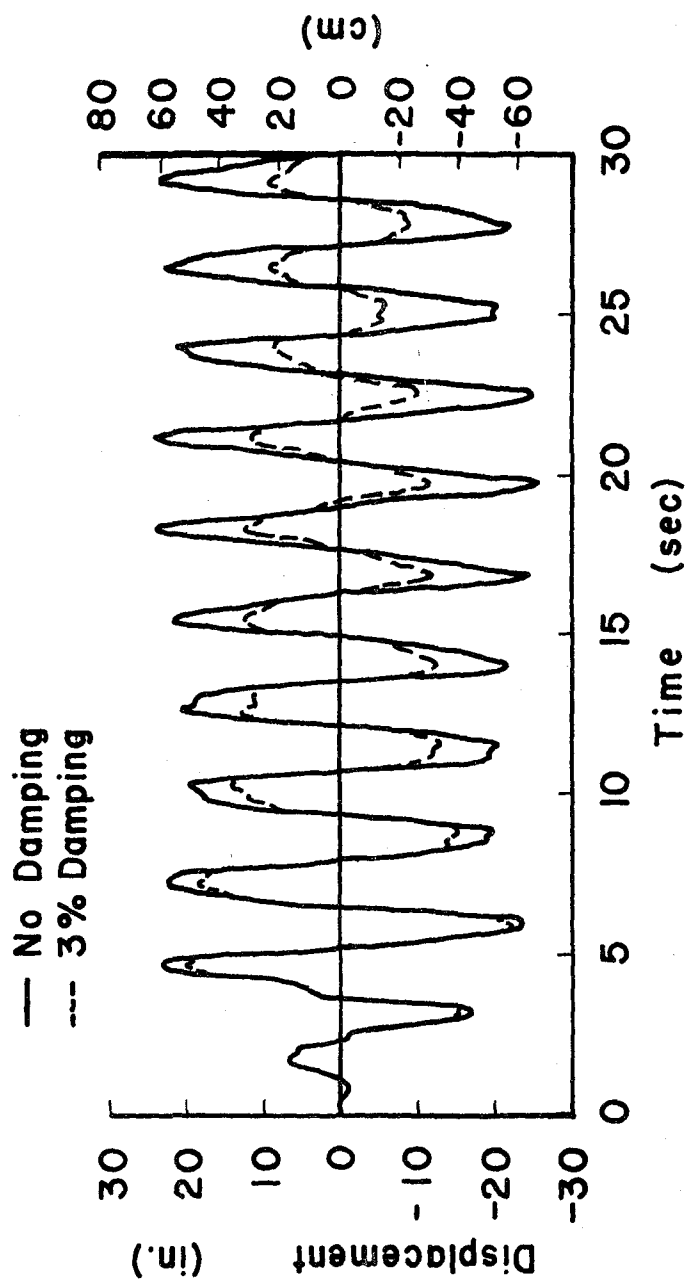


Figure 7.71. Effect of Damping on Displacement of Top Floor, Frame C, Elasto-Plastic System, 1940 El Centro, N-S Plus Vertical

VIII. REVIEW AND CONCLUSIONS

An analytical study is presented herein for the behavior of multi-story framed structures subjected to the interaction of horizontal and vertical components of an earthquake.

The energy absorption of elastic and inelastic systems has been considered in this research. The input energy is the result of the work produced by the horizontal and vertical support reactions acting through the corresponding support movements plus the horizontal floor forces due to the P-delta effect acting through the absolute horizontal floor displacements. The energy absorption is based on the kinetic energy due to velocity of the lumped masses, elastic strain energy due to bending in the frame members, dissipated strain energy due to the plastic rotations of the constituent members, and the dissipation due to viscous damping.

Bending deformation has been considered in this work for various elastic, elasto-plastic and bilinear structural systems. When considering the nonlinear moment-rotation relationship, a reduction in the plastic moment due to axial compression is included on the basis of the interaction formulation required by the AISC specifications. Other considerations include the P-delta effect and the effect of two different lumped mass models on response parameters.

The method of analysis as formulated in Chapter IV is chosen due to its adaptability to high speed digital computers and to the solution of nonlinear motion equations. The equations of motion are derived from a lumped mass system of the multi-story frame and are solved using Newmark's method with $\beta = 1/6$ which is the same as the linear

acceleration technique. The step-by-step approach lends itself to this type of analysis.

The response parameters in this study are mainly used to emphasize the deformation behavior of multi-story structures. Parameters include maximum horizontal and vertical displacements, maximum relative floor displacements, maximum vertical accelerations, ductility and excursion ratios, and energy absorptions of various structural models.

Observations and conclusions have been made in various appropriate chapters of this report. These observations and conclusions are based on the structures analyzed, the earthquake loading used, the assumptions applied in the formulation of the mathematical model, and the restrictions placed on the resulting response system. The assumptions in formulation and the restrictions placed on the resulting response are made in an attempt to simulate the realistic behavior of seismic structures. A summary of the more important observations and conclusions which are applicable to the objectives of this study is listed as follows:

- 1) The inclusion of the P-delta effect along with vertical earthquake motion can significantly influence the displacement response. The amount of change in response depends on the relationship between the fundamental frequency of the frame and the frequency spectrum of the earthquake loading.
- 2) The structures having a lumped mass at the center of each girder is an excellent model for a framed structure to respond to the energy produced by the vertical ground motion.

- 3) Even though the inclusion of the vertical earthquake component results in various changes in horizontal response according to the parameters of the system, this vertical motion can definitely cause an increase in the ductility requirement of the girders of the structures studied, especially in the upper floors.
- 4) The method used to integrate the motion equations in the step-by-step approach provides an accurate solution to the analysis of multi-story seismic frames. Newmark's method with $\beta = 1/6$ results in all errors less than 3% with the larger percent errors in the analysis of the 10-story frame at nearly the end of the earthquake record. The bulk of the errors is less than 1%.
- 5) For the analysis of damped structures, it is important to use an accurate fundamental frequency of the system for determining damping coefficient. Mass proportional damping has been shown to be an excellent damping formulation for accurate solution of nonlinear systems, because the variation in stiffness during a nonlinear response results in considerable error for other damping formulations expressed in terms of stiffness.
- 6) The overall effect of damping is a reduction in the response parameters of the system; however, the general behavior of the significant influence of vertical earthquake motion on response parameters remains the same as those of undamped systems.

BIBLIOGRAPHY

1. Anderson, J.C. and Bertero, V.V., "Discussion of Elasto-Plastic Seismic Response of Reinforced Concrete Frame," Journal of the Structural Division, ASCE, Vol. 96, No. ST6, Proc. Paper 7377, June, 1970, pp. 1246-1249.
2. Anderson, J.C. and Bertero, V.V., "Effects of Gravity Loads and Vertical Ground Acceleration on the Seismic Response of Multistory Frames," Proceedings, 5th World Conference on Earthquake Engineering, Rome, 1973.
3. Anderson, J.C. and Bertero, V.V., "Seismic Behavior of Multistory Steel Frames," Proceedings, Fourth Symposium on Earthquake Engineering, Roorkee, India, Nov., 1970.
4. Anderson, J.C. and Gupta, R.P., "Earthquake Resistant Design of Unbraced Frames," Journal of the Structural Division, ASCE, No. ST11, November 1972, pp. 2523-39.
5. Barr, O.D. and McWhannell, D.C., "Parametric Instability in Structures Under Support Motion," Journal of Sound and Vibration, Vol. 14, 1971, pp. 491-509.
6. Bathe, K.J. and Wilson, E.L., "Linear and Nonlinear Earthquake Analysis of Complex Structures," Proceedings, 5th World Conference on Earthquake Engineering, Rome, 1973.
7. Bathe, K.J. and Wilson, E.L., "Stability and Accuracy Analysis of Direct Integration Methods," Earthquake Engineering and Structural Dynamics, Vol. 1, pp. 283-291, 1973.
8. Berg, Glen V., "Response of Multi-Story Structures to Earthquake," Transactions, ASCE, Vol. 127, 1962, Part I, pp. 705-735.
9. Berg, G.V. and Housner, G.W., "Integrated Velocity and Displacement of Strong Earthquake Ground Motion," Bull. Seismol. Soc. Amer., Vol. 51, No. 2, pp. 175-189, April 1961.
10. Berg, G.V. and Thomaides, S.S., "Energy Consumption in Strong Motion Earthquakes," Proceedings, 2nd World Conference on Earthquake Engrg., Tokyo, 1960, Vol. II.
11. Biggs, John M., Introduction to Structural Dynamics, McGraw Hill, 1964.
12. Burney, S.Z.H. and Jaeger, L.G., "Dynamics of Plane Frames Subjected to Vertical Support Motion," Proceedings, First Canadian Conf. on Earthquake Engineering, Vancouver, B.C., May 1971, Cherry S., Ed., Univ. of British Columbia, Vancouver, Canada, pp. 187-202.

13. Cheng, F.Y., Computer Matrix Methods in Structural Dynamics and Earthquake Engineering, Notes for class CE 424, University of Missouri-Rolla.
14. Cheng, F.Y., "Finite Element Analysis of Structural Instability by Association of Pulsating Excitations," presented at the 1974 International Conference on Finite Element Methods in Engineering, August, 1974, Sydney, Australia, proceedings, pp. 597-610.
15. Cheng, F.Y. and Botkin, M.E., "P- Δ Effect of Optimum Design of Dynamic Tall Buildings," published by ASCE-IABSE Joint Committee for Conference on Tall Buildings, Bangkok, Thailand, January, 1974, Proceedings, pp. 621-632.
16. Cheng, F.Y., and Botkin, M.E., "Second-order Elasto-plastic Analysis of Tall Buildings with Damped Dynamic Excitations," Conference on the Finite Element Method in Civil Engineering, McGill University, Montreal, 1972, Proceedings, pp. 549-564.
17. Cheng, F.Y., and Oster, K.B., "Effect of Coupling Earthquake Motions on Inelastic Structural Models," Proc. of Intl. Symp. on Earthquake Structural Engineering, Vol. I, pp. 107-126, St. Louis, Mo., August, 1976.
18. Cheng, F.Y. and Oster, K.B., "The Effect of Parametric Earthquake Motions on Structural Ultimate Capacity," National Meeting of Universities Council for Earthquake Engineering Research, University of Michigan, May 1974, Proceedings.
19. Cheng, F.Y. and Oster, K.B., "Ultimate Instability of Earthquake Structures," presented at the ASCE Annual and National Environmental Engineering Convention (Oct. 21-25, 1974) Kansas City, Missouri, Preprint 2357.
20. Cheng, F.Y. and Oster, K.B., "Ultimate Instability of Earthquake Structures, Journal of the Structural Division, ASCE, Vol. 102, No. ST5, May, 1976, pp. 961-972.
21. Cheng, F.Y., and Oster, K.B., "Ductility Studies of Parametrically Excited Systems," 6th WCEE, paper No. 3-98, India, Jan., 1977.
22. Cheng, F.Y. and Tseng, W.H., Dynamic Instability and Ultimate Capacity of Inelastic Systems Parametrically Excited by Earthquakes--Part I, Technical Report prepared for the National Science Foundation, August, 1973, Civil Engineering Department, University of Missouri-Rolla.
23. Cheng, F.Y., Tseng, W.H., and Senne, J.H., "Dynamic Instability and Ultimate Capacity of Parametrically Excited Structures," Preprint No. 22, Vol. 1, presented at the Fifth World Conference on Earthquake Engineering, June 25-29, 1973, Rome, Italy, Proceedings.

24. Clough, R.W., Bensuka, K.L., Wilson, E.L., "Inelastic Earthquake Response of Tall Buildings," Proceedings, 3rd World Conf. on Earthquake Engrg., New Zealand, 1965.
25. Cooley, J.W. and Tukey, J.W., "An Algorithm for the Machine Calculation of Complex Fourier Series," Math. of Computation, Vol. 19, April 1965, pp. 297-301.
26. Disque, Robert O., Applied Plastic Design in Steel, Van Nostrand Reinhold Co., New York, 1971.
27. G-AE Subcommittee on Measurement Concepts, "What is the Fast Fourier Transform?," IEEE Transactions on Audio and Electro-acoustics, Vol. Au-15, No. 2, June 1967, pp. 45-55.
28. Giberson, M.F., "Two Nonlinear Beams with Definitions of Ductility," Journal of Structural Division, American Society of Civil Engineers, Vol. 95, ST2, pp. 137-157, 1969.
29. Giberson, M.F., "The Response of Nonlinear Multi-Story Structures Subjected to Earthquake Excitation," Ph.D. Dissertation, Calif. Institute of Technology, 1967.
30. Goel, S.C., "Inelastic Behavior of Multistory Building Frames Subjected to Earthquake Motion," Ph.D. Dissertation, University of Michigan, 1968.
31. Guru, B.P. and Heidebrecht, A.C., "Factor Influencing the Inelastic Response of Multi-Story Frames Subjected to Strong Motion Earthquakes," Proceedings, 4th World Conf. on Earthquake Engrg., Santiago, Chile, 1969.
32. Higdon, Archie and Stiles, William B., Engineering Mechanics, Vector Edition, Vol II, Prentice-Hall, Inc., Englewood Cliffs, N.J. 1962.
33. Langhaar, Henry L., Energy Methods in Applied Mechanics, John Wiley & Sons, Inc., New York 1962.
34. "Manual of Steel Construction," American Institute of Steel Construction, Inc., 1967.
35. Mendelson, Alexander, Plasticity: Theory and Application, The MacMillan Co., New York, 1968.
36. Newmark, N.M., "A Method of Computation for Structural Dynamics," Journal of the Engineering Mechanics Division, Proceedings, ASCE, Vol. 85, No. EM3, Proc. Paper, July, 1959, pp. 67-94.
37. Robinson, Ender A., Multichannel Time Series Analysis with Digital Computer Programs, Holden-Day, San Francisco, 1967.

38. Saul, W.E., Fleming, J.F. and Lee, S.L., "Dynamic Analysis of Bilinear Inelastic Multiple Story Shear Buildings," Proceedings, 3rd World Conf. on Earthquake Engineering, New Zealand, Vol II, pp. 533-51, 1965.
39. Saul, W.E., "Analysis of Bilinear Inelastic Structural Systems Subjected to Dynamic Loading," Ph.D. Dissertation, Northwestern University, 1964.
40. Sun, C.K., Berg, G.V. and Hanson, R.D., "Gravity Effect on Single-Degree Inelastic System," Journal of the Engineering Mechanics Division, ASCE, No. EM1, February 1973, pp. 183-200.
41. Thomaidis, Spiro S., "Earthquake Response of Systems with Bilinear Hysteresis," Journal of the Structural Division, ASCE, ST2, pp. 123-143, August 1964.
42. Timoshenko, S., Young, D.H., Weaver, W., Jr., Vibration Problems in Engineering, Fourth Edition, John Wiley & Sons, New York, 1974.
43. Titchkosky, K.A., Seismic Deconvolution, Vol II based on short course, "Summer Seminar for Digital Processing of Seismic Data," Calgary 1, Alta., Canada.
44. Wang, Chu-Kia, Matrix Methods of Structural Analysis, Second Edition, International Textbook Company, 1970.
45. Walpole, W.R. and Shepherd, R., "Elasto-Plastic Seismic Response of Reinforced Concrete Frame," Proceedings, ASCE Structural Division, Oct 1969, pp. 2031-55.

APPENDIX

DESCRIPTION OF INPUT DATA, FORTRAN IV LISTING OF PROGRAM, AND EXAMPLE
INPUT AND OUTPUT

Input Data

Information as to the size of structures, behavior conditions, loading conditions, type of analyses, and output format from the program must be provided as part of the input data. The five control cards following the heading card are used to provide this information.

Possible loads on the structure include initial static concentrated nodal loads, horizontal variable loads and vertical variable loads. The variable horizontal loading consists of either earthquake ground accelerations, a sinusoidal load or a triangular impulse load. The variable vertical loading consists of either earthquake ground accelerations, a sinusoidal variation in g-loads or a triangular impulse variation in g-loads. The program is written such that additional loading conditions can be added to the program without too much difficulty.

Information as to member locations, member properties, magnitude of lumped masses, elements of statics matrices and material properties are included in the structure information cards of X. A total of 11 possible card types are needed to provide this information.

I. Heading Card (20A4)

Columns 1-8, HDG, Contains information to be printed with
output

II. Structure Control Card (7I5)

Columns 1-5, JN,	No. assigned to structure analyzed
6-10, NP,	Total number of degrees of freedom
11-15, NPR,	Number of lumped masses
16-20, NPH,	Number of floor levels

- 21-25, NM, Number of members
 26-30, NSUPRT, Number of column supports
 31-35, NCOL, Number of columns

III. Behavior Control Card (5I5, 3F10.0)

- Columns 1-5, IELPL, The number 1 for a bilinear response
 Blank or 0 results in an elastic response
- 6-10, NCOND, Stress range condition
 = 0, elastic range = $2M_p$
 = 1, independent values for M_p
 = 2, M_p remains constant
- 11-15, IPDE, The number 1 causes the P-delta effect to be included
- 16-20, MP, The number 1 causes the reduction of the column M_p values due to axial compression
- 21-25, IDAM, Damping condition
 = 0, no damping
 = 1, mass proportional damping
 = 2, stiffness proportional damping
 = 3, mass plus stiffness proportional damping
- 26-35, ALAMDA, Critical damping factor
- 36-45, AOMEGA, Estimated fundamental frequency of structure
- 46-55, PVAL Strain hardening ratio, p

IV. Load Factors and Control Card (3I5, 3F10.0)

- Columns 1-5, IVA, The number 1 indicates inclusion of vertical loads
- 6-10, LPC, The number 1 causes the initial internal moments to be determined based on concentrated loads

- 11-15, LC, Loading condition number
 $= LC_h + 10*LC_v$, where:
 1 - earthquake record
 2 - sinusoidal load
 3 - triangular impulse load
 (vertical loads in g's)
- 16-25, BETAH, Factor to be applied to horizontal variable
 load (= 1.0 if left blank)
- 26-35, BETAV, Factor to be applied to vertical variable
 load (= 1.0 if left blank)
- 36-45, VGF, Factor to be applied to floor weights
 (= 1.0 if left blank)

V. Analysis Control Card (3F10.0)

- Columns 1-10, NMBM, Control number for Beta in Newmark's Beta
 Method.
 $= 0, \beta = 1/6$, linear acceleration
 $= 1, \beta = 1/12$
 $= 2, \beta = 1/4$

- 11-21, UDT, Time increment, sec
 22-31, TTOT, Total time of loading, sec

VI. Output Control Card (2F10.0, 7I5)

- Columns 1-10, PRDT, Increment of time for which output data is
 printed
- 11-20, PUDT, Increment of time for which output data is
 punched and/or plotted
- 21-25, INPRIN, The number 1 will cause the print of the initial
 stiffness matrices and moment-deformation matrix

- 26-30, IPLPR, The number 1 will cause the print of ductility and excursion data at time of plastic rotation
- 31-35, KPU, Control number for punched and/or plotted output
- = 0, No plot or punched output
 - = 1, Punched output only
 - = 2, Punched and/or plotted output
- 36-40, K1, Control for output of displacement history of top floor
- 41-45, K2, Control for output of total input energy history
- 46-50, K3, Control for output of total dissipated strain energy history
- 51-55, K4, Control for output of total dissipated energy due to damping

The controls K1-K4 for the above response parameters are based on the following designations:

- 0 - No plot or punch of output
- 1 - Plots of output
- 2 - Plot of dissipated strain energy when assigned to K3 and of dissipated energy due to damping when assigned to K4
- 3 - Plot of input energy, total dissipated energy and energy dissipated due to damping when assigned to K2

- 4 - Punches and plots of output
- 5 - Same as 2 with punched output included
- 6 - Same as 3 with punched output
- 7 - Punched output only

VII. Static Loads (7F10.0)(Use only when LPC = 1 in Card IV)

Concentrated transverse loads are applied in the directions of positive degree of freedom

PC(I), I = 1, NPS, where NPS = NP - NPR

VIII. Horizontal Variable Load Format depends on LC of Card IV

(Use only if LC > 0)

1. Earthquake Record (8F9.6)

Earthquake data is based on the time increment, UDT, and the total time of record, TTØT, as given in Card V. Data consists of the g-levels for time $t = 0.0$ to $t = TTØT$ in time increments of UDT

2. Sinusoidal Load on Top Floor (3F10.0)

Columns 1-10, AMEGØ, Forcing frequency, Hz

11-20, AMAX, Amplitude, kips

21-30, PHASE, Phase angle, degrees

3. Triangular Impulse Load on Top Floor (2F10.0)

Columns 1-10, F1, Initial value of force, kips

11-20, TD, Time which force reduces to zero, sec

IX. Vertical Variable Load Format depends on LC of Card IV

(Use only if LC > 10)

1. Earthquake Record (8F9.6)

Earthquake data is based on the time increment, UDT, and the total time of record, TTØT as given in Card V. Data consists of the g-levels for time $t = 0.0$ to $t = TTØT$ in increments of UDT

2. Sinusoidal Load

Columns 1-10, AMEGØ, Forcing frequency, Hz

11-20, AMAX, Amplitude, g's

21-30, PHASE, Phase angle, degrees

3. Triangular Impulse Load (2F10.0)

Columns 1-10, F1, Initial value of load, g's

11-20, TD Time which force reduces to zero, sec.

X. Structure Information Cards

The following cards are used for providing the structural parameters:

Card 1: Girder Members, IGIRD(I), I = 1, NGM(10I5)

This provides the girder member No.'s in the order of left to right for each span starting with the top floor. NGM = number of girder members = NM - NCØL.

Card 2: Support Members, ISUPRT(I), I = 1, NSUPRT (10I5)

This provides the support member No.'s in the order of left to right. NSUPRT = number of support members as indicated in Card II.

Card 3: Member M_p Values, VALMP(I), I = 1, NM(7F10.0)

The Plastic yield moment value for each member of increasing numerical order is provided, kip ft. NM = number of members in structure as indicated in Card II.

Card 4: Girder and Floor Masses, AMASS(I), I = 1, NPS(7F10.0)

The girder masses followed by the total mass of each floor are provided in increasing numerical order of the displacement degrees of freedom for the structure, kip-sec²/ft.

$NPS = NP - NPR = NPV + NPH$

More than 1 card can be used for each of the above structure information cards.

Card 5: Mass Magnification Factor, CMASS (F10.0)

Factor to be applied to all the masses of the lumped mass system as listed on previous card. (= 1 if left blank)

Card 6: Moment Statics Matrix (2I5, F10.0, 3I5)

The input of the moment statics matrix is accomplished by listing the location (Row I, Column J) and magnitude (AIJ) of each non-zero element of the matrix $AM(I,J)$.

Column 1-5, I, Row number of $AM(I,J)$
 6-10, J, Column number of $AM(I,J)$
 11-20, AIJ, Values of non-zero element of $AM(I,J)$

The remaining input values for these cards are optional. They are used to generate the $AM(I,J)$ matrix so that more than one non-zero element can be input per card.

21-25, NI, Number of non-zero elements included in this card

26-30, IADD, Increment to be added to I in generation of $AM(I,J)$

31-35, JADD, Increment to be added to J in generation of $AM(I,J)$

The above input data for Card 6 is followed by ONE BLANK CARD.

Card 7: Shear Statics Matrix (2I5, F10.0, 3I5)

The input of the shear statics matrix is accomplished by listing the location (Row I, Column J) and magnitude (ARZ) of each non-zero element of the matrix $AV(I,J)$

Column 1-5, I, Row number of $AV(I,J)$
 6-10, J Column number of $AV(I,J)$
 11-20, ARZ, Value of non-zero element of $AV(I,J)$

The remaining input values for these cards are optional. They are used to generate the $AV(I,J)$ matrix so that more than one non-zero element can be input per card.

21-25, NI, Number of non-zero elements included in this card

26-30, IADD, Increment to be added to I in generation of $AV(I,J)$

31-35, JADD, Increment to be added to J in generation of $AV(I,J)$

The above input data for Card 7 is followed by ONE BLANK CARD.

Card 8: Material Properties (2F10.0)

Column 1-10, E, Modulus of elasticity of material used in structure, ksi

11-20, F_y , Yield stress of material used in structure, ksi

Card 9: Moment of Inertia of Member Cross-sections (7F10.0)

$XI(I)$, $I = 1, NM$, where NM = Number of members.

This provides the moment of inertia values for all members.

The cards must be in member number sequence, in^4

Card 10: Length of Members (7F10.0)

$XL(I)$, $I = 1, NM$, where NM = Number of members. This provides the member lengths in member number sequence, ft.

Card 11: Member Properties Pertaining to M_p Reduction. Not used when $MP = 0$. (15, 3F10.0) One card per column member is provided in the order of left to right for each floor starting with the top floor.

Column 1-5, $ICOL(I)$, Column No.

6-15, $A(I)$, Cross sectional area of member I, in^2

16-25, $UBL(I)$, Unbraced length of member I, in.

26-35, $R(I)$, Radius of gyration of member I

XI. End Cards

The following two cards shall be provided to either end program or to continue to next set of data.

Card 1: End comment card or heading card for next set of data (20A4)

Card 2: Blank card or next set of data.


```

701 IF (IDAM.EQ.0) GO TO 704
711 GO TO (701,702,703),IDAM
711 PRINT 711
711 FORMAT(/8X,'MASS PROPORTIONAL DAMPING')
702 GO TO 705
712 PRINT 712
712 FORMAT(/8X,'STIFFNESS PROPORTIONAL DAMPING')
703 GO TO 705
713 PRINT 713
713 FORMAT(/8X,'MASS PLUS STIFFNESS PROPORTIONAL DAMPING
      *')
704 GO TO 705
714 PRINT 714
714 FORMAT(/8X,'DAMPING NOT CONSIDERED')
705 CONTINUE
498 PRINT 498
498 FORMAT (/ //5X,'OUTPUT CONTROL')
495 PRINT 495,PRDT,PUDT
495 FORMAT(/8X,'PRINTOUT INCREMENT',F10.2,
      /8X,'PUNCH OR PLOT INCREMENT',F10.3)
1 IF (INPRIN.EQ.0) GO TO 502
PRINT 501
501 FORMAT(8X,'PRINTOUT OF INITIAL MATRICES INCLUDED')
502 CONTINUE
IF (IPLPR.EQ.0) GO TO 504
PRINT 503
503 FORMAT(8X,'PRINTOUT OF PLASTIC HINGE RESULTS INCLUDED')
504 CONTINUE
CALL DAMP(IDAM,AA,BB,ALAMDA,AOMEGA)
LOADING INPUT
PRINT 721
721 FORMAT(/ //5X,'LOADING INFORMATION')
4322 IF (LPC) 4323,4323,4322
4322 READ 1002,(PC(I),I=1,NPS)
JS=1
PRINT 4328
4328 FORMAT(/ //6X,'CONCENTRATED LOAD VALUES')
PRINT 2009,(I,PC(I),I=1,NPS)
GO TO 4324
4323 CONTINUE
JS=0
DO 4350 I=1,NPS
4350 PC(I)=0.0
4324 CONTINUE
IERQK=0
ND=(TIOT+.0001)/UDT
IF (INPRIN.EQ.0) GO TO 301
PRINT 6001, ND

```

MAIN 720
 MAIN 730
 MAIN 740
 MAIN 750
 MAIN 760
 MAIN 770
 MAIN 780
 MAIN 790
 MAIN 800
 MAIN 810
 MAIN 820
 MAIN 830
 MAIN 840
 MAIN 850
 MAIN 860
 MAIN 870
 MAIN 880
 MAIN 890
 MAIN 900
 MAIN 910
 MAIN 920
 MAIN 930
 MAIN 940
 MAIN 950
 MAIN 960
 MAIN 970
 MAIN 980
 MAIN 990
 MAIN 1000
 MAIN 1010
 MAIN 1020
 MAIN 1030
 MAIN 1040
 MAIN 1050
 MAIN 1060
 MAIN 1070
 MAIN 1080
 MAIN 1090
 MAIN 1100
 MAIN 1110
 MAIN 1120
 MAIN 1130
 MAIN 1140
 MAIN 1150
 MAIN 1160
 MAIN 1170
 MAIN 1180

```

6001 FORMAT (/5X,'NUMBER OF TIMES FRAME IS LOADED=',I5)
301 CONTINUE
    IHV=1
    MULF=0
    IF(LC.EQ.0) GO TO 6050
    CONTINUE
    IF(LC.LT.10) GO TO 6020
    MULF=MULF+1
    LC=LC-10
    GO TO 6019
6020 CONTINUE
6021 CALL LOADNG(UDT,ND,IHV,LC)
    IF(MULF.EQ.0) GO TO 6060
    IHV=IHV+1
    CALL LOADNG(UDT,ND,IHV,MULF)
    GO TO 6061
6050 CONTINUE
    DO 6027 I=1,ND
6027 XSTT(I)=0.0
6060 CONTINUE
    DO 6028 I=1,ND
6028 YSTT(I)=0.0
6061 CONTINUE
C *****AMPLIFIED XSTT AND YSTT*****
    DO 627 I=1,ND
    XSTT(I)=XSTT(I)*BETAH
    YSTT(I)=YSTT(I)*BETAV*32.2
627 CONTINUE
710 CONTINUE
    XSTT(ND*1)=0.0
    XSTT(ND*2)=0.0
    YSTT(ND*1)=0.0
    YSTT(ND*2)=0.0
C *****AMPLIFIED XSTT AND YSTT*****
    PRINT 474
474 FORMAT (/5X,'STRUCTURE INFORMATION')
    READ 1005, (IGIRD(I),I=1,NGM)
    IF(INPV.NE.0) GO TO 4240
    IUT = LEFT AND RIGHT GIRDER MEMBERS FOR EACH SPAN
C STARTING AT TOP FLOOR, LEFT TO RIGHT.
    PRINT 4239, (IGIRD(I),I=1,NGM)
4239 FORMAT (18X,'GIRDER MEMBERS',/10X,23I5)
    GO TO 4109
4240 CONTINUE
    PRINT 4101, (IGIRD(I),I=1,NGM,2)
4101 FORMAT (/8X,'GIRDER MEMBERS LEFT SIDE OF SPAN',/10X,23I5)
    PRINT 4102, (IGIRD(I),I=2,NGM,2)
4102 FORMAT (18X,'GIRDER MEMBERS RIGHT SIDE OF SPAN',/10X,23I5)

```

```

MAIN1190
MAIN1200
MAIN1210
MAIN1220
MAIN1230
MAIN1240
MAIN1250
MAIN1260
MAIN1270
MAIN1280
MAIN1290
MAIN1300
MAIN1310
MAIN1320
MAIN1330
MAIN1340
MAIN1350
MAIN1360
MAIN1370
MAIN1380
MAIN1390
MAIN1400
MAIN1410
*****
MAIN1420
MAIN1430
MAIN1440
MAIN1450
MAIN1460
MAIN1470
MAIN1480
MAIN1490
MAIN1500
*****
MAIN1510
MAIN1520
MAIN1530
MAIN1540
*****
MAIN1550
MAIN1560
MAIN1570
MAIN1580
MAIN1590
MAIN1600
MAIN1610
MAIN1620

```

```

4109 CONTINUE
1005 READ 1005, (ISUPRT(I), I=1, NSUPRT)
1005 FORMAT (10I5)
2043 PRINT 2043, (ISUPRT(I), I=1, NSUPRT)
2043 FORMAT (/8X, 'SUPPORT COLUMNS', /10X, 23I5)
1002 READ 1002, (VALMP(I), I=1, NM)
1002 FORMAT(7F10.0)
IF (IELPL.EQ.1) GO TO 1310
*****MAGNIFIED MP-VALUE*****
DO 626 I=1, NM
VALMP(I)=VALMP(I)*100000.*100000.
*****MAGNIFIED MP-VALUE*****
626 VALMP(I)=VALMP(I)*100000.*100000.
*****MAGNIFIED MP-VALUE*****
1310 CONTINUE
PRINT 2002
2002 FORMAT(/ /6X, 'VALUE OF PLASTIC MOMENT FOR EACH MEMBER')
2009 PRINT 2009, (I, VALMP(I), I=1, NM)
2009 FORMAT(6I2X, I3, E15.6)
INITIALIZATION
I=0.
JJ=0
AHHA=XSTT(1)
AVVA=-YSTT(1)
BVVB=0.0
EIIE=0.0
EIEMAX=0.0
EIINPUT(I)=0.0
BPRC=0.0
BLSE=0.0
TDSE=0.0
EDD=0.0
XG=0.0
XGT=0.0
YG=0.0
XGTP1=0.0
YGTP1=0.0
DO 42 I=1, NEM
TBLSE(I)=0.0
DSEAB(I)=0.0
DO 43 I=1, NM
S(I)=0.0
DO 44 I=1, NPH
RELMAX(I)=0.0
DO 45 I=1, NEM
SLOPE(I)=0.0
TROT(I)=0.0
TANG(I)=0.0

```

```

45  BMOM(I)=0.
    NEM3=3*NEM
    DO 3963 I=1,NEM3
      DUCMAX(I)=0.0
      EXCUR(I)=0.0
    DO 50 I=1,NP
      X(I)=0.
    X10(I)=0.0
    DO 52 I=1,NPS
      XT(I)=0.
      XTT(I)=0.
    CONTINUE
    DO 55 I=1,NM
      JC1(I)=0
      JC2(I)=0
      JC3(I)=0
    DO 68 I=1,NEM
      K=(I+1)/2
      ALMP(I)=VALMP(K)
      ALMPN(I)=-VALMP(K)
    NTIM=0
    AVEYGT=0.0
    AVEYGT=0.0
    DO 60 I=1,NM
      PI(I)=1.
    DO 65 I=1,NEM
      RED(I)=1.0
      KI(I)=0
    DO 66 I=1,NPS
      ACCMAX(I)=0.0
      ACCMIN(I)=0.0
      XMAX(I)=0.0
      XMIN(I)=0.0
      TXMAX=0.0
      TXMIN=0.0
    DO 568 I=1,NEM
      BMIN(I)=0.0
      BMAX(I)=0.0
    CALL MAXTOR (NP,NPR,NPS,NEM,N1,N2,N3,N4,N5,N6,N7,N8,N9)
    K=N7-1
    DO 569 I=N6,K
      ATOZ(I)=0.0
      BEV=PRDT
      TRAC=PUDT
      KEN=1
    C
    FORM MASS MATRIX DIAGONAL
    YACC=YST(I)
    XACC=XST(I)

```

```

MAIN2080
MAIN2090
MAIN2100
MAIN2110
MAIN2120
MAIN2130
MAIN2140
MAIN2150
MAIN2160
MAIN2170
MAIN2180
MAIN2190
MAIN2200
MAIN2210
MAIN2220
MAIN2230
MAIN2240
MAIN2250
MAIN2260
MAIN2270
MAIN2280
MAIN2290
MAIN2300
MAIN2310
MAIN2320
MAIN2330
MAIN2340
MAIN2350
MAIN2360
MAIN2370
MAIN2380
MAIN2390
MAIN2400
MAIN2410
MAIN2420
MAIN2430
MAIN2440
MAIN2450
MAIN2460
MAIN2470
MAIN2480
MAIN2490
MAIN2500
MAIN2510
MAIN2520
MAIN2530
MAIN2540

```

```

      CALL FOMASM (NPH,NPS,TMASS,VMASS,XACC,YACC,LC)
      IF(LPC.GT.0) GO TO 4325
      IF(IERQK.EQ.0) GO TO 555
70  CONTINUE
      DT=UDT
      T=T+DT
      IF(LPC.EQ.0) GO TO 4325
      LPC=0
      GO TO 75
4325 CONTINUE
      FORM STIFFNESS AND INTERNAL MOMENT MATRICES
      CALL FOSTIM (NP,NPR,NPS,N1,N2,N3,N4,NCOL,INPRIN)
      IF(NTIM.GT.1) GO TO 676
      CALL FOK2M(NPS,NPH,NPV,N5,IREDK2,INPRIN)
676 CONTINUE
      IF(LPC.GT.0) GO TO 82
75 CONTINUE
      FORM FORCE MATRIX
      CALL FOFOME (NPS,NPV,LC,MULF)
      CONTINUE
77 CONTINUE
80 CONTINUE
      PERFORM NEWMARK BETA METHOD OF LINEAR ACCEL.
82  CALL NEMKBM(NP,NPS,NPV,N2,N3,N4,N5,N6,N7,N8,N9,LC,NCOL,
      * INPRIN,NMBM)
      CALL INWRK(XG,YG,LC,DT,IHV,VMASS,TMASS,NPV,NP, NPS,NPK,XGT,YGT,
      IREDK2,N5)
      IF(IERQK.EQ.0) GO TO 555
      CALL MAXIMA (NP,NPR,IXMAX,IXMIN,TEIE,NPV,EIEMAX,NEM)
      SAVE FOR PUNCH
      PEL=TRAC-.0001
      IF(T.LT.PEL) GO TO 84
      KEN=KEN + 1
      TRAC=KEN*PUDT
      DPL=X(NP)
      CALL CAPLS(KPU,K1,K2,K3,K4,KEN,NPS,TMASS,DPL,1)
84 CONTINUE
      PRINT OUT PUT
      BEV=BEV-.0001
      IF((XMAX(NPS).GT.50.0).OR.(XMIN(NPS).LT.-50.0)) GO TO 83
      IF(T.LT.BEL) GO TO 85
      BEV=BEV + PRDT
555 CONTINUE
      CALL PRIQUT(NP,NPR,NPS,NM,NEM,NPV,XG,XGT,YG,YGT,1)
      CALL ENERGY (NM,NPS,NPV,1,N6)
      CALL PRIQUT(NP,NPR,NPS,NM,NEM,NPV,XG,XGT,YG,YGT,2)
      IF(LPC.EQ.0) GO TO 308
      ISQS=0
      DO 302 I=1,NEM

```

```

MAIN2550
MAIN2560
MAIN2570
MAIN2580
MAIN2590
MAIN2600
MAIN2610
MAIN2620
MAIN2630
MAIN2640
MAIN2650
MAIN2660
MAIN2670
MAIN2680
MAIN2690
MAIN2700
MAIN2710
MAIN2720
MAIN2730
MAIN2740
MAIN2750
MAIN2760
MAIN2770
MAIN2780
MAIN2790
MAIN2800
MAIN2810
MAIN2820
MAIN2830
MAIN2840
MAIN2850
MAIN2860
MAIN2870
MAIN2880
MAIN2890
MAIN2900
MAIN2910
MAIN2920
MAIN2930
MAIN2940
MAIN2950
MAIN2960
MAIN2970

```

```

IF(KI(1).GT.0) ISOS=ISOS+1
302 CONTINUE
IF(IISOS.EQ.0) GO TO 308
PRINT 303, ISOS
303 FORMAT(/ /5X, 'PROGRAM TERMINATED DUE TO', I3, ' JOINT/S BECOMMING PLAS-
      TIC DURING STATIC ANALYSIS')
STOP
308 CONTINUE
IF(ILC.EQ.0) GO TO 99
IF(BPRC.GT.100.0) GO TO 83
IF(IEROK.EQ.0) GO TO 70
IF(T-TTOT+.0001) 86,83,83
83 CONTINUE
CALL PRIMAX (ITXMAX, TXMIN, EIMAX, TEIE, KEN, NPS, NPH, NEM)
IF(KPU.EQ.0) GO TO 99
PRINT 2223, KEN
2223 FORMAT(/ /5X, 'NUMBER OF DATA IN EACH OUTPUT=', I5)
CALL CAPLS(KPU, K1, K2, K3, K4, KEN, NPS, TMASS, DPL, 2)
GO TO 99
85 CONTINUE
CALL ENERGY (NM, NPS, NPV, 4, N6)
86 CONTINUE
IF(T.GE. TTOT) GO TO 83
IF(KJ.GT.1) GO TO 70
T=T+DT
GO TO 75
99 CONTINUE
GO TO 1
100 CONTINUE
STOP
END
SUBROUTINE MPRED (NCOL)
COMMON/MANECA/ DX(50), BMDM(80), ALMPP(80), ALMPN(80),
1 KI(80), VALMP(40), X(50), XT(20), XTT(20), DR(20),
2 UDT, PVAL, JJ, NCOND
COMMON/FAFEP/ AFA(20), AFEP(20), RED(80), ICOL(20), PY(20), MP
COMMON/AXIAL/ P(20)
DOUBLE PRECISION DX
1 CONTINUE
DO 50 I=1, NCOL
M=ICOL(I)
J2=2*M-1
J1=J2+1
IF(KI(J1).GT.0).AND.(KI(J2).GT.0)) GO TO 50
C=P(I)/PY(I)
IF(C.LE.0.15) GO TO 48
R1=1.18*(1.0-C)
R2=1.176*(1.0-P(I)/(1.7*AFA(I)))

```

```

MAIN2980
MAIN2990
MAIN3000
MAIN3010
MAIN3020
MAIN3030
MAIN3040
MAIN3050
MAIN3060
MAIN3070
MAIN3080
MAIN3090
MAIN3100
MAIN3110
MAIN3120
MAIN3130
MAIN3140
MAIN3150
MAIN3160
MAIN3170
MAIN3180
MAIN3190
MAIN3200
MAIN3210
MAIN3220
MAIN3230
MAIN3240
MAIN3250
MAIN3260
MAIN3270
MAIN3280
MPRE 11
MPRE 21
MPRE 31
MPRE 41
MPRE 51
MPRE 61
MPRE 71
MPRE 81
MPRE 91
MPRE 101
MPRE 111
MPRE 121
MPRE 131
MPRE 141
MPRE 151
MPRE 161

```

```

1 *(1.0-P(I)/(1.92*AFEP(I)))
  IF(R1-GT.R2) R1=R2
  IF(R1-GT.1.0) R1=1.0
  IF(KI(J1).GT.0) GO TO 20
  RED(J1)=R1
  IF(KI(J2).GT.0) GO TO 50
  RED(J2)=R1
  GO TO 50
48 CONTINUE
  IF(KI(J1).EQ.0) RED(J1)=1.0
  IF(KI(J2).EQ.0) RED(J2)=1.0
50 CONTINUE
  RETURN
END
SUBROUTINE INWORK(XG,YG,LC,DT,IHV,VMASS,TMASS,NPV,NP,NPS,NPR,
1 XGT,YGT,IREDK2,N5)
  COMMON/MAFDE/XSTT(3010),AHHA,IERQK
  COMMON/MANECA/ DX(50),BMDM(80),ALMPP(80),
1 KI(80),VALMP(40),XT(20),XTT(20),DR(20),
2 UDT,PVAL,JJ,NCGND
  COMMON/WORK/EIE,BPRC,ALONG,XGTPI,YGTPI,BPT,AVEXGT,CEIE,AVEYGT
  COMMON/SAVMDM/ ISUPRT(9),AVEMDM,NSUPRT,NGM,IGIRD(40),AVEBEL,JS
  COMMON/WHAT/IELPL,IPDE,IVA,IDAM,IPLPR
  COMMON/UPDOWN/ YSTT(3010),AVVA,BVVB,VGF
  COMMON/JUNK/ ATOT(8110)
  COMMON/PCLOD/ PC(20),LPC
  DIMENSION VK2(20,20)
  DOUBLE PRECISION DT,DX
  INPUT ENERGY DUE TO CONCENTRATED LOADS
  IF(LPC.EQ.0) GO TO 81
  DO 4326 I=1,NPS
    J=I+NPR
    EIE=EIE + PC(I)*DX(J)/2.0
4326 IF(IERQK.EQ.0) RETURN
    81 CONTINUE
    IF(LC.EQ.0) STOP
    XGPI=0.0
    YGPI=0.0
    YGTPI=0.0
    IF(LC.EQ.1) GO TO 6083
    INPUT ENERGY BASED ON HORIZONTAL FORCE ON TOP FLOOR
    EIE=EIE + (XSTT(IERQK+1) + XSTT(IERQK))*DX(NP)/2.0
    GO TO 6084
6083 CONTINUE
    INPUT ENERGY BASED ON EARTHQUAKE LOADING IN HORIZONTAL DIRECTION
    XGPI=XGT + (XSTT(IERQK)+XSTT(IERQK+1))*DT/2.0
    AVEYGT=(XGT+YGPI)/2.0

```

```

MPRE 171
MPRE 181
MPRE 191
MPRE 201
MPRE 211
MPRE 221
MPRE 231
MPRE 241
MPRE 251
MPRE 261
MPRE 271
MPRE 281
MPRE 291
MPRE 301
INWO 111
INWO 121
INWO 131
INWO 141
INWO 151
INWO 161
INWO 171
INWO 181
INWO 191
INWO 201
INWO 211
INWO 221
INWO 231
INWO 241
INWO 251
INWO 261
INWO 271
INWO 281
INWO 291
INWO 301

```

```

XGPI=XG+DT*XGT+DT*DT*(2.0*XSTT(IERQK)+XSTT(IERQK+1))/6.0
EIE=EIE+AVEVOM*(XGPI-XG)/ALONG
6084 IF(IHV.EQ.1) GO TO 6087
C INPUT ENERGY BASED ON VARIABLE VERTICAL G-LOAD
YGTPI=YGT + (YSTT(IERQK)+YSTT(IERQK+1))*DT/2.0
AVEYGT=(YGT+YGTPI)/2.0
YGPI=YG+DT*YGT+DT*DT*(YSTT(IERQK)+YSTT(IERQK+1))/4.0
IF(NPV.NE.0) GO TO 4105
EIE=EIE+TMASS*(YSTT(IERQK)+YSTT(IERQK+1))/2.0*(YGPI-YG)
GO TO 6087
4105 CONTINUE
DYGL=DT*YGT + DT*DT*(2.0*YSTT(IERQK)+YSTT(IERQK+1))/6.0
EIE=EIE + AVEBEL*DYGL + (TMASS-VMASS)*(YSTT(IERQK)+YSTT(IERQK+1))
1*(YGPI-YG)/2.0
6087 CONTINUE
IF(NPV.EQ.0) GO TO 6089
C INPUT ENERGY DUE TO CONCENTRATED LOADS ON GIRDERS.
DO 6088 I=1,NPV
J=I+NPR
EIE=EIE + PC(I)*(DX(J) + YGPI - YG)
6088 CONTINUE
IF(IPDE.EQ.0) GO TO 620
IF(IREDK2.EQ.0) GO TO 609
K=N5
DO 605 I=1,NPS
DO 605 J=1,NPS
VK2(I,J)=AIDZ(K)
605 K=K+1
609 CONTINUE
C INPUT ENERGY DUE TO P-DELTA EFFECT
AVER=-(YSTT(IERQK) + YSTT(IERQK+1))/2.0
DO 610 I=1,NPS
ADELX=DX(I+NPR) + XGPI - XG
DO 610 J=1,NPS
K=J+NPR
610 EIE=EIE + VK2(I,J)*(X(K)-.5*DX(K))*(AVER+32.2*VGF)*ADELX
620 CONTINUE
XG=XGPI
XGT=XGTPI
YG=YGPI
YGT=YGTPI
RETURN
END
SUBROUTINE MAXTOR(NP,NPR,NPS,NEM,N1,N2,N3,N4,N5,N6,N7,N8,N9)
C ALLOCATION OF VECTOR STORAGE
N1=1
N2=N1 + NEM*NP

```

```

INWO 311
INWO 321
INWO 331
INWO 341
INWO 351
INWO 361
INWO 371
INWO 381
INWO 391
INWO 401
INWO 411
INWO 421
INWO 431
INWO 441
INWO 451
INWO 461
INWO 471
INWO 481
INWO 491
INWO 501
INWO 511
INWO 521
INWO 531
INWO 541
INWO 551
INWO 561
INWO 571
INWO 581
INWO 591
INWO 601
INWO 611
INWO 621
INWO 631
INWO 641
INWO 651
INWO 661
INWO 671
INWO 681
INWO 691
INWO 701
INWO 711
MAXI
MAXI
MAXI

```



```

N3=N2 + NPR*NPR
N4=N3 + NPR*NPS
N5=N4 + NPS*NPS
N6=N5 + NPS*NPS
N7=N6 + NPS*NPS
N8=N7 + NPR*NPS
N9=N8 + NPS*NPS
N10=N9 + NPS*NPS
MAX=8110
IF(N10.LT.MAX) GO TO 6000
PRINT 6011, N10, MAX
FORMAT(//75X,'STORAGE REQUIREMENT EXCEEDS MAXIMUM',/7X,
1      'STORAGE NEEDED FOR THIS JOB=',I5,/7X,
2      ', MAXIMUM STORAGE POSSIBLE =',I5)
STOP
CONTINUE
RETURN
END
SUBROUTINE DAMP(I,AA,BB,AL,AO)
IF(I.EQ.O) GO TO 4
AO=AO*6.28319
GO TO (1,2,3), I
1 AA=2.O*AL*AO
BB=O.O
GO TO 5
2 AA=O.O
BB=2.O*AL/AO
GO TO 5
3 AA=AL*AO
BB=AL/AO
GO TO 5
4 CONTINUE
A=O.O
B=O.O
5 CONTINUE
RETURN
END
SUBROUTINE CAPLS(KPU,K1,K2,K3,K4,KEN,NPS,TMASS,DPL,N)
COMMON/MAXMIN/XMAX(20),XMIN(20),BMAX(80),BMIN(80),ACCMAX(20),
1 ACCOMIN(20),RELMAX(10),RELD(10)
COMMON/WORK/EIE,BPRC,ALONG,XGTP1,YGTP1,BPT,AVEXGT,CEIE,AVEYGT
COMMON/LOST/CMDOP(80),DSE(80),TDSE,EDD
COMMON/PLOUT/XIO(3010),EINPUT(3010),DENSI(3010),DEND(3010)
COMMON/WHAT/IELPL,IPDE,IWA,IDAM,IPLPR
COMMON/FONECA/DI,T,I,DXGM(20),JN,KJ
DOUBLE PRECISION DI,T
GO TO (1,2),N
1 CONTINUE

```

```

C THE FOLLOWING DATA TO BE PUNCHED OR PLOTTED
IF(KPU.EQ.0) GO TO 84
IF(K1.EQ.0) GO TO 6090
X10(KEN)=DPL
CONTINUE
EINPUT(KEN)=EIE
IF(IEPL.EQ.0) GO TO 777
DENS(KEN)=TDSE
CONTINUE
IF(ICAM.EQ.0) GO TO 778
DEND(KEN)=EDD
CONTINUE
GO TO 788
2 CONTINUE
KPU=KPU+1
GO TO 1788,5990,5989,KPU
CALL PENPOS('OSTER, KENNETH B.',17,0)
5989 CONTINUE
5990 IF(K1.LT.4) GO TO 6093
PUNCH 2222,{X10(I),I=1,KEN}
CONTINUE
6093 IF(K2.LT.4) GO TO 6095
PUNCH 2222,{EINPUT(I),I=1,KEN}
CONTINUE
6095 IF(K3.LT.4) GO TO 6097
PUNCH 2222,{DENS(I),I=1,KEN}
CONTINUE
6097 IF(K4.LT.4) GO TO 6099
PUNCH 2222,{DEND(I),I=1,KEN}
CONTINUE
6099 IF(K1.EQ.0) GO TO 6101
IF(K1.GT.3) K1=K1-3
IF(K1.GT.1) GO TO 6101
CALL SPLIT(XMAX,XMIN,KEN,I,NPS)
CONTINUE
6101 IF(K2.EQ.0) GO TO 6102
IF(K2.GT.3) K2=K2-3
IF(K2.EQ.4) GO TO 6102
CALL EPLIT(K2,IMASS,KEN,I,1)
CONTINUE
6102 IF(K3.EQ.0) GO TO 6103
IF(K3.GT.3) K3=K3-3
IF(K3.EQ.4) GO TO 6103
CALL EPLIT(K3,IMASS,KEN,I,2)
CONTINUE
6103 IF(K4.EQ.0) GO TO 6104
IF(K4.GT.3) K4=K4-3

```

```

IF(K4.EQ.4) GO TO 6104
CALL EPLOT(K4,IMASS,KEN,T,3)
CONTINUE
CALL LSTPLT
CONTINUE
FORMAT (8E10.3)
RETURN
END
SUBROUTINE CONDIT(NCOND,LC,MP,PVAL,NMBM)
COMMON/WHAT/IELPL,IPDE,IVA,IDAM,IPLPR
PRINT 475
FORMAT(//5X,'CONDITIONS OF ANALYSIS')
IF(IELPL) 302,301,302
PRINT 2034
301 FORMAT(/8X,'OUTPUT RESPONSE BASED ON LINEAR CONDITION')
2034 GO TO 303
302 PRINT 2035,PVAL
2035 FORMAT(/8X,'OUTPUT RESPONSE BASED ON BILINEAR CONDITION (P= ',F6.
14. ,)
CONTINUE
NC=NCOND+1
GO TO(480,481,482),NC
480 PRINT 580
580 FORMAT(/8X,'ELASTIC RANGE OF END MOMENTS = 2*PLASTIC MOMENT OF MEM
BER. ')
GO TO 483
PRINT 581
581 FORMAT(/8X,'INDEPENDENT VALUES FOR + AND - PLASTIC MOMENT')
GO TO 483
482 PRINT 582
582 FORMAT(/8X,'PLASTIC MOMENT OF A MEMBER REMAINS CONSTANT')
483 CONTINUE
IF(IPDE) 305,304,305
304 PRINT 2036
2036 FORMAT(/8X,'NO P-DELTA EFFECT')
GO TO 306
305 PRINT 2037
2037 FORMAT(/8X,'P-DELTA EFFECT INCLUDED')
306 CONTINUE
IF(IVA) 308,307,308
307 PRINT 2038
2038 FORMAT(/8X,'NO VARIABLE VERTICAL G-LOADING')
GO TO 309
308 PRINT 2039
2039 FORMAT(/8X,'VERTICAL VARIABLE G-LOADING INCLUDED')
309 CONTINUE
IF(MP) 485,484,485
484 PRINT 584

```

```

CAPL 581
CAPL 591
CAPL 601
CAPL 611
CAPL 621
CAPL 631
CAPL 641
CAPL 65
COND 111
COND 211
COND 311
COND 411
COND 511
COND 611
COND 711
COND 811
COND 911
COND 1011
COND 1111
COND 1211
COND 1311
COND 1411
COND 1511
COND 1611
COND 1711
COND 1811
COND 1911
COND 2011
COND 2111
COND 2211
COND 2311
COND 2411
COND 2511
COND 2611
COND 2711
COND 2811
COND 2911
COND 3011
COND 3111
COND 3211
COND 3311
COND 3411
COND 3511
COND 3611
COND 3711
COND 3811
COND 391

```

```

584  FORMAT(/8X,'REDUCTION OF THE PLASTIC MOMENT VALUES FOR COLUMN MEMB
      LERS DUE TO AXIAL COMPRESSION NOT CONSIDERED.')
```

401
411
421
431
441
451
461
471
481
491
501
511
521
531
541
551
561
571
581
591
601
611
621
631
641
651
661
671

```

      GO TO 486
485  PRINT 585
585  FORMAT(/8X,'REDUCTION IS MADE IN THE COLUMN PLASTIC MOMENT VALUES
      DUE TO AXIAL COMPRESSION.')
```

401
411
421
431
441
451
461
471
481
491
501
511
521
531
541
551
561
571
581
591
601
611
621
631
641
651
661
671

```

486  CONTINUE
315  IF(NMBM) 325,320,315
      CONTINUE
316  GO TO (316,317),NMBM
317  PRINT 2041
2041  FORMAT(/8X,'A BETA VALUE OF 1/12 IS USED IN NEWMARKS INTEGRATION
      *TECHNIQUE.')
```

401
411
421
431
441
451
461
471
481
491
501
511
521
531
541
551
561
571
581
591
601
611
621
631
641
651
661
671

```

      GO TO 330
317  PRINT 2042
2042  FORMAT(/8X,'A BETA VALUE OF 1/4 IS USED IN NEWMARKS INTEGRATION
      *TECHNIQUE.')
```

401
411
421
431
441
451
461
471
481
491
501
511
521
531
541
551
561
571
581
591
601
611
621
631
641
651
661
671

```

      GO TO 330
320  PRINT 2043
2043  FORMAT(/8X,'THE LINEAR ACCELERATION TECHNIQUE (BETA=1/6) IS USED
      *FOR INTEGRATION.')
```

401
411
421
431
441
451
461
471
481
491
501
511
521
531
541
551
561
571
581
591
601
611
621
631
641
651
661
671

```

      GO TO 330
325  PRINT 2044
2044  FORMAT(/8X,'BETA VALUE NOT CORRECTLY SPECIFIED.  JOB TERMINATED.')
```

401
411
421
431
441
451
461
471
481
491
501
511
521
531
541
551
561
571
581
591
601
611
621
631
641
651
661
671

```

      STOP
330  CONTINUE
      RETURN
END
SUBROUTINE MAXIMA (NP,NPR, TXMAX, TXMIN, TEIE, NPV, EIE MAX, NEM)
COMMON/ MANECA/ DX(50), BMDM(80), ALMP(80), ALMPN(80),
1  KI(80), VALMP(40), XT(20), XTI(20), DR(20),
2  UDI, PVAL, JJ, NCOND
COMMON/ MAXMIN/ XMAX(20), XMIN(20), BMAX(80), BMIN(80), ACCMAX(20),
1  ACCMIN(20), RELMAX(10), RFLD(10)
COMMON/ FONECA/ DT, T, DXGM(20), JN, KJ
COMMON/ WORK/ EIE, BPRC, ALONG, XGTPI, YGTPI, BPT, AVEXGT, CEIE, AVEYGT
DOUBLE PRECISION DT, T, DX
IF(EIE.LT.EIEMAX) GO TO 2300
EIEMAX=EIE
TEIE=T
2300  CONTINUE
      NPRI=NPRI+1
      DO 95 I=NPRI,NP
        J=I-NP
        IF(X(I).LT.XMAX(J)) GO TO 93
        XMAX(J)=X(I)
        IF(I.EQ.NP) TXMAX=T
      GO TO 95
```

11
12
13
14
15
16
17
18
19
20
21
22
23
24
25
26
27
28
29
30
31
32
33
34
35
36
37
38
39
40
41
42
43
44
45
46
47
48
49
50
51
52
53
54
55
56
57
58
59
60
61
62
63
64
65
66
67
68
69
70
71
72
73
74
75
76
77
78
79
80
81
82
83
84
85
86
87
88
89
90
91
92
93
94
95
96
97
98
99

```

93  CONTINUE
   IF(X(I).GT.XMIN(J)) GO TO 95
   XMIN(J)=X(I)
   IF(I.EQ.NP) TXMIN=T
95  CONTINUE
   NPS=NP-NPR
   DO 2580 I=1,NPS
     IF(XTT(I).GT.ACCMAX(I)) ACCMAX(I)=XTT(I)
     IF(XTT(I).LT.ACCMIN(I)) ACCMIN(I)=XTT(I)
2580 CONTINUE
     DO 105 I=1,NEM
       IF(BMM(I).LT.BMAX(I)) GO TO 103
       BMAX(I)=BMM(I)
       GO TO 105
103  CONTINUE
       IF(BMM(I).GT.BMIN(I)) GO TO 105
       BMIN(I)=BMM(I)
105  CONTINUE
       NPR2=NPR + NPV + 1
       DO 2690 I=NPR2,NP
         J=I-NPR-NPV
         IF(J.EQ.1) GO TO 2680
         RFLD(J)=ABS(X(I) - X(I-1))
         GO TO 2681
2680 RFLD(J)=ABS(X(I))
2681 CONTINUE
2690 IF(RFLD(J).GT.RELMAX(J)) RELMAX(J)=RFLD(J)
      CONTINUE
      RETURN
      END
      SUBROUTINE LOADING (UDT,ND,IHV,LC)
      COMMON/UPDOWN/ YSTT(3010),AVVA,BVVB,VGF
      COMMON/MAFOE/XSTT(3010),AHHA,IERQK
      DIMENSION A(3010)
      GO TO (10,20,30,40,50),LC
10  CONTINUE
C  EARTHQUAKE LOADING
   C=32.2
   READ 1001,(A(I),I=1,ND)
1001 FORMAT(8F9.6) C=1.0
      IF(IHV.EQ.2) C=1.0
      DO 15 I=1,ND
15  A(I)=A(I)*C
      GO TO (11,12),IHV
11  PRINT 2001
2001 FORMAT(/5X,'HORIZONTAL EARTHQUAKE COMPONENT')
12  PRINT 2002

```

```

MAXI 201
MAXI 211
MAXI 221
MAXI 231
MAXI 241
MAXI 251
MAXI 261
MAXI 271
MAXI 281
MAXI 291
MAXI 301
MAXI 311
MAXI 321
MAXI 331
MAXI 341
MAXI 351
MAXI 361
MAXI 371
MAXI 381
MAXI 391
MAXI 401
MAXI 411
MAXI 421
MAXI 431
MAXI 441
MAXI 451
MAXI 461
MAXI 471
MAXI 481
MAXI 491
LOAD 11
LOAD 21
LOAD 31
LOAD 41
LOAD 51
LOAD 61
LOAD 71
LOAD 81
LOAD 91
LOAD 101
LOAD 111
LOAD 121
LOAD 131
LOAD 141
LOAD 151
LOAD 161

```

```

2002 FORMAT(8X,'PLUS VERTICAL EARTHQUAKE COMPONENT')
      GO TO 60
20 CONTINUE
C SINUSOIDAL LOADING
  READ 1002, AMEGO, AMAX, PHASE
  1002 FORMAT(7F10.0)
      GO TO(21,22), IHV
21 PRINT 2003, AMEGO, AMAX, PHASE
2003 FORMAT(/5X,'HORIZONTAL SINUSOIDAL LOAD',
1      /10X,'OMEGA=',F8.5,
2      /10X,'AMPL=',F7.2,
3      /10X,'PHASE=',F7.2)
      GO TO 23
22 PRINT 2004, AMEGO, AMAX, PHASE
2004 FORMAT(8X,'PLUS VERTICAL G',S SINUSOIDAL LOAD',
1      /10X,'CMEGA=',F8.5,
2      /10X,'AMPL=',F8.5,
3      /10X,'PHASE=',F7.2)
23 TIM=0.0
   AMEGO=AMEGO*6.2832
   PHASE=PHASE/57.2958
   DO 25 I=1,ND
     A(I)=AMAX*SIN(AMEGO*TIM + PHASE)
     TIM=I*UDT
25 CONTINUE
      GO TO 60
30 CONTINUE
C TRIANGULAR IMPULSE LOAD
  READ 1002, F1,TD
  TIM=0.0
  NDT=TD/UDT
  IF(NDT.GE.ND) GO TO 37
  DO 35 I=1,NDT
    A(I)=F1*(1.0-TIM/TD)
    TIM=I*UDT + 1
35 NDTPI=NDT + 1
   DO 36 I=NDTPI,ND
     A(I)=0.0
36 GO TO 39
37 CONTINUE
   DO 38 I=1,ND
     A(I)=F1*(1.0-TIM/TD)
38 A(I)=F1*(1.0-TIM/TD)
39 CONTINUE
      GO TO(31,32), IHV
31 PRINT 2005, F1,TD
2005 FORMAT(/5X,'HORIZONTAL TRIANGULAR IMPULSE, F1 TO ZERO IN TD SECS.',
1      /10X,'F1=',F6.2,
2      /10X,'TD=',F6.3)

```

```

LOAD 171
LOAD 181
LOAD 191

LOAD 201
LOAD 211
LOAD 221
LOAD 231
LOAD 241
LOAD 251
LOAD 261
LOAD 271
LOAD 281
LOAD 291
LOAD 301
LOAD 311
LOAD 321
LOAD 331
LOAD 341
LOAD 351
LOAD 361
LOAD 371
LOAD 381
LOAD 391
LOAD 401
LOAD 411
LOAD 421

LOAD 431
LOAD 441
LOAD 451
LOAD 461
LOAD 471
LOAD 481
LOAD 491
LOAD 501
LOAD 511
LOAD 521
LOAD 531
LOAD 541
LOAD 551
LOAD 561
LOAD 571
LOAD 581
LOAD 591
LOAD 601
LOAD 611
LOAD 621

```

```

      GO TO 60
32  PRINT 2006, F1, TD
2006 FORMAT(8X, 'PLUS VERTICAL TRIANGULAR G'S IMPULSE DOWN, F1 TO ZERO
      1 IN TO SECS', /10X, 'F1=', F6.2,
      2 /10X, 'TD=', F6.3)
40  CONTINUE
50  CONTINUE
2010 PRINT 2010
      FORMAT(/5X, 'NO LOAD TYPE APPLIED TO THIS LOADING CONDITION NUMBER
      1 YET, LC=1,2,3 ONLY',
      2 IF(LC.GT.3) STOP
60  CONTINUE
      GO TO (61,63), IHV
61  CONTINUE
      DO 62 I=1, ND
62  XSTT(I)=A(I)
      RETURN
63  CONTINUE
      DO 64 I=1, ND
64  YSTT(I)=A(I)
      RETURN
      END
      SUBROUTINE FOK2M (NPS, NPH, NPV, N5, IREDK2, INPRIN)
      COMMON/ABC/AMASS(20), AMASSI(20), XL(40)
      COMMON/WHAT/IELPL, IPDE, IVA, IDAM, IPLPR
      COMMON/JUNK/ ATQZ(8110)
      DIMENSION VK2(20,20)
      IF(IPDE.EQ.0) GO TO 670
      IF(IREDK2.EQ.0) GO TO 665
      SUM1=0.
      DO 5 I=1, NPS
      DO 5 K=1, NPS
      VK2(I,K)=0.
      IF(NPV.GT.1) GO TO 7
      VK2(K,K)=AMASS(K)/XL(1)
      GO TO 21
7  CONTINUE
      SUM1=SUM1 + AMASS(I)
      SUM2=SUM1 - AMASS(K)
      FORM MATRIX VK2(NPS,NPS)
      DO 20 J=K, NPS
      JM1=J-1
      JP1=J+1
      JJ=J-NPV
      KK=K-1

```

LOAD 631
LOAD 641
LOAD 651
LOAD 661
LOAD 671
LOAD 681
LOAD 691
LOAD 701
LOAD 711
LOAD 721
LOAD 731
LOAD 741
LOAD 751
LOAD 761
LOAD 771
LOAD 781
LOAD 791
LOAD 801
LOAD 811
LOAD 821
LOAD 831
LOAD 841
FOK2 11
FOK2 21
FOK2 31
FOK2 41
FOK2 51
FOK2 61
FOK2 71
FOK2 81
FOK2 91
FOK2 101
FOK2 111
FOK2 121
FOK2 131
FOK2 141
FOK2 151
FOK2 161
FOK2 171
FOK2 181
FOK2 191
FOK2 201
FOK2 211
FOK2 221
FOK2 231

```

10 IF(JM1.EQ.KK) GO TO 10
   VK2(I,J,JM1)=VK2(JM1,J)
   VK2(J,J)=SUM1/XL(JJ) + SUM2/XL(JJ+1)
15 IF(JP1.GT.NPS) GO TO 20
   VK2(J,J,JP1)=-SUM2/XL(JJ+1)
   CONTINUE
   SUM1=SUM2
   IF(J.EQ.NPS) GO TO 20
   SUM2=SUM2 - AMASS(J+1)
20 CONTINUE
21 IF(INPRIN.EQ.0) GO TO 40
   PRINT 2023
   FORMAT(/,5X,'P-DELTA STIFFNESS MATRIX AS FORMED IN PROGRAM, K2')
2023 DO 30 I=1,NPS
      PRINT 2022,I, (VK2(I,J),J=1,NPS)
2022 FORMAT(4H ROW,I3,1X,6E15.6/(8X,6E15.6))
30 CONTINUE
   GO TO 40
665 CONTINUE
1002 READ 1002,((VK2(I,J),J=1,NPS),I=1,NPS)
      FORMAT(7F10.0)
      ***** TO MULTIPLY A FACTOR TIMES VK2 *****
      READ 1002, CVK2
      DO 67 I=1,NPS
      DO 67 J=1,NPS
        VK2(I,J)=CVK2* VK2(I,J)
        ***** TO MULTIPLY A FACTOR TIMES VK2 *****
67 IF(INPRIN.EQ.0) GO TO 40
   PRINT 2021
   FORMAT(/,5X,'P-DELTA STIFFNESS MATRIX AS INPUT DATA, K2')
2021 DO 72 I=1,NPS
      PRINT 2022,I, (VK2(I,J),J=1,NPS)
72 CONTINUE
   GO TO 40
670 CONTINUE
   DO 673 I=1,NPS
   DO 673 J=1,NPS
     VK2(I,J)=0.0
673 CONTINUE
   K=N5
   DO 6005 I=1,NPS
   DO 6005 J=1,NPS
     AT0Z(K)=VK2(I,J)
6005 K=K+1
   RETURN
   END
   SUBROUTINE FOMASM(NPH,NPS,TMASS,VMASS,XACC,YACC,LC)

```



```

COMMON/ABC/AMASS(20),AMASSI(20),XL(40)
COMMON/MANECA/ DX(50),BMDM(80),ALMPP(80),ALMPN(80),
1 KI(80),VALMP(40),X(50),XT(20),XIT(20),DR(20),
2 UDT,PVAL,JJ,NCQND
COMMON/WHAT/IELPL,IPDE,IVA,IDAM,IPLPR
DOUBLE PRECISION DX
NPV=NPS - NPH
K=NPV+1
READ 101,(AMASS(I),I=1,NPS)
IF(NPV.EQ.0) GO TO 12
PRINT 203
FORMAT(2X,'FLOOR MASSES CONSIDERED LUMPED AT GIRDER NODES')
203 CONTINUE
12 ***** TO MULTIPLY A FACTOR TIMES AMASS(I) *****
C *****
C READ 101,CMASS
IF(CMASS.EQ.0.) CMASS=1.0
DO 15 I=1,NPS
15 AMASS(I)=AMASS(I)*CMASS
C ***** TO MULTIPLY A FACTOR TIMES AMASS(I) *****
C *****
C IF(NPV.EQ.0) GO TO 303
PRINT 301,NPV
PRINT 202,(I,AMASS(I),I=1,NPV)
301 FORMAT(5X,'GIRDER MASSES FOR FLOORS 1 THRU',I3)
303 CONTINUE
PRINT 201,NPH
PRINT 202,(I,AMASS(I),I=K,NPS)
TMASS=0.0
K=NPV+1
DO 659 I=K,NPS
659 TMASS=TMASS + AMASS(I)
VMASS=0.0
IF(NPV.EQ.0) GO TO 6086
DO 6085 I=1,NPV
6085 VMASS=VMASS + AMASS(I)
6086 CONTINUE
GO TO (6071,6072,6072,6072,6072),LC
6071 CONTINUE
IF(IVA.EQ.0) GO TO 4002
DO 4001 I=1,NPV
4001 XIT(I)=-YACC
4002 CONTINUE
DO 660 I=K,NPS
660 XIT(I)=-XACC
GO TO 6073
6072 CONTINUE
IF(IVA.EQ.0) GO TO 4004
DO 4003 I=1,NPV

```

11 FOMA
 21 FOMA
 31 FOMA
 41 FOMA
 51 FOMA
 61 FOMA
 71 FOMA
 81 FOMA
 91 FOMA
 101 FOMA
 111 FOMA
 121 FOMA
 131 FOMA

 141 FOMA
 151 FOMA
 161 FOMA
 171 FOMA

 181 FOMA
 191 FOMA
 201 FOMA
 211 FOMA
 221 FOMA
 231 FOMA
 241 FOMA
 251 FOMA
 261 FOMA
 271 FOMA
 281 FOMA
 291 FOMA
 301 FOMA
 311 FOMA
 321 FOMA
 331 FOMA
 341 FOMA
 351 FOMA
 361 FOMA
 371 FOMA
 381 FOMA
 391 FOMA
 401 FOMA
 411 FOMA
 421 FOMA
 431 FOMA
 441 FOMA
 451 FOMA

```

4003      XTT(I)=-YACC
4004      CONTINUE
6073      XTT(NPS)=XACC/AMASS(NPS)
101      CONTINUE
201      FORMAT(7F10.0)
202      FORMAT(5X,'FLOOR MASSES FOR FLOORS 1 THRU',I3)
      RETURN
END
SUBROUTINE FOSTIM (NP,NPR,NPS,N1,N2,N3,N4,NCOL,INPRIN)
COMMON/STNECA/ JC1(40),JC2(40),JC3(40),P(40),NEM
COMMON/MAST/ S(40),NTIM
COMMON/WORK/EIE,BPRC,ALONG,XGTP1,YGTP1,BPT,AVEXGT,CEIE,AVEYGT
COMMON/ARCC/AMASS(20),AMASSI(20),XL(40)
COMMON/FAFEP/AFAP(20),AFEP(20),RED(80),ICOL(20),PY(20),MP
COMMON/JUNK/ ATQZ(8110)
DIMENSION AM(30,80),AV(20,80)
DIMENSION BSAT(80,50),SKI(30,30),SK2(30,20),SK3(20,20)
DIMENSION XI(40)
*****
STIFFNESS MATRIX
*****
NM=NEM/2
IF(NTIM.GT.0) GO TO 13
IF(NPR.EQ.0) GO TO 912
INITIALIZE AM(I,J) AND READ IN DATA. (BLANK CARD GOES AFTER DATA)
DO 201 I=1,NPR
DO 201 J=1,NEM
AM(I,J)=0.
201 AM(I,J)=0.
C *****
205 READ 202,I,J,AIJ,N1,IADD,JADD
202 FORMAT(2I5,F10.0,3I5)
203 IF(I) 204,204,203
CONTINUE
IF(N1.GT.0) GO TO 401
NI=1
401 DO 403 KZ=1,NI
AM(I,J)=AIJ
I=I+IADD
J=J+JADD
403 GO TO 205
204 CONTINUE
PRINT 104
104 FORMAT(/,' THE MATRIX AM---LOCATIONS NOT SHOWN ARE ZERO')
DO 911 I=1,NPR
KA=0
K8=0
DO 902 J=1,NEM

```

FOMA 461
FOMA 471
FOMA 481
FOMA 491
FOMA 501
FOMA 511
FOMA 521
FOMA 531
FOMA 541
FOST 111
FOST 211
FOST 311
FOST 411
FOST 511
FOST 611
FOST 711
FOST 811
FOST 911

FOST 101
FOST 111
FOST 121

FOST 131
FOST 141
FOST 151

FOST 161
FOST 171
FOST 181
FOST 191
FOST 201
FOST 211
FOST 221
FOST 231
FOST 241
FOST 251
FOST 261
FOST 271
FOST 281
FOST 291
FOST 301
FOST 311
FOST 321
FOST 331

```

          IF (AM(I,J).LT.1.) GO TO 902
          IF (KA.NE.0) GO TO 901
          KA=J
          KB=J
          901 CONTINUE
          902 PRINT 106, I,KA,KB,(AM(I,J),J=KA,KB)
          106 FORMAT(4H ROW,I3,5H COLS,I3,5H THRU,I3,1X,25F4.0/(24X,25F4.0))
          911 CONTINUE
          912 CONTINUE
          INITIALIZE AV(I,J) AND READ IN DATA. (BLANK CARD GOES AFTER DATA)
          DO 515 I=1,NPS
          DO 515 J=1,NEM
          515 AV(I,J)=0.
          *****
          C 517 READ 202,I,J,ARZ,NI,IADD,JADD
          521 IF(I) 519,519,521
          CONTINUE
          IF(NI.GT.0) GO TO 411
          NI=1
          411 DO 413 KZ=1,NI
          AV(I,J)=ARZ
          I=I+IADD
          413 J=J+JADD
          GO TO 517
          519 PRINT 716
          716 FORMAT(/, ' THE MATRIX AV---LOCATIONS NOT SHOWN ARE ZERO.')
          DO 931 I=1,NPS
          KA=0
          KB=0
          DO 922 J=1,NEM
          IF (AV(I,J).LT.1.) AND .AV(I,J).GT.-1.) GO TO 922
          IF (KA.NE.0) GO TO 921
          KA=J
          KB=J
          921 CONTINUE
          922 PRINT 106, I,KA,KB,(AV(I,J),J=KA,KB)
          931 CONTINUE
          *****
          C READ 4102, E,FY
          *****
          C 4102 FORMAT(2F10.0,2I5)
          102 READ 102,(XI(I),I=1,NM)
          FORMAT(7F10.4)
          *****
          C READ 102, (XL(I),I=1,NM)
          ALONG=XL(1)
          *****
          C IF (MP.LE.0) GO TO 4010

```

```

FOST 341
FOST 351
FOST 361
FOST 371
FOST 381
FOST 391
FOST 401
FOST 411
FOST 421
FOST 431
FOST 441
FOST 451
FOST 461
FOST 471
FOST 481
FOST 491
FOST 501
FOST 511
FOST 521
FOST 531
FOST 541
FOST 551
FOST 561
FOST 571
FOST 581
FOST 591
FOST 601
FOST 611
FOST 621
FOST 631
FOST 641
FOST 651
FOST 661
FOST 671
FOST 681
FOST 691
FOST 701
FOST 711
FOST 721
FOST 731
FOST 741
FOST 751

```

```

333 PRINT 333, E, FY
    FORMAT(/8X, 'E=', E9.2, 6X, 'FY=', F9.2)
    CALL ALLOW(NCOL, E, FY)
    GO TO 4011
4010 PRINT 4333, E
4333 FORMAT(/8X, 'E=', E9.2)
4011 CONTINUE
    C WHERE E IS IN KIP/SQ. IN., XL IN FT., XI IN IN.4
    XM IN KIP-SEC2/FT.
    DO 516 I=1, NM
    516 S(I)=E*XI(I)/(XL(I)*144.)
    PRINT 11
    11 FORMAT(/, ' THE STIFFNESS OF MEMBERS')
    12 PRINT 12, (I, S(I), I=1, NM)
    13 FORMAT(5(5X, I3, 1PE16.7))
    CONTINUE
    IF(NPR.EQ.0) GO TO 16
    NM=NEM/2
    DO 112 I=1, NPR
    DO 112 J=1, NPR
    SK1(I, J)=0.
    DO 15 K=1, NM
    L=2*K-1
    M=2*K
    15 SK1(I, J)=SK1(I, J)+P(K)*AM(I, L)*(4.*S(K)*AM(J, L)+2.*S(K)*AM(J, M))
    +P(K)*AM(I, M)*(2.*S(K)*AM(J, L)+4.*S(K)*AM(J, M))
    +(1.-P(K))*AM(I, L)*3.*S(K)*AM(J, L)*JC1(K)
    +(1.-P(K))*AM(I, M)*3.*S(K)*AM(J, M)*JC2(K)
    112 CONTINUE
    N=NPR+1
    DO 114 I=1, NPR
    DO 114 J=1, NPS
    JJ=J
    SK2(I, J)=0.
    DO 114 K=1, NM
    L=2*K-1
    M=2*K
    114 SK2(I, J)=SK2(I, J)
    +P(K)*AM(I, L)*(-6.*S(K)/XL(K))*AM(JJ, L)+AV(JJ, M))
    +P(K)*AM(I, M)*(-6.*S(K)/XL(K))*AM(JJ, L)+AV(JJ, M))
    3+{(1.-P(K))*AM(I, L)*(-3.*S(K)/XL(K))*AM(JJ, L)+AV(JJ, M))*JC1(K)
    4+{(1.-P(K))*AM(I, M)*(-3.*S(K)/XL(K))*AM(JJ, L)+AV(JJ, M))*JC2(K)
    16 CONTINUE
    DO 117 I=1, NPS
    III=I
    DO 117 J=1, NPS
    JJ=J
    SK3(I, J)=0.

```

FOST 761
FOST 771
FOST 781
FOST 791
FOST 801
FOST 811
FOST 821

FOST 831
FOST 841
FOST 851
FOST 861
FOST 871
FOST 881
FOST 891
FOST 901
FOST 911
FOST 921
FOST 931
FOST 941
FOST 951
FOST 961
FOST 971
FOST 981
FOST 991
FOST 1001
FOST 1011
FOST 1021
FOST 1031
FOST 1041
FOST 1051
FOST 1061
FOST 1071
FOST 1081
FOST 1091
FOST 1101
FOST 1111
FOST 1121
FOST 1131
FOST 1141
FOST 1151
FOST 1161
FOST 1171
FOST 1181
FOST 1191
FOST 1201
FOST 1211

```

118 DD 118 K=1,NM
L=2*K-1
M=2*K
118 SK3(I,J)=SK3(I,J)+P(K)*AV(III,L)*12.*S(K)/(XL(K)**2)*(AV(JJ,L)+
1AV(JJ,M)))+(1.-P(K))*AV(III,L)*3.*S(K)/(XL(K)**2)*(AV(JJ,L)+AV(JJ,M)
2))*JJC3(K)+P(K)*AV(III,M)*12.*S(K)/(XL(K)**2)*(AV(JJ,L)+AV(JJ,M))*JJC3(K)
3+{(1.-P(K))*AV(III,M)*3.*S(K)/(XL(K)**2)*(AV(JJ,L)+AV(JJ,M))*JJC3(K)
117 CONTINUE
C *****
C COEFFICIENTS FOR INTERNAL MOMENTS IN TERMS OF EXTERNAL DISPL. *****
C IF(NPR.EQ.0) GO TO 18 *****
DO 212 K=1,NM *****
DO 212 J=1,NPR *****
L=2*K-1 *****
M=2*K *****
BSAT(L,J)={4.*S(K)*AM(J,L)+2.*S(K)*AM(J,M))*P(K)
1+(1.-P(K))*3.*S(K)*AM(J,L)*JJC1(K)
BSAT(M,J)={2.*S(K)*AM(J,L)+4.*S(K)*AM(J,M))*P(K)
1+(1.-P(K))*3.*S(K)*AM(J,M)*JJC2(K)
212 CONTINUE
18 CONTINUE
N=NPR+1
DO 213 K=1,NM
DO 213 J=N,NP
JJ=J-NPR
L=2*K-1
M=2*K
BSAT(L,J)={-6.*S(K)/XL(K))*{(AV(JJ,L)+AV(JJ,M))*P(K)
1+(1.-P(K))*(-3.*S(K)/XL(K))*{(AV(JJ,L)+AV(JJ,M))*JJC1(K)
BSAT(M,J)={-6.*S(K)/XL(K))*{(AV(JJ,L)+AV(JJ,M))*P(K)
1+(1.-P(K))*(-3.*S(K)/XL(K))*{(AV(JJ,L)+AV(JJ,M))*JJC2(K)
213 CONTINUE
C THE FOLLOWING CARD CAUSES SKIP OF PRINT OF MOM. TO DEFL. RELAT.
C IF(NTIM.GE.1) GO TO 17
C IF(INPRIN.EQ.0) GO TO 17
PRINT 2002
FORMAT(2X,'END MOMENTS TO DISPLACEMENT RELATIONSHIP,')
DO 119 I=1,NEM
119 PRINT 702, I, (BSAT(I,J),J=1,NP)
702 FORMAT(4H ROW,I3,I3,10E12.4/(8X,10E12.4))
17 CONTINUE
NTIM=NTIM+1
K=N1
DO 6001 I=1,NEM
6001 DO 6001 J=1,NP
AT0Z(K)=BSAT(I,J)
K=K+1

```

FOST11221
FOST11231
FOST11241
FOST11251
FOST11261
FOST11271
FOST11281
FOST11291

FOST11301
FOST11311
FOST11321
FOST11331
FOST11341
FOST11351
FOST11361
FOST11371
FOST11381
FOST11391
FOST11401
FOST11411
FOST11421
FOST11431
FOST11441
FOST11451
FOST11461
FOST11471
FOST11481
FOST11491
FOST11501
FOST11511

FOST11521
FOST11531
FOST11541
FOST11551
FOST11561
FOST11571
FOST11581
FOST11591
FOST11601
FOST11611
FOST11621
FOST11631
FOST11641
FOST11651

```

IF(NPR.EQ.0) GO TO 6021
K=N2
DO 6002 I=1,NPR
DO 6002 J=1,NPR
  ATOZ(K)=SKI(I,J)
6002 K=K+1
  K=N3
DO 6003 I=1,NPR
DO 6003 J=1,NPS
  ATOZ(K)=SK2(I,J)
6003 K=K+1
6021 CONTINUE
  K=N4
DO 6004 I=1,NPS
DO 6004 J=1,NPS
  ATOZ(K)=SK3(I,J)
6004 K=K+1
  RETURN
END
SUBROUTINE FOFOME (NPS,NPV,LC,MULF)
COMMON/MAFOE/XSTT(3010),AHHA,IERQK
COMMON/UPDOWN/ YSTT(3010),AVVA,8VVB,VGF
COMMON/ABC/AMASS(20),AMASSI(20),XL(40)
COMMON/FONECA/ DT,I,DF(20),JN,KJ
DOUBLE PRECISION DT,I
DO 10 I=1,NPS
  DF(I)=0.0
  IERQK=IERQK + 1
  AHHA=XSTT(IERQK+1)
  K=NPV+1
  IF (LC.GT.1) GO TO 25
  DO 20 I=K,NPS
    DF(I)=-AMASS(I)*(XSTT(IERQK+1)-XSTT(IERQK))
  20 GO TO 30
  25 DF(NPS)=XSTT(IERQK+1) - XSTT(IERQK)
  30 CONTINUE
  IF(MULF.EQ.0) GO TO 33
  AVVA=-YSTT(IERQK+1)
  BVVB=-YSTT(IERQK+1) + YSTT(IERQK)
  IF(NPV.EQ.0) RETURN
  DO 32 I=1,NPV
    DF(I)=AMASS(I)*BVVB
  32 CONTINUE
  33 RETURN
END
SUBROUTINE PRIMAX (TXMAX,TXMIN,EIEMAX,TEIE,KEN,NPS,NPH,NEM)
COMMON/MAXMIN/XMAX(20),XMIN(20),BMAX(80),BMIN(80),ACCMAX(20),
  LACCMIN(20),RELMAX(10),RELD(10)

```

```

FOSTI1661
FOSTI1671
FOSTI1681
FOSTI1691
FOSTI1701
FOSTI1711
FOSTI1721
FOSTI1731
FOSTI1741
FOSTI1751
FOSTI1761
FOSTI1771
FOSTI1781
FOSTI1791
FOSTI1801
FOSTI1811
FOSTI1821
FOSTI1831
FOSTI1841
FOFO 1
FOFO 11
FOFO 21
FOFO 31
FOFO 41
FOFO 51
FOFO 61
FOFO 71
FOFO 81
FOFO 91
FOFO 101
FOFO 111
FOFO 121
FOFO 131
FOFO 141
FOFO 151
FOFO 161
FOFO 171
FOFO 181
FOFO 191
FOFO 201
FOFO 211
FOFO 221
FOFO 231
FOFO 241
FOFO 251
PRIM 11
PRIM 21
PRIM 31

```

```

COMMON/WORK/EIE,BPRC,ALONG,XGTPI,YGTPI,BPT,AVEXGT,CEIE,AVEYGT
COMMON/WHAT/IELPL,IPDE,IVA,IDAM,IPLPR
COMMON/GUTS/PBMDM(80),DMOM(80),BAVE(80),DUCMAX(240),EXCUR(240),
* BLSE
COMMON/FCNECA/DT,T,DXGM(20),JN,KJ
DOUBLE PRECISION T,DT
PRINT 2014, TXMAX, TXMIN, T
2014 FORMAT(//6X, 'MAXIMUM POSITIVE AND NEGATIVE DISPL. (NPV+NPH)',
1 /8X, '(MAX. TOP FLOOR DISPL. OCCUR AT', F7.3, ' SEC. AND', F7.3,
2 SEC. RESPECTIVELY.', F5.2)
PRINT 2020, (1,XMAX(I),XMIN(I),I=1,NPS)
2020 FORMAT(4(2X,I3,2E13.4))
PRINT 2316
2316 FORMAT(//6X, 'MAXIMUM RELATIVE FLOOR DISPLACEMENTS')
PRINT 2011, (1,RELMAX(I),I=1,NPH)
PRINT 2585, T
2585 FORMAT(//6X, 'MAXIMUM POSITIVE AND NEGATIVE ACCELERATIONS DURING F
1 FIRST', F5.2, ' SECONDS', /)
PRINT 2020, (1,ACCMAX(I),ACCMIN(I),I=1,NPS)
PRINT 2100, T
2100 FORMAT(//6X, 'MAXIMUM POSITIVE AND NEGATIVE END MOMENTS DURING FIR
1 ST', F5.2, ' SECONDS', /)
PRINT 2020, (1,BMAX(I),BMIN(I),I=1,NEM)
PRINT 2301, EIEMAX, TEIE
2301 FORMAT(//6X, 'THE MAXIMUM INPUT ENERGY FOR THIS JOB IS', E13.6,
1 /, ' FOUND PRESENT AT TIME', F7.3)
IF(IELPL.EQ.0) GO TO 91
PRINT 2501
2501 FORMAT(//6X, 'DUCTILITY AND EXCURSION RATIOS BASED'
1 /, ' ON ENERGY')
PRINT 2227
2227 FORMAT(//6X, 'MAXIMUM DUCTILITY RATIOS FOR EACH',
1 /, ' END OF MEMBERS', /)
PRINT 2011, (1,DUCMAX(I),I=1,NEM)
PRINT 2226
2226 FORMAT(//6X, 'EXCURSION RATIOS FOR EACH END OF '
1 /, ' MEMBERS', /)
PRINT 2011, (1,EXCUR(I),I=1,NEM)
2011 FORMAT(8X,I3,E13.4,2X,I3,E13.4,2X,I3,E13.4,2X,I3,E13.4,
1 2X,I3,E13.4,2X,I3,E13.4)
PRINT 2502
2502 FORMAT(//6X, 'DUCTILITY AND EXCURSION RATIOS '
1 /, ' BASED ON CURVATURE')
PRINT 2227
DO 10 I=1, NEM
K=I+NEM
DUCMAX(I)=DUCMAX(K)
EXCUR(I)=EXCUR(K)
10

```

PRIM 31
 PRIM 41
 PRIM 51
 PRIM 61
 PRIM 71
 PRIM 81
 PRIM 91
 PRIM 101
 PRIM 111
 PRIM 121
 PRIM 131
 PRIM 141
 PRIM 151
 PRIM 161
 PRIM 171
 PRIM 181
 PRIM 191
 PRIM 201
 PRIM 211
 PRIM 221
 PRIM 231
 PRIM 241
 PRIM 251
 PRIM 261
 PRIM 271
 PRIM 281
 PRIM 291
 PRIM 301
 PRIM 311
 PRIM 321
 PRIM 331
 PRIM 341
 PRIM 351
 PRIM 361
 PRIM 371
 PRIM 381
 PRIM 391
 PRIM 401
 PRIM 411
 PRIM 421
 PRIM 431
 PRIM 441
 PRIM 451
 PRIM 461
 PRIM 471
 PRIM 481
 PRIM 491
 PRIM 501

```

COMMON/JUNK/ ATOZ(8110)
DIMENSION A(20,20),U(20,20),Y(20),B(20),X(20)
DOUBLE PRECISION X
K=N8
DO 6008 I=1,N
DO 6008 J=1,N
A(I,J)=ATOZ(K)
6008 K=K+1
IF(N.EQ.1) GO TO 65
IF((I+J).EQ.0).AND.((J+J.GT.0)) GO TO 28
UPPER TRIANGULAR MATRIX *****
DO 25 J=1,N
DO 25 I=1,N
SUM=0.0
IF(I-J) 5,15,24
5 CONTINUE
8 IF(I-1) 10,8,10
10 GO TO 25
10 I=I-1
DO 12 K=1,IM1
SUM=SUM + U(K,I)*U(K,J)
12 U(I,J)=(A(I,J)-SUM)/U(I,I)
GO TO 25
15 CONTINUE
17 IF(I-1) 20,17,20
17 U(I,I)=SORT(A(I,I))
GO TO 25
20 I=I-1
DO 22 K=1,IM1
SUM=SUM + U(K,I)*U(K,I)
22 U(I,I)=SORT(A(I,I)-SUM)
GO TO 25
24 CONTINUE
25 U(I,J)=0.0
CONTINUE
K=N9
DO 6010 I=1,N
DO 6010 J=1,N
ATOZ(K)=U(I,J)
6010 K=K+1
GO TO 29
28 CONTINUE
K=N9
DO 6009 I=1,N
DO 6009 J=1,N
U(I,J)=ATOZ(K)
6009 K=K+1

```

```

DECO 211
DECO 311
DECO 411
DECO 511
DECO 611
DECO 711
DECO 811
DECO 911
DECO 1011
DECO 111
DECO 1211
DECO 1311
DECO 1411
DECO 1511
DECO 1611
DECO 1711
DECO 1811
DECO 1911
DECO 2011
DECO 2111
DECO 2211
DECO 2311
DECO 2411
DECO 2511
DECO 2611
DECO 2711
DECO 2811
DECO 2911
DECO 3011
DECO 3111
DECO 3211
DECO 3311
DECO 3411
DECO 3511
DECO 3611
DECO 3711
DECO 3811
DECO 3911
DECO 4011
DECO 4111
DECO 4211
DECO 4311
DECO 4411
DECO 4511
DECO 4611
DECO 4711
DECO 4811

```



```

C      29  CONTINUE SUBSTITUTION *****
      Y(I)=B(I)/U(I,1)
      DO 35 I=2,N
      SUM=0.0
      IM1=I-1
      DO 30 K=1,IM1
      SUM=SUM+U(K,I)*Y(K)
      30 Y(I)=(B(I)-SUM)/U(I,1)
      35 BACKWARD SUBSTITUTION *****
      I=N
      SUM=0.0
      IF(N-I) 50,55,50
      50 CONTINUE
      IPI=I+1
      DO 52 K=IPI,N
      SUM=SUM+U(I,K)*X(K)
      52 X(I)=(Y(I)-SUM)/U(I,I)
      55 I=I-1
      IF(I) 45,60,45
      60 CONTINUE
      RETURN
      65 X(I)=B(I)/ATOZ(N8)
      RETURN
      END
      SUBROUTINE ENERGY (NM,NPS,NPV,IAB,N6)
      THIS SUBROUTINE CALCULATES THE ELASTIC STRAIN ENERGY FOR
      THE ELASTIC CASE, TOTAL STRAIN ENERGY AND DISSIPATED
      ENERGY DUE TO DAMPING AND BILINEAR M-THETA RELATIONSHIPS.
      COMMON/STNECA/ JCI(40),JC2(40),JC3(40),P(40),NEM
      COMMON/DAMPNG/ AA,BB
      COMMON/MAST/ S(40),NTIM
      COMMON/MANECA/ DX(50),BMOM(80),ALMPP(80),ALMPN(80),
      1 K1(80),VALMP(40),X(50),XT(20),XTT(20),DR(20),
      2 UDT,PVAL,JJ,NCOND
      COMMON/WHAT/IELPL,IPDE,IVA,IDAM,IPLPR
      COMMON/FONECA/ DT,T,DXGM(20),JN,KJ
      COMMON/ABC/AMASS(20),AMASSI(20),XL(40)
      COMMON/CURDUC/ DELMP(80),YMOMP(80),YMQMN(80)
      COMMON/GUTS/PBMOM(80),DMOM(80),BAVE(80),DUCMAX(240),EXCJR(240),
      * BLSE
      COMMON/DUCEX/DSEAB(80),SESEAB(80),TBLSE(80),EMU(80)
      COMMON/LOST/CMDP(80),DSE(80),TDSE,EDD
      COMMON/WORK/EIE,BPRC,ALONG,XGTPI,YGTPI,BPT,AVEXGT,CEIE,AVEYGT
      COMMON/ANGLE/TROT(80),SLOPE(80),DROT(80),DVEL(20),TANG(80)
      COMMON/JUNK/ ATOZ(8110)
      DIMENSION XST(20),CMK(20,20)
      DIMENSION XT2(20)

```

DECO 491
DECO 501
DECO 511
DECO 521
DECO 531
DECO 541
DECO 551
DECO 561
DECO 571
DECO 581
DECO 591
DECO 601
DECO 611
DECO 621
DECO 631
DECO 641
DECO 651
DECO 661
DECO 671
DECO 681
DECO 691
DECO 701
DECO 711
ENER

ENER 11
ENER 21
ENER 31
ENER 41
ENER 51
ENER 61
ENER 71
ENER 81
ENER 91
ENER 101
ENER 111
ENER 121
ENER 131
ENER 141
ENER 151
ENER 161
ENER 171
ENER 181
ENER 191

C
C
C

```

DOUBLE PRECISION DT,I,DX
GO TO (1,2,3,1), IAB
1 CONTINUE
IF(S(I).NE.0.0) GO TO 30
PRC=0.0
EKE=0.0
ESE=0.0
TDSE=0.0
BLSE=0.0
EDD=0.0
TED=0.0
RETURN
2 CONTINUE
C INCREMENTAL JOINT ROTATIONS RELATIVE TO MEMBER
DO 110 I=1,NM
C1=(3.0+P(I))/(3.0*P(I))
C2=1.0/(4.0*S(I))
K=2*I-1
L=K+1
IF(JC3(I)).LT.1) GO TO 106
IF(JC2(I)).LT.1) GO TO 104
DROT(K)=(C1*DMOM(K)-2.0*DMOM(L))/3.0*C2
DROT(L)=(4.0*DMOM(L)-2.0*DMOM(K))*C2/3.0
GO TO 110
104 DROT(K)=(4.0*DMOM(K)-2.0*DMOM(L))*C2/3.0
DROT(L)=(C1*DMOM(L)-2.0*DMOM(K))/3.0*C2
GO TO 110
106 DROT(K)=(4.0*DMOM(K)-2.0*DMOM(L))*C2/(3.0*P(I))
DROT(L)=(4.0*DMOM(L)-2.0*DMOM(K))*C2/(3.0*P(I))
110 CONTINUE
C STRAIN ENERGY CALCULATIONS
DO 20 J=1,NEM
I=(J+1)/2
CMD=BAVE(J)*DROT(J)
TROT(J)=TROT(J)+DROT(J)
IF(K(I)).LT.1) GO TO 14
CMDP(J)=BAVE(J)*DROT(J)*(1.0-P(I))
SLOPE(J)=DSEAB(J)+ABS(DROT(J))
DSEAB(J)=DSEAB(J)+CMDP(J)
DSE(J)=DSE(J)+CMDP(J)
TDSE=TDSE+CMDP(J)
TANG(J)=TANG(J)+ABS(DROT(J))
14 CONTINUE
BLSE=BLSE+CMD
TBLSE(J)=TBLSE(J)+CMD
20 CONTINUE
RETURN
3 CONTINUE

```

```

2011
2211
2311
2411
2511
2611
2711
2811
2911
3011
3111
3211
3311
3411
3511
3611
3711
3811
3911
4011
4111
4211
4311
4411
4511
4611
4711
4811
4911
5011
5111
5211
5311
5411
5511
5611
5711
5811
5911
6011
6111
6211
6311
6411
6511

```

```

DO 120 J=1,NEM
I=(J+1)/2
IF(KI(J).NE.3) GO TO 120
DSEAB(J)=DSEAB(J)-CMDP(J)
TDSE=TDSE - CMDP(J)
K=2*I
L=K-1
SESEAB(I)=TBLSE(K) + TBLSE(L) - DSE(K) - DSE(L)
DUCTILITY BASED ON DISSIPATED ENERGY (OSTER) 2
EMU(J)=1.0 + DSEAB(J)/SESEAB(I)
IF(EMU(J)).LT.DUCMAX(J)) GO TO 15
DUCMAX(J)=EMU(J)
CONTINUE
15 EXCUR(J)=EXCUR(J) + ABS(EMU(J)-1.0)
IF(IPLPR.EQ.0) GO TO 214
PRINT 2011,J,DSEAB(J),SESEAB(I),EMU(J),DUCMAX(J),EXCUR(J)
2011 FORMAT(5X,I5,3X,'DSEAB=',E13.6,3X,'SESEAB=',E13.6,3X,'EMU=',E13.6,
*3X,'DUCMAX=',E13.6,3X,'EXCUR=',E13.6,' 1,')
214 CONTINUE
CURVATURE DUCTILITY (ANDERSON AND BERTERO)
N=J+NEM
IF(BMOM(J).LT.(ALMPP(J)+DELMP(J))) GO TO 150
EMU(J)=1.0 + (BMOM(J)-YMOMP(J)-DELMP(J))/(P(I)*YMOMP(J))
YMOM=YMOMP(J)
GO TO 160
150 EMU(J)=1.0 + (BMOM(J)-YMONN(J)-DELMP(J))/(P(I)*YMONN(J))
YMOM=YMOMN(J)
CONTINUE
160 IF(EMU(J).LT.DUCMAX(N)) GO TO 215
DUCMAX(N)=EMU(J)
CONTINUE
215 EXCUR(N)=EXCUR(N) + EMU(J) - 1.0
IF(IPLPR.EQ.0) GO TO 216
PRINT 2012,YMOM,DELMP(J),EMU(J),DUCMAX(N),EXCUR(N)
2012 FORMAT(14X,YMOM=,E13.6,4X,'DELMP=',E13.6,3X,'EMU=',E13.6,3X,'DUC
*MAX=',E13.6,3X,'EXCUR=',E13.6,' 2,')
216 CONTINUE
SYMMETRICAL DUCTILITY (WALPOLE AND SHEPHERD)
N=N+NEM
C2=6.0*S(I)
IF(BMOM(J).LT.(YMOMP(J)+DELMP(J))) GO TO 170
EMU(J)=1.0 + SLOPE(J)*C2/(ABS(YMOMP(J)))
GO TO 180
170 EMU(J)=1.0 + SLOPE(J)*C2/(ABS(YMONN(J)))
CONTINUE
180 IF(EMU(J).LT.DUCMAX(N)) GO TO 115
DUCMAX(N)=EMU(J)
CONTINUE
115

```

ENER 661
ENER 671
ENER 681
ENER 691
ENER 701
ENER 711
ENER 721
ENER 731

ENER 741
ENER 751
ENER 761
ENER 771
ENER 781
ENER 791
ENER 801
ENER 811
ENER 821
ENER 831

ENER 841
ENER 851
ENER 861
ENER 871
ENER 881
ENER 891
ENER 901
ENER 911
ENER 921
ENER 931
ENER 941
ENER 951
ENER 961
ENER 971
ENER 981
ENER 991
ENER 1001

ENER 1011
ENER 1021
ENER 1031
ENER 1041
ENER 1051
ENER 1061
ENER 1071
ENER 1081
ENER 1091
ENER 1101

```

EXCUR(N)=EXCUR(N) + EMU(J) -1.0
IF(IPLPR.EQ.0) GO TO 217
PRINT 2013, SLOPE(J), TANG(J), EMU(J), DUCMAX(N), EXCUR(N)
FORMAT(13X, 'ALPHA=', E13.6, 3X, 'ALPHA=', E13.6, 3X, 'EMU=', E13.6, 3X, 'D
2013 *UCMAX=', E13.6, 3X, 'EXCUR=', E13.6, ' 3.')
217 CONTINUE
DSEAB(J)=0.0
SLOPE(J)=0.0
120 CONTINUE
RETURN
30 CONTINUE
NE=0) GO TO 36
IF(IELPL.NE.0) GO TO 36
CALCULATION OF ELASTIC STRAIN ENERGY
ESE=0.0
DO 35 I=1,NM
K=2*I
J=K-1
C=1.0/(S(I)*6.0)
ESE=ESE + C*(BMOM(J)*BMOM(J) - BMOM(J)*BMOM(J) + BMOM(K)*BMOM(K))
35 CONTINUE
36 CONTINUE
CALCULATION OF KINETIC ENERGY
EKE=0.0
K=NPV+1
DO 40 I=K,NPS
XST(I)=XT(I) + XGTPI
EKE=EKE + AMASS(I)*XST(I)*XST(I)/2.0
40 CONTINUE
IF(NPV.EQ.0) GO TO 4002
DO 4001 I=1,NPV
K=I+NPV
VELY=YGTPI+XT(I)
EKE=EKE+AMASS(I)*VELY*VELY/2.0 +
4001 (AMASS(K)-AMASS(I))*YGTPI*YGTPI/2.0
GO TO 4004
4002 CONTINUE
I=1,NPS
DO 4003 EKE=EKE + AMASS(I)*YGTPI*YGTPI/2.0
4003 CONTINUE
4004 IF(IELPL.GT.0) GO TO 50
IF(IDAM.GT.0) GO TO 50
41 CONTINUE
TIE=ESE+EKE+EDD
IF(EIE) 45,47,45
45 PRC=(EIE-TIE)*100.0/EIE
GO TO 55
47 PRC=0.0
55 CONTINUE

```

ENER1111
ENER1112
ENER1113
ENER1114
ENER1115
ENER1116
ENER1117
ENER1118
ENER1119
ENER1120
ENER1121
ENER1122

ENER1231
ENER1241
ENER1251
ENER1261
ENER1271
ENER1281
ENER1291
ENER1301

ENER1311
ENER1321
ENER1331
ENER1341
ENER1351
ENER1361
ENER1371
ENER1381
ENER1391
ENER1401
ENER1411
ENER1421
ENER1431
ENER1441
ENER1451
ENER1461
ENER1471
ENER1481
ENER1491
ENER1501
ENER1511
ENER1521
ENER1531
ENER1541
ENER1551
ENER1561

```

1001 * IF(IAB.EQ.4) GO TO 48
      PRINT 1001, EIE,ESE,EKE,EDD,PRC
      FORMAT(8X, '-----')
      * /6X, 'ENERGY',5X, 'EIF=',E13.6,2X, 'ESE=',E13.6,2X,
48 PRC=ABS(PRC)
      IF(BPRC.GT.PRC) GO TO 49
      BPRC=PRC
      BPT=T
      CEIE=EIE
49 CONTINUE
      RETURN
50 CONTINUE
      ENERGY DISSIPATION DUE TO DAMPING
      IF(IDAM.EQ.0) GO TO 71
      K=N6
      DO 6006 I=1,NPS
      DO 6006 J=1,NPS
      CMK(I,J)=ATDZ(K)
6006 K=K+1
      DO 65 I=1,NPS
      XT2(I)=0.0
      DO 65 J=1,NPS
      XT2(I)=XT2(I) + CMK(I,J)*(XT(J)-DVEL(J))
65 IF(I.GT.NPV) GO TO 66
      EDD=EDD + XT2(I)*DT*(XT(I)-DVEL(I)+AVEYGT)
      GO TO 70
      EDD=EDD + XT2(I)*DT*(XT(I)-DVEL(I)+AVEXGT)
70 CONTINUE
      IF(LEPL.LT.1) GO TO 41
      TOTAL ENERGY DISSIPATED
      TED=EDD+TDSE
      GO TO 73
71 CONTINUE
      TED=TDSE
      GO TO 73
73 CONTINUE
      EDD=0.0
      TIE=BLSE +EDD+EKE
      PRC=(EIE-TIE)*100.0/EIE
      IF(IAB.EQ.4) GO TO 74
      PRINT 1002, EIE,BLSE,EKE,EDD,TDSE,PRC
      FORMAT(8X, '-----')
1002 * /6X, 'ENERGY',3X, 'EIE=',E13.6,2X, 'BLSE=',E13.6,
      * 2X, 'EKE=',E13.6,2X, 'EDD=',E13.6,3X, 'TDSE=',E13.6,
      * 2 3X, 'F10.4, '% ERROR')

```

ENER1571
 ENER1581
 ENER1591
 ENER1601
 ENER1611
 ENER1621
 ENER1631
 ENER1641
 ENER1651
 ENER1661
 ENER1671
 ENER1681
 ENER1691
 ENER1701
 ENER1711
 ENER1721
 ENER1731
 ENER1741
 ENER1751
 ENER1761
 ENER1771
 ENER1781
 ENER1791
 ENER1801
 ENER1811
 ENER1821
 ENER1831
 ENER1841
 ENER1851
 ENER1861
 ENER1871
 ENER1881
 ENER1891
 ENER1901
 ENER1911
 ENER1921
 ENER1931
 ENER1941
 ENER1951
 ENER1961
 ENER1971
 ENER1981
 ENER1991
 ENER2001
 ENER2011
 ENER2021

```

74 PRC=ABS(PRC)
   IF(BPRC.GT.PRC) GO TO 80
   BPRC=PRC
   BPT=T
   CEIE=EIE
   CONTINUE
80 RETURN
END
SUBROUTINE CAINMC(NP,NPS,NPV,N6,NCOL)
COMMON/MAFOE/XSTT(3010),AHHA,IERQK
COMMON/STNECA/JC1(40),JC2(40),JC3(40),P(40),NEM
COMMON/MASTI/S(40),NTIM
COMMON/MANECA/DX(50),BMOM(80),ALMPP(80),ALMPN(80),
1 KI(80),VALMP(40),XI(50),XT(20),XTT(20),DR(20),
2 UDT,PVAL,JJ,NCOND
COMMON/FONECA/DT,T,DXGM(20),JN,KJ
COMMON/SAVMQM/ISUPRT(9),AVEMOM,NSUPRT,NGN,IGIRD(40),AVEBEL,JS
COMMON/GUTS/PBMOM(80),DMOM(80),BAVE(80),DUCMAX(240),EXCUR(240),
* BLSE
COMMON/DUCEX/DSEAB(80),SESEAB(80),TBLSE(80),EMU(80)
COMMON/LOST/CMDPI(80),DSE(80),IDSE,EDD
COMMON/ANGLE/TROT(80),SLOPE(80),DROT(80),DVEL(20),TANG(80)
COMMON/WHAT/IELPL,IPDE,IVA,IDAM,IPLPR
COMMON/WORK/EIE,BPRC,ALONG,XGTPI,YGTPI,BPT,AVEXGT,CEIE,AVEYGT
COMMON/AXIAL/Q(20)
COMMON/FAFEP/FAF(20),AFEP(20),RED(80),ICOL(20),PY(20),MP
COMMON/UPDOWN/YSTT(3010),AVVA,BVVB,VGF
COMMON/ABC/AMASS(20),AMASSI(20),XL(40)
COMMON/CURDUC/DELMPI(80),YMOMPI(80),YMOMN(80)
COMMON/JUNK/ATOZ(8110)
DIMENSION IP(80),IE(80)
DIMENSION BSAT(80,50)
DOUBLE PRECISION DT,T,DX
CONTINUE
1 NM=NEM/2
K=1
DO 6001 I=1,NEM
DO 6001 J=1,NP
BSAT(I,J)=ATOZ(K)
K=K+1
6001 C CALCULATE POSSIBLE END MOMENTS
DO 5 I=1,NEM
DO 5 J=1,NP
4 DMOM(I)=0.0
5 DMOM(I)=DMOM(I)+BSAT(I,J)*DX(J)
DO 6 I=1,NEM
6 BAVE(I)=BMOM(I) + DMOM(I)/2.0
PBMOM(I)=DMOM(I)+BMOM(I)

```

ER2031
 ENER2041
 ENER2051
 ENER2061
 ENER2071
 ENER2081
 ENER2091
 ENER2101
 CAIN 111
 CAIN 121
 CAIN 131
 CAIN 141
 CAIN 151
 CAIN 161
 CAIN 171
 CAIN 181
 CAIN 191
 CAIN 201
 CAIN 211
 CAIN 221
 CAIN 231
 CAIN 241
 CAIN 251
 CAIN 261
 CAIN 271
 CAIN 281
 CAIN 291
 CAIN 301
 CAIN 311
 CAIN 321
 CAIN 331
 CAIN 341
 CAIN 351
 CAIN 361
 CAIN 371
 CAIN 381

```

111 IF(IELPL.EQ.0) GO TO 111
CALL ENERGY (NM,NPS,NPV,2,N6)
CONTINUE
IF(IMP.EQ.0) GO TO 4201
NPH=NPS-NPV
CALL COLLOD(NPH,NPV,IERQK,NCOL)
CALL MPRED(NCOL)
CONTINUE
4201 KJ=0
DO 20 I=1,NEM
M=KI(I)+1
GO TO (10,20,500,500),M
10 CONTINUE
K=(I+1)/2
IF(DMOM(I).LT.0.0) GO TO 11
BJ=ALMPP(I)*RED(I)
IF(PBMOM(I).GT.8J) GO TO 612
GO TO 20
11 BI=ALMPN(I)*RED(I)
IF(PBMOM(I).GT.BI) GO TO 20
612 CONTINUE
IF(DMOM(I).LT.0.0) GO TO 614
DELMPI=PBMOM(I) -ALMPP(I)
GO TO 615
614 CONTINUE
DELMPI=PBMOM(I) - ALMPN(I)
615 CONTINUE
P(K)=PVAL
KI(I)=1
JJ=-1
KJ=2
KA=I/K
GO TO (14,15),KA
14 JC2(K)=1
JC3(K)=1
GO TO 20
15 JC1(K)=1
JC3(K)=1
GO TO 20
500 K=(I+1)/2
BI=ALMPN(I)*RED(I)
IF(DMOM(I).LT.BI) GO TO 511
IF(DMOM(I).GT.8J) GO TO 512,20
CONTINUE
512 IF(NCOND.NE.2) GO TO 6050
IF(NCOND.NE.2) GO TO 6050
YMOMPI=ALMPP(I)
YMOMN(I)=ALMPN(I)
GO TO 513

```

```

6050 CONTINUE
      IF(BMCM(I).LT.BI) GO TO 405
      YMOMPM(I)=ALMPP(I)
      ALMPP(I)=PRMOM(I)
      IF(NCONC.EQ.1) GO TO 513
      ALMPP(I)=ALMPP(I) - 2.*VALMP(K)
      GO TO 513
405  YMOMN(I)=ALMPN(I)
      ALMPN(I)=PRMOM(I)
      IF(NCONC.EQ.1) GO TO 513
      ALMPP(I)=ALMPN(I) + 2.*VALMP(K)
513  CONTINUE
      IF(IPLPR.EQ.0) GO TO 4202
      PRINT 4176
4176 FORMAT(3X,'THE FOLLOWING ADDITIONAL INFORMATION APPLIES TO PLASTIC
      1 HINGES.')
      PRINT 205,I,ALMPP(I),ALMPN(I),TROTT(I)
205  FORMAT(5X,I5X,'MP MAX.=',E13.6,5X,'MP MIN.=',E13.6,
      1 5X,'JOINT ROTATION=',E13.6)
4202 CONTINUE
      KI(I)=3
      KJ=3
      KA=I/K
      GO TO (514,515),KA
514  JC2(K)=0
      GO TO 20
515  JC1(K)=0
      GO TO 20
511  IF(DMCM(I)) 20,512,512
20  CONTINUE
      IF(IELPL.EQ.0) GO TO 112
      CALL ENERGY (NM,NPS,NPV,3,N6)
112  CONTINUE
      IF(KJ.LT.1) GO TO 34
      M1=0
      M2=0
      DO 502 I=1,NEM
      IF(KI(I).NE.1) GO TO 503
      M1=M1+1
      IP(M1)=I
      IF(KI(I)=2)
501  CONTINUE
503  IF(KI(I).NE.3) GO TO 502
      M2=M2+1
      IE(M2)=I
      IF(KI(I)=0)
502  CONTINUE
      IF(M2.LT.1) GO TO 620

```

CAIN 881
 CAIN 891
 CAIN 901
 CAIN 911
 CAIN 921
 CAIN 931
 CAIN 941
 CAIN 951
 CAIN 961
 CAIN 971
 CAIN 981
 CAIN 991
 CAIN 1001
 CAIN 1011
 CAIN 1021
 CAIN 1031
 CAIN 1041
 CAIN 1051
 CAIN 1061
 CAIN 1071
 CAIN 1081
 CAIN 1091
 CAIN 1101
 CAIN 1111
 CAIN 1121
 CAIN 1131
 CAIN 1141
 CAIN 1151
 CAIN 1161
 CAIN 1171
 CAIN 1181
 CAIN 1191
 CAIN 1201
 CAIN 1211
 CAIN 1221
 CAIN 1231
 CAIN 1241
 CAIN 1251
 CAIN 1261
 CAIN 1271
 CAIN 1281
 CAIN 1291
 CAIN 1301
 CAIN 1311
 CAIN 1321
 CAIN 1331
 CAIN 1341


```

PRINT 202, T, (IE(I), I=1, M2)
202 FORMAT(2X, 'NOTE, AT TIME=', F6.2, ' SEC. THE FOLLOWING MEMBER ENDS
1 RETURNED TO THEIR ELASTIC RANGE', 10I4, / (2X, 30I4))
620 CONTINUE
IF(M1.LT.1) GO TO 622
PRINT 201, T, (IP(I), I=1, M1)
201 FORMAT(/2X, 'NOTE, AT TIME=', F6.2, ' SEC. THE FOLLOWING MEMBER ENDS
1 BECAME PLASTIC', 15I4, / (2X, 30I4))
622 CONTINUE
DO 504 I=1, NEM, 2
IF(KI(I).NE.0) GO TO 504
IP1=I+1
IF(KI(I), NE.KI(IP1)) GO TO 504
K=(I+1)/2
P(K)=1.
504 CONTINUE
DO 30 K=1, NM
IF(JC1(K)-JC2(K)) 30, 28, 30
28 JC1(K)=0
JC2(K)=0
30 JC3(K)=0
34 CONTINUE
IF(KJ.EQ.3) JJ=-1
AVEMOM=0.0
DO 555 I=1, NSUPRT
KL=ISUPRT(I)*2-1
KU=ISUPRT(I)*2
AVEMOM=AVEMOM+(BMOM(KL)+BMOM(KU)+PBMMOM(KL)+PBMMOM(KU))/2.0
555 CONTINUE
AVEBEL=0.0
IF(INPV.EQ.0) GO TO 4557
DO 4555 I=1, NGM, 2
KL=IGIRD(I)*2-1
KU=KL+1
J=IGIRD(I)
AVEBEL=AVEBEL+(BMOM(KL)+BMOM(KU)+PBMMOM(KL)+PBMMOM(KU))/(2.0*XL(J))
4555 CONTINUE
DO 4556 I=2, NGM, 2
KL=IGIRD(I)*2-1
KU=KL+1
J=IGIRD(I)
AVEBEL=AVEBEL-(BMOM(KL)+BMOM(KU)+PBMMOM(KL)+PBMMOM(KU))/(2.0*XL(J))
4556 CONTINUE
DO 40 I=1, NEM
40 BMOM(I)=PBMMOM(I)
50 CONTINUE
CAIN1351
CAIN1361
CAIN1371
CAIN1381
CAIN1391
CAIN1401
CAIN1411
CAIN1421
CAIN1431
CAIN1441
CAIN1451
CAIN1461
CAIN1471
CAIN1481
CAIN1491
CAIN1501
CAIN1511
CAIN1521
CAIN1531
CAIN1541
CAIN1551
CAIN1561
CAIN1571
CAIN1581
CAIN1591
CAIN1601
CAIN1611
CAIN1621
CAIN1631
CAIN1641
CAIN1651
CAIN1661
CAIN1671
CAIN1681
CAIN1691
CAIN1701
CAIN1711
CAIN1721
CAIN1731
CAIN1741
CAIN1751
CAIN1761
CAIN1771
CAIN1781
CAIN1791
CAIN1801
CAIN1811
CAIN1821

```

```

RETURN
END
SUBROUTINE PRIOUT(NP,NPR,NPS,NM,NEM,NPV,XG,XGT,YG,YGT,N)
COMMON/MAST/ S(40),NTIM
COMMON/MANECA/ DX(50),BMOM(80),ALMPP(80),ALMPN(80),
1 KI(80),VALMP(40),X(50),XT(20),XTT(20),DR(20),
2 UDT,PVAL,JJ,NCOND
COMMON/MAFOE/XSTT(3010),AHHA,IERQK
COMMON/FCNECA/ DT,I,DXGM(20),JN,KJ
COMMON/UPDOWN/ YSTT(3010),AVVA,BVVB,VGF
DIMENSION DISPL(20)
DOUBLE PRECISION DX,DT,T
GO TO (10,20),N
10 CONTINUE
PRINT 2006
FORMAT(/,2X,'*****')
1*****
PRINT 2007,T,NTIM
FORMAT(/,2X,'TIME=',F7.3,4X,'NUMBER OF TIMES STIFFNESS HAS BEEN CAL
1CULATED =',I3)
AVVA=-AVVA
PRINT 2031,AHHA,AVVA
FORMAT(8X,'- - - - -',10X,'HORIZONTAL=',E15.6,
* /6X,'LOADING
1 5X,'VERTICAL=',E15.6)
PRINT 3001,XG,XGT,YG,YGT
FORMAT(9X,'XG=',E13.6,' XGT=',E13.6,' YG=',E13.6,' YGT=',E13.6)
RETURN
20 CONTINUE
PRINT 2008
FORMAT(8X,'- - - - -',10X,'HORIZONTAL FLOOR DISPL., VEL. AND ACCEL. RELATIVE TO
* /6X,'HORIZONTAL FLOOR DISPL., VEL. AND ACCEL. RELATIVE TO
1ASE., /9X,'NO.,6X,'DISPL.,9X,'VEL.,10X,'ACCEL.')
```

DISPL.,9X,'VEL.,10X,'ACCEL.')

NPRI=NPRI+1+NPV

DO 625 I=NPRI,NP

J=I-NPR

DISPL(J)=X(I)

KK=NPV+1

PRINT 2030,(I,DISPL(I),XT(I),XTT(I),I=KK,NPS)

2030 FORMAT(8X,I3,3E15.6,4X,I3,3E15.6)

IF(NPV.EQ.0) GO TO 4008

PRINT 4005

FORMAT(/,6X,'VERTICAL DISPL., VEL. AND ACCEL. OF NODAL POINTS ON GIP
1RDERS RELATIVE TO BASE.')


```

DIMENSION A(20),B(20),DX2(20),DXI(20),DXII(20),VK2(20,20),INDEX(30)
1 SKI(30,30),SK2(30,20),SK3(20,20),STIP(30,20),DXI(30),INDEX(30)
2 SKI(20,20),AKS(20,20),STIPP(20,20),XMAI(20),DXI(30),INDEX(30)
DOUBLE PRECISION SIXOI2,DI,I,A,B,DXI,DXII,XMI,DX,DX2,THRDI
*****
NEWMARK BETA METHOD
NPR=NP-NPS
IF(IERQK.EQ.0) GO TO 510
IF(NMBM) 100,105,100
CONTINUE
GO TO (101,102),NMBM
100 THRDI=6.0/DI
SIXDI2=12.0/(DI*DI)
A(I)={-12.0/DI}*XI(I) - 6.0*XTI(I)
B(I)=-6.0*XI(I) - 2.0*DI*XTI(I)
GO TO 510
102 THRDI=2.0/DI
SIXDI2=4.0/(DI*DI)
A(I)={-4.0/DI}*XI(I) - 2.0*XTI(I)
B(I)=-2.0*XI(I)
GO TO 510
105 CONTINUE
THRDI=3.0/(DI*DI)
SIXDI2=6.0/(DI*DI)
*****
CALCULATE VECTORS A AND B
*****
DO 905 I=1,NPS
A(I)={-6.0/DI}*XTI(I)-3.*XTI(I)
B(I)=-3.*XI(I)-{DI/2.}*XTI(I)
CONTINUE
CONTINUE
IF(JJ.GT.0) GO TO 486
M=NPR+1
IF(NPR.EQ.0) GO TO 6021
K=N2
DO 6002 I=1,NPR
DO 6002 J=1,NPR
SKI(I,J)=ATOZ(K)
K=K+1
6002 K=N3
DO 6003 I=1,NPR
DO 6003 J=1,NPS
SK2(I,J)=ATOZ(K)
K=K+1
6003 K=N4
6021 CONTINUE

```

NEMK 211
NEMK 221
NEMK 231
NEMK 241

NEMK 251
NEMK 261
NEMK 271
NEMK 281
NEMK 291
NEMK 301
NEMK 311
NEMK 321
NEMK 331
NEMK 341
NEMK 351
NEMK 361
NEMK 371
NEMK 381
NEMK 391
NEMK 401
NEMK 411
NEMK 421

NEMK 431
NEMK 441
NEMK 451
NEMK 461
NEMK 471
NEMK 481
NEMK 491
NEMK 501
NEMK 511
NEMK 521
NEMK 531
NEMK 541
NEMK 551
NEMK 561
NEMK 571
NEMK 581
NEMK 591
NEMK 601
NEMK 611
NEMK 621


```

486      CONTINUE
      DO 21 I=1,NPS
      DO 21 J=1,NPS
      STIPP(I,J)=0. GO TO 21
      IF(NPR.EQ.0) GO TO 21
      DO 20 L=1,NPR
      T1=SK2(L,I)*STIP(L,J)
      STIPP(I,J)=STIPP(I,J)+T1
20      CONTINUE
21      IF(IERQK.GT.0) GO TO 22
      K=N8
      DO 4324 I=1,NPS
      DO 4324 J=1,NPS
      ATOZ(K)=STIPP(I,J) + SK3(I,J)
4324      K=K+1
      CALL DECOMP (NPS,N8,N9,PC,DX2,JJ)
      GO TO 4325
22      CONTINUE
      IF(IPDE) 300,302,300
      300 AVVAP1=AVVA + 32.2*VGF
      GO TO 303
      302 AVVAP1=AVVA
      303 CONTINUE
      K=N5
      DO 6005 I=1,NPS
      DO 6005 J=1,NPS
      VK2(I,J)=ATOZ(K)
      K=K+1
      DO 485 I=1,NPS
      DO 485 J=1,NPS
      STIPP(I,J)=STIPP(I,J) + SK3(I,J) - AVVAP1*VK2(I,J)
485      CONTINUE
720      K=N6
      DO 4320 I=1,NPS
      DO 4320 J=1,NPS
      CMK(I,J)=ATOZ(K)
      K=K+1
4320      IF((IDAM.LE.1).AND.(IERQK.GT.1)) GO TO 4322
      IF((JJ.GT.0).AND.(IVA.EQ.0)) GO TO 4322
      DO 301 I=1,NPS
      DO 301 J=1,NPS
      CMK(I,J)=STIPP(I,J)*BB
      301      CONTINUE
      DO 304 I=1,NPS
      DO 304 CMK(I,I)=CMK(I,I) + AMASS(I)*AA
      K=N6
      DO 6006 I=1,NPS
      DO 6006 J=1,NPS
      ATOZ(K)=CMK(I,J)

```

```

NEMK1051
NEMK1061
NEMK1071
NEMK1081
NEMK1091
NEMK1101
NEMK1111
NEMK1121
NEMK1131
NEMK1141
NEMK1151
NEMK1161
NEMK1171
NEMK1181
NEMK1191
NEMK1201
NEMK1211
NEMK1221
NEMK1231
NEMK1241
NEMK1251
NEMK1261
NEMK1271
NEMK1281
NEMK1291
NEMK1301
NEMK1311
NEMK1321
NEMK1331
NEMK1341
NEMK1351
NEMK1361
NEMK1371
NEMK1381
NEMK1391
NEMK1401
NEMK1411
NEMK1421
NEMK1431
NEMK1441
NEMK1451
NEMK1461
NEMK1471
NEMK1481
NEMK1491
NEMK1501
NEMK1511
NEMK1521

```

```

6006 6006 K=K+1
4322 4322 CONTINUE
C C C C
C C C C *CALCULATE DELTA R
C C C C *****
C C C C DO 907 I=1,NPS
C C C C XMA(I)=AMASS(I)*A(I)
C C C C DO 908 J=1,NPS
C C C C XMA(I)=XMA(I) + CMK(I,J)*VK2(I,J)*X(J*NPR)*BVVB
908 908 XMA(I)=DXGM(I)-XMA(I)
907 907 DR(I)=DXGM(I)-XMA(I)
C C C C *****
C C C C *CALCULATE K ASTERISK
C C C C *****
C C C C DO 910 I=1,NPS
C C C C DO 910 J=1,NPS
910 910 AKS(I,J)=STIPP(I,J) + THROT*CMK(I,J)
912 912 DO 912 I=1,NPS
912 912 AKS(I,I)=AKS(I,I) + SIXDT2*AMASS(I)
C C C C K=N8
C C C C DO 6008 I=1,NPS
C C C C DO 6008 J=1,NPS
C C C C ATDZ(K)=AKS(I,J)
6008 6008 K=K+1
C C C C IF(I=IERQK.GT.1) GO TO 725
C C C C IF(I=INPRIN.EQ.0) GO TO 725
C C C C PRINT 723
723 723 FORMAT(5X,'MATRIX AKS')
C C C C DO 724 I=1,NPS
724 724 PRINT 702, I, (AKS(I,J),J=1,NPS)
C C C C CONTINUE
C C C C IF(I=IDAM.EQ.0) GO TO 725
C C C C PRINT 730
730 730 FORMAT(5X,'MATRIX CMK')
C C C C DO 731 I=1,NPS
731 731 PRINT 702, I, (CMK(I,J),J=1,NPS)
725 725 CONTINUE
C C C C IF(AKS(I,I).LE.0.) GO TO 951
C C C C *****
C C C C *CALCULATE DELTA X DISPLACEMENT
C C C C *****
C C C C $$$$$$*****
C C C C CALL DECOMP(NPS,N8,N9,DR,DX2,JJ)
C C C C $$$$$$*****
C C C C JJ=1
C C C C *****
4325 4325 CONTINUE
C C C C CALCULATE DELTA ROTATION
C C C C *****

```

```

C *****
C IF(NPR.EQ.0) GO TO 605
C DO 487 I=1,NPR
C DX1(I)=0.
C DO 487 J=1,NPS
C DX1(I)=DX1(I) + STIP(I,J)*DX2(J)
C *****
C FORM DELTA X MATRIX
C *****
C DO 490 I=1,NPR
C DX1(I)=DX1(I)
C CONTINUE
C DO 495 I=M,NP
C J=I-NPR
C DX1(I)=DX2(J)
C *****
C *CALCULATE INTERNAL MOMENTS AND CHECK STRESS RANGE OF ALL JOINTS.
C *****
C CALL CAINMO(NP,NPS,NPV,N6,NCOL)
C DO 915 I=1,NP
C X(I)=X(I)+DX(I)
C IF(IERQK.EQ.0) RETURN
C DO 917 I=1,NPS
C J=I+NPR
C DX1(I)=THROD*DX(J) + B(I)
C DO 9919 I=1,NPS
C DVEL(I)=DX1(I)/2.0
C XT(I)=X(I)+DX1(I)
C DO 9921 I=1,NPS
C J=I+NPR
C DX1(I)=SIXDI2*DX(J) + A(I)
C DO 9923 I=1,NPS
C XT(I)=XT(I)+DX1(I)
C RETURN
C PRINT 952
C FORMAT(5X,'AKS(1,1).LE.0.')
C STOP
C FORMAT(4H ROW,13,1X,10E12.4/(8X,10E12.4))
C END
C SUBROUTINE COLLOD(NPH,NPV,IERQK,NCOL)
C COMMON/ABC/AMASS(20),AMASS1(20),XL(40)
C COMMON/SAVMOM/ ISUPRT(9),AVERDM,NSUPRT,NGM,IGIRD(40),AVEBEL,JS
C COMMON/GUTS/P8MOM(80),DMOM(80),BAVE(80),DUCMAX(240),EXCUR(240),
C * BLSE
C COMMON/UPDOWN/YSTI(3010),AVVA,BVVB,VGF
C COMMON/AXIAL/P(20)
C THE PURPOSE OF THIS SUBROUTINE IS TO CALCULATE THE COLUMN LOADS.
C 1 CONTINUE

```

NEMK1881
NEMK1891
NEMK1901
NEMK1911
NEMK1921

NEMK1931
NEMK1941
NEMK1951
NEMK1961
NEMK1971
NEMK1981

NEMK1991
NEMK2001
NEMK2011
NEMK2021
NEMK2031
NEMK2041
NEMK2051
NEMK2061
NEMK2071
NEMK2081
NEMK2091
NEMK2101
NEMK2111
NEMK2121
NEMK2131
NEMK2141
NEMK2151
NEMK2161
NEMK2171
NEMK2181
NEMK2191
COLL 11
COLL 21
COLL 31
COLL 41
COLL 51
COLL 61
COLL 71


```

K=NPV+NPV
IF(IERQK.NE.0) GO TO 4
C=32.2
GO TO 5
4 CONTINUE
C=32.2-Y*STT(IERQK)
5 CONTINUE
I6=NPV+NPV
IF(NPV.EQ.0) GO TO 6
I7=4*(NSUPRT-1)
IF(IJS.EQ.1) GO TO 8
I7=I7/2
GO TO 8
6 CONTINUE
I7=2*NSUPRT-2
8 CONTINUE
DO 10 I=1,NCOL
10 P(I)=0.0
I1=0
B=AMASS(I6)*C/I7
I8=1
I1=0
DO 50 I=1,NGM
15=IGIRD(I)
I3=2*I5-1
I4=I3+1
A=(PBMQM(I3) + PBMQM(I4))/XL(I5)
IF(NPV.NE.0) GO TO 30
I1=I+I
IF(I6.EQ.K) GO TO 20
I2=I1-NSUPRT
P(I1)=P(I1) + P(I2) - A + B
I1=I1+1
I2=I2+1
P(I1)=P(I1) + A + B
GO TO 40
20 P(I1)=P(I1) - A + B
I1=I1+1
P(I1)=P(I1) + A + B
GO TO 40
30 J=(I-1)/2
I9=I1
I1=I+I-I-J
IF(I9.EQ.I1) E=0.0
I8=-I*I8
IF(I6.EQ.K) GO TO 35
I2=I1-NSUPRT
P(I1)=P(I1) + P(I2)*E + I8*A + B

```

```

COLL 81
COLL 91
COLL 101
COLL 111
COLL 121
COLL 131
COLL 141
COLL 151
COLL 161
COLL 171
COLL 181
COLL 191
COLL 201
COLL 211
COLL 221
COLL 231
COLL 241
COLL 251
COLL 261
COLL 271
COLL 281
COLL 291
COLL 301
COLL 311
COLL 321
COLL 331
COLL 341
COLL 351
COLL 361
COLL 371
COLL 381
COLL 391
COLL 401
COLL 411
COLL 421
COLL 431
COLL 441
COLL 451
COLL 461
COLL 471
COLL 481
COLL 491
COLL 501
COLL 511
COLL 521
COLL 531
COLL 541
COLL 551

```

COLL 561
COLL 571
COLL 581
COLL 591
COLL 601
COLL 611
COLL 621
COLL 631
COLL 641
COLL 651
COLL 661
COLL 671
COLL 681
COLL 691

```

E=1.0
GO TO 40
P(I1)=P(I1) + I8*A + B
35 E=1.0
40 CONTINUE
J=NSUPRT*(I1+1)
IF(I1.LT.J) GO TO 50
I1=I1+1
I6=I6-1
IF(I6.LE.0) GO TO 50
B=AMASS(I6)*C/I7
50 CONTINUE
RETURN
END

```

C C THE FOLLOWING TWO SUBROUTINES ARE USED AT UMR FOR PLOTTING OUTPUT.

```

SUBROUTINE SPLOT(XMAX,XMIN,ND,I,NPS)
COMMON/PLOUT/X10(3010),EINPUT(3010),DENS(3010),DEND(3010)
DIMENSION XMAX(10),XMIN(10)
DIMENSION U(3010)
DO 50 I=1,ND
X10(I)=X10(I)*12.0
50 XMA=12.0*XMAX(NPS)
XMI=12.0*XMIN(NPS)
PRINT 2001
2001 FORMAT(/'/6X,'PLOT OF THE HORIZONTAL DISPLACEMENT FOR THE TOP FLOOR
1R MADE AS A RESULT OF THIS PROGRAM')
AN=0.01
AXMA=ABS(XMA)
AXMI=ABS(XMI)
IF(AXMA.LT.AXMI) GO TO 20
SMA=AXMA
GO TO 22
SMA=AXMI
20 CONTINUE
22 CHEK=SMA/AN
25 IF(CHEK.LT.1.0) GO TO 30
AN=10.0*AN
GO TO 25
30 CONTINUE
DAN=AN/20.0
CALL NEWPLT(1.5,5.5,9.0)
CALL ORIGIN(0.0,0.0)
CALL TSCALE(0.0,T,5.00)
CALL YSCALE(-AN,AN,8.0)
CALL TAXIS(1.0)
CALL YAXIS(DAN)

```

SPLD 1
SPLD 11
SPLD 21
SPLD 31
SPLD 41
SPLD 51
SPLD 61
SPLD 71
SPLD 81
SPLD 91
SPLD 101
SPLD 111
SPLD 121
SPLD 131
SPLD 141
SPLD 151
SPLD 161
SPLD 171
SPLD 181
SPLD 191
SPLD 201
SPLD 211
SPLD 221
SPLD 231
SPLD 241
SPLD 251
SPLD 261
SPLD 271
SPLD 281
SPLD 291
SPLD 301

```

CALL SYM(0.5,4.0,0.14,'HEADING FOR PLOT GOES HERE
CALL SYM(0.5,3.8,0.14,'HEADING FOR PLOT GOES HERE
CALL SYM(0.5,3.6,0.14,'XMAX=',0.0,5)
CALL SYM(0.5,3.4,0.14,'XMIN=',0.0,5)
CALL NUM(1.3,3.6,0.14,XMA,0.0,3)
CALL NUM(1.3,3.4,0.14,XMI,0.0,3)
CALL TPLT(XLO,ND,1,-1)
CALL ENDPLT
RETURN
END
SUBROUTINE EPLOT(K,IMASS,ND,I,N)
COMMON/PLOUT/XLO(3010),EINPUT(3010),DENS(3010),DEND(3010)
AN=0.001
EMA=0.0
GO TO(1,2,3),N
1 CONTINUE
IF(K.EQ.3) GO TO 4
PRINT 101
101 FORMAT('PLOT OF THE INPUT ENERGY MADE AS A RESULT OF THIS PR
*OGRAM',)
J=1 TO 29
GO TO 29
4 CONTINUE
DO 5 I=1,ND
DENS(I)=DENS(I) + DEND(I)
PRINT 102
102 FORMAT('PLOT OF THE INPUT ENERGY, TOTAL DISSIPATED ENERGY, ANE
*D DISSIPATED ENERGY DUE TO DAMPING MADE AS A RESULT OF THIS PROGRA
*M',)
J=2 TO 9
GO TO 9
5 CONTINUE
IF(K.EQ.2) GO TO 6
PRINT 103
103 FORMAT('PLOT OF THE DISSIPATED STRAIN ENERGY MADE AS A RESULT
*F OF THIS PROGRAM',)
J=3
GO TO 19
6 CONTINUE
PRINT 104
104 FORMAT('PLOT OF THE INPUT ENERGY AND DISSIPATED STRAIN ENERGY
*Y MADE AS A RESULT OF THIS PROGRAM',)
J=4
GO TO 19
3 CONTINUE
IF(K.EQ.2) GO TO 7
PRINT 105
105 FORMAT('PLOT OF THE DISSIPATED ENERGY DUE TO DAMPING MADE ASE

```

```

* A RESULT OF THIS PROGRAM' )
J=5
GO TO 9
7 CONTINUE
106 PRINT 106
106 FORMAT(//5X,'PLOT OF THE INPUT ENERGY AND THE DISSIPATED ENERGY DUE TO DAMPING MADE AS A RESULT OF THIS PROGRAM',)
J=6
9 CONTINUE
DO 10 I=1,ND
DEND(I)=DEND(I)*144.0/TMASS
IF(DEND(I).GT.EMA) EMA=DEND(I)
10 CONTINUE
IF (J.GT.4) GO TO 28
19 CONTINUE
DO 20 I=1,ND
DENS(I)=DENS(I)*144.0/TMASS
IF(DENS(I).GT.EMA) EMA=DENS(I)
20 CONTINUE
IF(J.EQ.3) GO TO 50
28 CONTINUE
IF(J.EQ.5) GO TO 50
29 CONTINUE
DO 30 I=1,ND
EINPUT(I)=EINPUT(I)*144.0/TMASS
IF(EINPUT(I).GT.EMA) EMA=EINPUT(I)
30 CONTINUE
50 CHECK=EMA/AN
55 IF(CHECK.LT.1.0) GO TO 60
AN=AN*10.0
GO TO 55
60 CONTINUE
EMAX=AN
DEMAX=EMAX/20.0
CALL NEWPLT(1.5,2.5,10.0)
CALL ORIGIN(0.0,0.0)
CALL TSCALE(0.0,1.4,18)
CALL YSCALE(-DEMAX,EMAX,6.3)
CALL TAXIS(1.0)
CALL YAXIS(DEMAX)
CALL SYM(0.5,7.0,0.14,'HEADING FOR PLOT GOES HERE
CALL SYM(0.5,6.8,0.14,'HEADING FOR PLOT GOES HERE
CALL SYM(0.5,6.6,0.14,'MAXIMUM ENERGY=',0.0,15)
CALL NUM(2.4,6.6,0.14,EMA,0.0,0)
CALL SYM(-0.5,1.0,0.10,'ENERGY PER UNIT MASS, IV. -SEC.',90.0,31)
CALL SYM(4.3,0.02,0.10,'TIME',0.0,4)
CALL SYM(4.3,-.12,0.10,'SEC.',0.0,4)

```

```

EPL0 381
EPL0 391
EPL0 401
EPL0 411
EPL0 421
EPL0 431
EPL0 441
EPL0 451
EPL0 461
EPL0 471
EPL0 481
EPL0 491
EPL0 501
EPL0 511
EPL0 521
EPL0 531
EPL0 541
EPL0 551
EPL0 561
EPL0 571
EPL0 581
EPL0 591
EPL0 601
EPL0 611
EPL0 621
EPL0 631
EPL0 641
EPL0 651
EPL0 661
EPL0 671
EPL0 681
EPL0 691
EPL0 701
EPL0 711
EPL0 721
EPL0 731
EPL0 741
EPL0 751
EPL0 761
EPL0 771
EPL0 781
EPL0 791
EPL0 801
EPL0 811
EPL0 821
EPL0 831
EPL0 841
EPL0 851

```

```

EPL0 861
EPL0 871
EPL0 881
EPL0 891
EPL0 901
EPL0 911
EPL0 921
EPL0 971
EPL0 981
EPL0 991
EPL0 1001
EPL0 1011
EPL0 1021
EPL0 1031
EPL0 1041
EPL0 1051
EPL0 1061
EPL0 1071

```

```

MAIN 10
MAIN 20
MAIN 30

```

```

MAIN 40
MAIN 50
MAIN 60
MAIN 70
MAIN 80
MAIN 90
MAIN 100
MAIN 110
MAIN 120
MAIN 130
MAIN 140

```

```

MAIN 150
MAIN 160
MAIN 170
MAIN 180
MAIN 190
MAIN 200

```

```

CALL SYM(0.5,6.4,0.14,'TOTAL TIME=',0.0,11)
CALL NUM(1.9,6.4,0.14,1,0.0,2)
GO TO(110,120,130,140,150,160),J
CALL TPLT(EINPUT,ND,1,-1)
110 GO TO 170
CALL TPLT(EINPUT,ND,1,-1)
120 CALL TPLT(DENS,ND,1,-1)
CALL TPLT(DENS,ND,1,-1)
140 CALL TPLT(EINPUT,ND,1,-1)
CALL TPLT(EINPUT,ND,1,-1)
150 GO TO 170
CALL TPLT(DEND,ND,1,-1)
GO TO 170
160 CALL TPLT(DEND,ND,1,-1)
CALL TPLT(EINPUT,ND,1,-1)
170 CONTINUE
CALL ENDPLT
RETURN
END

```

THE FOLLOWING PROGRAM IS USED TO PRODUCE A FREQUENCY SPECTRUM.

```

DIMENSION YSTT(3000),X(4096)
DIMENSION FR(2050),AMPL(2048),PHASE(2048)
COMPLEX X

```

READ AND WRITE INPUT

```

READ (1,101) JN,ND,N,DELTAT,AMMIN
WRITE(3,111) JN,ND,N,DELTAT,AMMIN
101 FORMAT(//5X,'JOB NUMBER',I4,
120 RECORDS',I6,
130 'POINTS CONSIDERED',I6,
140 'ACCEL. INCREMENT',F10.4,
150 'TIME INCREMENT',F10.4,
160 'MINIMUM AMPLITUDE CONSIDERED',F10.4,
170 'RESULTS',/)
READ(1,102)(YSTT(I),I=1,ND)
102 FORMAT(8F9.6)

```

PLACE ACCEL. DATA INTO AN ARRAY HAVING A SIZE OF N**2

```

DO 20 I=1,ND
X(I)=YSTT(I)
CONTINUE
20 ND1=ND+1
NP=2**N
DO 30 I=ND1,NP

```

```

30      X(1)=0.0
      CONTINUE
      PERFORM FAST FOURIER TRANSFORM
      CALL NLOGN (N,X,-1.0)
      CALCULATE DATA FOR FREQUENCY SPECTRUM AND PHASE ANGLE
      CALL SPECRA (NP,X,DELTAT,AMMIN,FR,AMPL,PHASE,J)
      PLOT OF FREQUENCY SPECTRUM AND PHASE ANGLE
      CALL SPLOT(NP,DELTAT,AMMIN,FR,AMPL,PHASE,J)
      STOP
      END
      SUBROUTINE NLOGN(N,X,SIGN)
      DIMENSION M(12)
      DIMENSION X(4096)
      COMPLEX X,WK,HOLD,Q,CMLPX
      LX=2**N
      DO 1 I=1,N
      M(I)=2**{N-I}
      DO 4 L=1,N
      NBLOCK=2**{L-1}
      LBLOCK=LX/NBLOCK
      LBHALF=LBLOCK/2
      K=0
      DO 4 IBLOCK=1,NBLOCK
      FLX=LX
      FK=K
      V=SIGN*6.2831853*FK/FLX
      WK=CMLPX{COS(V),SIN(V)}
      ISTART=LBLOCK*(IBLOCK-1)
      DO 2 I=1,LBHALF
      J=ISTART+I
      JH=J+LBHALF
      Q=X(JH)*WK
      X(JH)=X(J)-Q
      X(J)=X(J)+Q
      CONTINUE
      DO 3 I=2,N
      II=I
      IF(K.LT.M(II)) GO TO 4
      K=K-M(II)
      K=K+M(II)
      K=0
      DO 7 J=1,LX

```

MAIN 210
MAIN 220

MAIN 230

MAIN 240

MAIN 250
MAIN 260
MAIN 270
NLOG 111
NLOG 211
NLOG 311
NLOG 411
NLOG 511
NLOG 611
NLOG 711
NLOG 811
NLOG 911
NLOG 1011
NLOG 1111
NLOG 1211
NLOG 1311
NLOG 1411
NLOG 1511
NLOG 1611
NLOG 1711
NLOG 1811
NLOG 1911
NLOG 2011
NLOG 2111
NLOG 2211
NLOG 2311
NLOG 2411
NLOG 2511
NLOG 2611
NLOG 2711
NLOG 2811
NLOG 2911
NLOG 3011
NLOG 311

```

114 IF(K.LT.J) GO TO 5
    HOLD=X(J)
    X(J)=X(K+1)
    X(K+1)=HOLD
5 DO 6 I=1,N
    II=I
    IF(K.LT.M(I)) GO TO 7
6 K=K-M(I)
7 K=K+M(II)
    IF(SIGN.LT.0.0)RETURN
    DO 8 I=1,LX
8 X(I)=X(II)/FLX
    RETURN
    END
    SUBROUTINE SPECRA(NP,X,DELTA,AMMIN,FR,AMPL,PHASE,J)
    THIS PROGRAM CALCULATES DATA FOR FREQUENCY SPECTRUM
    AND PHASE ANGLE
    DIMENSION X(4096),FR(2050),AMPL(2048),PHASE(2048)
    COMPLEX X
    NDIV2=NP/2
    J=0
    TN=DELTA*NP
    WRITE(3,114)
114 FORMAT(//8X,'I',6X,'FREQUENCY',6X,'REAL X(I)',6X,'IMAG X(I)',6X,
    1,AMPL X(I)',6X,'PHASE(I)')
    FR(1)=0.0
    DO 40 I=1,NDIV2
    II=I+1
    FR(II)=I/TN
    X(I)=X(II)/NP
    AMPL(I)=CABS(X(I))
    IF (AMMIN-AMPL(I)) 35,35,40
35 CONTINUE
    A=REAL(X(I))
    B=AIMAG(X(I))
    IF(A)38,36,38
36 PHASE(I)=90.0
    IF(B)37,39,39
37 PHASE(I)=-90.0
    GO TO 39
    PHASE(I)=ATAN(B/A)*57.29578
38 IF(A.GT.0) GO TO 39
    PHASE(I)=PHASE(I) + 180.0
39 CONTINUE
    WRITE(3,115) I,FR(I),X(I),AMPL(I),PHASE(I)
115 FORMAT(110,4E15.5,F15.2)
    J=J+1

```

[illegible]

EXAMPLE PROBLEM NO. 1, 3-STORY, 1-BAY FRAME, H+V OF FL CENTRO, ELASTO-PLASTIC

STRUCTURE CONTROL DATA

STRUCTURE NO. 131
 DEGREES OF FREEDOM 15
 LUMPED MASSES 9
 NODES ON GIRDER SPANS 3
 FLOOR LEVELS 3
 NUMBER OF MEMBERS 12
 NUMBER OF SUPPORT COLUMNS 2
 NUMBER OF COLUMNS 2

CONDITIONS OF ANALYSIS

OUTPUT RESPONSE BASED ON BILINEAR CONDITION (P=0.0000)
 PLASTIC MOMENT OF A MEMBER REMAINS CONSTANT
 P-DELTA EFFECT INCLUDED
 VERTICAL VARIABLE S-LADING INCLUDED
 REDUCTION IS MADE IN THE COLUMN PLASTIC MOMENT VALUES DUE TO AXIAL COMPRESSION
 THE LINEAR ACCELERATION TECHNIQUE (BETA=1/4) IS USED FOR INTEGRATION
 HORIZONTAL LOADING MULTIPLIED BY 1.000
 VERTICAL LOADING MULTIPLIED BY 1.000
 FLOOR WEIGHTS MULTIPLIED BY 1.000
 DELTA T 0.010000
 TOTAL TIME CONSIDERED 1.50
 CRITICAL DAMPING FACTOR 0.0
 ESTIMATED FUNDAMENTAL FREQUENCY 0.8330 CPS
 DAMPING NOT CONSIDERED

OUTPUT CONTROL

PRINTOUT INCREMENT 0.50
 PUNCH OR PLOT INCREMENT 2.000
 PRINTOUT OF INITIAL MATRICES INCLUDED
 PRINTOUT OF PLASTIC HINGE RESULTS INCLUDED
 DAMPING NOT CONSIDERED

LOADING INFORMATION

CONCENTRATED LOAD VALUES
 1 0.929400E+02 2 0.837000E+02 3 0.435000E+02 4 0.0 5 0.0 6 0.0

NUMBER OF TIMES FRAME IS LOADED= 150

HORIZONTAL EARTHQUAKE COMPONENT
 PLUS VERTICAL EARTHQUAKE COMPONENT

STRUCTURE INFORMATION

GIRDER MEMBERS LEFT SIDE OF SPAN
 GIRDER MEMBERS RIGHT SIDE OF SPAN
 SUPPORT COLUMNS

VALUE OF PLASTIC MOMENT FOR EACH MEMBER
 1 0.393000E+03 2 0.342000E+03 3 0.342000E+03 4 0.345000E+03 5 0.345000E+03 6 0.306000E+03
 7 0.345000E+03 8 0.345000E+03 9 0.306000E+03 10 0.390000E+03 11 0.342000E+03 12 0.342000E+03

FLOOR MASSES CONSIDERED LUMPED AT GIRDER NODES

GIRDER MASSES FOR FLOORS 1 THRU 3
 1 0.288629E+01 2 0.253861E+01 3 0.135101E+01
 FLOOR MASSES FOR FLOORS 1 THRU 3
 4 0.577250E+01 5 0.537215E+01 6 0.270202E+01

THE MATRIX AM---LOCATIONS NOT SHOWN ARE ZERO

ROW 1 COLS 2 THRU 7 1. 1. 0. 0. 0. 0.
 ROW 2 COLS 4 THRU 9 1. 1. 0. 0. 0. 0.
 ROW 3 COLS 6 THRU 11 1. 0. 0. 0. 0. 0.
 ROW 4 COLS 12 THRU 17 1. 0. 0. 0. 0. 0.
 ROW 5 COLS 10 THRU 15 1. 0. 0. 0. 0. 0.
 ROW 6 COLS 8 THRU 13 1. 0. 0. 0. 0. 0.
 ROW 7 COLS 14 THRU 21 1. 0. 0. 0. 0. 0.
 ROW 8 COLS 16 THRU 23 1. 0. 0. 0. 0. 0.
 ROW 9 COLS 18 THRU 24 1. 0. 0. 0. 0. 0.

THE MATRIX AV---LOCATIONS NOT SHOWN ARE ZERO

ROW 1 COLS 8 THRU 13 1. 0. 0. 0. 0. 0.
 ROW 2 COLS 10 THRU 15 1. 0. 0. 0. 0. 0.
 ROW 3 COLS 12 THRU 17 1. 0. 0. 0. 0. 0.
 ROW 4 COLS 2 THRU 21 1. 0. 0. 0. 0. 0.
 ROW 5 COLS 4 THRU 23 1. 0. 0. 0. 0. 0.
 ROW 6 COLS 6 THRU 24 1. 0. 0. 0. 0. 0.

E= 0.30E+05 FY= 36.00

THE CROSS-SECTIONAL AREA OF COLUMN MEMBERS, IN.2

3 2.6199997E+01 12 2.6199997E+01 2 2.6199997E+01 11 2.6199997E+01 1 2.9399994E+01
 10 2.9399994E+01

THE UNBRACED LENGTH OF COLUMN MEMBERS, IN.

3 1.2000000E+02 12 1.2000000E+02 2 1.2000000E+02 11 1.2000000E+02 1 1.8000000E+02

Reproduced from
 best available copy.



[illegible]

ROW	P-DELTA	STIFFNESS MATRIX	AS FORMED IN	PROGRAM, K2			
ROW 1	0.0	0.0	0.0	0.0	0.0	0.0	0.0
ROW 2	0.0	0.0	0.0	0.0	0.0	0.0	0.0
ROW 3	0.0	0.0	0.0	0.0	0.0	0.0	0.0
ROW 4	0.0	0.0	0.0	0.0	0.173470E+01	-0.809973E+00	0.0
ROW 5	0.0	0.0	0.0	0.0	-0.809973E+00	0.108012E+01	-0.270202E+00
ROW 6	0.0	0.0	0.0	0.0	0.0	-0.270202E+00	0.270202E+00

```

TIME= 0.0      NUMBER OF TIMES STIFFNESS HAS BEEN CALCULATED = 1
LOADING
XG= 0.0      XGT= 0.0      HORIZONTAL= 0.353105E+00      VERTICAL= -0.276337E+01
YG= 0.0      YGT= 0.0      EDO= 0.0      TDSE= 0.0
ENERGY EIE= 0.346472E+01      ALSC= 0.346470E+01      EKE= 0.0
HORIZONTAL FLOOR DISPL., VEL. AND ACCEL. RELATIVE TO BASE.
NO.      DISPL.      VEL.      ACCEL.      NO.      DISPL.      VEL.      ACCEL.
1      -0.36214E-07      0.0      -0.333105E+00      5      -0.563794E-07      0.0      -0.333105E+00
6      -0.522914E-07      0.0      -0.333105E+00
VERTICAL DISPL., VEL. AND ACCEL. OF NODAL POINTS ON GIRDERS RELATIVE TO BASE.
NO.      DISPL.      VEL.      ACCEL.      NO.      DISPL.      VEL.      ACCEL.
1      0.364778E-01      0.0      0.276337E+01      2      0.305455E-01      0.0      0.276337E+01
3      0.203403E-01      0.0      0.276337E+01
JOINT ROTATIONS
1      0.2161E-02      2      0.1308E-02      3      0.1354E-02      4      -0.5471E-09      5      0.4889E-10      6      0.8671E-09      7      -0.2141E-02
8      -0.1308E-02      9      -0.1354E-02
JOINT MOMENTS, K=0, ELASTIC RANGE, K=2, PLASTIC RANGE
NO.      NO.      MOMENT      K      NO.      NO.      MOMENT      K      NO.      NO.      MOMENT      K      NO.      NO.      MOMENT      K
1      0.3631E+02      0      2      0.7263E+02      0      3      0.1271E+03      0      4      0.1079E+03      0      5      0.8965E+02      0
6      0.9067E+02      0      7      -0.1975E+03      0      8      -0.1975E+03      0      9      -0.2370E+03      0
11     -0.9057E+02      0      12     -0.1268E+03      0      13     0.2649E+03      0      14     0.1998E+03      0      15     0.2370E+03      0
16     0.1975E+03      0      17     0.1268E+03      0      18     0.9067E+02      0      19     -0.3531E+02      0      20     -0.7263E+02      0
21     -0.1271E+03      0      22     -0.1079E+03      0      23     -0.8965E+02      0      24     -0.9357E+02      0
MATRIX SK1(NPR,NPS)
ROW      1      0.1391E+06      0.2258E+05      0.0      0.0      0.0      0.3017E+05      0.3017E+05      0.0      0.0      0.0
ROW      2      0.258E+05      0.2258E+05      0.0      0.258E+05      0.0      0.0      0.0      0.0      0.0      0.0
ROW      3      0.0      0.2258E+05      0.2571E+05      0.0      0.0      0.0      0.0      0.0      0.0      0.2571E+05
ROW      4      0.0      0.0      0.2571E+05      0.1008E+06      0.0      0.0      0.0      0.0      0.0      0.0
ROW      5      0.0      0.3017E+05      0.0      0.0      0.1207E+06      0.0      0.0      0.0      0.3017E+05      0.0
ROW      6      0.3017E+05      0.0      0.0      0.0      0.1207E+06      0.0      0.3017E+05      0.0      0.0      0.0
ROW      7      0.0      0.0      0.0      0.0      0.0      0.1391E+06      0.2258E+05      0.0      0.2258E+05      0.0
ROW      8      0.0      0.0      0.0      0.0      0.0      0.2258E+05      0.1527E+06      0.2258E+05      0.2258E+05      0.998E+05
ROW      9      0.0      0.0      0.0      0.2571E+05      0.0      0.0      0.2258E+05      0.2258E+05      0.998E+05
MATRIX SK2(NPR,NPS)
ROW      1      -0.9050E+04      0.0      0.0      0.3414E+04      -0.6775E+04      0.0      0.0
ROW      2      0.0      -0.9050E+04      0.0      0.3414E+04      -0.6775E+04      0.0      0.0
ROW      3      0.0      0.0      -0.8012E+04      0.0      0.6775E+04      -0.6775E+04      0.0

```

```

ROW 2 0.0 0.0 0.0 0.0 0.0 0.0
ROW 3 0.0 0.0 0.0 0.0 0.0 0.0
ROW 4 0.0 0.0 0.0 0.0 0.0 0.0
ROW 5 0.0050E+04 0.0050E+04 0.0 0.0 0.0 0.0
ROW 6 0.0 0.0 0.0 0.0 0.0 0.0
ROW 7 0.0 0.0 0.0 0.0 0.0 0.0
ROW 8 0.0 0.0 0.0 0.0 0.0 0.0
ROW 9 0.0 0.0 0.0 0.0 0.0 0.0

```

```

MATRIX SK3INPS,NPS1
ROW 1 0.3620E+04 0.0 0.0 0.0 0.0 0.0
ROW 2 0.0 0.3620E+04 0.0 0.0 0.0 0.0
ROW 3 0.0 0.0 0.0 0.0 0.0 0.0
ROW 4 0.0 0.0 0.0 0.0 0.0 0.0
ROW 5 0.0 0.0 0.0 0.0 0.0 0.0
ROW 6 0.0 0.0 0.0 0.0 0.0 0.0

```

```

MATRIX STIPINPR,NPS1
ROW 1 0.6674E-01 -0.1036E-01 -0.2101E-02 -0.1903E-01 0.5381E-01 -0.7226E-02
ROW 2 -0.1036E-01 0.6381E-01 -0.1274E-01 -0.4404E-01 0.4475E-02 0.3968E-01
ROW 3 -0.2373E-02 -0.1462E-01 0.3424E-01 0.1299E-01 -0.8308E-01 0.6898E-01
ROW 4 -0.7656E-09 0.3226E-03 -0.2471E-07 -0.6437E-02 0.3348E-01 -0.3449E-01
ROW 5 0.7054E-09 -0.1411E-07 0.6495E-08 0.2432E-01 -0.2238E-02 0.1484E-01
ROW 6 0.0 -0.2825E-01 -0.3512E-02 0.2493E-02 -0.2593E-01 0.1613E-02
ROW 7 -0.6674E-01 0.1036E-01 -0.2101E-02 -0.1903E-01 0.5381E-01 -0.7226E-02
ROW 8 -0.1036E-01 0.6381E-01 -0.1274E-01 -0.4404E-01 0.4475E-02 0.3968E-01
ROW 9 -0.2373E-02 -0.1462E-01 0.3424E-01 0.1299E-01 -0.8308E-01 0.6898E-01

```

```

MATRIX SKS
ROW 1 0.1756E+06 0.1875E+03 0.1875E+03 -0.1678E-03 0.4833E-03 0.0
ROW 2 0.1875E+03 0.1644E+06 0.2342E+03 0.4833E-03 -0.1678E-03 0.0
ROW 3 -0.3403E+02 0.2342E+03 0.8242E+05 -0.1221E-03 0.4833E-03 0.0
ROW 4 -0.2788E+03 0.2342E+03 0.8242E+05 -0.1221E-03 0.4833E-03 0.0
ROW 5 0.1875E+03 0.2342E+03 0.8242E+05 -0.1221E-03 0.4833E-03 0.0
ROW 6 0.1526E+04 0.1526E-03 0.2441E-03 0.4833E-03 -0.1678E-03 0.1633E+06

```

```

*****
TIME= 0.500 NUMBER OF TIMES STIFFNESS HAS BEEN CALCULATED = 1
LOADING XG= 0.278535E-01 XGT= 0.850170E-01 YG= 0.9414E-01 YGT= 0.257259E-01
ENERGY EIE= 0.281556E+01 ELSE= 0.245260E+01 EKE= 0.361864E+00 EDD= 0.0 TDS= 0.0 0.0426% ERROR
HORIZONTAL FLOOR DISPL., VEL. AND ACCEL. RELATIVE TO BASE.
NO. DISPL. VEL. ACCEL. NO. DISPL. VEL. ACCEL.
4 -0.941370E-02 0.607914E-02 -0.345355E+00 5 -0.147451E-01 0.137780E-01 -0.133347E+00
6 -0.173190E-01 0.170417E-01 -0.74349E-01
VERTICAL DISPL., VEL. AND ACCEL. OF NODAL POINTS ON GIRDERS RELATIVE TO BASE.
NO. DISPL. VEL. ACCEL. NO. DISPL. VEL. ACCEL.
3 0.321851E-01 -0.447816E-01 0.562751E+01 2 0.241439E-01 0.585345E-01 0.821297E+01
3 0.158617E-01 0.670861E+00 0.881514E+01
JOINT ROTATIONS
1 0.1438E-02 2 0.7103E-03 3 0.9325E-03 4 0.6366E-03 5 0.1458E-03 6 0.2466E-03 7 -0.2624E-02
8 -0.1294E-02 9 -0.1187E-02
JOINT MOMENTS, K=0, ELASTIC RANGE, K=2, PLASTIC RANGE
NO. MOMENT K NO. MOMENT K NO. MOMENT K NO. MOMENT K NO. MOMENT K NO. MOMENT K
4 0.7288E+02 0 7 -0.1971E+03 0 8 -0.2337E+03 0 9 -0.1713E+03 0 10 -0.1883E+03 0
6 0.7288E+02 0 7 -0.1971E+03 0 8 -0.2337E+03 0 9 -0.1713E+03 0 10 -0.1883E+03 0
11 -0.7288E+02 0 12 -0.1971E+03 0 13 -0.2337E+03 0 14 -0.1713E+03 0 15 -0.1883E+03 0
21 -0.1026E+03 0 22 -0.7706E+02 0 23 -0.6700E+02 0 24 -0.6539E+02 0
11 -0.7288E+02 0 12 -0.8888E+02 0 13 -0.2337E+02 0 14 -0.3523E+03 0 15 -0.1883E+03 0
21 -0.1026E+03 0 22 -0.7706E+02 0 23 -0.6700E+02 0 24 -0.6539E+02 0

```

```

*****
TIME= 1.000 NUMBER OF TIMES STIFFNESS HAS BEEN CALCULATED = 1
LOADING XG= 0.784732E-01 XGT= 0.178999E+00 YG= 0.241181E-01 YGT= 0.14115E+00
ENERGY EIE= 0.461873E+01 ELSE= 0.360733E+01 EKE= 0.101311E+01 EDD= 0.0 TDS= 0.0 -0.0371% ERROR
HORIZONTAL FLOOR DISPL., VEL. AND ACCEL. RELATIVE TO BASE.
NO. DISPL. VEL. ACCEL. NO. DISPL. VEL. ACCEL.
4 0.230855E-01 0.274219E+00 0.191391E+01 5 0.351294E-01 0.439702E+00 0.185093E+01
6 0.437897E-01 0.195930E+00 0.743280E+00
VERTICAL DISPL., VEL. AND ACCEL. OF NODAL POINTS ON GIRDERS RELATIVE TO BASE.
NO. DISPL. VEL. ACCEL. NO. DISPL. VEL. ACCEL.
3 0.359080E-01 0.274445E+00 0.363657E+01 2 0.338657E-01 0.317454E+00 0.129322E+01
3 0.112242E-01 0.243647E+00 0.154238E+02
JOINT ROTATIONS
1 0.3268E-02 2 0.2412E-02 3 0.9410E-03 4 -0.2027E-03 5 -0.3842E-03 6 -0.5994E-03 7 -0.8704E-03
8 -0.8753E-03 9 -0.1104E-03
JOINT MOMENTS, K=0, ELASTIC RANGE, K=2, PLASTIC RANGE
NO. MOMENT K NO. MOMENT K NO. MOMENT K NO. MOMENT K NO. MOMENT K NO. MOMENT K
4 -0.2261E+02 0 7 -0.3231E+02 0 8 -0.1137E+03 0 9 -0.9424E+02 0 10 -0.7430E+02 0
6 0.4508E+02 0 7 -0.1459E+03 0 8 -0.2625E+03 0 9 -0.1722E+03 0 10 -0.2569E+03 0
11 -0.4508E+02 0 12 -0.7263E+02 0 13 -0.2625E+03 0 14 -0.2569E+03 0 15 -0.2569E+03 0
16 -0.4476E+03 0 17 -0.7297E+02 0 18 -0.9439E+02 0 19 -0.9210E+02 0 20 -0.1066E+03 0
21 -0.4476E+03 0 22 -0.7297E+02 0 23 -0.9439E+02 0 24 -0.9210E+02 0
NOTE, AT TIME= 1.04 SEC. THE FOLLOWING MEMBER ENDS BECAME PLASTIC 8 10 13 14 15
THE FOLLOWING ADDITIONAL INFORMATION APPLIES TO PLASTIC HINGES
10 MP MAX= 0.345000E+03 MP MIN= -0.345000E+03 JOINT ROTATION= -0.492289E-02
THE FOLLOWING ADDITIONAL INFORMATION APPLIES TO PLASTIC HINGES
10 DSEAB= 0.140543E-01 DSEAB= 0.101309E+01 EMP= 0.101309E+01 DSEAB= 0.101309E+01 EXCUR= 0.138731E-01 1
YMON= 0.345000E+03 DELAP= -0.228687E+01 EMP= 0.100000E+01 DSEAB= 0.100000E+01 EXCUR= 0.0 2
ALPHA= 0.13263E-03 ALPHAT= 0.192888E-03 EMP= 0.104985E+01 DSEAB= 0.104985E+01 EXCUR= 0.1496531E-01 3
DSEAB= 0.137136E-02 DSEAB= 0.129878E+01 EMP= 0.998788E+00 DSEAB= 0.998788E+00 EXCUR= 0.121184E-02 1
YMON= 0.345000E+03 DELAP= -0.228687E+01 EMP= 0.100000E+01 DSEAB= 0.100000E+01 EXCUR= 0.0 2
ALPHA= 0.200141E-03 ALPHAT= 0.200141E-03 EMP= 0.105250E+01 DSEAB= 0.105250E+01 EXCUR= 0.524998E-01 3
NOTE, AT TIME= 1.05 SEC. THE FOLLOWING MEMBER ENDS RETURNED TO THEIR ELASTIC RANGE 10 15
THE FOLLOWING ADDITIONAL INFORMATION APPLIES TO PLASTIC HINGES
8 MP MAX= 0.345000E+03 MP MIN= -0.345000E+03 JOINT ROTATION= -0.600014E-02
THE FOLLOWING ADDITIONAL INFORMATION APPLIES TO PLASTIC HINGES
13 MP MAX= 0.345000E+03 MP MIN= -0.345000E+03 JOINT ROTATION= 0.360098E-02
THE FOLLOWING ADDITIONAL INFORMATION APPLIES TO PLASTIC HINGES
14 MP MAX= 0.345000E+03 MP MIN= -0.345000E+03 JOINT ROTATION= 0.447191E-02
8 DSEAB= 0.12623E-02 DSEAB= 0.023267E+00 EMP= 0.113715E+01 DSEAB= 0.113715E+01 EXCUR= 0.137146E+00 1
YMON= 0.345000E+03 DELAP= -0.541162E+01 EMP= 0.100300E+01 DSEAB= 0.100300E+01 EXCUR= 0.0 2
ALPHA= 0.417637E-03 ALPHAT= 0.417637E-03 EMP= 0.110355E+01 DSEAB= 0.110355E+01 EXCUR= 0.109553E+00 3
DSEAB= 0.276126E-01 DSEAB= 0.134180E+01 EMP= 0.97942E+00 DSEAB= 0.97942E+00 EXCUR= 0.203786E-01 1
YMON= 0.345000E+03 DELAP= -0.541162E+01 EMP= 0.100300E+01 DSEAB= 0.100300E+01 EXCUR= 0.0 2
ALPHA= 0.369224E-03 ALPHAT= 0.369224E-03 EMP= 0.109695E+01 DSEAB= 0.109695E+01 EXCUR= 0.968542E-01 3
DSEAB= 0.216715E+00 DSEAB= 0.134180E+01 EMP= 0.116151E+01 DSEAB= 0.116151E+01 EXCUR= 0.161510E+00 1

```


MAXIMUM POSITIVE AND NEGATIVE ACCELERATIONS DURING FIRST 1.50 SECONDS

1	0.1557E+02	-0.1511E+02	2	0.2174E+02	-0.1967E+02	3	0.2866E+02	-0.2662E+02	4	0.4571E+01	-0.5197E+01
5	0.2386E+01	-0.4104E+01	6	0.3194E+01	-0.4934E+01						

MAXIMUM POSITIVE AND NEGATIVE END MOMENTS DURING FIRST 1.50 SECONDS

1	0.7670E+02	-0.1799E+03	2	0.1082E+03	-0.7798E+02	3	0.1827E+03	0.0	4	0.1617E+03	-0.3550E+02
5	0.1411E+03	0.0	6	0.1632E+03	0.0	7	0.2039E+02	-0.2756E+03	8	0.0	-0.3528E+03
9	0.0	-0.2691E+03	10	0.0	-0.3572E+03	11	0.0	-0.1632E+03	12	0.0	-0.2358E+03
13	0.3528E+03	0.0	14	0.3565E+03	0.0	15	0.3572E+03	0.0	16	0.356E+03	0.0
17	0.2358E+03	0.0	18	0.1814E+03	0.0	19	0.8535E+01	-0.2473E+03	20	0.0	-0.2030E+03
21	0.0	-0.1958E+03	22	0.0	-0.2374E+03	23	0.0	-0.1481E+03	24	0.0	-0.1814E+03

THE MAXIMUM INPUT ENERGY FOR THIS JOP IS 0.157112E+02, FOUND PRESENT AT TIME 1.500

DUCTILITY AND EXCURSION RATIOS BASED ON ENERGY

MAXIMUM DUCTILITY RATIOS FOR EACH END OF MEMBERS

1	0.0	2	0.0	3	0.0	4	0.0	5	0.0	6	0.0	7	0.0
8	0.1137E+01	9	0.0	10	0.1121E+01	11	0.0	12	0.0	13	0.1330E+01	14	0.1323E+01
15	0.1084E+01	16	0.1161E+01	17	0.0	18	0.0	19	0.0	20	0.0	21	0.0
22	0.0	23	0.0	24	0.0								

EXCURSION RATIOS FOR EACH END OF MEMBERS

1	0.0	2	0.0	3	0.0	4	0.0	5	0.0	6	0.0	7	0.0
8	0.2790E+00	9	0.0	10	0.1675E+00	11	0.0	12	0.0	13	0.6274E-01	14	0.7892E+00
15	0.9169E-01	16	0.1609E+00	17	0.0	18	0.0	19	0.0	20	0.0	21	0.0
22	0.0	23	0.0	24	0.0								

DUCTILITY AND EXCURSION RATIOS BASED ON CURVATURE

MAXIMUM DUCTILITY RATIOS FOR EACH END OF MEMBERS

1	0.0	2	0.0	3	0.0	4	0.0	5	0.0	6	0.0	7	0.0
8	0.1000E+01	9	0.0	10	0.1000E+01	11	0.0	12	0.0	13	0.1000E+01	14	0.1212E+01
15	0.1000E+01	16	0.1071E+01	17	0.0	18	0.0	19	0.0	20	0.0	21	0.0
22	0.0	23	0.0	24	0.0								

EXCURSION RATIOS FOR EACH END OF MEMBERS

1	0.0	2	0.0	3	0.0	4	0.0	5	0.0	6	0.0	7	0.0
8	0.0	9	0.0	10	0.0	11	0.0	12	0.0	13	0.0	14	0.4245E+00
15	0.0	16	0.7076E-01	17	0.0	18	0.0	19	0.0	20	0.0	21	0.0
22	0.0	23	0.0	24	0.0								

DUCTILITY AND EXCURSION RATIOS BASED ON SYMMETRICAL BENDING

MAXIMUM DUCTILITY RATIOS FOR EACH END OF MEMBERS

1	0.0	2	0.0	3	0.0	4	0.0	5	0.0	6	0.0	7	0.0
8	0.1110E+01	9	0.0	10	0.1098E+01	11	0.0	12	0.0	13	0.1097E+01	14	0.1614E+01
15	0.1107E+01	16	0.1192E+01	17	0.0	18	0.0	19	0.0	20	0.0	21	0.0
22	0.0	23	0.0	24	0.0								

EXCURSION RATIOS FOR EACH END OF MEMBERS

1	0.0	2	0.0	3	0.0	4	0.0	5	0.0	6	0.0	7	0.0
8	0.2519E+00	9	0.0	10	0.1784E+00	11	0.0	12	0.0	13	0.1766E+00	14	0.9957E+00
15	0.1821E+00	16	0.1917E+00	17	0.0	18	0.0	19	0.0	20	0.0	21	0.0
22	0.0	23	0.0	24	0.0								

LARGEST ERROR IN ENERGY= 0.6695% AT TIME= 0.970 SEC. AT THIS TIME EIE= 0.285036E+01

